The role of the ETS factor ELF3 in the normal and malignant prostate

Leanne K Archer

PhD

University of York

Biology

September 2018

Abstract

The ETS transcription factor family members are involved in multiple cancers, including prostate cancer. Whilst extensive literature exists on the highly prevalent TMPRSS2-ERG gene fusion, the role of other ETS factors in prostate cancer is less well understood. ELF3 has been ascribed both oncogenic and tumour suppressive roles in prostate cancer and has been highlighted as a regulator of epithelial cell differentiation in other tissues. The overarching aim of this project was to elucidate the role of ELF3 in the context of both normal prostate development and prostate cancer.

This study details an extensive expression profile of ELF3 in prostate epithelial cell lines, primary prostate cell subpopulations and prostate tissue. ELF3 expression was restricted to the basal compartment of epithelial glands, specifically to the committed basal cell subpopulation of the basal epithelial hierarchy. Appropriate cell models were used to investigate the role of ELF3 in the prostate. By silencing ELF3 in BPH-1 and PC3 cells, ELF3 was established as a regulator of the cell cycle. This manifested as a decrease in colony forming ability, migration and cell viability caused by G2 cell cycle arrest. Furthermore, manipulating ELF3 expression altered the differentiation status of cell lines and primary cells, highlighting that a balance of ELF3 expression is required to maintain proper differentiation of the epithelial hierarchy. Finally, a possible link of ELF3 to more advanced prostate tumours using tissue microarray analysis, a potential association with neuroendocrine differentiation and putative survival advantage of ELF3 expression in cancer vs normal cells, was identified.

These results suggest that ELF3 acts as an oncogene in the prostate cancer setting. However, its importance in normal prostate epithelial cell growth and differentiation has also been demonstrated. Work should now focus on identifying appropriate downstream effectors that could be targeted to exploit these properties for prostate cancer treatment.

List of Contents

List of Figures

List of Tables

Acknowledgements

This work is dedicated to my mum, the strongest woman I know and provider of exceptional potato scones when needed. Everything I am is because of you.

Thank you to Norman and Prostate Cancer UK for giving me the opportunity to be part of the CRU and providing essential funding.

Thanks to Hannah, Michelle, Dominika and the rest of the CRU, past and present, for their support and always being a friendly face.

Thank you to Mandy, for truly being my lab mum and supplying biscuits on tap during desperate times.

Thank you to Georgie, my partner in crime, for sharing that bottle of prosecco with me and always making me feel clever, may you always be bright and shiny.

Thank you to John P., Ban, Conor and John H., for providing endless banter and always laughing at my jokes.

Last and foremost, thank you to Fiona, for being the best mentor I could have ever hoped for. This would not have been achievable without your guidance, pep talks and friendship.

Author's Declaration

I declare that this thesis is a presentation of my own unaided work, except where acknowledged otherwise in the text. This work has not previously been presented for an award at this, or any other, University. All sources are acknowledged as References.

This work has been presented at the following meetings:

Oct 2016 23rd Meeting of the EAU Section of Urological Research, Parma, Italy.

Poster presentation

Sep 2017 European Society for Medical Oncology Congress, Madrid, Spain

Poster presentation

The following review article was published during this PhD and has been used in part in this thesis:

ARCHER, L. K., FRAME, F. M. & MAITLAND, N. J. 2017. Stem cells and the role of ETS transcription factors in the differentiation hierarchy of normal and malignant prostate epithelium. J Steroid Biochem Mol Biol, 166, 68-83.

1. Introduction

1.1 Function and anatomy of the prostate

The prostate is a male secretory gland comprised of a series of glandular epithelial acini and muscular stroma. It is responsible for producing proteins, such as prostatic acid phosphatase (PAP) and prostate specific antigen (PSA) and secreting the fluid which constitutes semen via ducts which lead to the urethra. The prostate is located below the bladder, surrounding the urethra, and is in close proximity to a collection of nerves called the prostatic plexus which is responsible for controlling urinary output as well as erection and ejaculation. As a result of this position, enlargement of the prostate can lead to both urinary and sexual symptoms (Figure 1.1). The prostate can be divided into separate zones, each with its own propensity for disease. The peripheral zone is found at the base of the prostate and forms ~70% of the tissue. This area is where the majority of prostate cancers (PCa) arise (>70%) and can be assessed during a digital rectal examination. The central zone lies just below the bladder. Prostate tumours rarely arise from the central zone however they are associated with an aggressive phenotype and poor prognosis (Lee et al., 2011). Finally, the transitional zone is located in front of the central zone surrounding the urethra and is the site where the majority of benign enlargement of the prostate occurs, known as benign prostatic hyperplasia (BPH) (McNeal, 1981).

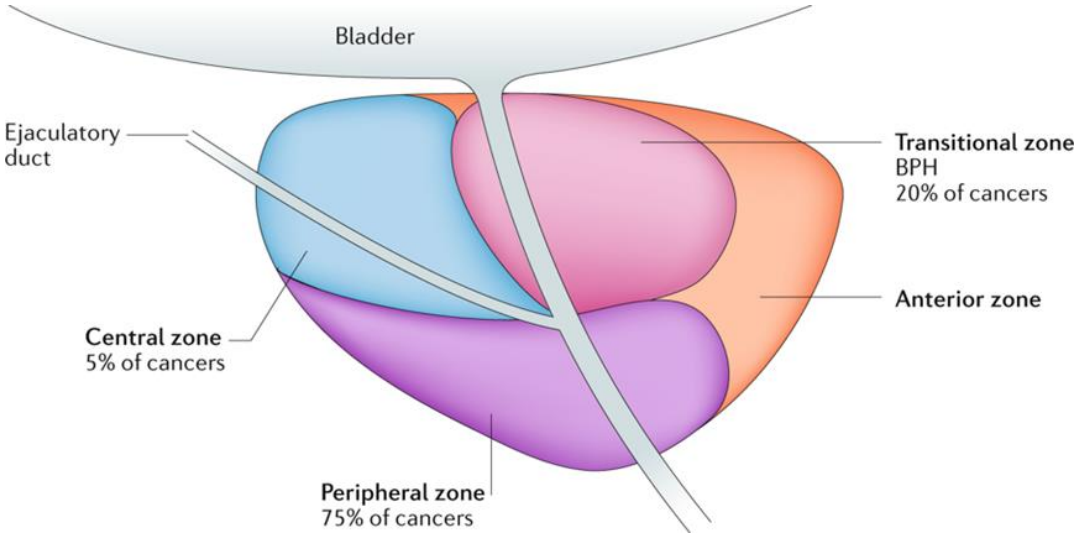

Figure 1.1. The zonal anatomy of the prostate.

The prostate gland is situated below the bladder, surrounding and linking the urethra to the ejaculatory duct. The prostate consists of four zones; the peripheral zone, anterior zone, central zone and transitional zone, each of which has its own propensity for prostate pathology. Reprinted from (Sathianathen et al., 2018), with Copyright permission from Springer Nature.

1.2 Cellular organisation of the normal prostate

The normal prostate epithelium is composed of an hierarchy of cells that can be split into a basal compartment, which is attached to the basement membrane (BM), and a luminal compartment, which is the inner layer lining the lumen (Figure 1.2). Androgen-independent basal cells comprise the proliferative compartment of the adult prostate and can be distinguished by their expression of specific cytokeratins (CK) including CKs 5 and 14 (Schalken and van Leenders, 2003), and other cell markers such as p63 (Signoretti et al., 2000), CD44 (Terpe et al., 1994) and bcl-2 (McDonnell et al., 1992). The fully differentiated luminal cells are the secretory cells of the prostate. These are androgen-responsive, expressing high levels of the androgen receptor (AR) and PSA. Luminal cells also express CKs 8 and 18 (Schalken and van Leenders, 2003) and CD57 (Liu et al., 1997b). Distinct differentiation states have been found within the basal compartment, adding another level of complexity and heterogeneity to the prostate epithelium. The base of the hierarchy consists of normal basal stem cells (SC) which are largely quiescent (Oldridge et al., 2012). Some SCs asymmetrically divide into a proliferative, intermediate progenitor cell population which are termed transit amplifying (TA) cells. A third population committed to differentiation called committed basal (CB) cells completes the basal hierarchy (Oldridge et al., 2012, Isaacs and Coffey, 1989). Significantly, several studies have shown that both basal and luminal cells derive from the same rare SC precursors found in the basal compartment, providing further evidence for the presence of a differentiation hierarchy in the prostate (Isaacs and Coffey, 1989, Hudson et al., 2001, Lang et al., 2001b, van Leenders et al., 2001).

A rare neuroendocrine (NE) cell population is also scattered throughout the basal compartment of the prostate epithelium. These granular cells secrete peptide hormones such as serotonin and chromogranin A (ChrA) that regulate epithelial cell proliferation and differentiation (di Sant'Agnese, 1998, Rumpold et al., 2002). On the opposite side of the basal basement membrane lies the network of fibromuscular stroma which includes smooth muscle cells, fibroblasts, collagen fibres, endothelial cells and nerve fibres (Barron and Rowley, 2012). The stroma is important for maintaining prostate tissue growth and homeostasis through interactions with epithelial cells and secretion of growth factors.

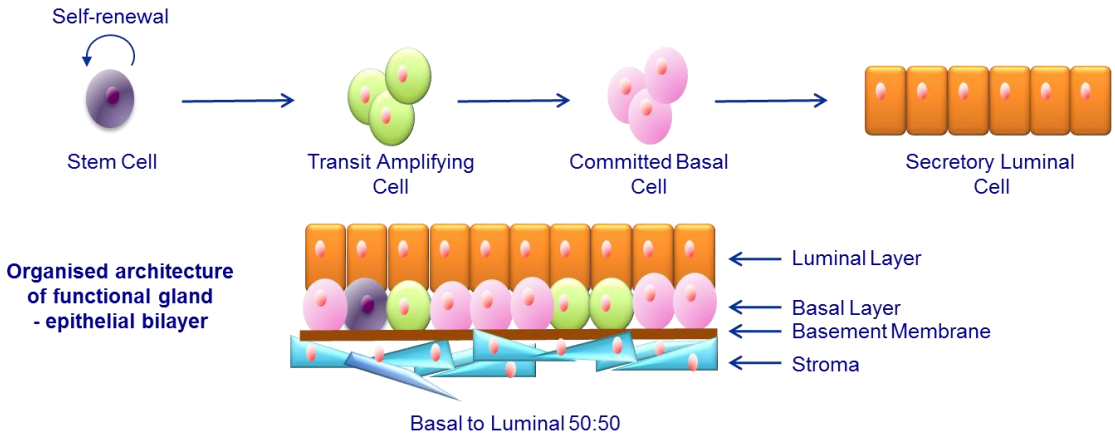

Figure 1.2. Differentiation hierarchy of the normal prostate.

The normal human prostate epithelium is composed of an hierarchical differentiation pathway. SCs differentiate into rapidly dividing transit amplifying cells by asymmetric division and thus also maintain themselves. Multipotent transit amplifying cells differentiate into committed basal cells, which then commit to terminal differentiation into secretory luminal cells. This tightly regulated pathway generates a highly organised glandular structure consisting of the luminal layer, the basal layer attached to the basement membrane and the surrounding stroma. Adapted from (Archer et al., 2017).

1.3 Disorders of the prostate

1.3.1 Benign prostatic hyperplasia

There are a number of disorders of the prostate which have all been linked by some means to the development of PCa. BPH involves an androgen-dependent abnormal increase in proliferation of the epithelial and stromal cells within the prostate (Roehrborn, 2008). This disorder primarily occurs in the transitional zone and can result in the obstruction of urine in the urethra which can be somewhat alleviated by transurethral resection of prostate (TURP) (Simpson, 1997). Like PCa, the presence of BPH increases with age, with 88% of autopsies of men over 80 presenting with BPH (Boyle, 1994). There is accumulating evidence that inflammation plays a key role in the development of BPH. The presence of immune cell infiltrates and cytokines in BPH lesions has been observed and this is thought to promote tissue remodelling and further proliferation and enlargement (Kramer et al., 2007, Bostanci et al., 2013, Fibbi et al., 2010).

1.3.2 Prostatic intraepithelial neoplasia

Prostatic intraepithelial neoplasia (PIN) is defined by accumulating abnormalities in the prostatic epithelium with progressive similarities to adenocarcinoma. These include an increase in proliferation in luminal epithelial cells and a decrease in basal cells (Shen and Abate-Shen, 2010). Whilst it does not increase the levels of prostate PSA, the presence of PIN is considered an early stage of carcinogenesis and the majority of patients presenting with PIN develop cancer within 10 years. The incidence of PIN also increases with age, but predominantly occurs in the peripheral zone of the prostate. Tissue with high-grade PIN lesions share both morphological and genetic similarities to PCa (Bostwick et al., 2004).

1.3.3 Prostatitis

Inflammation of the prostate, known as prostatitis, is divided into four categories; acute and chronic bacterial prostatitis, most commonly caused by *E.coli* and *Enterococcus spp*, asymptomatic inflammatory prostatitis and chronic prostatitis, also known as chronic pelvic pain syndrome (CPPS) (Murphy et al., 2009, Cai et al., 2011). It is estimated that 15% of US males will be affected by symptomatic prostatitis in their lifetime (Krieger, 2004). However, the presence of inflammation in prostatic biopsies and TURPs suggest that the prevalence of asymptomatic prostatitis may be much higher and that inflammation may be an important factor in prostate carcinogenesis (De Marzo et al., 2007, Nickel et al., 1999, Nickel et al., 2008).

1.4 Prostate cancer

1.4.1 Epidemiology and risk factors

PCa is the most common cancer of men in the UK, accounting for 26% of all new cancer cases. It is currently the second most common cause of cancer-related death (13%), following lung cancer and it is estimated that 1 in 8 males in the UK will develop the disease in their lifetime (Cancer Research UK, 2016).

Epidemiological and genetic studies have defined clear risk factors. PCa is most highly associated with age, with over a third of new cases found in men ≥75 (Figure 1.3). PCa is also more prevalent in black males than white males, with Asian males possessing significantly lower risk (Quinn and Babb, 2002).

Other PCa risks include familial factors which was first explored by Morganti et al. in 1956, and describes several members of the same family developing the disease due to environmental factors, genes or a combination of the two, accounting for 10-20% of all PCa cases (Morganti et al., 1956, Stanford and Ostrander, 2001). Hereditary PCa is a subset of familial PCa caused by the Mendelian inheritance of rare susceptibility genes (Potter and Partin, 2000). Hereditary PCa is considerably more prevalent in relatively younger diagnosed patients, accounting for 43% of cases diagnosed below the age of 55. There are now over 70 susceptibility loci that confer an increased risk for PCa, identified through genome wide association studies (Eeles et al., 2013). An example of susceptibility genes that are of current interest are BRCA1 and BRCA2, gene mutations of which are most widely associated with a predisposition for breast cancer. BRCA2 mutations have now been confirmed as a risk factor for early and aggressive PCa and patients show poorer outcomes following localised PCa treatment than those who do not harbour mutations (Mottet et al., 2017, Castro et al., 2015). Phase II clinical trials have found patients with BRCA2 mutations and other DNA repair defects respond favourably to PARP inhibitors such as olaparib, highlighting the need for stratified therapies (De Felice et al., 2017).

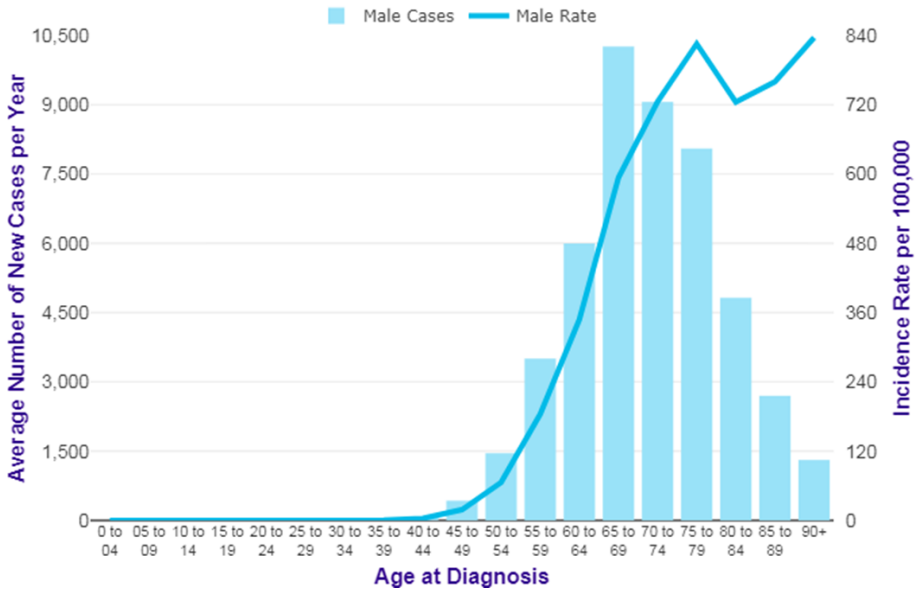

Figure 1.3. Prostate cancer is highly associated with age.

The average number of new cases per year and incidence rate with age from 2013-2015, compiled by Cancer Research UK. https://www.cancerresearchuk.org/health-professional/cancer-statistics/statistics-by-cancer-type/prostate-cancer/incidence#heading-One.

1.4.2 Diagnosis and grading

PSA testing of men over 50 remains the gold standard for the screening of PCa. Normal levels of PSA in the blood is <4ng/ml, however this figure rises naturally with age. Although the introduction of PSA testing led to a dramatic increase in PCa incidence in the late 1980s, this method of detection remains imperfect. PSA levels not only rise in the incidence of PCa but also due to infection, prostatitis and BPH (Obort et al., 2013). Furthermore, although PSA is termed a prostate-specific protein, detectable expression has also been found in other tissues including the breast, lung, ovary and salivary glands (Smith et al., 1995). PSA detection and subsequent PCa diagnosis can often lead to the overtreatment of many patients. Several alternative biomarkers specific to PCa have been investigated, such as PCA3 and TMPRSS2:ERG (Romero Otero et al., 2014, McGrath et al., 2016). However, PSA still remains the most advantageous screening method to date.

Following high level PSA detection, multiple transrectal ultrasound (TRUS) biopsies are usually taken. The Gleason grading system is the most widely used technique for grading prostate carcinomas (Gleason, 1966). H&E stained histological sections of prostate are graded according to the most common patterns of cells observed under the microscope. The system has been updated in recent years to reduce ambiguity between grades for pathologists (Figure 1.4) (Epstein, 2010). Patterns are graded 1-5 by their degree of differentiation and visual abnormalities compared to normal prostate tissue, with 1 representing normal glandular structures and 5 representing abnormal sheets of undifferentiated tissue. The sum of the most common (primary) and second most common (secondary) patterns produces the total Gleason score. A new classification system divides patients into the grade groups defined in Figure 1.4 (Epstein et al., 2016). The Gleason system has been a powerful tool in predicting prognosis and aiding the decision of treatment options. Furthermore, the upgraded classification has resulted in a reduction in overtreatment of Gleason 6 cancers (as more aggressive patterns are now associated with a Gleason score of 7) and distinguishes the prognostic differences in Gleason scores 3 + 4 and 4 + 3 (Epstein et al., 2016). However, its limitations include the absence of consideration of the heterogeneity of PCa, as several different Gleason patterns have been found in single prostate tumours (Humphrey, 2004). Discovery of a PCa-specific biomarker capable of determining progression and aggressiveness would aid to avoid overtreatment and allow for a more appropriate treatment regime for individual patients.

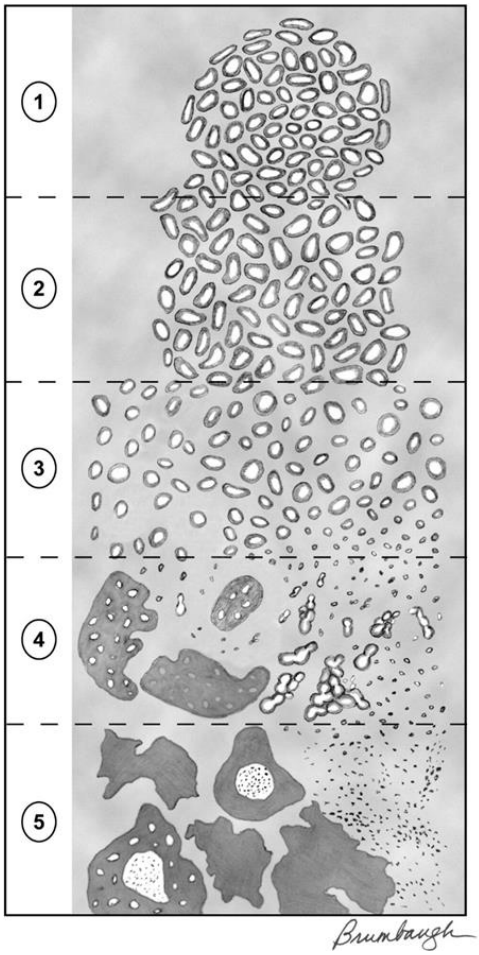

Grade Group	Gleason Score
1	≤6
2	3 + 4 = 7
3	4 + 3 = 7
4	8
5	9 - 10

Figure 1.4. Gleason grading system of prostate adenocarcinoma.

Updated Gleason grading system of prostate adenocarcinomas. Histological patterns are scored 1 to 5 according to degree of disorder. Reprinted from (Epstein, 2010), with Copyright permission from Elsevier.

1.4.3 Treatment of localised prostate cancer

A patient with low Gleason grade, localised PCa has the option to either receive treatment or undergo active surveillance (Kollmeier and Zelefsky, 2012). Both tumour grade and patient preference will impact this decision.

As some low Gleason grade adenocarcinomas will never progress, overtreatment of these men is an ongoing problem. A case for active surveillance as an alternative option is growing, whereby the patient receives routine PSA level checks and biopsies. The inability to determine which patients will undergo disease progression is a cause for reservation. However, the quality of life of the patient following treatment must also be taken into consideration (Bul et al., 2013, Klotz, 2006, Xia et al., 2012, Bellardita et al., 2014).

If immediate treatment is favoured, options include surgical removal of the prostate, known as radical prostatectomy (RP), radiotherapy or focal treatment. The most common treatment is RP, which risks undesirable side effects, most notably incontinence and impotence.

Radiotherapy is an option for local and locally advanced PCa in conjunction with hormone therapy, and can be delivered by external beam radiation therapy (EBRT) or directed brachytherapy. EBRT includes three-dimensional conformal radiation therapy (3D-CRT) and image-guided intensity-modulated radiation therapy (IMRT) (Heidenreich et al., 2014a). IMRT is presently favoured due to the capacity for higher doses of radiation without increasing off-target toxicity (Bauman et al., 2012). Brachytherapy involves direct radiation of the prostate by either a temporary high dose implant or permanent low dose radioactive seeds. An advantage to brachytherapy is the limited radiation to the surrounding tissues, whereas EBRT risks rectal toxicity (Crook, 2011). However, many authors have demonstrated that a high dose of radiation is required for a better outcome in patients (Zelefsky et al., 2001, Kupelian et al., 2005). A ten year follow-up study monitoring patients undergoing active surveillance, RP or EBRT found there was no significant difference in PCa-related deaths (Hamdy et al., 2016). However, RP and ERBT were associated with lower risk of disease progression and metastases compared to active surveillance.

At present there are various focal therapies for PCa available which aim to target a tumour directly and limit damage to the surrounding tissue in order to avoid the undesirable side effects of the alternative therapies already discussed. Given PCa is often a multifocal disease, focal therapy is generally selected for patients considered low-risk of progression, where the tumour is restricted to one lobe and unifocal (Eggener et al., 2010). High-intensity focused ultrasound (HIFU) utilises targeted thermal damage with magnetic resonance imaging (MRI) as guidance (Napoli et al., 2013). It is delivered transrectally and so avoids invasive surgery. As HIFU is a relatively new therapy, there is a lack of studies with long term follow up. However, the current cancer-free survival rates and low rates of serious side effects are promising (Cordeiro et al., 2012, Ramsay et al., 2015). Extreme low temperature and thawing cycles characterise cryotherapy which can be used to treat localised PCa or as salvage therapy following relapse (de la Taille et al., 2000). A transperineal argon gas or liquid nitrogen probe is used, guided by TRUS (Nomura and Mimata, 2012). Cryoablation is a relatively invasive treatment and also requires warming of the surrounding tissues to avoid damage (Cohen

and Miller, 1994). Photodynamic therapy (PDT) involves intravenous injection of photo-sensitive drugs which specifically act in the prostate by administration of light. This therapy induces necrosis of tumour material and largely avoids damaging other tissues (Koudinova et al., 2003). However, since the drug is administered intravenously, patients must avoid direct sunlight for a period of time depending on the half-life of the drug used (Moore et al., 2009). Results from a recent clinical trial show that after 3.5 years follow up, 75% of patients maintained complete tumour ablation in the treated lobe (Noweski et al., 2018).

1.4.4 Metastasis and epithelial-to-mesenchymal transition

Metastasis is the cause of over 90% of deaths from solid tumours (Valastyan and Weinberg, 2011, Gupta and Massague, 2006). Despite local therapy, up to 40% of men will develop metastatic PCa, most commonly to the bone (Beltran et al., 2011). Activation of invasion and metastasis is one of the hallmarks of cancer described by Hanahan and Weinberg, where transformed cells progress through a coordinated series of steps, coined the invasion-metastasis cascade, summarised in Figure 1.5 (Hanahan and Weinberg, 2000, Hanahan and Weinberg, 2011).

Following formation of a primary tumour, cells undergo a number of changes to facilitate local invasion of the BM and surrounding stroma. Epithelial-to-mesenchymal transition (EMT) is a process which occurs during normal organ development and wound healing (Thiery et al., 2009). EMT has also become recognised as a major mechanism by which transformed epithelial cells acquire the ability to invade surrounding tissue and disseminate to form distant metastases. It is a molecular switch from an epithelial cell phenotype to a mesenchymal cell phenotype, culminating in the loss of cell polarity and tight junctions between cells. The most well characterised alteration is the loss of epithelial cell marker E-cadherin and induced expression of mesenchymal cell marker N-cadherin, which results in the loss of cell-to-cell contacts and promotes a migratory mesenchymal cell phenotype (Valastyan and Weinberg, 2011). This switch in gene expression is controlled by several master transcription factors of EMT including Snail, Slug, ZEB1/2 and Twist (Thiery et al., 2009). EMT transcription factors are capable of promoting a cell phenotype which facilitates almost the entirety of the invasion-metastasis cascade. Mesenchymal-to-epithelial transition (MET), the reversal of EMT, may occur at distant tumour sites to permit establishment of invading tumour cells (Polyak and Weinberg, 2009).

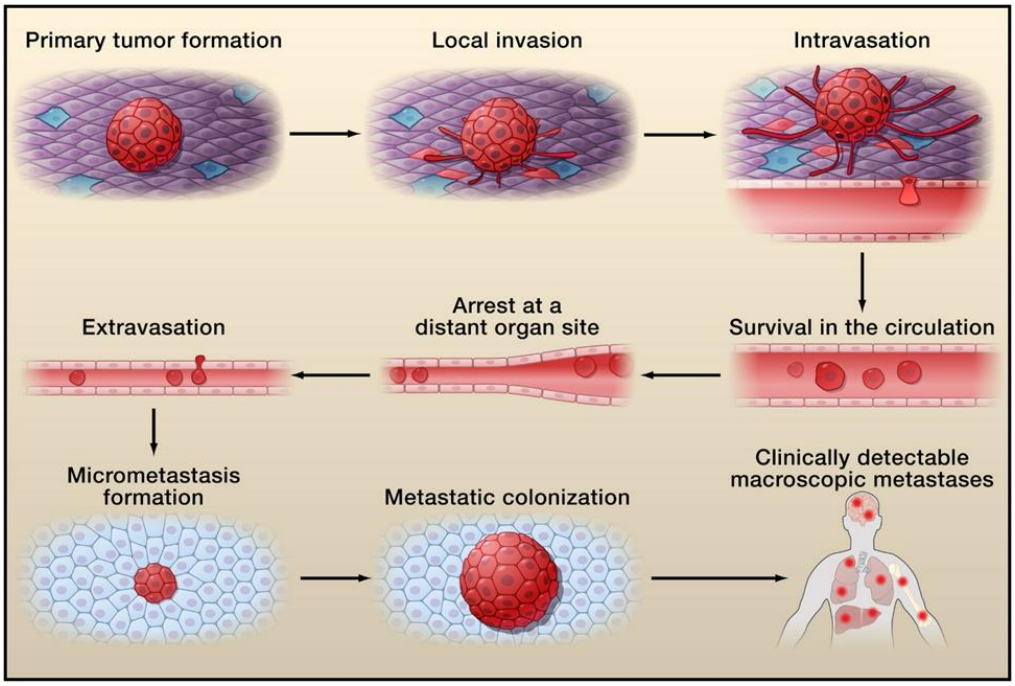

Figure 1.5. The invasion-metastasis cascade.

Schematic detailing the stages of the invasion-metastasis cascade. A metastatic cell must invade the local tissue and enter the circulation via intravasation. Should the cell survive transit, it must then invade the distant tissue site and adapt in order to survive and form metastatic lesions in the new foreign microenvironment. Reprinted from (Valastyan and Weinberg, 2011), with Copyright permission from Elsevier.

Whilst bone is the most prominent site of PCa metastases, occurring in 90% of patients with advanced PCa, they are also commonly known to occur in the lymph nodes, lungs and liver (Bubendorf et al., 2000, Kelly and Yin, 2008). This tropism for bone is thought to be regulated by chemokines. Chemokines are a class of chemotactic cytokine which are important for immune cell development and recruitment of immune cells to sites of inflammation. The chemokine CXCL12 is highly expressed at sites of PCa metastases, including bone (Mognetti et al., 2013). Its receptor, CXCR4, has been shown to be expressed in PCa cell lines as well as increased expression in tissue sections derived from primary prostate tumours and mestastases compared to normal prostate (Sun et al., 2003, Akashi et al., 2008, Chetram et al., 2011).

The surrounding stroma, both locally in the prostate and at sites of metastases, provide factors such as cytokines and growth factors, which interact with tumour cells and cooperatively facilitate invasion into the circulation from the primary tumour and also survival at the new tumour site (Josson et al., 2010, Morrissey and Vessella, 2007). The tumour-associated stroma (known as "reactive stroma") demonstrates changes in composition which can be distinguished from normal stroma, such as a switch from largely smooth muscle cell content in normal prostate stroma to a more myofibroblast and fibroblast cell content in reactive stroma (Tuxhorn et al., 2002). This process is thought to be regulated in part by TGF-β and Wnt signalling, which are also known regulators of EMT (Barron and Rowley, 2012).

1.4.5 Treatment of metastatic prostate cancer

High-grade and metastatic PCa is generally treated with pharmacological drugs which aim to deprive the tumour of androgens which are essential for growth, known collectively as androgen-deprivation therapy (ADT). The standard categories of ADT are as follows:

1) **Anti-androgen therapy**: prevents activation of target genes by interacting with the AR, e.g. bicalutamide (Iversen et al., 2000).
2) **Oestrogen treatment**: prevents testosterone production by inhibiting 5-α reductase, e.g. diethylstilbestrol (McLeod, 2003).
3) **Gonadotrophin-releasing hormone (GnRH) agonist**: inhibits androgen production by desensitising hormone feedback systems in the pituitary, initially used in conjunction with anti-androgens to prevent tumour flare, e.g. goserelin (Peeling, 1989).
4) **GnRH antagonist**: binds to GnRH receptor and inhibits testosterone production, e.g. degarelix (Shore, 2013).

Many different agents have been trialled with different mechanisms of action. Oestrogen therapy via diethylstilbestrol (DES) was the first hormonal therapy used for PCa in the 1960s. However, the overall mortality rate among patients treated with DES was higher due to increased cardiovascular disease, highlighting the need for alternative treatments (McLeod, 2003). GnRH agonists, such as goserelin, are used at present, which avoid the need for surgical castration (Peeling, 1989, Heidenreich et al., 2014b, Seidenfeld et al., 2000). The use of nonsteroidal anti-androgen therapy such as bicalutamide for locally advanced PCa does not have significant survival benefits over castration but does provide the patient with a better quality

of life (Tyrrell et al., 1998, Iversen et al., 2000, Iversen, 2003). Other agents include GnRH antagonists, which have been shown to decrease testosterone and PSA levels at a much faster rate than GnRH agonists (Klotz et al., 2008, Trachtenberg et al., 2002).

1.4.6 The androgen receptor and the emergence of castration-resistant prostate cancer

Androgens are necessary factors for pre- and post-natal development and growth of the prostate (Kellokumpu-Lehtinen et al., 1979, Aumuller, 1991). The AR is a member of the nuclear receptor superfamily and is a vital transcriptional regulator for both the normal prostate and PCa. The AR is expressed by luminal epithelial cells, which comprise the bulk of a prostate tumour and are therefore the main target of ADT.

In its unactivated form, the AR exists in the cytoplasm in complex with several proteins from the heat shock protein family. Upon ligand binding, most commonly to dihydrotestosterone (DHT), the AR undergoes a conformational change which triggers nuclear translocation. Here, the AR binds to the promoter/enhancer regions of genes which contain androgen response elements (ARE) such as PSA and PAP. AR-mediated transcription can be positively and negatively regulated in several ways. This includes interaction with co-regulators which modulate histones and either promote/prevent AR binding, and also by interaction with other transcription factors (Heinlein and Chang, 2004).

Patients with high grade PCa undergoing androgen-ablation treatment may show promising tumour regression and lowering of PSA initially. However, they eventually become hormone resistant and the cancer recurs, known as castration-resistant prostate cancer (CRPC). Several androgen-related mechanisms of resistance have been investigated including:

1) **AR mutations**: mutations can result in a receptor that is more sensitive to small amounts of hormone and increase sensitivity to other steroid hormones and molecules (Taplin et al., 1999).
2) **AR variants**: several AR splice variants have been identified in CRPC patients. Variants lacking a ligand-binding domain result in constitutive activation of the AR (Watson et al., 2010).
3) **AR amplification**: multiple copies of the AR gene resulting in an increase of AR protein (Linja et al., 2001).

An alternative hypothesis for the emergence of CRPC suggests that androgen-independent, and therefore ADT-resistant, cell populations of the prostate epithelium can survive treatment and subsequently reconstitute the tumour with other androgen-independent cells (Shen and Abate-Shen, 2010).

1.4.7 Treatment of CRPC

Therapy for CRPC includes treatment with cytotoxic chemotherapy agents such as docetaxel or cabazitaxel, which target rapidly dividing cells. Unfortunately, not all PCa patients respond to chemotherapeutic agents and others often become resistant, as the survival benefit with current agents is between a few months to 2 years (Seruga and Tannock, 2011, Bahl et al., 2013, Pezaro et al., 2014). Several novel therapies have now

been developed which are not curative but aim to prolong progression-free survival and improve quality of life, these include:

1) **Abiraterone acetate**: second-line anti-androgen that inhibits CYP17A, an enzyme involved in androgen synthesis (de Bono et al., 2011).
2) **Enzalutamide**: second-line anti-androgen that inhibits AR signalling by powerful blockade of the AR (Scher et al., 2012).
3) **Sipuleucel-T**: a personalised immunotherapy whereby the patients antigen-presenting cells are externally activated by granulocyte-macrophage colony stimulating factor (GM-CSF) which is fused to PAP as the antigen. The vaccine is then infused into the patient to stimulate an immune response against PAP-expressing cells (Kantoff et al., 2010, Anassi and Ndefo, 2011).
4) **Radium-223 dichloride**: an α-emitting radionuclide with a tropism for bone metastases (Deshayes et al., 2017).

The median life expectancy of a patient with CRPC is 2 years despite the development of these next generation therapies, which only increase life expectancy by a matter of months relative to a placebo (de Bono et al., 2011, Kantoff et al., 2010, Scher et al., 2012). Ongoing clinical trials aim to determine the best time at which to introduce these drugs during disease progression and the combinations which yield the greatest effects possible (James et al., 2016, James et al., 2017, Attard et al., 2018). Although the principal focus of drug design has been on androgen depletion, the use of these drugs has in fact now been linked to an increased risk of developing advanced PCa by the U.S. Food and Drug Administration (FDA) (Thompson et al., 2003, Andriole et al., 2010, FDA, 2011). Resistance suggests that AR-positive cells are not the only important cell type within the tumour. These current PCa drugs have been designed to target androgen-responsive luminal cells which comprise the bulk of a tumour, whilst overlooking the AR-negative basal cell populations which includes a stem-like population.

1.5 Cancer stem cells

The cancer stem cell (CSC) hypothesis proposes that only a subpopulation of cells within a tumour is able to initiate, propagate and maintain tumour growth (Greaves, 2010). In addition to self-renewal and multipotency, CSCs also have dysregulated proliferation and differentiation. Thus, a CSC can maintain itself, whilst also differentiating into the distinct heterogeneous cell types that constitute the bulk of a tumour (Figure 1.6). These bulk tumour populations are considered non-tumourigenic, although it should be noted that CSC properties may not only be originally acquired by normal tissue SCs but also by a more differentiated cell type within the hierarchy. The original cell type which is targeted for genetic mutation and transformation, whether or not it is a SC, is known as the cell of origin. Since CSCs are the only cells capable of driving tumour growth, these cells therefore require targeting to achieve long term cancer therapy. However, consistent with normal tissue SCs, CSCs possess inherent resistance mechanisms which allow them to evade standard cancer treatments including chemotherapy and radiation (Alison et al., 2012, Morrison et al., 2011, Ishii et al., 2008).

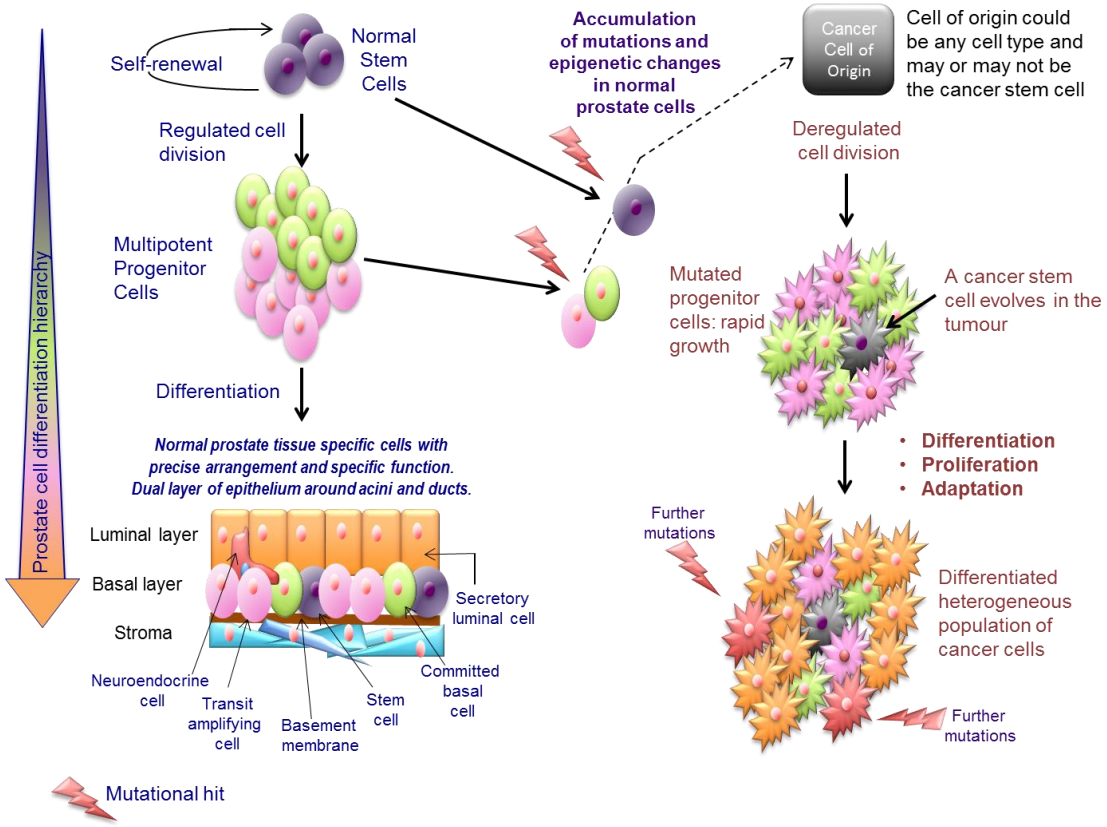

Figure 1.6. The cancer stem cell hypothesis and progression of prostate cancer.

This model shows the progression from a normal prostate differentiation hierarchy to the deregulated growth of a prostate tumour. Although it is more likely for the cancer stem cell to arise from a normal stem cell, due to its longevity and self-renewal properties, this model does not exclude the possibility that a progenitor cell could become the cancer stem cell following a series of mutations. This cancer stem cell is then able to maintain tumour growth and differentiate into the different cell types that compose the tumour. In addition, it is possible for other mutations to occur within bulk tumour cells altering their behaviour and contributing to a more aggressive cancer phenotype. Taken from (Archer et al., 2017).

Multiple studies, going back over a hundred years implied the existence of CSCs (Maitland and Collins, 2014). The first "modern age" evidence presenting CSCs as the cause and maintenance of cancer was elegantly demonstrated in acute myeloid leukaemia (AML) by John Dick's laboratory in 1994 (Lapidot et al., 1994). Since then our understanding of CSCs has been refined and their identification in multiple other leukaemias and solid tumours has supported the CSC hypothesis of cancer (Visvader and Lindeman, 2008). However, accumulating evidence for the CSC hypothesis has posed significant challenges, including the identification of markers that can accurately distinguish CSCs and expedite isolation of these relatively rare cells from a complex tumour environment. The two functional caveats for identifying CSCs are that they must 1) be tumourigenic, forming heterogeneous tumours reminiscent of those from which they were derived and 2) be serially transplantable when xenografted in mice. An array of markers, including CD133, CD44, CD24 and ALDH1, have been used to isolate CSCs from different solid tumours. Moreover, as there is no single CSC marker for each tumour type, multiple markers are generally used to isolate as homogeneous a population as possible. These markers usually include normal SC markers of the same tissue (Park et al., 2007). Whilst it has previously been hypothesised that CSCs constitute a rare population of tumour cells, studies in melanoma have shown that the current models could be significantly underestimating the size of the CSC population. In NOD/SCID mice the proportion of cells with tumourigenic capacity was 0.1-0.0001%, which rose to 25% in more immunocompromised NOD/SCID/IL2Rγ^{null} mice (Quintana et al., 2008). However, the original hypothesis seems true in tumours of other tissues such as human pancreatic adenocarcinoma, lung squamous cell carcinoma, lung adenocarcinoma, and head and neck squamous cell carcinoma (HNSCC). In these tumours, the CSC population only accounted for 0.0028-0.04% of total tumour cells in NOD/SCID/IL2Rγ^{null} mice (Ishizawa et al., 2010). The proportion of tumour cells with a CSC phenotype is therefore likely to be a quality that is dependent on tissue of origin and cancer subtype within that tissue, and in some cases tumour grade may also be important (Marcato et al., 2011, Thirant et al., 2011). Although serial transplantation in mice is considered to be the gold standard as the means of identifying CSCs, this data also highlights the host's immune response and differences in vital growth factors as limiting factors in studying CSCs in model systems.

1.5.1 A basal cell is the cell of origin of prostate cancer

Substantial evidence exists for a basal SC origin of PCa. By introducing ERG expression and constitutive PI3K signalling into the basal and luminal epithelial cells of mice, Lawson et al. demonstrated that whilst luminal cells were unresponsive, the basal population was able to form fully differentiated tumours reminiscent to those seen in humans (Lawson et al., 2010). Significantly, evidence from human prostate cells also indicates a basal SC origin of PCa. The CD44^{+}/CD133^{+}/$\alpha_2\beta_1^{hi}$ markers in basal cells identify normal prostate SCs (Collins et al., 2001, Richardson et al., 2004). These cells showed self-renewal and differentiation properties, were highly proliferative and reconstituted prostate glands *in vivo* (Richardson et al., 2004). To isolate primary prostate CSCs which constitute approximately 0.1% of tumour cells from PCa biopsies the same markers were used; cells were first selected for high $\alpha_2\beta_1$ integrin expression by rapid adhesion to collagen I-coated plates and CD133^{+} cells were then enriched from α2β1^{hi} cells (Collins et al.,

2005). These $CD133^+/\alpha_2\beta_1^{hi}$ cells exhibited enhanced proliferative potential and secondary colony-forming efficiency *in vitro* compared to other populations, i.e. they were able to expand and self-renew through several generations as the proportion of $CD133^+$ cells remained constant. As well as possessing the fundamental SC properties, the cells also demonstrated classic cancer cell characteristics of invasion and anchorage-independent growth, confirming that the cells were of tumour origin. Furthermore, $CD133^+/\alpha_2\beta_1^{hi}$ cells were able to differentiate into AR^+ luminal cells, recapitulating the characteristics of a primary prostate tumour (Collins et al., 2005). It should also be noted that these cells are normally studied at as low a passage as possible, minimising any changes that may occur due to long-term culture. Patrawala et al also demonstrated that primary human PCa $CD44^+$ basal cells had increased tumourigenic and proliferative capabilities *in vitro* and *in vivo* than $CD44^-$ cells (Patrawala et al., 2006). Then, similarly to Lawson, Goldstein et al. confirmed that human benign basal cells, but not luminal cells, could produce tumours with a luminal phenotype in NOD/SCID/IL2Rγ^{null} mice following AKT, ERG and AR expression (Goldstein et al., 2010). Furthermore, it was recently shown by high-throughput RNA sequencing that a basal SC phenotype was associated with more aggressive types of PCa (Smith et al., 2015). Various combinations of markers including CD133, CD49f, CD44 and Trop2 are commonly used to detect prostate CSCs (Trerotola et al., 2010, Patrawala et al., 2006, Goldstein et al., 2010).

In contrast, Wang et al identified castration-resistant Nkx3.1-expressing cells (CARNs) which were defined as a subset of luminal cells in the mouse prostate (Wang et al., 2009). These cells comprised 1% of cells in the total prostate and were able to survive following androgen deprivation. CARN cells were proposed to be the origin of PCa, due to the presence of high grade PIN and carcinoma lesions following PTEN deletion and their ability to form organoids in culture (Wang et al., 2009, Chua et al., 2014). Similarly, luminal progenitors have also been found in other mouse models of PCa (Korsten et al., 2009, Liu et al., 2011, Agarwal et al., 2015). However, the normal mouse and human prostates display significant differences. For instance, the murine prostate consists of a single layer of epithelia where luminal cells contact the basement membrane directly, and has a lower basal cell content compared to human. It is therefore possible that the development of PCa differs between the two species and this CARN progenitor could be a unique cell found in mice. However, a putative luminal CSC was found in the BM18 xenograft model derived from a human PCa bone metastasis (Germann et al., 2012). A quiescent population of cells co-expressing stem-like (NANOG or ALDH1A1) and luminal (NKx3.1 and CK18) markers was able to reconstitute a tumour in the presence of androgen following previous castration. However, these specific cells were not selected and serially transplanted into different mice, so it remains unclear whether the cells truly have tumour-initiating properties. It should also be noted that this xenograft model only represents one patient and it is well known that PCa is a very heterogeneous disease. Furthermore, the xenograft had been passaged many times since it was established in 2005 and is likely to have evolved significant changes since then (McCulloch et al., 2005). Critically, a luminal CSC has yet to be isolated from a primary human prostate tumour (Collins et al., 2005).

1.6 Cancer stem cells and treatment resistance in prostate cancer

The CSC hypothesis also logically explains the development of metastases. Complex sequencing studies have shown that the cancer cell clones present in a primary prostate tumour are also present in metastases (Hong et al., 2015, Haffner et al., 2013). Theoretically, in order to maintain the founder mutations present in the original tumour through to metastasis, this must be carried out by a primitive, long-lived cell that is capable of both clonal expansion and the ability to accumulate further abnormalities that allow the cell to develop independence from the extracellular matrix and migrate to extraprostatic sites (Gundem et al., 2015). Prostate CSCs possess enhanced invasive qualities in comparison to other tumour cell populations (Smith et al., 2015, Klarmann et al., 2009). Successfully targeting the CSC population alongside cytotoxic hormone therapies to kill the rapidly dividing tumour bulk may be curative, and should prevent the initiation of lethal secondary metastases (Figure 1.7). However, heterogeneity within the CSC population itself makes drug design for the rare CSC population even more challenging (Guenechea et al., 2001, Greaves, 2010). Furthermore, CSCs are thought to be the cause of cancer recurrence following radiation and chemotherapy, and the emergence of CRPC following ADT (Frame and Maitland, 2011, Rane et al., 2012). This seems logical, given that a characteristic of normal SCs is their robustness and inherent resistance to toxic substances. The quiescent nature of SCs poses a further challenge, since most cancer therapies target actively dividing cells. So, whilst conventional cancer therapies reduce the bulk population of tumour cells, these treatments consequently have the potential to enrich for CSCs (Dylla et al., 2008, Freitas et al., 2014, Li et al., 2008).

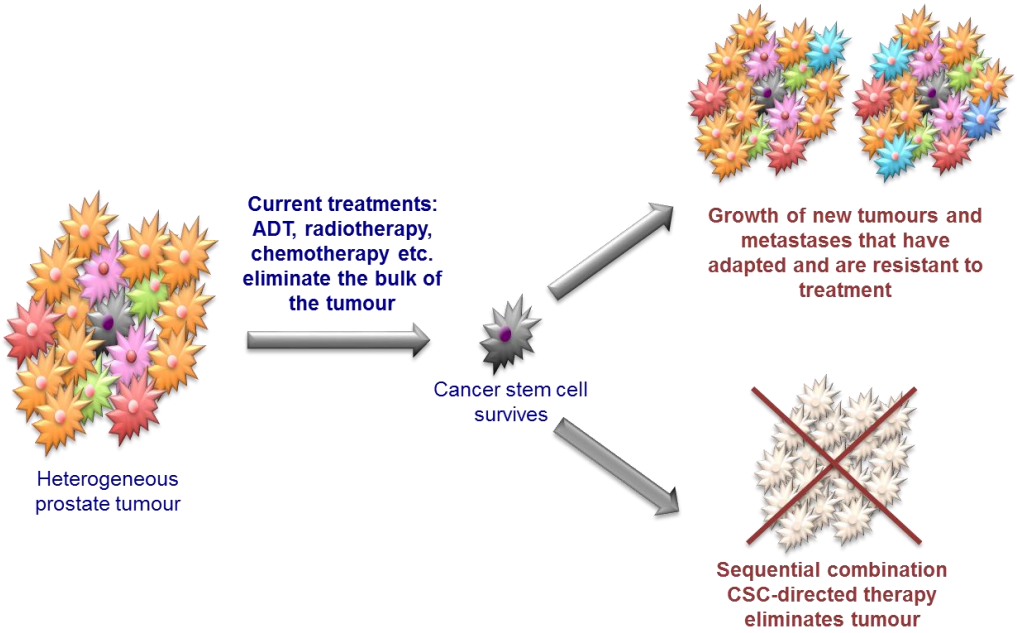

Figure 1.7. Prostate cancer cell response and resistance to treatment.

Whilst current PCa therapies can effectively eradicate the differentiated luminal cells which compose the bulk of the tumour, cancer stem cells can survive via extensive therapy resistance mechanisms. The CSCs are then able to initiate the growth of new tumours and metastases and may themselves have evolved to thrive in the post-treatment microenvironment. The discovery of novel CSC-directed therapies may be curative and eliminate all tumour cells in conjunction with conventional therapies. Taken from (Archer et al., 2017).

1.6.1 Drug efflux transporters and anti-apoptotic molecules

Normal SCs and CSCs express drug efflux transporters of the ABC transporter superfamily that can efficiently pump chemotherapeutic drugs out of the cells (Moitra et al., 2011). ABCG2 has been shown to be expressed in prostate CSCs and is more highly expressed in prostate tumours which have recurred following treatment compared to non-recurrent tumours, suggesting that the transporter does indeed play a part in drug resistance in PCa (Pascal et al., 2007, Guzel et al., 2014). There have been numerous clinical trials for ABC inhibitors, but outcomes have been poor due to high toxicity and low efficacy (Fletcher et al., 2010). Many CSCs also express anti-apoptotic molecules, essentially allowing them to bypass signals which would ordinarily lead to cell death. This includes members of the Bcl2 family (Madjd et al., 2009, Konopleva et al., 2002) and inhibitor of apoptosis (IAP) family (Liu et al., 2006). Affymetrix gene-expression arrays comparing the gene expression of human primary prostate CSCs and committed basal cells fractionated from benign and cancerous prostate tissue showed that SCs and CSCs also have significantly higher expression of IAP family members survivin and BIRC6 (Birnie et al., 2008).

1.6.2 DNA damage response

Enhanced DNA damage response is another characteristic of CSCs, which allows them to survive exposure to radiation and chemotherapy. Under normal circumstances, when DNA damage is irreversible, cell death pathways are activated, resulting in the upregulation of pro-apoptotic molecules. However, given the DNA damage repair mechanisms and upregulation of cell cycle checkpoint molecules in CSCs, they are able to survive such genotoxic stresses (Maugeri-Sacca et al., 2012). In glioma, $CD133^+$ CSCs were more resistant to radiation than the $CD133^-$ tumour cell populations. Inhibitors of checkpoint kinases Chk1 and Chk2 induced radiosensitivity, demonstrating that glioma CSCs have a permissive DNA damage checkpoint in response to radiation (Bao et al., 2006). In cell line models, prostate CSCs also have increased expression of DNA damage repair molecules (Yan and Tang, 2014, Kim et al., 2013). In human prostate tissue the $CD133^+/\alpha_2\beta_1^{hi}$ CSCs exhibited higher levels of heterochromatin, which rendered them more resistant to the lethal double strand breaks induced by radiation. (Frame et al., 2013). Radio-sensitivity could be induced by combination treatment with the histone deacetylase (HDAC) inhibitor Trichostatin A, i.e. CSC therapy resistance in this case is defined at the chromatin level. Radiotherapy produces reactive oxygen species (ROS), causing oxidative stress and subsequently DNA damage in cells. Breast CSCs possess low levels of ROS compared to normal SCs due to increased expression of free radical scavengers and thus survive following radiation (Diehn et al., 2009).

1.6.3 The tumour microenvironment and CSC niche

As well as possessing several mechanisms that confer drug resistance, CSCs may also persist due to signals from the local microenvironment. The normal SC niche is a distinct area within a tissue that supports and provides SCs with the factors they require to maintain stemness (Li and Xie, 2005). A special niche may also exist for CSCs (Sneddon and Werb, 2007). For instance, CSCs are often found in niches in close proximity to vasculature, where VEGF-secreting endothelial cells can promote CSC-induced angiogenesis

and metastasis (Beck et al., 2011, Alvero et al., 2009, Veeravagu et al., 2008). The stroma surrounding solid tumours is altered from its normal state, sometimes referred to as "reactive stroma" in the prostate (Dakhova et al., 2009, Thalmann et al., 2010). The reactive stroma (or cancer-associated fibroblasts, CAFs) isolated from primary prostate tumours was sufficient to induce tumorigenesis in selected basal cells from the benign BPH-1 cell line, resulting in tumour formation in immunocompromised mice (Taylor et al., 2012). Additionally, with help from the reactive stroma, PCa cells are able to continuously adapt to their environment promoting EMT which allows cells to become motile and disseminate. This inevitably results in invasion and metastasis with a particular tropism for bone (Thalmann et al., 2010, Josson et al., 2010, Scheel and Weinberg, 2011, van der Pluijm, 2011). The innate plasticity of CSCs, which allows them to thrive in distant environments from the original tumour also makes them a difficult therapeutic target. Treatments to target the surrounding microenvironment may also be required to treat PCa more effectively (Bracarda et al., 2011).

1.6.4 Other CSC targets

Given the extensive therapy resistance mechanisms of CSCs discussed above, it is therefore likely that both the CSC and clonal evolution models occur in unison in PCa (Greaves and Maley, 2012). Whilst the tumour is probably initiated by a long-lived CSC, following treatment, the selection pressures will dictate which CSCs will mutate and thrive and cause metastases by clonal evolution. This makes the continually adapting CSCs an essential but challenging target. Inhibitors of key developmental pathways such as Wnt, Notch and Hedgehog, all crucial for CSC maintenance, are currently being tested (Morrison et al., 2011, Alison et al., 2012, Takebe et al., 2011). For instance galiellalactone, a STAT3 inhibitor which blocks the binding of activated STAT3 to target gene DNA, decreased the proportion of $ALDH^+$ cells in PCa cell lines, another commonly used CSC marker (Hellsten et al., 2011). Other inhibitors of the STAT3 pathway have also proved successful in human primary PCa cultures and xenograft models (Kroon et al., 2013). Siltuximab (anti-IL-6) and LLL12, a specific inhibitor of activated STAT3, supressed the colony forming ability of prostate CSCs. Following *ex vivo* treatment, LLL12 also prevented tumour initiation of a xenograft derived from a castrate-resistant patient (Kroon et al., 2013).

It should be noted that since these pathways are also crucial in many normal cell types, including SCs, the off-target effects and toxicity must be carefully monitored. Two phase 2 clinical trial targeting CSCs in late stage pancreatic cancer (ALPINE trial) and small cell lung cancer (PINNACLE trial) have so far provided disappointing results (OncoMed Pharmaceuticals, 2016, OncoMed Pharmaceuticals, 2017). The lack of success with tarextumab, a Notch2 and Notch3 receptor inhibitor, to produce a beneficial response in patients is most likely due to the off-target side effects of blocking this critical signalling pathway. However, encouragingly, NF-κB pathway blockade by parthenolide treatment has been shown to decrease the viability of human primary prostate CSCs without affecting the normal SC population, highlighting that selective cell death of prostate CSCs may be possible (Birnie et al., 2008).

1.7 Transcriptional regulation in the prostate

To maintain normal prostate homeostasis, a delicate balance of cell renewal, differentiation and cell death within the prostate epithelium must occur. This equilibrium is dictated by specific gene expression patterns which are in part controlled by transcription factors.

As mentioned previously, androgens and the AR are essential for both prostate development and maintenance of the adult prostate. Specifically, androgens are required for the survival of adult luminal epithelial cells, as demonstrated by involution–regeneration experiments in rats (English et al., 1987). Other important factors include Nkx3.1 and FoxA1, which are also required for normal prostate luminal cell differentiation (Dutta et al., 2016, Gao et al., 2005). In addition, p63 is essential for maintaining the basal progenitor cell populations of the prostate (Signoretti et al., 2005).

There are several key signalling pathways involved in the development and maintenance of the complex differentiation hierarchy of the prostate including Notch, Wnt and Hedgehog signalling (Leong and Gao, 2008, Deng et al., 2016, Simons et al., 2012, Shaw and Bushman, 2007). These vital signalling pathways are also involved in regulating SC survival (Shahi et al., 2011, Bisson and Prowse, 2009, Chang et al., 2011). It should be noted that signals from the surrounding stroma also play an important role in prostate cell differentiation and homeostasis (Hall et al., 2002, Berry et al., 2008).

1.8 ETS transcription factors control of cell differentiation and the stem cell phenotype in prostate cancer

The E26 transformation-specific (ETS) family of transcription factors are critical for the control and regulation of a variety of cellular processes such as haematopoiesis, differentiation, survival, and the immune response (Kastner and Chan, 2008, Russell and Garrett-Sinha, 2010, Kar and Gutierrez-Hartmann, 2013, Scott et al., 1994). Notably, ETS factors are also important in the maintenance of SCs of different tissues (Hock et al., 2004, Chen et al., 2005). Many ETS factors are ubiquitously expressed in several different cell types, whilst some factors are restricted to specific cell lineages and tissues (Oikawa and Yamada, 2003). ETS proteins are exclusively found in metazoans and there are at least 30 human genes, which have been divided into specific subfamilies according to the gene homology of their characteristic ETS domains (Table 1.1). All ETS family members contain the unique 85 amino acid ETS DNA-binding domain (Figure 1.8) which consists of a winged-helix-turn-helix (WHTH) structure and binds to core purine-rich sequences of GGAA/T in DNA target genes. This domain is also involved in protein-protein interactions which regulate DNA binding (Sharrocks, 2001). ETS factors vary widely outside the ETS domain and variations within the ETS domain itself between the transcription factors can affect the proteins that can bind and also how they are regulated, demonstrating the vast potential for regulation within this family.

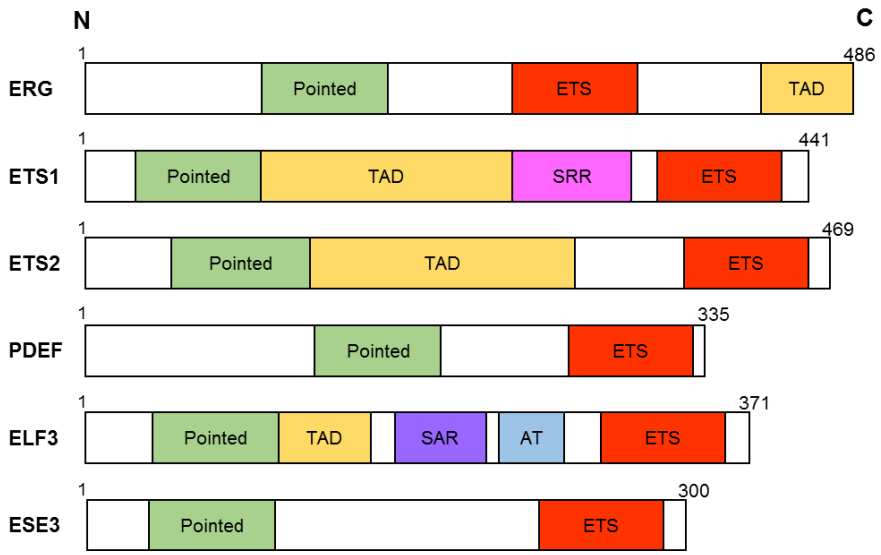

Figure 1.8. Domain structure of ETS factors which have proposed roles in prostate cancer.

The amino acid number and positions of known domains of ETS factors which have been shown to have a role in PCa are displayed above. ETS factors are characterised by a unique 85 amino acid long sequence known as the ETS DNA binding domain (ETS). A subset of ETS factors also possess a pointed domain (Pointed) involved in protein-protein interactions. The transactivation domain (TAD) is essential for activation of transcription factor activity. Other regions important for DNA binding have also been identified such as the serine-rich region (SRR) of ETS1 and the AT hook domain (AT) of ELF3. ELF3 also contains a serine- and aspartic acid-rich domain (SAR) which may play a role in cellular transformation. It should also be noted that some ETS factors such as ERG, ETS1 and ELF3 have been found to possess auto-inhibitory regions flanking the ETS domain. N = N-terminus, C = C-terminus. Taken from (Archer et al., 2017).

ETS Subfamily	Family Members (alternative names)
ERG	ERG, FLI1, FEV
ERF	ERF (PE2), ETV3 (PE1)
ETS	ETS1, ETS2
ELG	GABPα
PDEF	PDEF (SPDEF, PSE)
TEL	ETV6 (TEL), ETV7 (TEL2)
SPI	PU.1 (SPI), SPIB, SPIC
ESE	ELF3 (ESE1, ESX), ESE2 (ELF5), ESE3 (EHF)
ELF	ELF1, ELF2 (NERF), ELF4 (MEF)
TCF	ELK1, ELK4 (SAP1), ELF3 (NET, SAP2)
PEA3	ETV4 (PEA3, E1AF), ETV5 (ERM), ETV1 (ER81), ETV2 (ER71)

Table 1.1. ETS transcription factor subfamilies. Taken from (Archer et al., 2017).

A subset of ETS factors including ETS1, ETS2, ETV6 and ELF3 also possess a pointed (PNT) domain at their N-terminal which is important for protein-protein interactions and can further influence the transcriptional regulation of target genes (Figure 1.8). For instance, the PNT domain of ETS1 acts as a docking site for signalling molecule ERK2 (Seidel and Graves, 2002). Also, the PNT domain of ETV6 allows it to form oligomers which are important for the function of fusion proteins found in many leukaemias (Jousset et al., 1997, Mackereth et al., 2004). Overlapping functions and redundancy in promoter occupancy have been found between ETS proteins, making investigation of native biological interactions challenging (Hollenhorst et al., 2007, Oikawa and Yamada, 2003). Many ETS factors were discovered due to their integral roles in leukaemias and cancers, and a number of ETS family members have since been linked to various different cancers (Zelent et al., 2004, May et al., 1993, Panagopoulos et al., 1994, Golub et al., 1996, de Nigris et al., 2001). In PCa, ERG is the most overexpressed oncogene in patient tumour samples and the TMPRSS2-ERG fusion, which can be formed by translocation or interstitial deletion, is a suspected driver of tumourigenesis and progression (Adamo and Ladomery, 2015, Tomlins et al., 2008, Taylor et al., 2010). Additional key roles for other members of the ETS family in PCa are emerging in the literature (Li et al., 2012, Sementchenko et al., 1998, Turner et al., 2011, Shatnawi et al., 2014, Longoni et al., 2013, Albino et al., 2012).

1.8.1 Aberrant expression of ETS factors

ETS1 is the founding member of the ETS transcription factor family (Laudet et al., 1993). Its expression in cancers other than prostate is generally associated with negative prognosis and is most frequently linked to high grade tumours and metastasis (Takai et al., 2000, Nakayama et al., 2001). Studies of primary prostate tissue have shown that ETS1 expression is also associated with poorly differentiated, high Gleason grade prostate tumours as well as faster progression to castration-resistant disease following ADT (Li et al., 2012, Alipov et al., 2005). A series of studies by Shaikhibrahim and Wernert also identified metastasis-associated genes that were differentially expressed in PC3 cells after ETS1 knockdown. These were then subsequently correlated to primary PCa tissue by gene expression microarray (Shaikhibrahim et al., 2011a, Shaikhibrahim and Wernert, 2012). There is also evidence that ETS1 contributes to the castration-resistant phenotype by directly interacting with the AR and decreasing LNCaP sensitivity to the AR antagonist flutamide following ETS1 overexpression (Smith et al., 2012). Furthermore, ETS1 knockdown in C4-2 cells (a castration-resistant progression model of LNCaP cells) resulted in decreased invasion and anchorage-independent growth. Angiotensin II is an important mediator of angiogenesis and is a potent upregulator of VEGF (Chen et al., 2013). Kosaka et al explored the effects of angiotensin II and angiotensin II type I receptor blockers (ARBs) in PCa cell lines (Kosaka et al., 2010). Interestingly, angiotensin II upregulates ETS1, and is inhibited following treatment with the ARB candesartan. Collectively the evidence shows that ETS1 is strongly associated with PCa metastasis and castration-resistant disease.

Closely related to ETS1, ETS2 expression is also upregulated in PCa. Similar to ETS1, downregulation of ETS2 in Du145 and PC3 cells reduces colony forming ability and cell survival, both characteristics of CSCs, whilst increasing apoptosis (Carbone et al., 2004, Sementchenko et al., 1998). Interestingly, both ETS1 and ETS2 are highly expressed in androgen-insensitive and more invasive PCa cell lines PC3 and Du145, but are expressed at lower levels in androgen-sensitive (luminal) cell lines LNCaP and VCaP, providing further evidence that ETS2 expression is associated with more malignant disease (Sementchenko et al., 1998, Shaikhibrahim et al., 2011b). An early study by Liu et al using a series of PCR primers showed that ETS2 mRNA was expressed in 5 tumour foci derived from frozen tissue sections from one patient (Liu et al., 1997a). On the other hand, ETS1 was only expressed in one of these tumour foci. This suggests that individual ETS factor expression may arise in independent tumour foci and thus display different expression patterns between focuses. These studies highlight that PCa is a heterogeneous disease with intra- and inter-patient heterogeneity. Interestingly, ETS2 can regulate telomerase action. Telomerase is a reverse transcriptase which maintains the elongation of telomeres on chromosomes permitting an extended life span. Telomerase is essential during development and remains active in long-lived cells, namely germ cells and some SCs, whilst it is downregulated in most other cell types. Telomerase is also present in >85% of human cancers (Hiyama and Hiyama, 2002). ETS2 is an activator and repressor of hTERT, the enzymatic component of telomerase, by binding to different ETS binding sites within its promoter (Dwyer and Liu, 2010). This was found in breast cancer cell lines, and ETS2 knockdown resulted in decreased cell survival

(Xu et al., 2008). Since ETS2 is often overexpressed in PCa, its regulation of telomerase and therefore potential of maintaining cell survival, a CSC characteristic, in prostate cells could be of importance.

1.8.2 ETS fusion genes

The TMPRSS2-ERG fusion gene is formed in 50% of PCas between the androgen-regulated promoter of the transmembrane protease TMPRSS2 and the ETS factor (ERG) gene, both encoded on chromosome 21 (Tomlins et al., 2005, Clark et al., 2008). There have been 14 distinct variants of the TMPRSS2-ERG transcript reported in literature, which can result in the translation of either normal full-length ERG, various N-terminal truncations of ERG and one which encodes a TMPRSS2-ERG fusion protein (Clark et al., 2007, Tu et al., 2007, Wang et al., 2006). The most common isoform is that between TMPRSS2 exon 1 and ERG exon 4. Significantly, most of these transcripts retain the ETS DNA binding domain of ERG, together with the PNT domain and C-terminal transactivation domain, ultimately resulting in the overexpression of a functional ERG protein. The incidence of the fusion in precancerous prostate intraepithelial neoplasia (PIN) lesions suggests it could be an early event in PCa development (Carver et al., 2009a). Some fluorescent in situ hybridisation (FISH) and immunohistochemistry (IHC) studies have correlated fusion positive prostate tumours with poor prognosis and disease recurrence (Perner et al., 2006, Rajput et al., 2007, Huang et al., 2014) . Increased copy number of the TMPRSS2 or ERG loci, as well as fusion formation by deletion rather than translocation, has also been linked to poor prognosis (Fine et al., 2010, Mehra et al., 2008, Attard et al., 2008). To add to the complexity, PCa is a heterogeneous, multifocal disease (Arora et al., 2004, Bostwick et al., 1998, Wise et al., 2002). Reverse transcriptase (RT) PCR and FISH studies of prostate tumours have revealed that multiple independent TMPRSS2-ERG rearrangements can occur in a single patient in separate tumour foci (Cooper et al., 2015, Mehra et al., 2007, Clark et al., 2007, Clark et al., 2008).

The TMPRSS2-ERG fusion results in overexpression of ERG oncoprotein. Whilst ERG is not expressed in the normal prostate, it is consistently overexpressed in a large subset of prostate tumours, corresponding to the frequency of fusion positive patients (Tomlins et al., 2008). ERG overexpression has been proposed to be an inducer of epithelial-to-mesenchymal transition (EMT), increased migration and invasion, and subsequently metastasis through the upregulation of associated target genes (Leshem et al., 2011, Gupta et al., 2010, Carver et al., 2009b). ERG target genes include activation of FZD4, MMP1, VEGFR2 and repression of E-cadherin, all of which directly promote EMT and invasion (Adamo and Ladomery, 2015). Additionally, ERG stimulates the expression of the chemokine receptor CXCR4. Its ligand, CXCL12, is highly expressed in bone marrow, resulting in the chemoattraction of PCa cells to bone, the most common site of metastasis (Singareddy et al., 2013, Cai et al., 2010, Carver et al., 2009b). Two ChIP-seq studies in PCa cell lines showed that ERG disrupts the expression of androgen-regulated genes such as PSA in cooperation with epigenetic-modifying enzymes HDAC1 and EZH2 (Yu et al., 2010, Chng et al., 2012). ERG overexpression also promotes c-myc expression, as well as downregulating prostate-specific differentiation associated genes (Sun et al., 2008). This disruption of androgen-regulation retains cells in a de-differentiated progenitor state that is thought to promote invasion and metastasis (Figure 1.9).

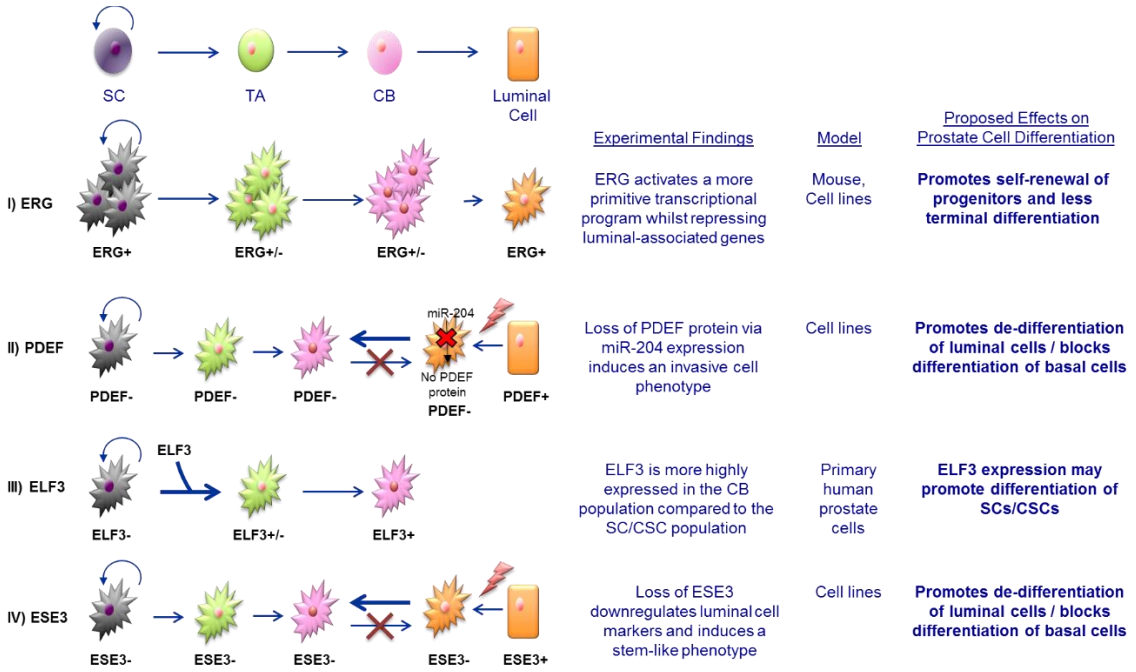

Figure 1.9. Proposed mechanisms of ETS factor-induced de-differentiation of prostate cancer epithelial cells.

The majority of the discussed ETS factors may play a role in prostate cell differentiation. It appears that in PCa these factors are regulated in a manner which disrupts the normal differentiation pathway and allows cells to remain in a progenitor state which allows them to possess stem-like qualities promoting cancer growth and spread. I) ERG is overexpressed in PCa patients who possess the TMPRSS2-ERG fusion gene. ERG has been shown to both activate genes which initiate EMT and repress luminal-associated genes, characteristics associated with cancer stem cells. II) PDEF expression may be lost in terminally differentiated luminal cells due to miR-204 expression in cancer cells. PDEF loss results in an invasive cell phenotype associated with less differentiated cells. III) Microarray data shows ELF3 is more highly expressed in differentiated committed basal cells compared to SCs from both benign and cancerous primary prostate tissue. This suggests ELF3 expression may promote prostate SC differentiation (work in this thesis). IV) Knockdown of ESE3 results in the upregulation of EMT markers and downregulation of luminal cell marker Nkx3.1. Together with characteristic SC functions such as colony forming ability, this suggests that ESE3 loss may promote a SC phenotype. (SC = stem cell, TA = transit amplifying cell, CB = committed basal cell). Taken from (Archer et al., 2017).

Initial mouse models to investigate the effects of TMPRSS2-ERG utilised ERG cDNA driven by the prostate-specific modified probasin promoter. Although some studies observed the development of PIN lesions following ERG overexpression (Klezovitch et al., 2008, Tomlins et al., 2008), others required concomitant PTEN deletion to observe a disease phenotype (King et al., 2009, Carver et al., 2009b), probably due to the different genetic backgrounds of the mice used. Since the TMPRSS2-ERG fusion is suspected to be an early event in PCa initiation and evidence from mouse models suggests that other mutation events such as PTEN loss are also required for cancer progression, it is reasonable to hypothesise that these initial events are likely to occur in long-lived, self-renewing cells where mutations can accumulate. Casey et al produced a bacterial artificial chromosome (BAC) by recombination to express the ERG gene under the control of the TMPRSS2 promoter (Casey et al., 2012). Once again PIN lesions and progression to carcinoma were only evident in mice with an additional heterozygous PTEN deletion. They observed a more genuine, cell specific expression pattern of TMPRSS2-ERG which revealed expression in not only the $EpCAM^{+}/Sca\text{-}1^{-}/NKx3.1^{+}$ luminal cells but also in a fraction of the $EpCAM^{+}/Sca\text{-}1^{+}/p63^{+}$ basal/progenitor cell population. The $Sca\text{-}1^{+}$ (stem cell antigen-1) basal cells from TMPRSS2-ERG mice possessed greater sphere-forming and colony-forming ability than their counterparts from wild-type mice, illustrating that TMPRSS2-ERG positive stem-like cells have increased self-renewal capabilities.

The study by Casey et al. highlighted the importance of investigating critical genetic aberrations in the individual cell populations of the prostate as opposed to total epithelial cells, which may mask any variations found in the rarer basal epithelial cell populations, including SCs (Casey et al., 2012). Polson et al examined this further by growing epithelial cells from human prostate biopsies in culture and fractionating the cell populations into SC, TA and CB populations based on CD133 and $\alpha_2\beta_1$ expression as discussed previously (Polson et al., 2013, Collins et al., 2005). Using FISH, RT-PCR and southern blotting the status and expression of TMPRSS2-ERG in the SC fraction from primary patient samples was demonstrated. They also showed that prostate basal epithelial cells, particularly SCs, do not express AR or the oestrogen receptor (ER), and therefore demonstrated that TMPRSS2-ERG must be regulated in these cells in an androgen-independent manner (Maitland et al., 2011, Polson et al., 2013). There was also heterogeneity in the expression patterns of TMPRSS2-ERG. For instance, in one patient TMPRSS2-ERG was expressed in both the SC and TA populations and lost in the CB population. Most commonly, whilst TMPRSS2-ERG was expressed in the SC population, in several patients fusion expression was lost in TA cells and regained in CB cells. This can be explained by a phenomenon called monoallelic expression, whereby one inherited allele of a gene is preferentially expressed and the other is silenced (Chess, 2012). In cases of genetic abnormality where one allele is normal and the other mutated, such as TMRPSS2-ERG, the mechanism of monoallelic expression becomes significant. Silencing of a mutated allele may prevent the early removal of a potential cancer-initiating clone thereby allowing a higher chance of accumulating additional necessary mutations required for cancer progression.

TMPRSS2 fusions can also occur with other ETS factors, albeit at much reduced frequencies. Along with ERG, TMPRSS2 fusions to ETV1 and ETV4 were also discovered by Tomlins et al. in PCa cell lines and

primary tissue (Tomlins et al., 2005, Tomlins et al., 2006). The presence of the fusions again coincides with the overexpression of the corresponding ETS factor and each appears to be mutually exclusive in most cases (Svensson et al., 2011). Unlike ERG, ETV1 and ETV4 are located on different chromosomes from TMPRSS2 and fusions are therefore formed solely by translocation rather than interstitial deletion. This may be relevant when deducing the prognostic significance of different fusions, given that TMPRSS2-ERG fusions formed by deletion are associated with poor prognosis (Mehra et al., 2008). The propensity of ETS factors to form tumourigenic fusions has also led to the discovery of several other non-TMPRSS2 ETS factor fusions in PCa (Barros-Silva et al., 2013, Helgeson et al., 2008, Tomlins et al., 2007). The incidence of several mutually exclusive ETS factor fusions in PCa, which is also the case in Ewing's sarcoma, is an occurrence which should be investigated. This may be an example of redundancy seen in ETS factors, where in the absence of one fusion another may be able to exert the same effects.

1.8.3 Epithelial-specific ETS factors

Within the ETS transcription factor family there is a subset of genes whose expression is limited to epithelial cells. ESE2, ESE3 and ELF3 (also known as ESE1) are highly related and form a distinct gene subfamily. PDEF is another epithelial-specific ETS factor, although it differs from the others due to its preferential binding to GGAT core sequences in target genes, as opposed to the more common GGAA (Oettgen et al., 2000). This relatively new category of ETS factors, the first of which was discovered in 1997, display important roles in epithelial cell differentiation. Notably, there is now mounting evidence that several of these factors play a role in PCa.

1.8.3.1 PDEF

Prostate-derived ETS factor (PDEF) is most highly expressed in the prostate but is also found at lower levels in other hormone-regulated organs including the breast, ovaries and salivary glands and also in the lung and intestine (Oettgen et al., 2000, Noah et al., 2010). PDEF protein is exclusively expressed in the terminally-differentiated secretory luminal cells of normal prostate epithelium and has a role in the differentiation of intestinal progenitor cells into the secretory cell types of the intestinal epithelium (Oettgen et al., 2000, Gregorieff et al., 2009). Consistent with this expression pattern, PDEF was first described as an upregulator of PSA both in the presence of and independently of androgen (Oettgen et al., 2000). In PCa, loss of PDEF expression is associated with more aggressive tumours, and patients with $PDEF^-$ tumours have a decreased survival rate compared to $PDEF^+$ patients (Turner et al., 2011, Ghadersohi et al., 2011). Several studies have shown PDEF loss to enhance the migratory and invasive phenotype of PCa cell lines and thus have tumour suppressor qualities upon its re-expression (Johnson et al., 2010, Turner et al., 2011, Gu et al., 2007). This coincides with evidence found in other cancers showing loss of PDEF protein expression, including colon and breast cancer (Moussa et al., 2009, Steffan and Koul, 2011, Feldman et al., 2003). In PCa, PDEF expression loss is in part regulated by microRNA miR-204 expression (Turner et al., 2011).

Conversely, some studies claim PDEF expression increases in prostate and breast cancers compared to their normal tissues and induces invasiveness of a non-tumourigenic breast epithelial cell line when co-expressed with tyrosine kinases ErbB2 and CSF-1 (Gunawardane et al., 2005, Sood et al., 2007). This dichotomy can be explained since the studies that show PDEF to be a tumour suppressor in breast cancer are of the more invasive basal cell subtype and those that describe it as an oncogene are of the more differentiated luminal subtype (associated with better prognosis). This implies that in different cancer cell subtypes, PDEF can influence tumour growth in different ways. Since PDEF is normally expressed in luminal cells in the prostate and associated with luminal cell markers such as PSA, loss of protein expression could potentially result in cells dedifferentiating, which would correlate with an increase of invasiveness (Figure 1.9). Whether PDEF knockdown in more differentiated (luminal) PCas could be beneficial therapeutically remains to be seen, but this seems to be the situation in breast cancer (Buchwalter et al., 2013). Using this rationale, one would therefore expect PDEF expression to be lost in more aggressive, less differentiated PCas (high Gleason grade) resulting in suppression of luminal markers such as PSA. If PDEF loss also promotes a stem-like phenotype in PCa cells then EMT and invasion (also properties of CSCs) should be seen. These proposals are yet to be experimentally demonstrated.

1.8.3.2 ELF3

ELF3 (also known as ESE1, ESX, and Jen) is mainly expressed in epithelial-rich tissues such as the gut, kidneys, bladder and prostate (Tymms et al., 1997, Oettgen et al., 1997, Bock et al., 2014). Two papers have been published describing a role for ELF3 in PCa with conflicting views. Shatnawi et al described ELF3 as a repressor of PCa. By interfering with AR DNA binding, ELF3 could repress the upregulation of AR target genes known to be drivers of PCa (Shatnawi et al., 2014). Knockdown of ELF3 using siRNA induced AR target gene expression resulting in increased cell migration and proliferation of the PCa cell line LNCaP. Furthermore, overexpression of ELF3 repressed tumour growth in an LNCaP xenograft model. ELF3 protein loss was also associated with PCa progression by IHC from tissue sections, although the patient cohort was relatively small.

In contrast, Longoni et al described ELF3 as a driver of PCa (Longoni et al., 2013). They observed high ELF3 expression at the mRNA level in several patient datasets. Immunohistochemical staining for ELF3 in 207 tumours revealed that 63% of tumours significantly expressed the protein, whereas ELF3 was poorly expressed in normal tissues. ELF3 mRNA was also more highly expressed in metastases compared with primary prostate tumours. The mechanism by which ELF3 drives PCa was proposed to be a positive feedback loop with the transcription factor NF-κB, a known upregulator of ELF3 (Rudders et al., 2001, Grall et al., 2005). This required pro-inflammatory IL1-β stimulation for NF-κB activation and subsequent ELF3 induction, which was then able to sustain NF-κB activation. ELF3 induction resulted in an increased malignant phenotype of LNCaP and 22RV1 cell lines by increasing colony forming ability in soft agar, anoikis resistance and cell migration. Xenograft tumours produced by ELF3 over-expressing 22RV1 cells in nude mice presented with larger and faster growing tumours and also produced metastases in the lung compared to control cells. However, since 22RV1 cells are known to migrate and promote angiogenesis, other cell

lines may have been more appropriate to validate an effect in vivo (Stieler et al., 2012). It should also be taken into account that both of these studies did not use a normal cell comparison as a control. Elucidating the roles of ELF3 in the normal prostate will aid further experiments in cancer models.

ELF3 has oncogenic and suppressive roles in colorectal cancer (CRC). It can upregulate β-catenin and subsequently activate downstream targets of the Wnt/β-catenin signalling pathway to drive colon cancer progression (Wang et al., 2014). ELF3 expression can also directly promote the apoptotic effects of non-steroidal anti-inflammatory drugs (NSAIDs) in CRC (Lee et al., 2008). An explanation for these conflicting findings is that ELF3 could be under similar regulation to that of PDEF in cancer where it has different roles in different cell types. ELF3 also plays major roles in epithelial cell differentiation, including the terminal differentiation of keratinocytes as well as a high expression in the most differentiated cells of the normal human urothelium (Cabral et al., 2003, Bock et al., 2014). Furthermore, a recent study has shown that ELF3 is linked to differentiation of the human embryonal carcinoma stem cell line NCCIT, after differentiation was promoted using retinoic acid treatment. This treatment resulted in the downregulation of early differentiation transcription factor OCT4 and upregulation of ELF3 (Park et al., 2014). OCT4 is important for maintaining the pluripotency and self-renewal characteristics of SCs and its expression has been linked to enhanced malignant phenotype of cells and cancer progression in glioma, bladder and PCa (Du et al., 2009, Linn et al., 2010, Chang et al., 2008).

When Affymetrix gene-expression arrays of 15 BPH and cancer tissues obtained from patients, comparing prostate SC/CSC ($CD133^{+}/\alpha_2\beta_1^{hi}$) gene expression to the committed basal cell population ($\alpha_2\beta_1^{lo}$), 581 genes associated with cancer and inflammation were found to have significantly altered expression in the CSC population (Birnie et al., 2008). This information has allowed investigation of specific targets and pathways to further our understanding of prostate cell heterogeneity and CSC biology and identify potential therapeutic targets for PCa (Maitland and Collins, 2008). Here, ELF3 was found to have consistently higher expression in committed basal cells compared to SCs. Since low expression of ELF3 was found in both benign and malignant SCs across all patients, ELF3 may be involved in SC differentiation (Figure 1.9). Using the different fractions of primary prostate epithelial cells to investigate ELF3 should provide a more precise account of its roles in prostate cell differentiation and PCa and will be addressed in this study.

1.8.3.3 ESE3

ESE3 is an epithelial-specific ETS factor belonging to the same subfamily as ELF3. The ESE3 ETS DNA-binding domain shares 84% homology with ELF3 (Kas et al., 2000). However, each has a distinct PNT domain, suggesting that whilst they may bind to similar target genes, their effects could ultimately vary depending on the protein-protein interactions achieved via their PNT domains. This was shown for prostate-specific promoters PSA and PSMA (prostate-specific membrane antigen). The PSMA promoter was upregulated 3-fold in the presence of ELF3, whilst ESE3 had no effect. Conversely, ESE3 was able to activate the PSA promoter over 2-fold whereas ELF3 repressed the PSA promoter (Kas et al., 2000). This

study was carried out in (non-prostate) HEK-293 cells, and so studies in more appropriate prostate models should be carried out to determine if ESE3 and ELF3 have opposing roles in prostate cell differentiation.

In a microarray analysis of 59 primary prostate tumour samples and 14 normal prostate samples, differential ETS factor protein expression in PCa has been evaluated. ERG, ELF3 and ESE3 were the most dysregulated genes, with ERG and ELF3 upregulated and ESE3 downregulated in cancer samples compared to normal prostate (Kunderfranco et al., 2010). This study found a tumour-suppressor role for ESE3 in PCa as a result of its ability to regulate the expression of Nkx3.1; a tumour-suppressor commonly lost in PCa partly by heterozygous deletion of the gene located at chromosome 8p21.2 (Bowen et al., 2000, Vocke et al., 1996). Knockdown of ESE3 in LNCaP and LHS cells (normal prostate epithelial cells [PrECs] which have been immortalised via hTERT and SV40 large T antigen expression) resulted in reduced Nkx3.1 transcription. Since Nkx3.1 is also an androgen-regulated marker of prostate epithelial cell differentiation (Iwata et al., 2010), downregulation of ESE3 and upregulation of ELF3 and ERG may act in concert to produce similar effects.

To complement this theory, a study by the same group further examined the role of ESE3 suppression in PCa cells (Albino et al., 2012). ESE3 shRNA knockdown in immortalised PrECs and RWPE-1 cells resulted in the upregulation of EMT markers vimentin and twist-1 as well as downregulation of epithelial cell marker E-cadherin. Furthermore, ESE3 repression induced both colony-forming ability in soft agar and sphere-forming ability, both hallmarks of SCs. Gene set enrichment studies of 3 independent datasets of primary prostate tumours indicated that ESE3 suppression is found in approximately 25% of tumours and can occur both cooperatively or independently of ERG overexpression. The highest upregulated gene sets in tumours with ESE3 suppression include EMT, adhesion and cytoskeleton remodelling related genes (Albino et al., 2012). Therefore, since loss of ESE3 downregulates luminal cell markers and appears to induce stem-like properties it could be speculated that this would allow the de-differentiation of luminal cells and/or block the differentiation of basal cells (Figure 1.9).

1.9 Models of the prostate

1.9.1 Prostate epithelial cell lines

To understand the mechanisms which contribute to prostate cell differentiation and the development and progression of cancer, a number of models of the prostate exist, each with their own advantages and disadvantages. A range of human-derived cell lines are available for studying the normal and malignant prostate, most of which are detailed in an extensive two-part review (Sobel and Sadar, 2005). Cell lines are a good model of study as they are obtainable without the need for comprehensive ethical considerations, they can be genetically modified and easily transfected and can be grown in culture almost indefinitely. However, as a consequence of immortalisation and long-term culture, cell lines have adapted to life outside the patient by a series of genetic and epigenetic changes (Lee et al., 2006, Izadpanah et al., 2008, Kawai

et al., 1994, Meissner et al., 2008). This demonstrates that whilst cell lines are suitable models for initial studies, they do not fully represent what occurs in a patient.

1.9.2 Primary prostate epithelial cultures

Primary prostate cultures derived from patient tissue are valuable models of study as they not only represent an individual patient as unaltered as possible, but also represent the heterogeneity found between patients in a disease. However, it should be noted that patient biopsies may not be easy to source and requires ethical permission. Furthermore, they are expensive to maintain and in order to keep cultures as near to the patient as possible they can only be grown for a limited time.

1.9.3 3D models of the prostate

2D *in vitro* models are limited due to the fact that they do not grow in a fashion which recapitulates the normal tissue architecture. Notably, prostate cell lines and primary cells can also be grown in 3D cultures. Resuspension of cells in a solid matrix such as matrigel promotes growth of spheroids which can recapitulate the architecture of prostate acini (Pellacani et al., 2014, Lang et al., 2006, Lang et al., 2001a). More specifically, a basal and luminal bilayer with a hollow lumen in the centre.

1.9.4 *In vivo* models of the prostate

As PCa only occurs naturally in elderly canines, alternative routes of study are required for *in vivo* investigation of PCa (Leav and Ling, 1968). *In vivo* models of PCa include the transplantation of cell lines and primary cells into immunocompromised mice (known as xenografts) such as NOD/SCID or RAG2$^{-/-}$ IL2RγC$^{-/-}$ (Stephenson et al., 1992, Shultz et al., 1995, Lawrence et al., 2013, Taurozzi et al., 2017). There are also transgenic mouse models of PCa available, with TRAMP and LADY amongst the most commonly used (Greenberg et al., 1995, Kasper et al., 1998). However, as discussed previously (Section 1.5.1), it must be taken into consideration that the mouse prostate bears significant differences to the normal human prostate. Further limitations include a non-fully-functioning immune system and interference of the host's cells with the human tumour. As such, it is important to note that mouse models may not fully represent what would occur in a human patient with regards to potential drug efficacy and toxicity.

1.10 Aims of research

The current treatment regimen for advanced PCa is not curative and a shift away from ADT, towards novel therapies which take into consideration the heterogenous cell populations present in a prostate tumour is needed.

The role of ELF3 in the prostate is currently controversial, with literature describing both oncogenic and tumour suppressor roles (Longoni et al., 2013, Shatnawi et al., 2014). Furthermore, ELF3 was significantly downregulated in the SC subpopulation compared to the CB subpopulation derived from benign and cancerous prostate tissue, suggesting an additional link to prostate cell differentiation (Birnie et al., 2008). The main aims of this study were to investigate ELF3 expression in the prostate and elucidate its roles in both normal prostate development and malignancy. The specific objectives were as follows:

1) Identify the pattern of ELF3 expression in prostate epithelial cell lines and primary prostate subpopulations at the protein level.

2) Determine whether ELF3 is differentially expressed between benign and cancerous prostate tissue.

3) Explore the roles of ELF3 in the normal and malignant prostate by manipulating its expression through knockdown and overexpression.

4) Investigate potential regulatory pathways by observing global gene changes following ELF3 gene expression knockdown.

The complex regulation of the prostate epithelial differentiation hierarchy is not fully understood and so a further understanding of the mechanisms involved in cell differentiation is key to developing novel long term therapies for advanced PCa. By resolving these questions and furthering our understanding of prostate epithelial cell development and maintenance, we could clarify the conflicting findings in literature and contribute to our understanding of PCa.

2. Materials and Methods

2.1 Mammalian cell culture

2.1.1 Maintenance of cell lines

Cell lines were maintained in T-25 or T-75 tissue culture flasks (Corning or Sarstedt) at 37°C with 5% CO_2 and were sub-cultured by washing in phosphate buffered saline (PBS) and then incubation with 0.05% (v/v) trypsin-EDTA in PBS at 37°C. Trypsin was inactivated with R10 media. Cells were collected and washed in PBS and centrifuged at 1500 RPM for 5 minutes. Depending on the growth rate of each cell line, they were passaged at a ratio of 1:3-1:20. Cells were also harvested for analysis by this method unless otherwise stated. A summary of cell lines used in this study and culture conditions are shown in Tables 2.1 and 2.2.

Cell Line	Culture Conditions	Reference
PNT1a	R10	(Cussenot et al., 1991)
PNT2-C2	R10	(Berthon et al., 1995)
BPH-1*	R5	(Hayward et al., 1995)
P4E6**	K2	(Maitland et al., 2001)
PC3	H7	(Kaighn et al., 1979)
Du145	R10	(Sobel and Sadar, 2005)
LNCaP	R10	(Horoszewicz et al., 1983)
22RV1	R10	(Sramkoski et al., 1999)
HEK-293T	D10	(DuBridge et al., 1987, Pear et al., 1993)
U-87 MG	D10	(Ponten and Macintyre, 1968)

* Gifted from Simon Hayward

** Derived in York

Table 2.1. Cell lines and their culture conditions.

Media	Constituents
R10	Roswell Park Memorial Institute-1640 (RPMI, Gibco),10% (v/v) foetal calf serum (FCS) (Gibco) and 2mM L-Glutamine (Gibco)
R5	RPMI, 5% (v/v) FCS, 2mM L-Glutamine
K2	Keratinocyte Serum-Free Medium (KSFM, Invitrogen), 2% (v/v) FCS, 2mM L-Glutamine, 50µg/ml bovine pituitary extract (Gibco), 5ng/ml human epidermal growth factor (EGF) (Gibco)
H7	Ham's F-12 medium (Lonza), 7% (v/v) FCS, 2mM L-Glutamine
D10	Dulbecco's Modified Eagle's Medium (DMEM) (Gibco), 10% (v/v) FCS, 2mM L-Glutamine

Table 2.2. Culture media constituents.

2.1.2 Primary prostate tissue processing and cell culture

A detailed account of primary prostate tissue processing and cell culture is described in Frame et al. (2016). Prostate tissue was obtained from patients with ethical permission and consent by a tissue procurement officer (Ethics Number: 07/H1304/121). Tissue received was anonymised and derived from either BPH by TURP or targeted needle core biopsies of tumours and adjacent normal tissue following RP. Cancer cores were taken from palpable tumours when possible or alternatively from cancerous areas detected by MRI and TRUS biopsies. The tissue was submerged in transport media, composed of RPMI with 5% (v/v) FCS and 100U/ml antibiotic/antimycotic solution (100 IU/ml penicillin, 100µg/ml streptomycin and 0.25 µg/ml fungizone (ABM, Invitrogen)) and maintained at 4°C during transport.

Upon arrival, tissue fragments were chopped into small pieces with a scalpel. A small piece was submerged in formalin for paraffin-embedding whilst the rest was digested in collagenase (200U/mg, Worthington Biochemical Corporation) in 2.5ml KSFM and 5ml R10. After incubation overnight at 37°C on an orbital shaker at 80 RPM, the digested tissue was then triturated through a 5ml pipette followed by a blunt cannula (0.813mm x 2.5mm, Covidien) and centrifuged at 1500 RPM for 10 minutes. The supernatant was removed with a Pasteur pipette and cells washed with 10ml PBS and centrifuged at 1500 RPM for 4 minutes. Cells were then incubated in 5ml trypsin at 37°C for 30 minutes on an orbital shaker at 80 RPM, trypsin inactivated with 5ml of R10 and centrifuged at 1500 RPM for 4 minutes. The supernatant was removed and cells resuspended in 5ml stem cell media (SCM) which consisted of KSFM, bovine pituitary extract (50µg/ml), human EGF (5ng/ml), granulocyte macrophage colony stimulating factor (1ng/ml, Miltenyi Biotec), stem cell

factor (2ng/ml, First Link UK Ltd), leukaemia inhibitory factor (2ng/ml, Chemicon), cholera toxin (100ng/ml, Sigma Aldrich) and L-Glutamine (2mM).

Primary cells were cultured on collagen-I coated 10cm dishes (BD Biosciences) with murine STO fibroblast feeder cells (irradiated) and maintained with fresh SCM every other day and passaged at a ratio of 1:2-1:4 by trypsinisation. Following the first passage after processing, STOs were no longer used.

2.1.3 Irradiation of murine fibroblasts

Murine STO fibroblasts were added to primary epithelial cell cultures as a feeder culture. To ensure STOs did not overwhelm the primary cell cultures, they were treated with a 60Gy dose of radiation. Irradiation of STOs was routinely carried out by Fiona Frame and Dominika Butler using an X-RAD iR225 irradiator. STOs were maintained in T-175 tissue culture flasks (Sarstedt) in D10, harvested by trypsinisation at 90% confluency and centrifuged at 1500 RPM for 5 minutes. They were then sub-cultured at a ratio of 1:20. STOs that were to be irradiated were resuspended in 25ml KSFM per T-175 flask. Irradiated STOs were kept at 4°C until use for up to 5 days.

2.1.4 Cryopreservation of cell cultures

Cultured cells to be transferred to liquid nitrogen for long term storage were harvested via trypsinisation and centrifuged at 1500 RPM for 5 minutes. They were then resuspended at a concentration of 1-2x10^6 cells/ml in freezing medium (10% (v/v) dimethyl sulfoxide (DSMO), 20% (v/v) FCS in RPMI) and transferred into 2ml cryovials (Greiner Bio-One). Cells were stored at -80°C for 24 hours before transferring to liquid nitrogen.

2.1.5 Live cell count using haemocytometer

Live cell number was determined using Trypan Blue Stain (0.4%, Sigma Aldrich). 10µl Trypan Blue was mixed with 10µl cell suspension and cells counted using a haemocytometer (Neubauer). Number of unstained cells was equivalent to live cell number.

2.1.6 Enrichment of basal cell subpopulations from primary cell cultures

The prostate differentiation hierarchy is composed of three basal cell subpopulations. TA and CB cells were enriched for from primary prostate epithelial cell cultures by using cell surface markers, as described previously by Collins et al. and Frame et al. TA cells are $\alpha_2\beta_1$-integrin^{high} and CB cells are $\alpha_2\beta_1$-integrin^{low} (Collins et al., 2001, Frame et al., 2016). $\alpha_2\beta_1$-integrin expression allows enrichment by collagen adherence.

Collagen-I coated 10cm dishes were blocked with heat inactivated, filtered 0.3% (w/v) bovine serum albumin (BSA) in PBS at 37°C for 1 hour and washed once with PBS. The number of blocked plates was half the number of plates of cultured cells to be enriched. Primary cultures were harvested by trypsinisation and resuspended in SCM. 3ml of cell suspension was added to each blocked plate and incubated for 20 minutes at 37°C. The media was collected, together with three 3ml PBS washes, and centrifuged at 1500 RPM for 5 minutes; this constitutes the CB subpopulation. The adherent cells were then trypsinised and pelleted and

these constitute the TA subpopulation. The TA and CB subpopulations were then harvested for protein or plated onto collagen-I coated plates for knockdown experiments (CB cells only) or vorinostat treatment.

2.1.7 Vorinostat treatment of primary cells

Primary prostate epithelial cells (whole population, TA or CB) were plated at a density of 5 x 10^5 onto collagen-I coated 6 well plates and left to adhere overnight. Cells were treated with Vorinostat at a concentration of 0.625μM, 2.5μM or 10μM for 4 hours or 24 hours before harvesting for protein analysis.

2.2 Cell transfection

2.2.1 siRNA transfection of prostate cell lines

Silencer Select siRNAs (ThermoFisher Scientific) were used to knock down ELF3 expression in prostate epithelial cell lines and primary cells. Cells were plated at a density of 4 x 10^4 – 3 x 10^5 and left to adhere overnight. A 10μM stock of ELF3 siRNA (siELF3, Assay ID: s4623) or scrambled siRNA (siSCR, Negative control no. 1) was added to OptiMEM reduced serum medium to produce mix 1 and Lipofectamine RNAiMAX (Invitrogen) was added to OptiMEM to produce mix 2 (Table 2.3). The mixtures were added together at a ratio of 1:1 and incubated for 15 minutes at room temperature. The transfection mix was then added dropwise into media of wells. Cells were harvested at various time points for protein analysis and functional assays (Section 2.7).

Plate Size	Mix 1		Mix 2		Total Transfection Mix/well (µl)	Media Volume (ml)
	OptiMEM (µl)	10µM siRNA (µl)	OptiMEM (µl)	RNAiMAX (µl)		
6 well	125	2.5	125	7.5	250	2
12 well	50	1	50	3	100	1
24 well	25	0.5	25	1.5	50	0.5

Table 2.3. Components of siRNA transfection mixes for cell lines.

2.2.2 siRNA transfection of primary prostate cells

Cell were plated at a density of 3 x 10^4 – 2 x 10^5 in 12-well or 6-well collagen-I coated plates and left to adhere overnight. Transfection mixes were prepared as follows; siELF3 or siSCR (stock concentration of 10µM) was added to OptiMEM reduced serum medium to produce mix 1 and Oligofectamine transfection reagent was added to OptiMEM medium to produce mix 2 (Table 2.4) and tubes were incubated for 10 minutes at room temperature. All reagents were equilibrated to room temperature before use. The tubes were then added together and incubated for a further 25 minutes at room temperature. Media was aspirated from cells and OptiMEM was added to each well. The siRNA/Oligofectamine mixture was then added dropwise to wells and cells were incubated for 4 hours at 37°C. The transfection mixture was then removed, cells were washed once in PBS and 2ml of SCM was added. Cells were harvested from 6 well plates at 72 hours post-transfection for protein analysis and from 12 well plates at 72 hours for cell cycle analysis.

Plate Size	Mix 1		Mix 2		OptiMEM Volume (µl)	Total Transfection Mix/well (µl)	Total Media Volume (ml)
	OptiMEM (µl)	10µM siRNA (µl)	OptiMEM (µl)	Oligofectamine (µl)			
6 well	245	5	66	4	175	320	2
12 well	122.5	2.5	33	2	87.5	160	1

Table 2.4. Components of siRNA transfection mixes for primary cells.

2.3 Mammalian cell RNA analysis

2.3.1 RNA extraction

An RNeasy Mini Kit (QIAGEN) was used to extract RNA from mammalian cells as per manufacturer's instructions. Briefly, up to $5x10^6$ cells were harvested by washing in PBS and incubated at 37°C with 0.05% trypsin-EDTA. Trypsinisation was stopped with R10 medium and cells were pelleted by centrifugation at 1500 RPM for 5 minutes. The supernatant was removed and the remaining cell pellet was lysed in 350µl of Buffer RLT with 1:100 (v/v) β-mercaptoethanol (β-Me) and vortexed. The lysate was transferred to a QIAshredder spin column in a 2ml collection tube (QIAGEN) and centrifuged at 13,000 RPM for 2 minutes to homogenise the samples. 350µl of 70% ethanol was added to the homogenate and transferred to an RNeasy Mini spin column. The mixture was centrifuged at 13,000 RPM for 15 seconds and the flow-through discarded. The column was washed with 350µl of Buffer RW1 and centrifuged at 13,000 RPM for 15 seconds. DNase digestion was performed by preparing a master mix of 10µl DNaseI stock solution and 70µl of Buffer RDD per sample and mixed by inverting the tube a few times. 80µl of the mix was added to each column and incubated at room temperature for 10 minutes. 350µl of Buffer RW1 was added to the each column and centrifuged at 13,000 RPM for 15 seconds. Each column was transferred to a fresh collection tube and washed with 500µl Buffer RPE and centrifuged at 13,000 RPM for 15 seconds. A final wash was carried out with 500 µl Buffer RPE and centrifuged at 13,000 RPM for 2 minutes. The columns were then transferred to a fresh collection tube and centrifuged at 13,000 RPM for 1 minute to remove any residual ethanol. To elute the RNA, each column was placed in a 1.5ml Eppendorf and 30µl RNase-free water was added directly to the column and centrifuged at 13,000 RPM for 1 minute. A NanoDrop ND-1000 spectrophotometer (ThermoFisher Scientific) was used to determine RNA quality and concentration. RNA samples were kept at -80°C for long term storage.

2.3.2 cDNA synthesis and PCR purification

Equal quantities of RNA were reverse transcribed into complementary DNA (cDNA) for each experiment (5µg of cell line RNA, 15-270ng primary cell RNA). Two master mixes were prepared as shown in Table 2.5 (all components from Invitrogen). The appropriate volume of RNA was added to PCR tubes and samples were made up to 10µl with sterile molecular biology grade water (Sigma Aldrich). 2µl of Mastermix 1 was added to each sample and incubated at 65°C for 5 minutes. Samples were then put on ice and 8µl of Mastermix 2 was added and mixed by pipetting. The samples were then incubated at 25°C for 10 minutes, 42°C for 50 minutes and 72°C for 15 minutes on a GeneAmp PCR Sytem 9700 (Applied Biosystems).

Mastermix	Component (concentration)	Volume per sample (µl)
1	Random hexamer primer (50ng/µl)	1
	dNTP (10mM)	1
2	5x First Strand Buffer	4
	DDT (0.1M)	2
	RNase OUT (40U/µl)	1
	Superscript III (200U/µl)	1

Table 2.5. Mastermix components for cDNA synthesis.

The QIAquick PCR purification Kit (QIAGEN) was used to remove excess dNTPs and salts from the cDNA samples. 100µl of Buffer PB was added to the 20µl cDNA reactions and transferred to a QIAquick spin column. The samples were centrifuged at 13,000 RPM for 45 seconds. The flow-through was discarded and the column washed in 750µl of Buffer PE and centrifuged 13,000 RPM for 1 minute. The flow-through was discarded and the column was centrifuged again at 13,000 RPM for 1 minute. The column was then transferred to a 1.5ml Eppendorf and the column incubated with 30µl of water (Sigma Aldrich) for 1 minute before eluting the cDNA by centrifugation at 13,000 RPM for 1 minute. A NanoDrop ND-1000 spectrophotometer was used to determine cDNA quality and concentration. cDNA samples were kept at -80°C for long term storage.

2.3.3 Quantitative reverse-transcriptase PCR (qRT-PCR)

Quantitative reverse-transcriptase PCR (qRT-PCR) was carried out using a CFX96 Real-Time PCR Detection System (Bio-Rad). Reactions were prepared in a dedicated PCR hood with 5µl SsoFast Probes Supermix (Bio-Rad) or Taqman Gene Expression Master Mix (Applied Biosystems), 0.5µl TaqMan assay probe (ELF3: Hs00963881_m1, Applied Biosystems) (GAPDH: qHsaCEP0041396, Bio-Rad) and 1.5µl ddH_2O. 3µl cDNA was added outside the hood to make a total reaction volume of 10µl. A standard curve was used for absolute quantification of gene expression. 5-fold serial dilutions of pGEM-TEasy-ELF3 plasmid (obtained from Prof Jenny Southgate, University of York) were prepared with a known number of copies of ELF3. Each sample and standard were run in triplicate on MicroAmp Optical 96 well plates (Applied Biosystems) and covered with StarSeal Advanced Polyolefin Film (STARLAB).

Results were analysed using the Bio-Rad CFX Manager 2.0. The standard curve equation was used to determine the expression in unknown samples. Relative quantification was also carried out on a selection of samples using the delta-delta C_T method, with GAPDH as the housekeeping gene.

2.4 Gene expression microarray analysis

2.4.1 Sample preparation

RNA was extracted from cells using the RNeasy Mini Kit (QIAGEN) according to Section 2.2.1. Sample sets were in triplicate and included untransfected, mock transfected, siSCR and siELF3 BPH-1 and PC3 cells. The RNA integrity number (RIN) of all samples was 9.8 or above (analysed by the University of York Bioscience Technology Facility using an Agilent Bioanalyzer). Each sample was carried out in duplicate to also obtain protein for western blot analysis. ELF3 knockdown was verified at the protein level before microarray analysis.

2.4.2 Data analysis

An Affymetrix Clariom D gene expression microarray was performed by Eurofins Genomics on RNA extracted from the samples described above. Transcriptome Analysis Console (TAC) Software 4.0 was used to analyse the data (ThermoFisher Scientific). A significance threshold of 2-fold increase or decrease and a p-value <0.05 was used. Gene ontology (GO) analyses were carried out using the Database for Annotation, Visualization and Integrated Discovery (DAVID) and visualised using REViGO.

Data was also analysed by an external bioinformatician (Alastair Droop). He used LIMMA (Linear Models for Microarray and RNA-seq Data) within the R numerical environment, with a false discovery rate threshold of 0.025 after empirical Bayes smoothing of the standard errors (Ritchie et al., 2015, R Core Team, 2014).

Multidimensional scaling (MDS) showed that BPH-1 and PC3 cells are different from each other and samples within each set are consistent and can therefore be compared (Figure 2.1).

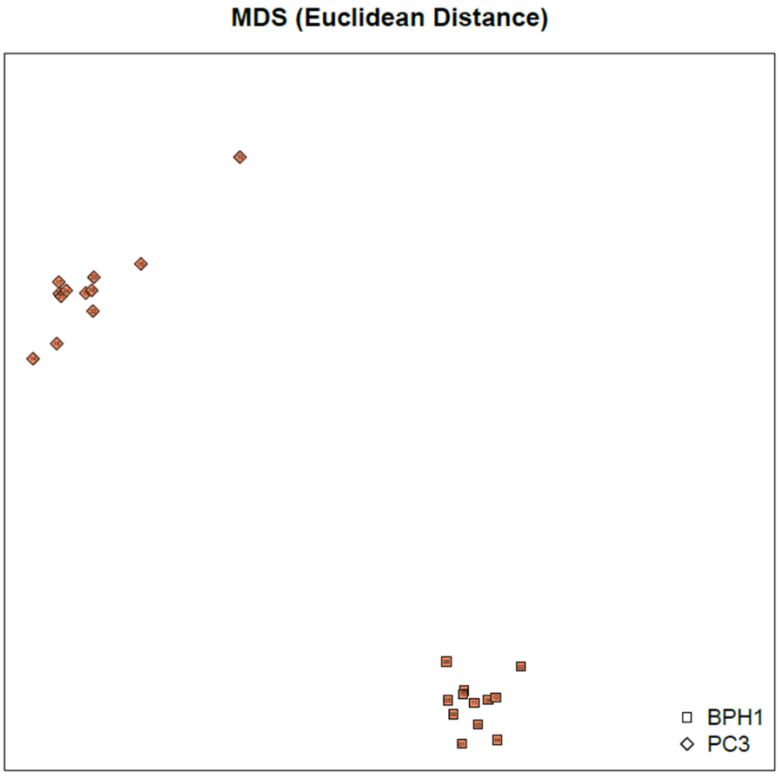

Figure 2.1. Multidimensional scaling of microarray samples.

Multidimensional scaling (MDS) of BPH-1 and PC3 samples analysed by gene expression microarray. Produced by Alastair Droop. Sample sets were in biological triplicate and included untransfected, mock transfected, siSCR and siELF3 of BPH-1 and PC3 cells.

2.5 Protein analysis

2.5.1 Protein extraction

Cells were harvested using trypsin and the resulting pellets were lysed in radioimmunoprecipitation assay (RIPA) buffer or CytoBuster lysis buffer (Novagen) with the addition of protease inhibitors (cOmplete™, Mini, EDTA-free Protease Inhibitor Cocktail, Roche). Phosphatase inhibitors were also added if appropriate (PhosSTOP Roche). Cells lysed in CytoBuster were incubated on ice for 5 minutes and then centrifuged at 13,000 RPM for 5 minutes. The supernatant was then transferred into a new 1.5ml microcentrifuge tube as the whole cell lysate. Cells lysed in RIPA buffer were incubated at 4°C for 20 minutes on a cyclical spinner. Samples were then spun at 14,000 RPM for 10 minutes at 4°C and the supernatant kept as the whole cell lysate.

2.5.2 Protein quantification

A Bicinchoninic acid (BCA) assay (Thermofisher Scientific) was used to quantify protein concentration from whole cell lysates according to the manufacturer's instructions. Standards of known concentrations of BSA were made in the same lysis buffer as the unknown samples. 10µl of each standard or unknown sample were added to a 96 well plate in triplicate. 200µl of the pre-made BCA assay working solution was then added to each well and the plate was incubated at 37°C for 30 minutes. The plate was cooled down to room temperature and then read on a POLARstar OPTIMA microplate reader (BMG Labtech) for absorbance at 562nm. A standard curve was generated from the BSA standards and protein concentration of unknown samples was calculated from the line of best fit.

2.5.3 Cytoplasmic and nuclear fractionation

$5x10^6$ cells (PNT1a, PNT2-C2, BPH-1, P4E6, LNCaP, PC3) were harvested and washed twice in cold PBS. The supernatant was discarded and the cell pellet was resuspended in 500µl of hypotonic buffer (20mM Tris-HCl pH 7.4, 10mM NaCl, 3mM $MgCl_2$) and transferred to a pre-chilled 1.5ml microcentrifuge tube. The lysate was then incubated on ice for 15 minutes. 25µl of 10% NP40 was added and mixed by vortexing for 10 seconds. The lysate was centrifuged at 3000 RPM for 10 minutes at 4°C. The supernatant was removed and kept as the cytoplasmic fraction. The remaining cell pellet was then was then resuspended in 50µl cell extraction buffer (100mM Tris-HCl pH 7.4, 2mM $NaVO_4$, 100mM NaCl, 1% (v/v) Triton X-100, 1mM EDTA, 10% (v/v) glycerol, 1mM EGTA, 0.1% (w/v) SDS, 1mM NaF, 0.5% (w/v) sodium deoxycholate, 20mM $Na_4P_2O_7$). The lysate was incubated on ice for 30 minutes with vortexing at 10 minute intervals. They were then centrifuged at 12,000 RPM for 30 minutes at 4°C. The supernatant was transferred to a fresh Eppendorf as the nuclear fraction. Lysates were kept at -80°C for long term storage.

2.5.4 SDS-PAGE gel electrophoresis

8-12% Tris-SDS acrylamide gels were prepared using the Bio-Rad Protean II system. 20-30µg of protein lysate was added to 4x Laemmli Sample Buffer (Bio-Rad) and heated to 95°C for 5 minutes. Up to 50µl of samples were added to wells with the Precision Plus Protein Kaleidoscope ladder (Bio-Rad) in a separate lane to determine size of proteins. Proteins were subjected to electrophoresis at 50V for 30 minutes, followed by 100V for 90 minutes.

2.5.5 Western blot

Immobilon-P membrane (Millipore) was activated by immersion in methanol for 30 seconds, and washed in dH_2O. Gels were placed onto the membrane and transferred using the Bio-Rad Protean II system in transfer buffer (48mM Tris, 39mM glycine, 10% (v/v) methanol) at 100V for 90 minutes. Membranes were then blocked with 5% (w/v) non-fat skimmed milk (Marvel) at room temperature for 1 hour. Primary antibody diluted in 1% (w/v) Marvel or 5% (w/v) BSA in TBST (150mM NaCl, 50mM Tris-HCl pH7.5, 0.1% (v/v) Tween 20) was added and incubated overnight at 4°C; a list of primary antibodies used is shown in Table 2.6. The following day, membranes were washed in TBST buffer three times for 5 minutes. Membranes were incubated with secondary antibodies (goat anti-rabbit IgG HRP-linked, Cell Signalling Technologies or goat anti-mouse IgG HRP-linked, Affinipure) for 1 hour at room temperature at a working concentration of 1:10,000. After washing in TBST three times for 10 minutes, the BM Chemiluminescence Blotting Substrate (Roche) was used to develop the membranes. Solution A was added to Solution B at a dilution of 1:100 and added to the membrane for 2 minutes. The excess was removed and the membranes were exposed to hyperfilm ECL (GE Healthcare) and processed using an X-ray processor (SRX-101A, Konica Minolta) or a GeneGnome (Syngene).

Antibody	Manufacturer	Catalogue no.	Species	Working Concentration	Diluent
ELF3	Abcam	Ab133621	Rabbit mono	1:1000-1:5000	1% Milk
CK5	Abcam	Ab52635	Rabbit mono	1:2000	1% Milk
CK18	Sigma Aldrich	C8541	Mouse mono	1:2000	1% Milk
E-cadherin	Abcam	Ab1416	Mouse mono	1:250	1% Milk
Total β-catenin	Sigma Aldrich	C2206	Rabbit poly	1:4000	1% Milk
Active β-catenin	Cell Signalling Technology (CST)	8814S	Rabbit poly	1:1000	5% BSA
NSE	Abcam	Ab53025	Rabbit poly	1:500	1% Milk
PLK1	CST	4513	Rabbit mono	1:1000	5% BSA
CDC25C	CST	4688	Rabbit mono	1:1000	5% BSA
Cleaved caspase 3	CST	9661	Rabbit poly	1:1000	5% BSA
Cyclin B1	CST	4135	Mouse mono	1:1000	5% BSA
p-Cyclin B1 (Ser133)	CST	4133	Rabbit mono	1:1000	5% BSA
p21	CST	2947	Rabbit mono	1:1000	5% BSA
GAPDH	Abcam	Ab9485	Rabbit poly	1:10,000	1% Milk
Actin	Merck	04-1040	Rabbit mono	1:10,000	1% Milk

Table 2.6. Antibodies used for protein detection by western blot.

2.5.6 Western blot stripping

Once membranes had been exposed they were washed in TBST four times for 5 minutes and then incubated in stripping buffer (0.0625M Tris-HCl pH6.8, 2% (w/v) SDS, 0.007% (v/v) β-Me) for 30 minutes at 50°C on a rocker. The membrane was then washed in TBST six times for 5 minutes and blocked in 5% Marvel for 1 hour at room temperature before incubating with the primary antibody overnight at 4°C.

2.6 Paraffin-embedding and sectioning of prostate tissue

2.6.1 Preparation of prostate tissue for paraffin-embedding

Small segments of prostate tissue biopsies and TURPs were submerged in formalin overnight. The following day, the tissue was moved to a histocassette and placed in 70% ethanol until paraffin embedding. Filter paper was added to the histocassette to avoid small pieces of tissue being lost through the gaps.

2.6.2 Preparation of cell pellets for paraffin-embedding

BPH-1 cells were grown in a monolayer in a 10cm dish until confluent. Cells were detached via incubation with trypsin and collected by centrifugation at 1500 RPM for 5 minutes. The pellet was then washed once in PBS and transferred to a 1.5ml microcentrifuge tube. Cells were centrifuged at 6500 RPM for 2 minutes and the pellet was resuspended in 225µl of blood plasma with 5.6µl of 1M calcium chloride added. 22.5µl of thrombin (120 NIH-U/ml, Sigma) was added to the cell mixture, stirred with a pipette tip and left to coagulate for a few minutes.

A histocassette was set up as follows; a layer of filter paper at the bottom, a sponge layer with a hole cut out of the middle to insert the coagulated cell pellet followed by another filter paper on top. The assembled histocassette was then placed in formalin to replicate fixation of prostate tissue. After four hours (the pellet did not require as long as tissue for the formalin to penetrate) the histocassette was moved to 70% ethanol until paraffin embedding.

2.6.3 Paraffin-embedding of cell pellets and prostate tissue

Prepared tissues and cell pellets in histocassettes were transferred from storage 70% ethanol into fresh 70% ethanol for 10 minutes. Histocassettes were then placed in 100% ethanol 3 x 10 minutes, propan-2-ol 2 x 10 minutes and xylene 4 x 10 minutes. Excess xylene was blotted on blue roll. Four paraffin wax pots were melted in an oven at 60°C the previous evening and the histocassettes were placed in each pot for 15 minutes consecutively. The samples were then removed from the histocassette and placed and orientated in metal moulds partially filled with molten wax from an urn. The lid of the histocassette (with label) was placed on top of the sample and the mould was filled up with molten wax. The samples were set on a cold plate for 20 minutes and removed from the mould. Samples were stored at room temperature until sectioning.

2.6.4 Sectioning of paraffin-embedded samples

SuperFrost Plus Slides (ThermoFisher Scientific) were first coated in 3-Aminopropyltriethoxysilane (APES) as follows: submerged in 2% APES in acetone for 1 minute, 2 x acetone washes, 2 x distilled water washes and placed on a slide dryer overnight.

Paraffin-embedded tissues and cell pellets were sectioned on a Leica RM2235 microtome. Sections were 5µm thick and placed on APES coated slides and placed on a slide dryer overnight.

2.7 Immunostaining

2.7.1 Immunohistochemistry (IHC) – prostate tissue and cell pellets

Paraffin-embedded prostate tissue sections were baked at 45°C for 20 minutes on a slide dryer. Deparaffinisation and rehydration were performed by immersing slides in the following baths; xylene 2 x 10 minutes, xylene 1 x 1 minute, 100% ethanol 3 x 1 minute and 70% ethanol 1 x 1 minute. Slides were then washed for 5 minutes under running tap water. Heat-induced epitope retrieval (HIER) was carried out in sodium citrate buffer (pH 6) using the 2100 Antigen Retriever (Aptum Biologics) pressure cooker overnight.

Slides were washed three times in PBS for 5 minutes on an orbital shaker. A PAP pen (Dako) was used to create a hydrophobic barrier around each tissue section, which was subsequently blocked in 10% (v/v) FCS in PBS for 1 hour at room temperature in a dark, moist box. The block was removed and sections were incubated in primary antibody diluted in 10% (v/v) FCS in PBS overnight at 4°C in the box (Table 2.7).

The following day, slides were washed three times in PBS for 5 minutes and treated with 3% (v/v) hydrogen peroxide in PBS for 30 minutes to remove endogenous peroxidases. Slides were rinsed in PBS and then incubated with the secondary biotinylated antibody diluted in 10% (v/v) FCS in PBS for 30 minutes at room temperature. After washing three times in PBS for 5 minutes, they were then incubated with the tertiary antibody (streptavidin-HRP) diluted in 10% FCS for 30minutes at room temperature. Slides were washed twice in PBS for 5 minutes and sections were then incubated with diaminobenzidene (ImmPACT DAB peroxidase substrate, Vector Laboratories) until sections started to turn brown (10 seconds – 2 minutes). Following rinsing in distilled water and then running tap water for 5 minutes, sections were counterstained with haematoxylin for 3 seconds, rinsed with water and then dehydrated through the following baths; 70% ethanol 1 x 1 minute, 100% ethanol 3 x 1 minute and xylene 2 x 1 minute. The slides were then mounted with DPX (Sigma Aldrich) and covered with a coverslip.

Antibody	Primary (P)/ Secondary (S) /Tertiary (T)	Manufacturer	Cat no.	Species	Working Dilution
ELF3	P	Abcam	Ab97310	Rabbit poly	1:1000
p63	P	Dako	M7317	Mouse mono	1:500
HMW-CK	P	Dako	M0630	Mouse mono	1:800
Nkx3.1	P	Menapath	MP-422-CR01	Rabbit poly	1:800
AMACR	P	Dako	M3616	Rabbit mono	1:100
Rabbit anti-mouse biotinylated	S	Dako	E0354	Rabbit poly	1:200
Goat anti-rabbit biotinylated	S	Dako	E0432	Goat poly	1:500
Streptavidin-HRP	T	Dako	P0397		1:100

Table 2.7. Antibodies used for protein detection by immunohistochemistry.

2.7.2 IHC using the ImmPRESS Excel Amplified HRP Polymer Staining Kit

The ImmPRESS Excel Amplified HRP Polymer Staining Kit (anti-rabbit IgG kit: MP-7601, anti-mouse IgG kit: MP7602, Vector Laboratories) was employed to amplify signal of potentially weakly expressed antigens. Baking, deparaffinisation, hydration and antigen retrieval was carried out as described in section 2.5.1. All further reagents used were provided in the kit.

The following day sections were incubated with BLOXALL blocking solution for 10 minutes to quench endogenous peroxide activity and subsequently washed in running water for 10 minutes. Sections were then blocked in 2.5% normal horse serum for 20 minutes. The block was removed and sections were incubated in primary antibody diluted in 2.5% normal horse serum overnight at 4°C in a dark moist box.

Slides were washed three times in TBST for 5 minutes and then incubated with Amplifier Antibody for 15 minutes followed by another two washes in TBST for 5 minutes. Sections were then incubated with ImmPRESS Excel Reagent for 30 minutes and washed once in TBST and then in dH_2O for 5 minutes. Equal

volumes of ImmPACT DAB *EqV* Reagent 1 and 2 were combined and added to sections until they turned brown (10 seconds – 2 minutes). Sections were then rinsed in dH_2O followed by running tap water. Slides were counterstained with haematoxylin for 3 seconds, rinsed with water and dehydrated and mounted as described in section 2.5.1.

2.7.3 Immunocytochemistry (ICC) – fixed cells

Cells were plated onto 8 well chamber slides and left to adhere overnight (~10,000 cells/well). Corning Biocoat collagen-I coated slides were used for primary prostate cells whilst uncoated Falcon culture slides were used for cell lines (Corning). Following two PBS washes, cells were then fixed with either 200µl 4% paraformaldehyde (PFA) pH 7.4 for 10 minutes at room temperature or 1:1 methanol:acetone for 30 seconds at room temperature. After washing in PBS three times for 5 minutes, cells were permeabilised using 200µl 0.5% (v/v) Triton X-100 in PBS for 10 minutes at room temperature. Following a further three PBS washes for 5 minutes, cells were then blocked in 10% (v/v) goat serum in PBS for 1 hour at room temperature. Cells were then incubated with primary antibody diluted in 10% goat serum overnight at 4°C. Secondary antibody only controls were performed by incubating in 10% goat serum only overnight. Primary and secondary antibodies used are shown in Table 2.8.

The following day, slides were washed three times in PBS for 5 minutes and incubated with 200µl secondary antibody at a dilution of 1:1000 in 10% goat serum. Cells were washed a final five times with PBS for 5 minutes whilst protected from light and the chambers were then removed. Nuclear staining was performed using Vectashield mounting medium with 4',6-diamidino-2-phenylindole (DAPI) (Vector Laboratories) and slides covered with a coverslip (22x50mm, SLS) and sealed with clear nail varnish.

Slides were analysed on a Leica DMIL LED fluorescent microscope or a Zeiss LSM 880 confocal microscope.

Antibody	Primary (P)/ Secondary(S)	Manufacturer	Cat no.	Species	Working Dilution
ELF3	P	Abcam	Ab133621	Rabbit mono	1:1000
ELF3	P	Santa Cruz	sc-376055	Mouse mono	1:50-1:500
ELF3	P	Sigma Prestige	HPA003479	Rabbit poly	1:50
Ki67	P	Abcam	Ab15580	Rabbit poly	1:800
Active β-catenin	P	Cell Signalling Technology	8814S	Rabbit poly	1:600
Cytokeratin 5	P	Abcam	Ab52635	Rabbit mono	1:500
Cytokeratin 18	P	Sigma	C8541	Mouse mono	1:800
Tubulin	P	Abcam	Ab7291	Mouse mono	1:250
Phospho-histone 3	P	Merck	06-570	Rabbit poly	1:500
Goat anti-rabbit IgG Alexa Fluor 568	S	Invitrogen	A-11036	Goat poly	1:1000
Goat anti-mouse IgG Alexa Fluor 488	S	Invitrogen	A-11029	Goat poly	1:1000

Table 2.8. Antibodies used for protein detection by immunocytochemistry.

2.8 Lentiviral cloning and virus production

2.8.1 *attB* sequence flanking of ELF3

Invitrogen Gateway Cloning Technology (ThermoFisher Scientific) was utilised to produce lentiviral vectors for ELF3 overexpression, which is based on bacteriophage lambda *att* site recombination. For the desired sequence to be incorporated into the vector, it was first flanked with *attB* sequences via two rounds of PCR amplification and gel extraction. A reaction mix of 20µl was prepared according to Tables 2.9 and 2.10. PCR reactions were performed using the Phusion polymerase kit (New England Biolabs) and all components were kept on ice. Thermocycling conditions were as follows; 98°C for 30 seconds, 30 cycles of 98°C for 10

seconds, 66°C for 30 seconds and 72°C for 30 seconds, with a final extension of 72°C for 10 minutes on the GeneAmp PCR System 9700 (Applied Biosystems). Plasmid DNA template pGEMT-easy-ELF3-WT was provided by Prof Jenny Southgate and pEGFP-ELF3-ΔAT was provided by Prof Arthur Gutierrez-Hartmann.

Component	Volume per sample
5x HF Phusion Buffer	4
Forward primer (10μM)	1
Reverse primer (10μM)	1
dNTPs (10mM)	0.4
DNA template	100ng
Phusion polymerase	0.1
Nuclease free H_2O	Up to 20μl

Table 2.9. Components used for *attB* flanking of ELF3 by PCR.

Primer Name	Description	Sequence
ELF3-overhang	Outer ELF3 and inner *attB* sequence	F: 5' – CAAAAAAGCAGGCTCCAT GGCTGCAACCTGTGAG – 3' R: 5' – CAAGAAAGCTGGGTCTCA GTTCCGACTCTGGAGAA – 3'
Outer *attB*	Outer *attB* sequence	F: 5' – GGGGACAAGTTTGTACAA AAAAGCAGGCT – 3' R: 5' – GGGGACCACTTTGTACAA GAAAGCTGGGT – 3'

Table 2.10. Primer sequences for sequential *attB* flanking of ELF3.

2.8.2 Gel extraction

PCR products were run on a 1% (w/v) agarose gel in Tris-acetate EDTA (TAE) buffer with SYBR Safe DNA gel stain (Invitrogen) at 60V for 90 minutes. Bands were visualised, excised into a 2ml microcentrifuge tube

and DNA was recovered using the QIAquick Gel Extraction kit (QIAGEN). Briefly, the amount of gel was weighed and the appropriate volume of QG buffer was added (100µl for every 100mg of gel). Tubes were incubated at 50°C for 10 minutes and vortexed every 3 minutes until the gel dissolved. An equal volume of isopropanol was then added to the tubes and mixture was transferred to a QIAquick column and centrifuged for 1 minute at 13,000 RPM. 500µl of Buffer QG was added and centrifuged for a further minute and the flow through discarded. The column was centrifuged for 1 minute at 13,000 RPM to remove residual buffer and then placed into a clean 1.5ml microcentrifuge tube. 30µl Sigma water was added to the column and left standing for 4 minutes before eluting the DNA by centrifuging for 1 minute at 13,000 RPM.

2.8.3 BP reaction

The BP recombination reaction was performed by adding 25ng of the ELF3-*att*B PCR product to 150ng of the empty DONR vector (pDONR221) and Sigma water to make a total volume of 8µl. The BP clonase was thawed on ice and 2µl was added to each sample. The samples were incubated overnight at 25°C using the GeneAmp PCR Sytem 9700 (Applied Biosystems) and then stopped using 1µl of proteinase K (Invitrogen) before transformation into DH5α competent cells (Section 2.6.4).

2.8.4 Transformation and bacterial cultures

MAX Efficiency DH5α competent cells (Invitrogen) were thawed on ice for 20 minutes. Meanwhile, lysogeny broth (LB) agar plates containing the appropriate antibiotic were warmed to 37°C. DONR vectors were selected on kanamycin plates (30µg/ml) whilst Destination vectors were selected on carbenicillin plates (50µg/ml). The recombination reaction mixture was added to the competent cells, mixed by swirling the pipette tip and incubated on ice for 30 minutes. The mixture was heat shocked at 42°C for 45 seconds in a waterbath and incubated on ice for a further 2 minutes. 200µl of S.O.C media (ThermoFisher Scientific) without antibiotic was added and the mixture was incubated at 37°C whilst shaking at 225 RPM for 1 hour. The transformation mixture was then spread on warmed agar plates using a glass spreader and incubated overnight at 37°C.

Single colonies were picked and used to inoculate a 5ml LB broth with the appropriate antibiotic and incubated at 37°C for 16-18 hours with shaking at 225 RPM. Glycerol stocks of each clone were generated by adding 850µl of bacterial culture to 150µl of glycerol into a cryovial before vortexing and storing at -80°C.

2.8.5 Miniprep

Plasmid DNA was purified using the QIAprep Spin Miniprep Kit (QIAGEN) using the manufacturer's instructions. Briefly, bacterial cells from overnight cultures were harvested by centrifuging at 3000 RPM for 10 minutes at room temperature in a Heraeus Megafuge 1.0R centrifuge (Thermo Scientific). Cells were then resuspended in 250µl Buffer P1 and transferred to a microcentrifuge tube. 250µl Buffer P2 was added and mixed by tapping the tube until the mixture became viscous. After 5 minutes at room temperature, 350µl of Buffer N3 was added, mixed immediately and thoroughly by inverting the tube until the mixture became

white and cloudy. Tubes were then centrifuged at 13,000 RPM for 10 minutes and the resulting supernatant was transferred to a QIAprep spin column and centrifuged at 13,000 RPM for 1 minute. The flow-through was discarded and the column was washed with 500µl of Buffer PB. Columns were centrifuged at 13,000 RPM for 1 minute and the flow through was discarded. Columns were then washed in 750µl of Buffer PE. The flow-through was discarded and the columns were centrifuged again at 13,000 RPM for 1 minute to remove any remaining wash buffer. The QIAprep column was transferred to a clean 1.5ml microcentrifuge tube, 50µl of Sigma water was added and allowed to absorb into the column for 1 minute. DNA was eluted by centrifuging for 1 minute at 13,000 RPM. DNA concentration and quality was calculated by a NanoDrop ND-1000 spectrophotometer (Thermo Scientific).

2.8.6 LR reaction

The LR recombination reaction was performed by adding 1µl of the empty Destination vector (pDest298 or pDest159) at 100ng/µl to 1µl of the pENTR vector produced during the BP reaction (pDONR227-ELF3-WT clone 7) at 50ng/µl into a PCR tube. 1µl of Sigma water was added to the reaction and finally 1µl of LR Clonase which was thawed on ice. The reaction was incubated overnight at 25°C using the GeneAmp PCR Sytem 9700 (Applied Biosystems) and then stopped using 1µl of proteinase K (Invitrogen) before transformation into DH5α competent cells (Section 2.6.4).

2.8.7 PCR

PCR amplification was carried out to determine if ELF3 was present in plasmid clones. A reaction mix of 20µl was prepared according to Table (Section 2.7.1). Primers used are shown in Table 2.11. PCR reactions were performed using the Phusion polymerase kit (New England Biolabs) and all components were kept on ice. Thermocycling conditions were as follows; 98°C for 30 seconds, 30 cycles of 98°C for 10 seconds, 66°C for 30 seconds and 72°C for 30 seconds, with a final extension of 72°C for 10 minutes. Products were analysed on a 1% (w/v) agarose gel in TAE buffer with GelRed nucleic acid stain (1:10,000, Biotium). Size of bands was determined using the MassRuler Express Reverse DNA ladder (ThermoFisher Scientific). Gels were visualised using GeneSnap ID software (Syngene).

Primer	Sequence
ELF3 Forward	5' – TCGGAGGACTCCACCCTG – 3'
ELF3 Reverse	5' – CCCAACCAGCTGGCCTTC – 3'

Table 2.11. ELF3 primer sequences for PCR.

2.8.8 Restriction digest

Restriction digests were carried out on single selected clones. 250ng of DNA was added to 2µl of the appropriate buffer and 1µl of enzyme (EcoRI, BamHI or PvuII, New England Biolabs). Reactions were made up to 10µl in Sigma water and incubated at 37°C for 1 hour. The products were subjected to gel electrophoresis on a 1% (w/v) agarose gel in TAE buffer with GelRed nucleic acid stain (1:10,000) at 60V for 90 minutes.

2.8.9 Plasmid transfection

HEK-293T cells were transfected with several clones of each generated ELF3-overexpressing plasmid using X-tremeGENE HP DNA transfection reagent (Roche). 3 x 10^5 cells were plated on 6 well poly-L-lysine (0.1mg/ml, Sigma Aldrich) coated plates and left to adhere overnight. A total reaction volume of 200µl was prepared. All reagents were warmed to room temperature before use consisting of 2µg of plasmid and 6µl of X-tremeGENE HP DNA transfection reagent, topped up with Opti-MEM reduced serum media. The transfection mix was incubated for 45 minutes at room temperature before adding dropwise to wells. GFP expression was examined on a Leica DMIL LED fluorescent microscope at 24 and 48 hours post-transfection.

2.8.10 Lentivirus production and concentration

Lentivirus production was carried out in HEK-293T cells which had been modified from HEK-293T cells by transformation with SV40 large T antigen. This modification results in a highly transfectable cell line which is beneficial for lentivirus production (Pear et al., 1993). 7.5 x 10^5 HEK-293T cells were plated into 6 well poly-L-lysine coated plates and left to adhere overnight. The following day 2ml of fresh D10 media was added to wells 2 hours before transfection. The transfection mixture was prepared to a total volume of 200µl. All reagents were warmed to room temperature before use. Reduced serum Opti-MEM was added to a 1.5ml microcentrifuge tube. The plasmid mix was then added and gently mixed. This was composed of the desired Destination vector (2µg/well) and the viral packaging plasmids pVSV-G (0.5µg/well) and psPAX2 (1.5µg/well). X-tremeGENE HP DNA transfection reagent (Roche) was then added at a ratio of 3:1 (12µl/well) and mixed gently. The transfection mixture was incubated at room temperature for 45 minutes and then added dropwise to wells.

The viral supernatant was collected at 48 hours post-transfection and filtered using a Millex-HV 0.45µm PVDF syringe filter (Merck). The virus was concentrated using PEG-*it* precipitation solution. 1ml of PEG-*it* solution was added for every 4 volumes of filtered viral supernatant and incubated at 4°C overnight. The supernatant was centrifuged at 1500G for 30 minutes at 4°C, transferred to a new vial and residual virus was centrifuged at 1500G for a further 5 minutes. The resulting pellets were resuspended and combined in PBS at 1:10 of the original volume. This was then aliquoted into cryovials and stored at -80°C.

The control pDest298-GUS plasmid was provided by Alberto Taurozzi.

2.8.11 Lentivirus titre

5 x 10^4 P4E6 cells were transduced in suspension with 10-fold serial dilutions of concentrated virus between a range of 1:10 and 1:100,000. Cells were plated onto 24 well plates and the media was changed 16 hours after transduction. Cells were analysed at 48 hours post-transduction by flow cytometry on a CyAn ADP (Beckman Coulter). Results were analysed using Summit software. The population of interest was gated on using FS Lin/SS Log and singlets were gated on using pulse width. The GFP-positive population was gated on using FITC Log. Viral titre was determined using dilutions which produced between 1 and 20% of GFP-positive P4E6 cells. Viral titre was calculated using the following formula:

$$Titre = \frac{number\ of\ starting\ cells\ \times dilution\ factor\ \times (\%\ GFP\ positive\ cells\ \div 100)}{volume}$$

2.8.12 Lentiviral transduction of primary prostate epithelial cells

3 x 10^5 primary prostate epithelial cells were transduced in suspension with pDest298-GUS, pDest298-ELF3-WT or pDest298-ELF3-ΔAT at a ratio of three infectious particles for each cell. The cells were plated onto a 10cm dish topped up with 5ml of SCM. The media was changed 16 hours post-transduction, changed every two days thereafter until the 10cm dishes were 90% confluent. The cells were then used for various functional assays.

1 x 10^4 primary prostate epithelial cells were transduced in suspension with pDest159-GUS, pDest159-ELF3-WT or pDest159-ELF3-ΔAT at a ratio of three infectious particles for every one cell. The pDest159-GUS virus was provided by Alberto Taurozzi. The cells were plated onto a collagen-coated chamber slide (Corning) and topped up with 200ul of SCM. The media was changed 16 hours post-transduction and cells were fixed in 4% PFA the following day.

2.9 Cell function assays

2.9.1 Cell viability assay

AlamarBlue quantitatively measures cell viability since actively metabolising cells can reduce its active ingredient resazurin to a fluorescent molecule (resorufin) which can be subsequently analysed on a plate reader. Cells were plated in 24 well plates in triplicate at a density of 4 x 10^4 BPH-1 cells/well and 6 x 10^4 PC3 cells/well and left to adhere overnight in 500µl media. The following day cells were transfected according to section 2.6.11. At days 1, 2 and 3, 50µl of alamarBlue reagent (diluted 1:10 in the corresponding media for each cell line) was added to each well and incubated at 37°C for 2 hours. Fluorescence intensity was determined using a microplate reader (Polarstar Optima, BMG Labtech) at excitation/emission values

of 544/590nm. As cells were approaching confluency at day 3, they were trypsinised and replated at the original plating density, viability was analysed on days 4, 5 and 6.

2.9.2 Cell adhesion assay

To assess the effect of ELF3 knockdown on cell adhesion, BPH-1 cells following knockdown were detached by incubation with trypsin and replated in a 6-well plate at three different densities; low (40,000), medium (100,000) and high (300,000). Cells were left to adhere for 4 hours at which point non-adherent cells were washed off and adherent cells were trypsinised and counted using the Vi-Cell Cell Viability Analyser (Beckman Coulter).

2.9.3 Wound healing assay following ELF3 knockdown in prostate epithelial cell lines

Cells were plated onto 12 well plates in triplicate (2 x 10^5 BPH-1, 2.5 x 10^5 PC3 per well) and left to adhere overnight. Cells were transfected the following day according to Section 2.5.1. At 24 hours post-transfection, a wound was made in the confluent monolayer using the end of a blue tip. Images were taken at zero hours using an EVOS XL transmitted light microscope (AMG) at 10x. The end point was determined by monitoring the wounds until the first triplicate set of one condition (mock, siSCR or siELF3) had closed. The average width of the wounds was determined between 10 points using Image J software. Percent wound closure was calculated at the end point relative to zero hour images.

2.9.4 Wound healing assay following ELF3 overexpression in primary prostate epithelial cells

Primary prostate epithelial cells were transduced with lentiviral ELF3 overexpression vectors as described in Section 2.7.12. 2.1 x 10^4 cells were plated into each well of a 2-well insert (Ibidi) in 12 well plates in triplicate according to manufacturer's instructions. The insert ensures the cell-free gap is consistent between wells. Cells were left to adhere overnight and the following day the inserts were removed and the plates were put onto the VL21 microscope (Phasefocus, www.phasefocus.com) to monitor wound closure via live cell real time imaging. The data was processed by Amanda Noble using Cell Analysis Toolbox (CAT) software and analysed by myself.

2.9.5 Colony forming assay

Colony forming assays were carried out by plating 200 BPH-1 or PC3 cells into 12 well plates in triplicate. Cells were plated 24 hours after knockdown treatment (mock, siSCR or siELF3), and were supplemented with fresh media every two days. At day 7, cells were stained with crystal violet (1% (w/v) crystal violet, 10% (v/v) ethanol in PBS). Colonies consisting of >32 cells were counted (representative of 5 population doublings) (Puck and Marcus, 1956, Francipane et al., 2008).

2.9.6 Cell cycle analysis

Cell cycle analysis was carried out by flow cytometry using the Click-iT Plus EdU Pacific Blue Flow Cytometry Kit (ThermoFisher Scientific) and propidium iodide according to the manufacturer's instructions.

Briefly, 4 x 10^4 BPH-1 and 8 x 10^4 PC3 cells were plated onto a 12 well plate. The following day cells were transfected for knockdown according to section 2.6.11. On days 1, 2 and 3 post-transfection cells were treated with 10μM EdU. After 4 hours, cells were trypsinised and harvested and washed in 3ml 1% BSA in PBS. The pellet was resuspended in 100μl Click-iT fixative and incubated at room temperature for 15 minutes away from light. Cells were washed in 3ml 1% BSA in PBS and then stored in PBS at 4°C until the day they were to be analysed by flow cytometry.

Cells were centrifuged and resuspended in 100μl of 1x Click-iT saponin-based permeabilisation and wash reagent and incubated at room temperature for 15 minutes. 500μl of the Click-iT Plus reaction cocktail (438μl PBS, 10μl copper protectant, 2.5μl fluorescent dye picolyl azide, 50μl reaction buffer additive) was added to each tube, mixed well and incubated at room temperature for 30 minutes away from light. Cells were then washed in 1x Click-iT saponin-based permeabilisation and wash reagent, centrifuged and resuspended in 400μl of the same reagent. 50μl of RNase A (1mg/ml, Sigma) and 50μl propidium idodide (400μg/ml, Sigma) were added to each sample and incubated at 37°C for 30 minutes before analysing on the flow cytometer.

Results were analysed using Summit software. The cell population of interest was gated using a FS Lin/SS Log histogram and doublets were excluded using a PE-Texas Red Lin/PE-Texas-Red Area histogram. PE-Texas Red Area/Violet 1 Log was used to determine the proportion of cells in G1, S and G2 phases of the cell cycle. At least 10,000 events were collected for significance.

A pulse-chase experiment was also set up to assess progression of cells through the cell cycle. Cells were treated with 10μM EdU for 4 hours (pulse) and one well was then harvested and the medium was replaced in duplicate wells with normal growth medium. These cells were then harvested at 24 hours (chase). Cells were then analysed using the above protocol.

2.10 Statistical analyses

Unless otherwise stated, statistical analyses were carried out using GraphPad Prism 6/7 software (San Diego, USA). Functional assays were carried out in technical replicate (at the same time with the same passage of cells, n=3) and biological replicate (at a separate time point with a different passage of cells, n≥3). Significance was calculated on at least three biological replicates using tests described in figure legends. Results were expressed as the mean with associated standard deviation unless otherwise stated. Statistical significance was represented on graphs as * $p = 0.01$ to 0.05, ** $p = 0.001$ to 0.01, *** $p = 0.0001$ to 0.001, **** $p < 0.0001$.

3. Results

3.1 ELF3 expression in prostate epithelial cell lines

3.1.1 ELF3 is ubiquitously expressed in a range of prostate cell lines

ELF3 has been ascribed both oncogene and tumour suppressor roles in the prostate (Longoni et al., 2013, Shatnawi et al., 2014). These reported studies focused on manipulating ELF3 expression in the prostate cell lines LNCaP, Du145 and 22RV1. To ascertain the expression pattern of ELF3 in all epithelial cell types in the prostate, qRT-PCR was carried out on a range of cell lines derived from normal prostate, benign prostate, localised PCa and PCa metastases (Table 3.1). The absolute transcript copy number of ELF3 was determined using a standard curve of serial dilutions of the pGEM-TEasy-ELF3 plasmid. The standard curve was then used to determine the gene expression levels of ELF3 in the prostate cell lines. ELF3 was most highly expressed in the normal PNT2-C2 cell line, but had relatively low expression in the PNT1a cell line which is also derived from normal prostate and both represent androgen-independent luminal cells. The intermediate BPH-1, PC3 and Du145 cell lines showed moderate expression and P4E6 (intermediate), LNCaP (luminal), and 22RV1 (luminal) expressed relatively low levels of ELF3 (Figure 3.1A). The level of ELF3 expression in each cell line was predominantly mirrored at the protein level (Figure 3.1B). These results demonstrate that there was no clear pattern of expression of ELF3 in relation to diagnosis or basal/luminal phenotype.

Cell Line	Origin	Selected Epithelial Hierarchy Markers	Basal/Luminal /Intermediate	AR Expression	PSA Expression	Reference
PNT1a	Normal prostate	CK8, CK18	Androgen-independent Luminal	-	-	(Mitchell et al., 2000)
PNT2-C2	Normal prostate	CK8, CK18	Androgen-independent Luminal	-	-	(Berthon et al., 1995, Lang et al., 2001a)
BPH-1	BPH	CK5, CK8, CK18	Intermediate	-	-	(Hayward et al., 1995, Pellacani et al., 2014)
P4E6	Localised PCa	CK8, CD44	Intermediate	-	+	(Maitland et al., 2001)
PC3	Lumbar vertebral bone metastasis	CK5, CK8, CK18 CD44	Intermediate	-	-	(Kaighn et al., 1979, van Leenders et al., 2001)
Du145	Brain metastasis	CK5, CK8, CK18,	Intermediate	-	-	(Sobel and Sadar, 2005)
LNCaP	Lymph node metastasis	CK8, CK18	Luminal	+	+	(Horoszewicz et al., 1983)
22RV1	Xenograft of relapsed CWR22 xenograft	CK8, CK18	Luminal	+	+	(Sramkoski et al., 1999)

Table 3.1. Origin and phenotypic characteristics of prostate epithelial cell lines.

CK = cytokeratin, AR = androgen receptor, PSA = prostate specific antigen, BPH = benign prostatic hyperplasia, PCa = prostate cancer. Markers of basal cells – CD44, CK5. Markers of luminal cells – CK8, CK18, AR. Expression of CK5 in absence of CK14 indicated an intermediate phenotype.

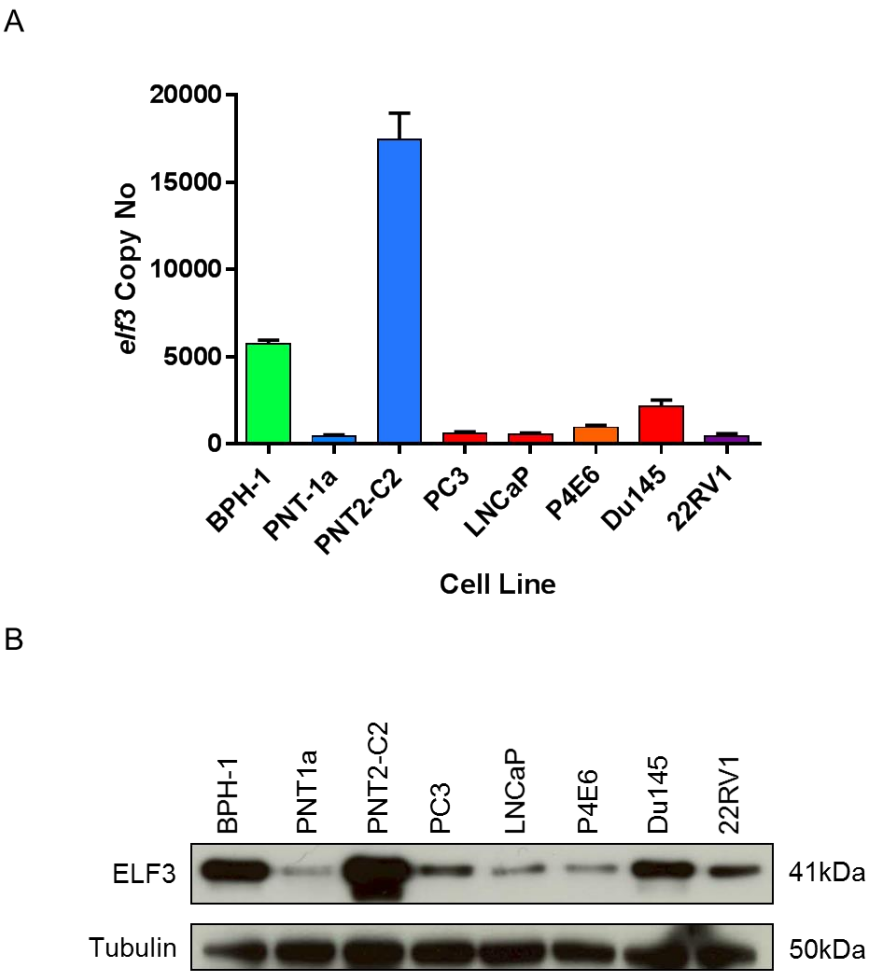

Figure 3.1. mRNA and protein expression of ELF3 in prostate epithelial cell lines.

Expression of ELF3 was examined in a range of prostate cell lines at the mRNA and protein level. (A) 30ng of cDNA was analysed by qRT-PCR. A standard curve of 5-fold serial dilutions of pGEM-TEasy-ELF3 plasmid was used for absolute quantification of ELF3 gene expression. Colours indicate diagnosis of respective cell lines. Blue = normal, green = benign prostatic hyperplasia, orange = primary PCa, red = metastatic PCa, purple = derived from mouse model of PCa. (B) Protein expression was analysed by western blot analysis. 20µg of protein was loaded per lane onto a 10% SDS gel, transferred onto a PVDF membrane and probed for the indicated proteins. Tubulin was used as a loading control.

3.2 ELF3 expression in primary prostate epithelial cells

3.2.1 ELF3 is more highly expressed in the committed basal cell population of primary prostate cultures as detected by microarray analysis

An Affymetrix gene expression microarray was previously carried out in our lab, on enriched SC and CB epithelial cell populations derived from both human benign prostatic hyperplasia (BPH) and PCa tissue (Birnie et al., 2008). A total of seven BPH and twelve PCa tissues were processed and enriched for SC ($\alpha_2\beta_1^{hi}$/CD133$^+$) and CB cells ($\alpha_2\beta_1^{lo}$/CD133$^-$). Only treatment naïve PCa samples with a Gleason score of 7 or above were included in the analysis as this resulted in clustering of samples based on diagnosis and differentiation state. The data was reanalysed to determine the expression of ELF3.

There was a significant increase in ELF3 expression in CB cells compared to SC across three individual probes (Figure 3.2). However, there was no significant difference in ELF3 expression between benign and malignant samples when cell types were pooled. This suggests that, ELF3 expression is linked to the differentiation state of prostate epithelial cells regardless of diagnosis.

A

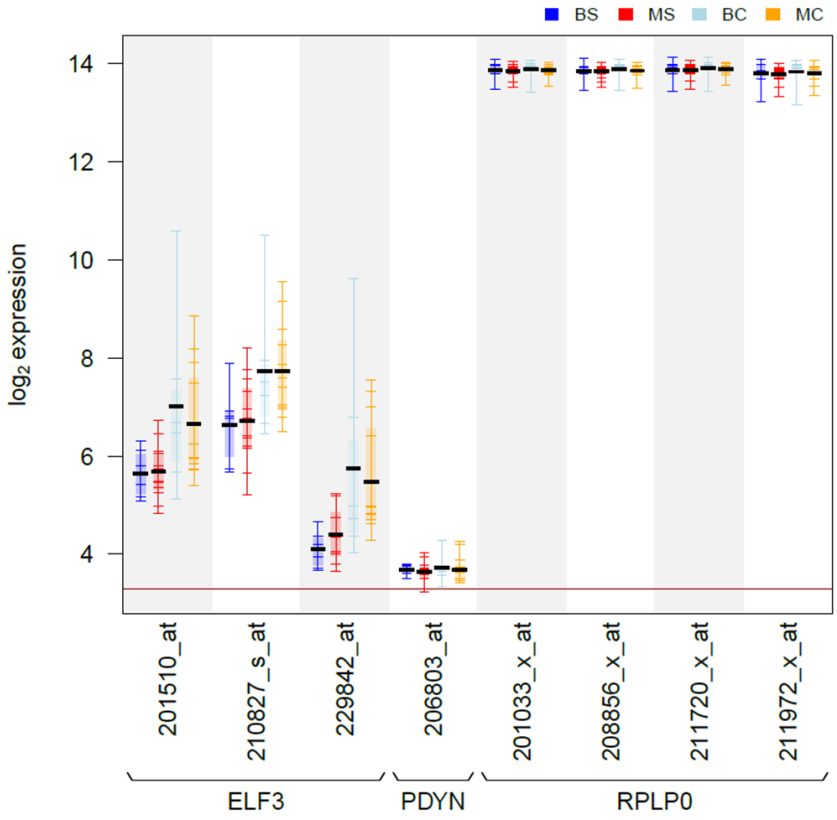

B

Probe	BPH SC vs BPH CB	PCa SC vs PCa CB	SC vs CB
201510_at	0.1258	0.0152	0.0038
210827_s_at	0.1461	0.0145	0.0035
229842_at	0.0898	0.0114	0.0020

Probe	BPH SC vs PCa SC	BPH CB vs PCa CB	BPH vs PCa
201510_at	0.9016	0.6270	0.7074
210827_s_at	0.8613	0.9987	0.9225
229842_at	0.2874	0.7297	0.9814

P < 0.05
P < 0.01

Figure 3.2. Affymetrix gene expression microarray data analysis from benign and malignant prostate suggests ELF3 is expressed at higher levels in the committed basal cell subpopulation compared to stem cells.

Affymetrix gene-expression arrays were carried out on the sorted cell populations from seven benign prostatic hyperplasia (BPH) and twelve prostate cancer (PCa) tissues obtained from patients. (A) ELF3 gene expression was compared between stem cell (SC) and committed basal (CB) cell populations derived from BPH and cancer tissues. RPLPO (ribosomal protein lateral stalk subunit P0) and PDYN (prodynorphin) were used as positive and negative control genes, respectively. BS = benign stem cells, MS = malignant stem cells, BC = benign committed cells, MC= malignant committed cells. (B) Tables indicate the P values of individual ELF3 probes in SC vs CB (top panel) and BPH vs cancer (bottom panel). Statistical significance was measured using the Student's T-test (unpaired, two-tailed). Significant values are highlighted in blue. Data generated by mining array from (Birnie et al., 2008).

3.2.2 ELF3 is expressed in the CB population of primary prostate cultures at the protein level

To add to the RNA expression profile of ELF3 found in the microarray data, ELF3 protein expression was examined in primary prostate samples by SDS-PAGE and western blotting. Initial blots showed that lysates containing whole epithelial populations did not express ELF3 (data not shown). BPH and PCa tissues were then cultured and enriched for TA and CB subpopulations. ELF3 was consistently expressed in the CB population of both BPH (n=4) and PCa (n=4) samples (Figure 3.3). There was very little expression or no detection of ELF3 in the TA population of any samples. Furthermore, there was no differential expression between BPH and PCa.

When performing western blot analysis on lysates derived directly from BPH tissue homogenates, ELF3 was not detected (Figure 3.4A). This suggests the threshold of ELF3 expression is below the limit of detection due to the heterogeneous nature of the cells. Since the tissue homogenates contain stroma as well as epithelial glands and CB cells only comprise a fraction within the basal layer, this may not be surprising.

Stromal cells can also be separated and cultured from prostate tissue. Lysates from six primary prostate stromal cultures (1 BPH and 5 PCa) showed no ELF3 expression by western blot (Figure 3.4B). As luminal cells are terminally differentiated, they cannot be grown in culture. Likewise, the SC population is so rare that upon CD133 microbead selection from six 10cm dishes only a few thousand are generally recovered. For these reasons the luminal and SC populations were excluded from protein analysis.

Together these results correspond with the initial microarray data with regards to high ELF3 expression in the CB population and no significant difference in expression between BPH and PCa. ELF3 is also not expressed in prostate stroma, which may be expected as ELF3 is an epithelial-specific transcription factor (Oettgen et al., 1997). Since ELF3 is expressed at low levels in the SC and TA populations, the more primitive cell types of the prostate epithelial differentiation hierarchy, this further reinforces the hypothesis that ELF3 may be involved in prostate epithelial cell differentiation, either as cause or consequence.

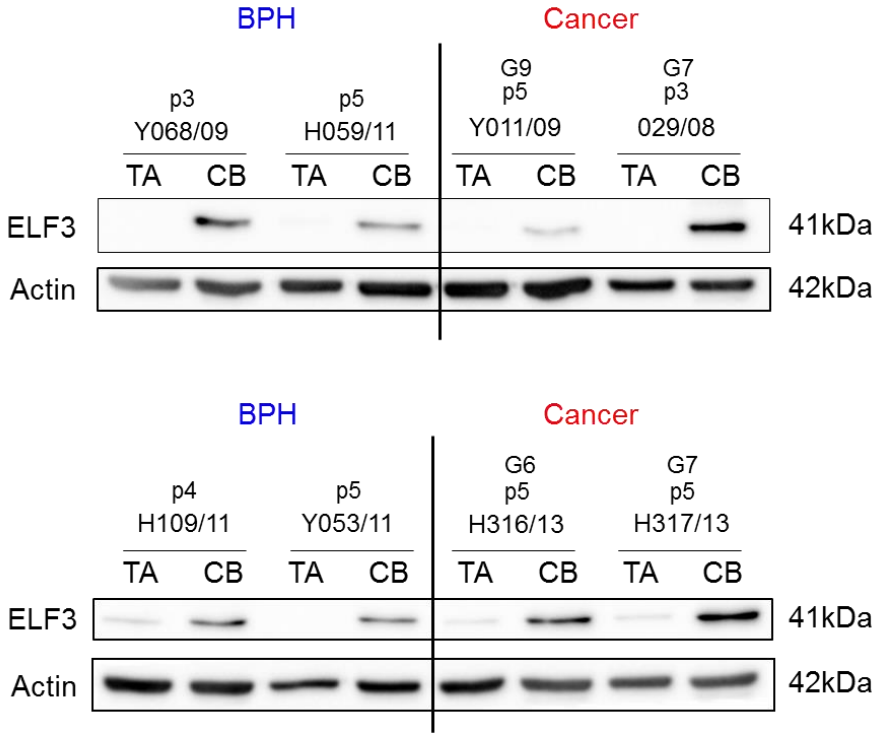

Figure 3.3. Protein expression of ELF3 in the fractionated cell subpopulations from primary prostate benign and tumour samples.

Western blot analysis of ELF3 protein expression in the TA and CB cell subpopulations of primary BPH and PCa samples. 20µg of protein was loaded per lane onto a 10% SDS gel, transferred onto a PVDF membrane and probed for the indicated proteins. Actin was used as a loading control. p = passage number. G = Gleason score of cancer sample.

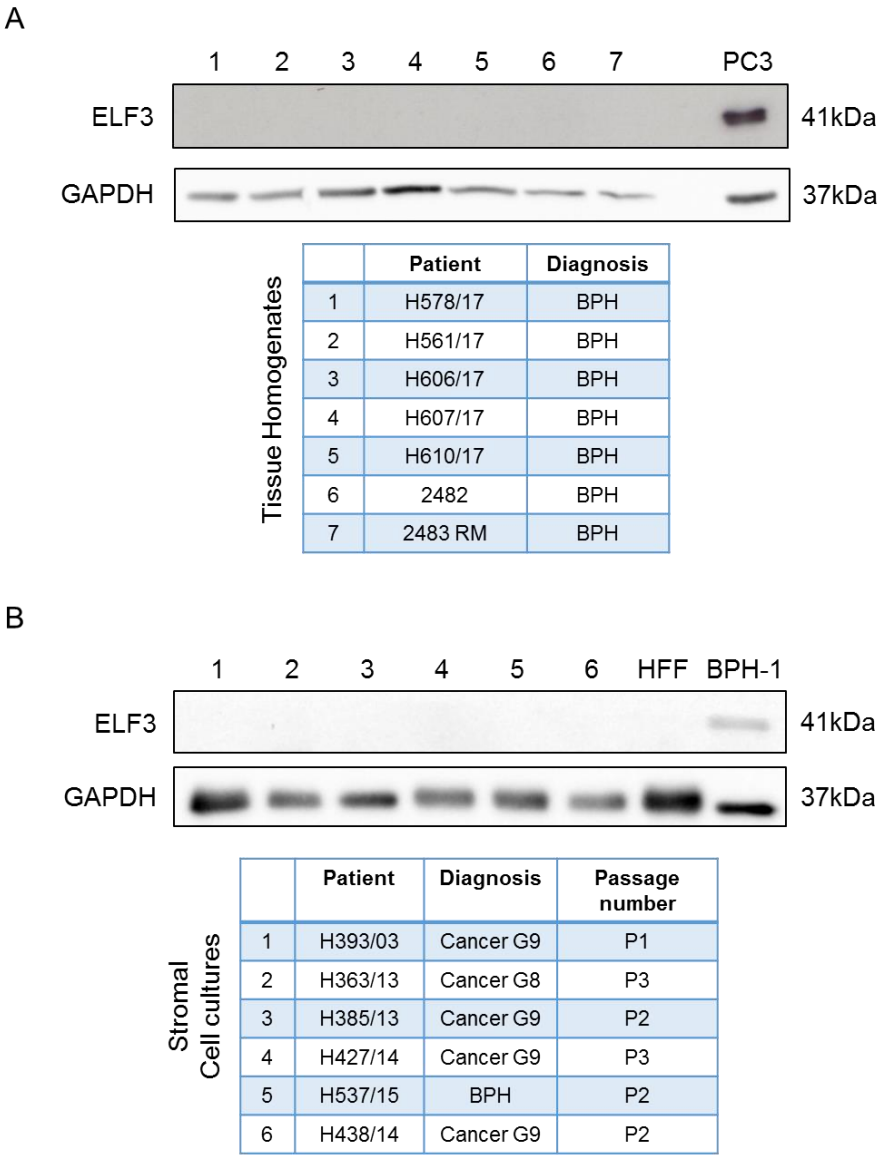

	Patient	Diagnosis
1	H578/17	BPH
2	H561/17	BPH
3	H606/17	BPH
4	H607/17	BPH
5	H610/17	BPH
6	2482	BPH
7	2483 RM	BPH

	Patient	Diagnosis	Passage number
1	H393/03	Cancer G9	P1
2	H363/13	Cancer G8	P3
3	H385/13	Cancer G9	P2
4	H427/14	Cancer G9	P3
5	H537/15	BPH	P2
6	H438/14	Cancer G9	P2

Figure 3.4. Protein expression of ELF3 in prostate tissue homogenates and stromal cells.

Western blot analysis of ELF3 expression in lysates derived from (A) BPH tissue homogenates (provided by Mandy Noble) and (B) enriched stromal cells cultured from tissue (provided by Katrina Reilly). 20µg of protein was loaded per lane onto a 10% SDS gel, transferred onto a PVDF membrane and probed for the indicated proteins. GAPDH was used as a loading control. Tables show patient details for each corresponding lane. HFF = human foreskin fibroblast cell line. G = Gleason score.

3.3 Cellular and tissue localisation of ELF3

3.3.1 ELF3 is expressed in both the cytoplasmic and nuclear compartments of prostate epithelial cells

To accurately determine the function of ELF3 in prostate cells it was important to establish its cellular localisation. To achieve this, ICC was carried out on fixed cell lines. Despite testing three antibodies and different methods of optimisation, it was concluded that these antibodies were unsuitable for ICC.

BPH-1 cells with ELF3 knockdown were used as a negative control and stained using two commercially available antibodies (Ab133621, Abcam and sc-376055, Santa Cruz). Figures 3.5A & B show that whilst there was significant ELF3 knockdown, as detected by western blot, there was no corresponding decrease in ICC staining, which is positive in all samples and presents with a pan-cellular pattern. A third commercial antibody was then tested (HPA003479, Sigma). BPH-1 cells were plated, transfected and stained on hydrochloric acid-treated coverslips to avoid the need to detach (Figure 3.5C). However, similar results were observed. As an additional control the three antibodies were also tested on an ELF3-negative cell line, U-87 MG, with PNT2-C2 cells as a positive control. The Santa Cruz antibody showed low/negative staining in both cell lines, whilst the Abcam and Sigma antibodies were positive in both cell lines (Figure 3.6). U-87 MG negativity was verified by western blot (Figure 3.6B). As 4% paraformaldehyde was initially used for cell fixation, an alternative method of 50:50 methanol:acetone was also performed to observe whether this would reduce background staining and improve specificity (Figure 3.7). In this case PC3 cells were chosen as ELF3 high cells, PNT1a as ELF3 low cells and HEK-293 as ELF3 negative cells. However, whilst PC3 cells showed high expression compared to PNT1a, there was still some staining present in the HEK-293 cells suggesting there was non-specific binding occurring.

To overcome this issue, an alternative technique to determine protein localisation was employed. A cell fractionation protocol was used on a panel of prostate cell lines, which involved a hypotonic buffer to extract cytoplasmic proteins and the remaining nuclear pellet was subsequently lysed with a whole cell extraction buffer (Figure 3.8). Western blot analysis revealed that ELF3 was predominantly expressed in the nucleus of all cell lines, with some present in the cytoplasm. Furthermore, the resulting expression pattern between cell lines was consistent with that from the whole cell lysates (Section 3.3.1).

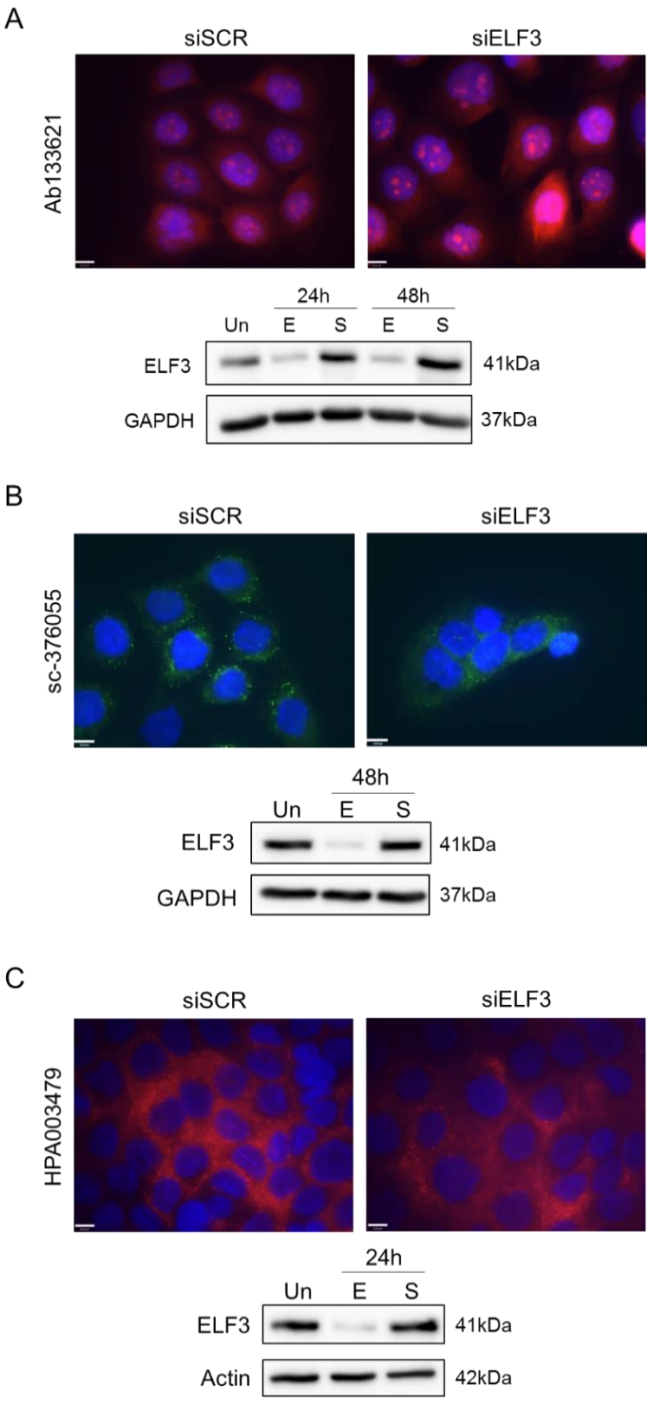

Figure 3.5. Testing ELF3 antibodies for immunocytochemistry using BPH-1 cells with ELF3 knockdown.

BPH-1 cells were transfected with ELF3 (siELF3) and scrambled siRNA (siSCR), fixed in 4% paraformaldehyde and stained using commercial ELF3 antibodies. Cells stained with (A) Ab133621 and (B) sc-376055 were transferred to chamber slides 24h following transfection and fixed at 48h post-transfection. (C) Cells stained with HPA003479 were transfected and stained directly on hydrochloric acid-treated coverslips to avoid replating of cells. Cells were fixed 24h post-transfection. Western blots show knockdown of ELF3 for each experiment. 20µg of protein was loaded per lane onto a 10% SDS gel, transferred onto a PVDF membrane and probed for the indicated proteins. GAPDH and Actin were used as loading controls. E = ELF3 siRNA, S = Scrambled siRNA. Red or green = ELF3, Blue = DAPI. 60x oil lens. Scale bar = 10µm.

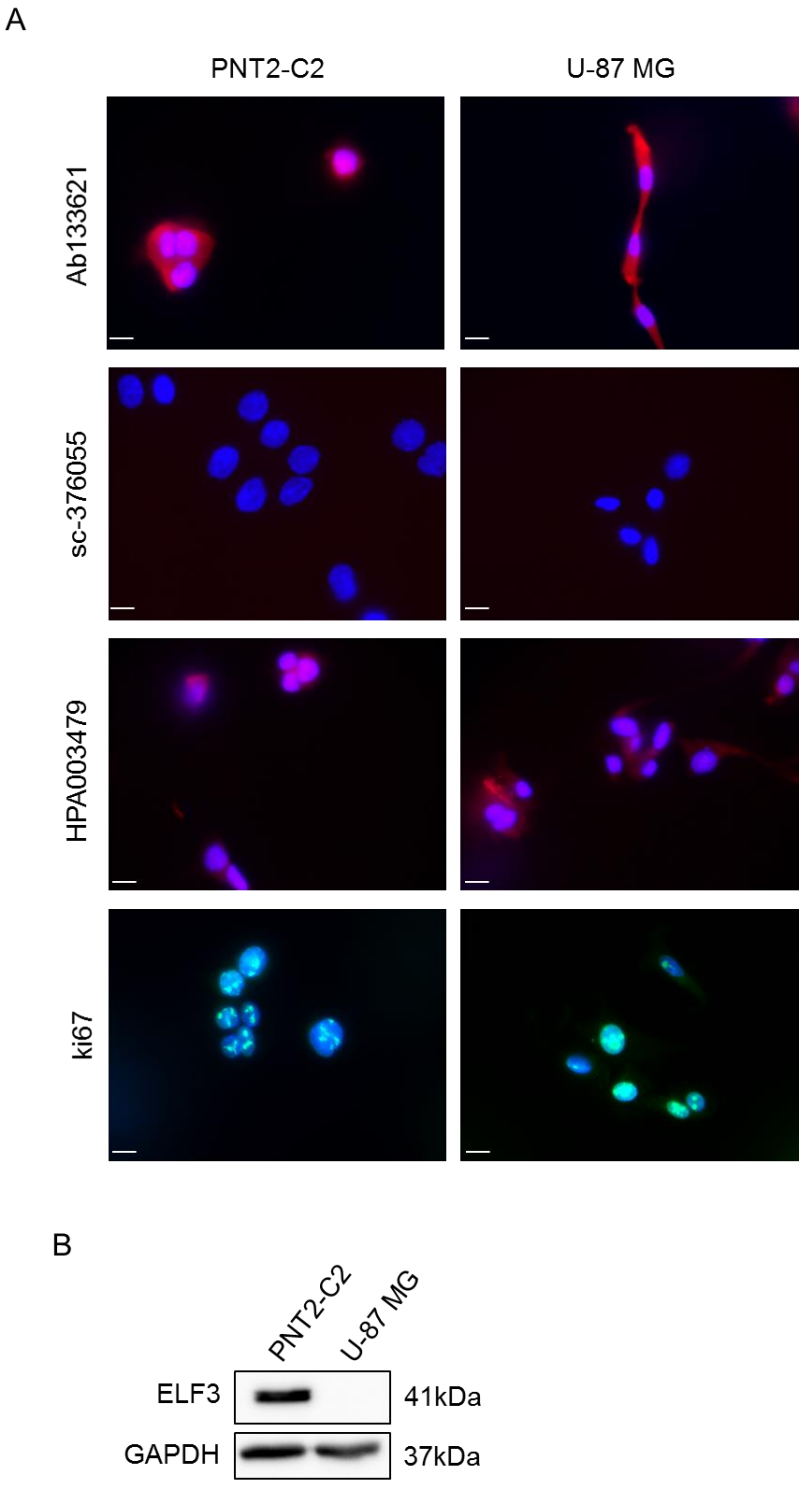

Figure 3.6. Testing ELF3 antibodies for immunocytochemistry using ELF3-negative cell line U-87 MG.

(A) PNT2-C2 (ELF3-positive) and U-87 MG (ELF3-negative) cells were fixed on chamber slides with 4% PFA and subsequently stained using three commercial ELF3 antibodies; Ab133621 (Abcam), sc-376055 (Santa Cruz) and HPA003479 (Sigma). Ki67 was used as a positive control for antibody staining. Scale bar = 10µm (B) Western blot analysis indicating protein expression of ELF3 in PNT2-C2 and U-87 MG cells. 20µg of protein was loaded per lane onto a 10% SDS gel, transferred onto a PVDF membrane and probed for the indicated proteins. GAPDH was used as a loading control.

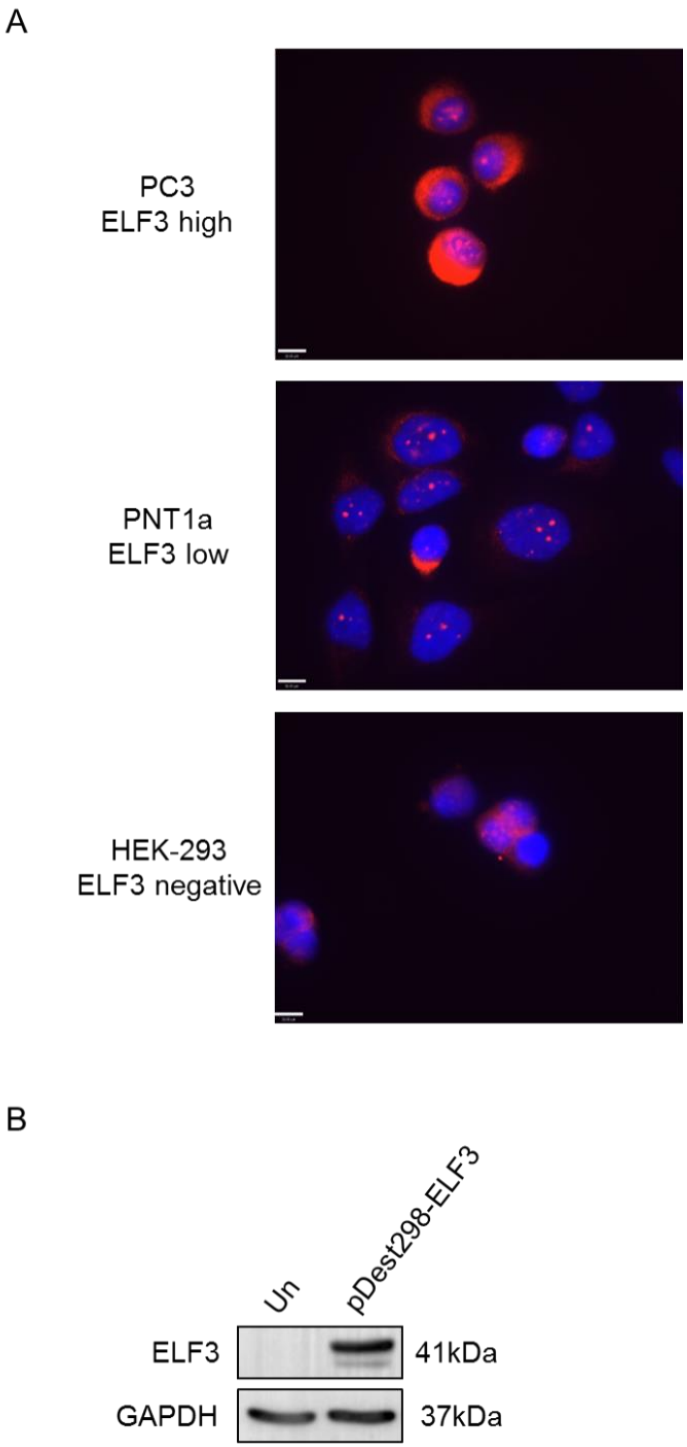

Figure 3.7. Testing ELF3 antibodies for immunocytochemistry using alternative fixation method.
An alternative method of cell fixation was tested using three cell lines, which were chosen due to their varying degrees of ELF3 expression. (A) PC3 (ELF3 high), PNT1a (ELF3 low) and HEK-293 (ELF3 negative) cells were fixed using 50:50 methanol:acetone and stained using ELF3 antibody Ab133621. Scale bar = 10µm (B) Western blot analysis of ELF3 expression in untransfected HEK-293 cells and following ELF3 overexpression via plasmid transfection (pDest298-ELF3). 20µg of protein was loaded per lane onto a 10% SDS gel, transferred onto a PVDF membrane and probed for the indicated proteins. GAPDH was used as a loading control.

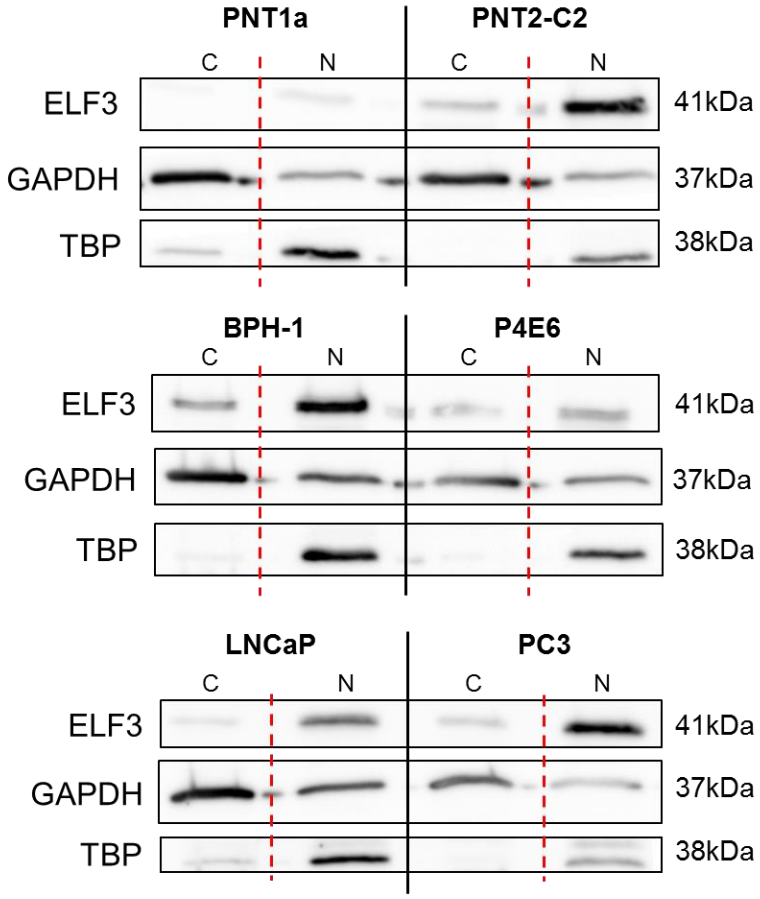

Figure 3.8. ELF3 cellular localisation in prostate cell lines.

A cell fractionation protocol was employed to determine the cellular localisation of ELF3 in a panel of prostate cell lines. Cells were harvested and lysed in a hypotonic buffer to extract cytoplasmic proteins. The remaining pellet was subsequently lysed with a whole cell extraction buffer to extract nuclear proteins. Western blot analysis was then carried out. 30µg of protein was loaded per lane onto a 10% SDS gel, transferred onto a PVDF membrane and probed for the indicated proteins. C = cytoplasmic fraction, N = nuclear fraction, GAPDH = cytoplasmic control, TATA-binding protein (TBP) = nuclear control.

3.3.2 ELF3 expression is restricted to the basal layer of the prostate epithelium in tissue

Tissue staining was carried out to assess ELF3 expression *in situ* in benign and cancer prostate tissue. Paraffin-embedded BPH tissue sections were stained with ELF3 by immunofluorescence. There was a very distinct pattern of expression where ELF3 staining was present in the basal epithelial cell population, but absent from the luminal layer and surrounding stroma (Figure 3.9). p63 was used as a nuclear basal cell marker and high molecular weight cytokeratin (HMW-CK, recognises cytokeratins 1, 5, 10 and 14) as a cytoplasmic basal cell marker. Secondary antibody only controls were satisfactorily void of staining (data not shown). The cellular localisation of ELF3 was predominantly cytoplasmic, as shown by the colocalization with HMW-CK. However, low nuclear staining was also present in some cells. The fractionated western blots showed that ELF3 is present in the cytoplasm of cell lines, however there was higher expression in the nucleus. To address the possibility that expression in the nucleus was below the limit of detection in the tissue sections, an IHC amplification kit (ImmPRESS Excel Amplified HRP Polymer Staining Kit, Vector Laboratories), which utilises horseradish peroxidase micropolymers to amplify the signal, was employed to establish if any ELF3 signal could be visualised in the nuclear compartment of basal cells. First, BPH sections generated by our lab were stained using IHC with the amplification kit. Results confirmed that ELF3 was specifically expressed in the basal layer of prostate epithelial glands and absent from luminal cells and stroma (Figure 3.10). With regards to cellular localisation, positive ELF3 staining was observed in both the cytoplasm and nucleus of basal cells. Since the staining pattern was specific only to basal cells and agreed with findings from western blot analyses, we were satisfied that this antibody was suitable for IHC.

Tissue microarrays (TMAs) of both BPH (102 sections from 34 patients) and PCa (40 sections from 13 patients) tissue were obtained from the Orchid tissue bank (in collaboration with Professor Dan Berney, Barts Hospital, London) to evaluate the expression of ELF3 across multiple patients. ELF3 was present in all BPH tissue sections from 34 patients which contained epithelial glands. Some patient sections showed exclusively cytoplasmic staining (Figure 3.11A) whilst others also exhibited nuclear ELF3 (Figure 3.11B). Results were less clear in PCa tissue. Loss of the basal cell population and expression of AMACR are indicators of cancer used in prostate histology and contributes to a cancer diagnosis (Humphrey, 2007). This marker was therefore used to distinguish areas of cancer in the PCa tissue sections. Sections of Gleason 6 grade PCa which contained no obvious glandular structures did not express ELF3. However, some sections contained glandular structures both with and without AMACR staining. For example, patient WXP11C exhibited histology with a Gleason score of 6 (Figure 3.12). In these sections ELF3 tended to be detected in the basal-like cells of AMACR negative glands. In less differentiated sections, with Gleason score ≥7, which had no obvious glandular structures, but were entirely AMACR positive, some did not stain for ELF3 (Figure 3.13A), whilst others showed positive ELF3 staining (Figure 3.13B). It was difficult to distinguish the cellular localisation of ELF3 expression in these more advanced cancers.

These results suggest that ELF3 expression may initially be lost in lower grade (Gleason 6) tumours. Additionally, there may be a subset of higher grade prostate tumours (Gleason ≥7) which then re-express ELF3.

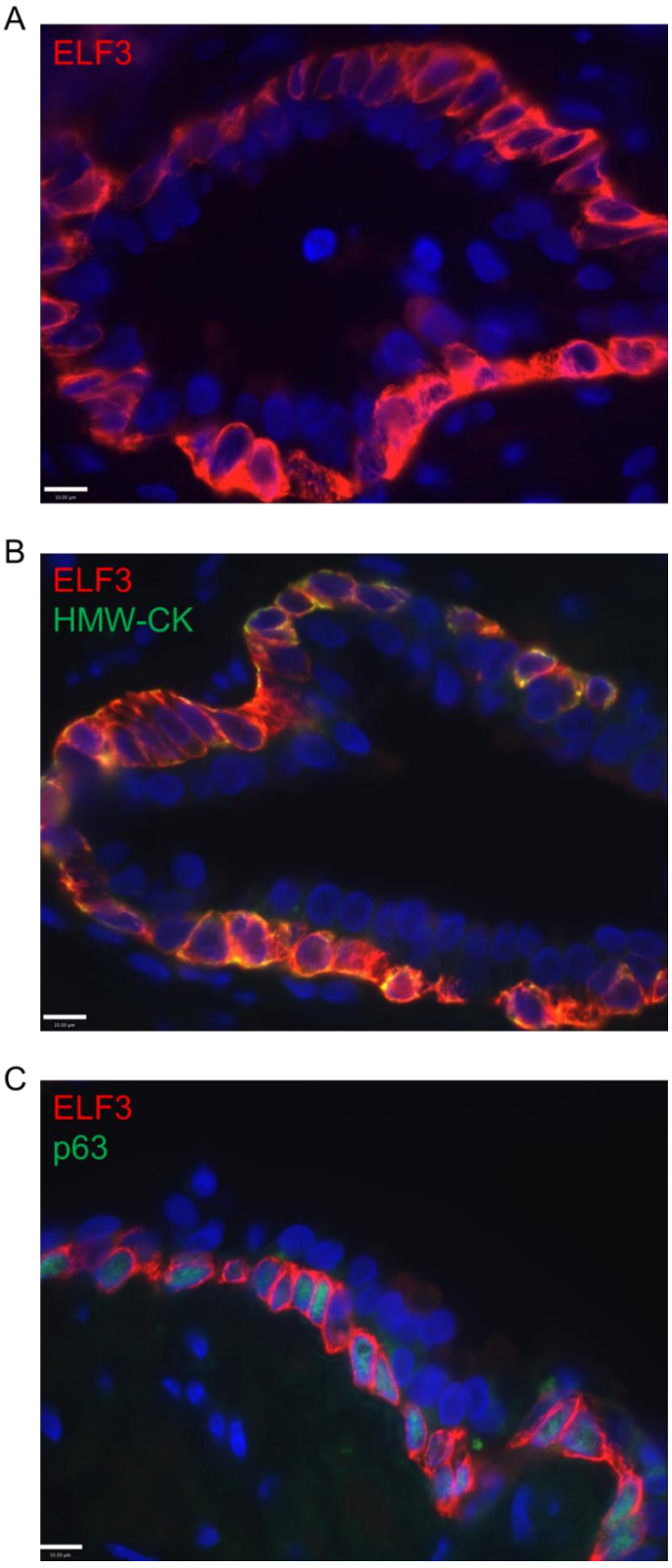

Figure 3.9. ELF3 expression in BPH tissue by immunohistochemistry (immunofluorescence).
Formalin-fixed, paraffin-embedded BPH tissue was deparaffinised and rehydrated before undergoing heat-induced antigen retrieval in sodium citrate buffer. IHC was carried out and sections were incubated with fluorescent Alexa Fluor secondary antibodies. (A) ELF3 alone (Ab97310), (B) ELF3 co-stained with high molecular weight cytokeratin (cytoplasmic basal cell marker) and (C) ELF3 co-stained with p63 (nuclear basal cell marker). Red = ELF3, Green = HMW-CK / p63, Blue = DAPI. 60x oil lens. Scale bar = 10µm.

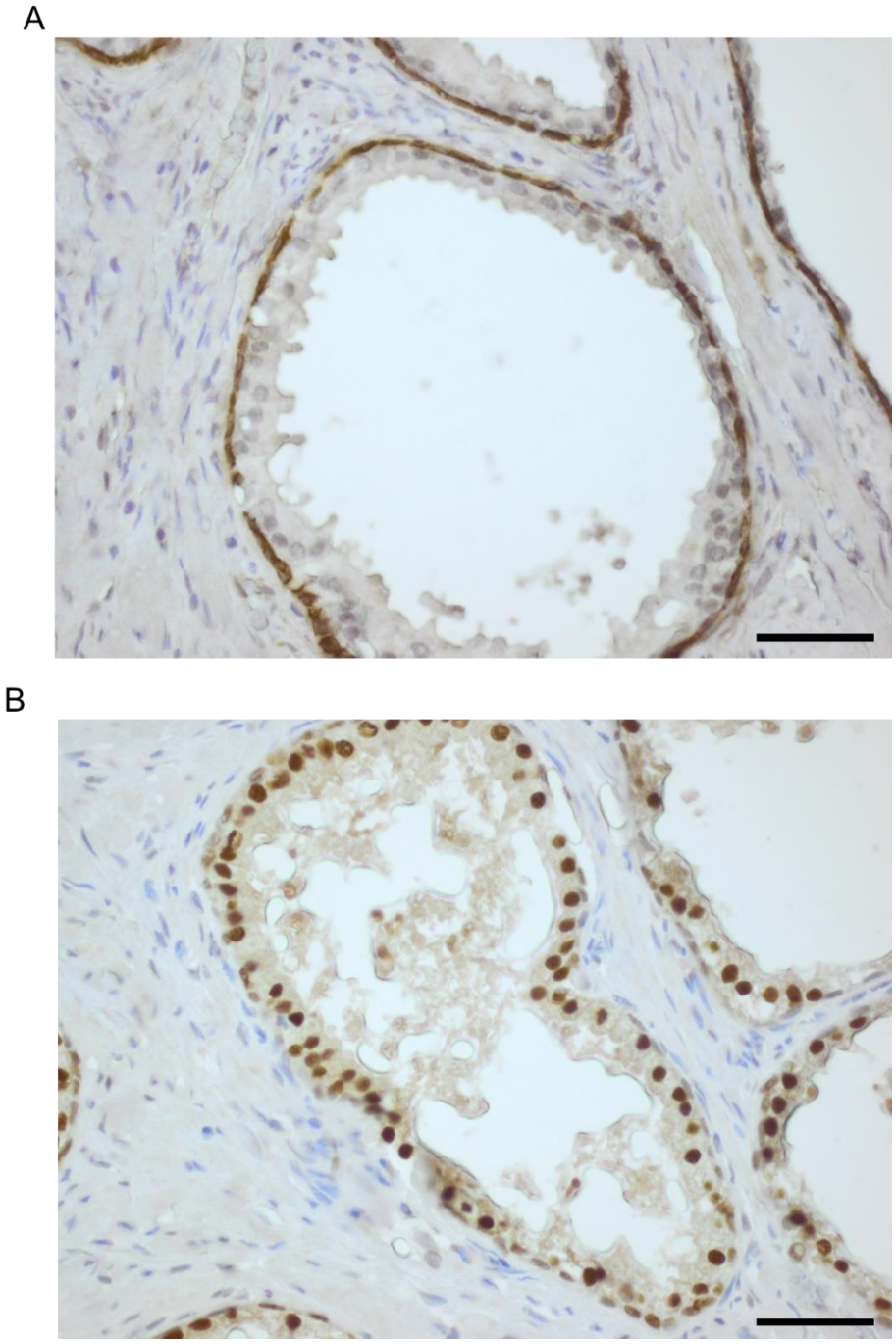

Figure 3.10. ELF3 expression in BPH tissue using the ImmPRESS Excel Amplified HRP Polymer Staining Kit.

Formalin-fixed, paraffin-embedded BPH tissue was deparaffinised and rehydrated before undergoing heat-induced antigen retrieval in sodium citrate buffer. IHC was carried out using the ImmPRESS Excel Amplified HRP Polymer Staining Kit (Vector Labs) and sections were incubated with DAB until they turned brown and then counterstained with haematoxylin. (A) ELF3 (Ab97310) and (B) Nkx3.1 (nuclear luminal cell control). Scale bar = 50μm.

Figure 3.11. ELF3 expression in BPH tissue microarrays (TMAs).

102 tissue sections from 34 patients were stained for ELF3 expression using Ab97310 using the Vector ImPRESS Excel Kit. Representative images of sections from two patients are shown. (A) Patient 9C exhibits more cytoplasmic staining whilst (B) Patient 5A exhibits more nuclear staining. Sections were stained for Nkx3.1 as a nuclear luminal cell control. Sec only = tissues stained with secondary antibody only. 20x scale bar = 100µm, 40x scale bar = 50µm. (TMAs provided through collaboration with Professor Dan Berney, Barts and London School of Medicine and Dentistry).

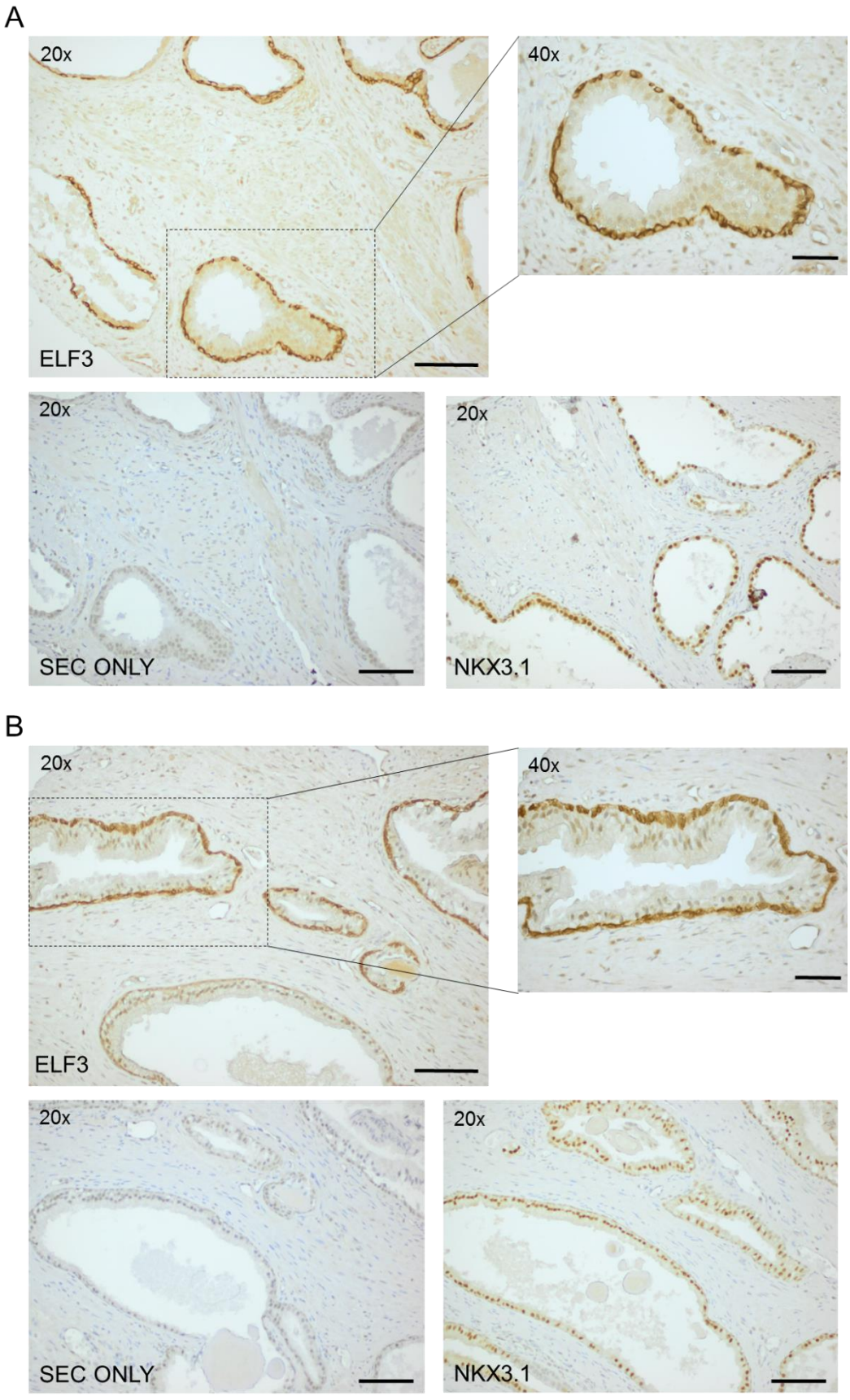
A
20x
40x
ELF3
20x
SEC ONLY
20x
NKX3.1
B
20x
40x
ELF3
20x
SEC ONLY
20x
NKX3.1

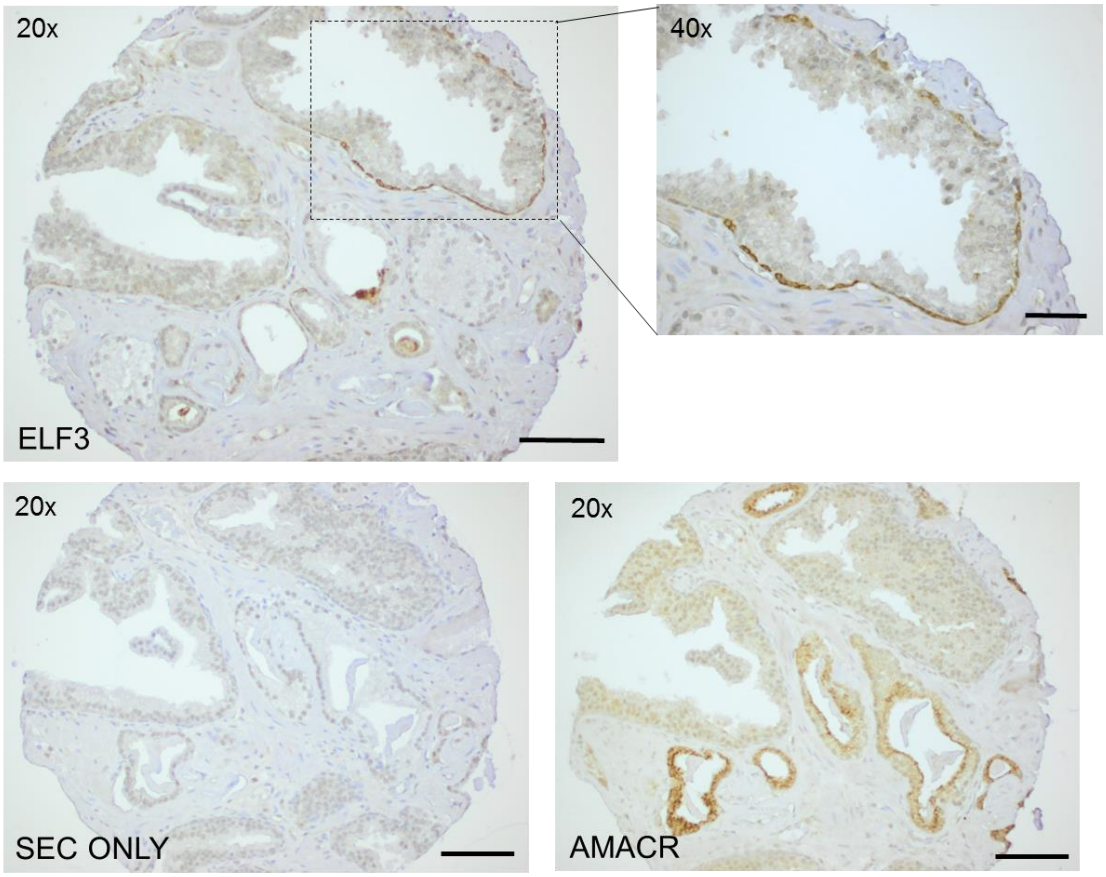

Figure 3.12. ELF3 expression in Cancer tissue microarrays (TMAs) – Low Gleason grade prostate cancer.

40 tissue sections from 13 patients were stained for ELF3 expression using Ab97310 using the Vector ImPRESS Excel Kit. Representative images from one patient, WXP11C (classed as Gleason grade 3+3), where AMACR positive and negative regions are shown. Sections were stained for AMACR as a cancer marker. Sec only = tissues stained with secondary antibody only. 20x scale bar = 100µm, 40x scale bar = 50µm. (TMAs provided through collaboration with Professor Dan Berney, Barts and London School of Medicine and Dentistry).

Figure 3.13. ELF3 expression in Cancer tissue microarrays (TMAs) – High Gleason grade prostate cancer.

40 tissue sections from 13 patients were stained for ELF3 expression using Ab97310 using the Vector ImPRESS Excel Kit. Sections were stained for AMACR as a cancer marker. (A) Patient WXP10C (Gleason grade 4+3). (B) WXP7B (Gleason grade 4+4). Sec only = tissues stained with secondary antibody only. 20x scale bar = 100µm, 40x scale bar = 50µm. (TMAs provided through collaboration with Professor Dan Berney, Barts and London School of Medicine and Dentistry).

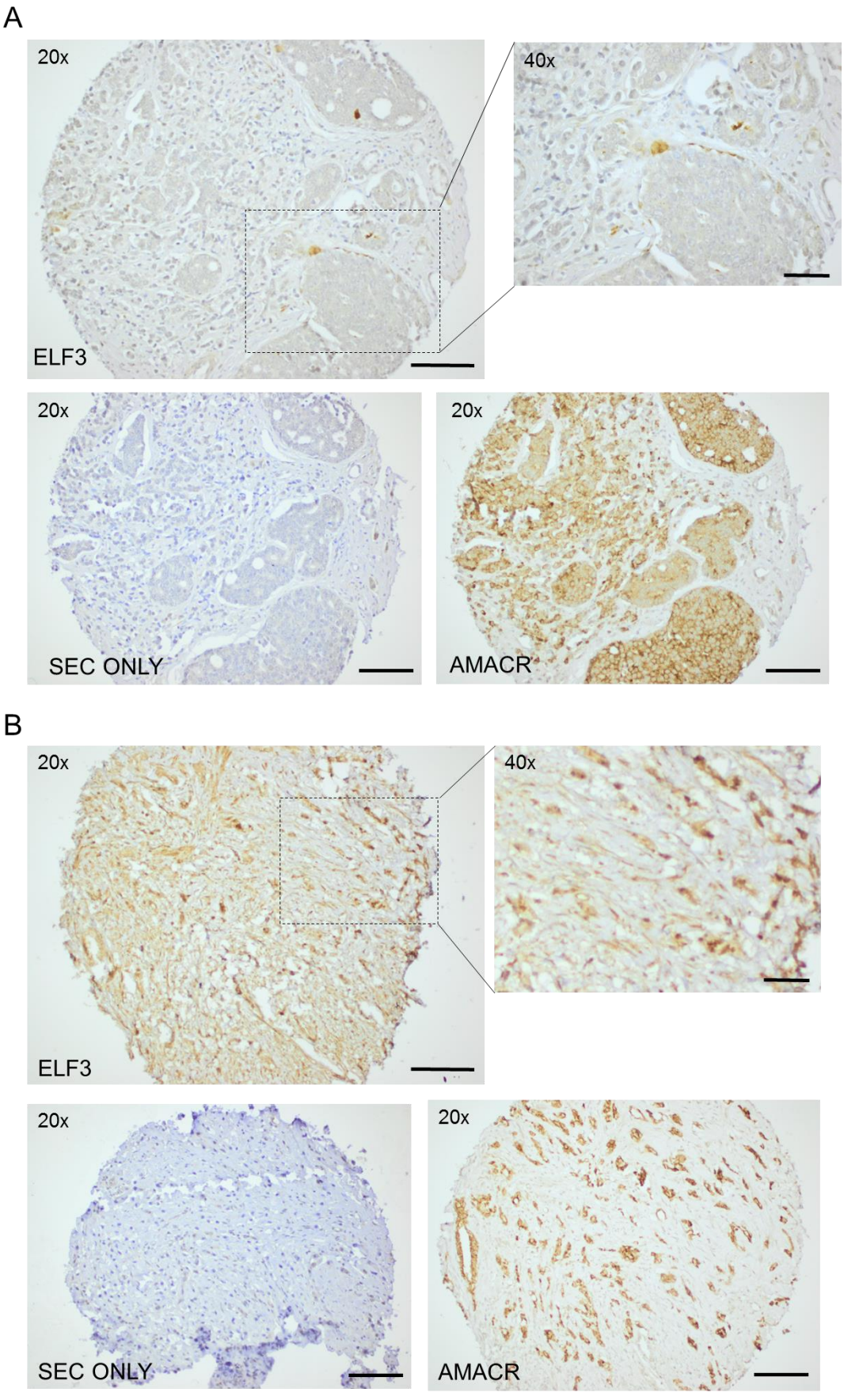
A
20x
40x
ELF3
20x
SEC ONLY
20x
AMACR
B
20x
40x
ELF3
20x
SEC ONLY
20x
AMACR

3.4 The effects of ELF3 knockdown on prostate epithelial cell lines

3.4.1 siRNA transfection maintains long-term ELF3 knockdown in prostate epithelial cell lines

Following confirmation that ELF3 is expressed in prostate tissue, initial mechanistic studies were carried out using BPH-1 and PC3 cell lines. Since ELF3 is expressed in primary prostate basal epithelial cells, BPH-1 and PC3 cells were considered the most appropriate cell lines to initially characterise the effects of ELF3 knockdown in prostate benign and cancer cells because they both express significant levels of ELF3 (Section 3.1.1, Figure 3.1) and do not possess the characteristics of a luminal cell phenotype (Section 3.1.1, Table 3.1).

ELF3 knockdown was achieved using a siRNA oligonucleotide targeting exon 3 of ELF3 (siELF3), which targets all known protein coding transcripts of the ELF3 gene. A non-specific scrambled siRNA (siSCR) was used as a control to ensure any changes seen with ELF3 knockdown were specific. A mock transfection control which contained transfection reagent only was also included. SiRNAs are an efficient method of modulating expression as they are generally better tolerated by a range of cells, including primary cells, compared to plasmid transfection.

ELF3 siRNA transfection using Lipofectamine RNAiMAX (Invitrogen) sustained knockdown for at least 6 days post-transfection (Figure 3.14). This ensured that ELF3 expression remained at a very low level for the duration of all functional experiments that were carried out. The percentage of knockdown achieved was 79-96% in BPH-1 cells and 88-100% in PC3 cells.

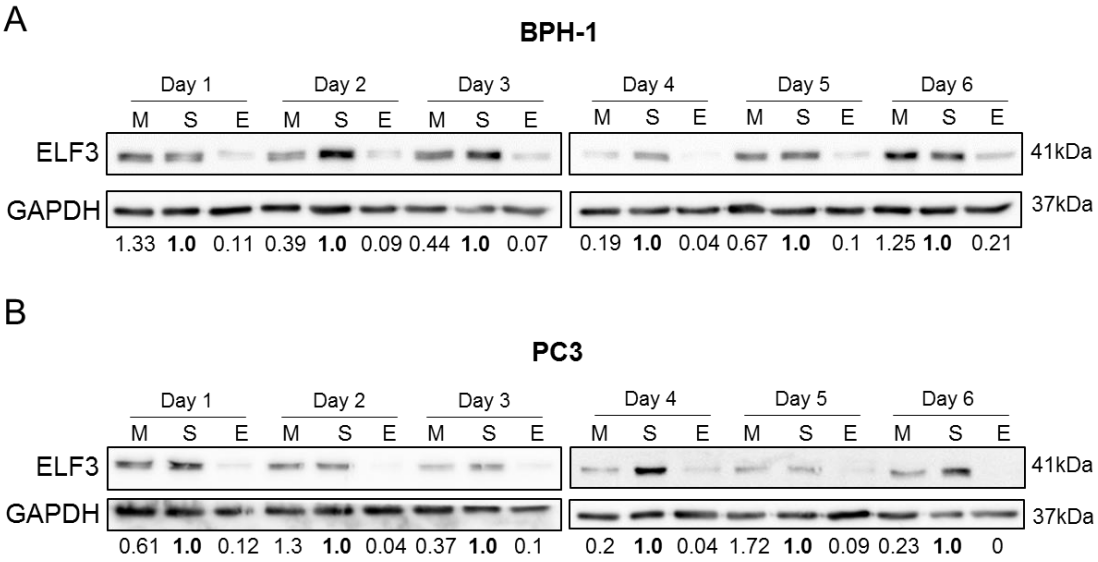

Figure 3.14. Time course of ELF3 knockdown in benign (BPH-1) and cancer (PC3) prostate epithelial cell lines.

ELF3 protein expression was analysed by western blot in (A) BPH-1 and (B) PC3 cells following ELF3 knockdown over a 6 day time course. 20µg of protein was loaded per lane onto a 10% SDS gel, transferred onto a PVDF membrane and probed for the indicated proteins. GAPDH was used as a loading control. Densitometry was carried out using Image J software. Numbers below blots indicate levels of knockdown compared to samples treated with siSCR on the same day. siSCR samples were normalised to 1.0. M = Mock, S = siSCR, E = siELF3.

3.4.2 ELF3 knockdown significantly reduces the cell viability of prostate epithelial cell lines by a process other than apoptosis

An alamarBlue assay was carried out to assess the effects of ELF3 knockdown on prostate cell viability. Cells were analysed for six consecutive days following transfection. After obtaining the reading from day 3, cells were trypsinised and replated at the original starting density. This was due to the confluency of cells by this point in the time course and also to assess the cells ability to recover following replating. Figure 3.15 shows that in both BPH-1 and PC3 cells, the viability of cells with ELF3 knockdown begins to decrease at day 3 and is significantly decreased following replating at days 4, 5 and 6. In both BPH-1 and PC3 cells the viability decreased by around 40% by day 6. Therefore, there is no distinct effect on benign vs. cancer cells in this case.

Since the significant decrease in viability did not occur until after replating the transfected cells, it was hypothesised that the cells with ELF3 knockdown had disrupted adhesion capabilities. This was confirmed by an adhesion assay in which BPH-1 cells were transfected with mock, siSCR or siELF3 and once confluent were replated at three different densities (high, medium and low) and allowed to adhere for 4hrs. Results showed that ELF3 knockdown decreased BPH-1 cell adhesion regardless of starting density (Figure 3.16A). However, since there is a continued decrease in cell viability following day 3, as opposed to an increase which would be evident with normally proliferating cells, this suggests that there is another mechanism contributing to the progressive decrease in viability over time.

To assess whether cell death was occurring by apoptosis, western blot analysis was carried out on BPH-1 and PC3 cells using cleaved caspase 3 as a marker of apoptosis. BPH-1 cells treated with 1μM staurosporine for 24 hours were used as a positive control. The ELF3 expression of these samples was analysed at a previous time and therefore does not include the staurosporine control. Figures 3.16B & C show that cleaved caspase 3 was only present in staurosporine-treated cells and therefore ELF3 knockdown cells were not dying via apoptosis. This correlates with the observation that little cell death was observed down the microscope and therefore suggests the decrease in viable cell number may be due to reduced proliferation.

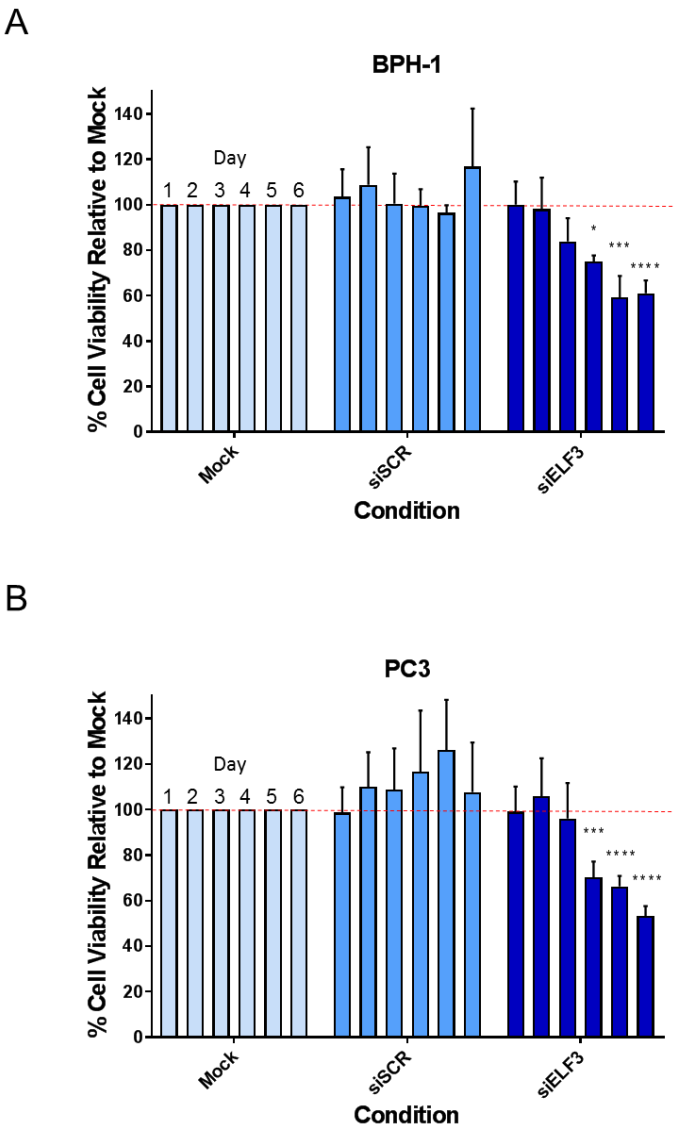

Figure 3.15. ELF3 knockdown decreases the viability of prostate epithelial cell lines after replating. AlamarBlue cell viability assays were performed 24 hours after transfection and every day for six consecutive days. Due to confluency, cells were re-plated after the day 3 reading at the original density of 40,000 cells for BPH-1 and 60,000 cells for PC3 in a 24 well plate. (A) BPH-1 cells. (n=3) (B) PC3 cells (n=3). Mock samples were normalised to 100% viability. Statistical significance was determined using a 2-way ANOVA with Tukey's multiple comparison test.

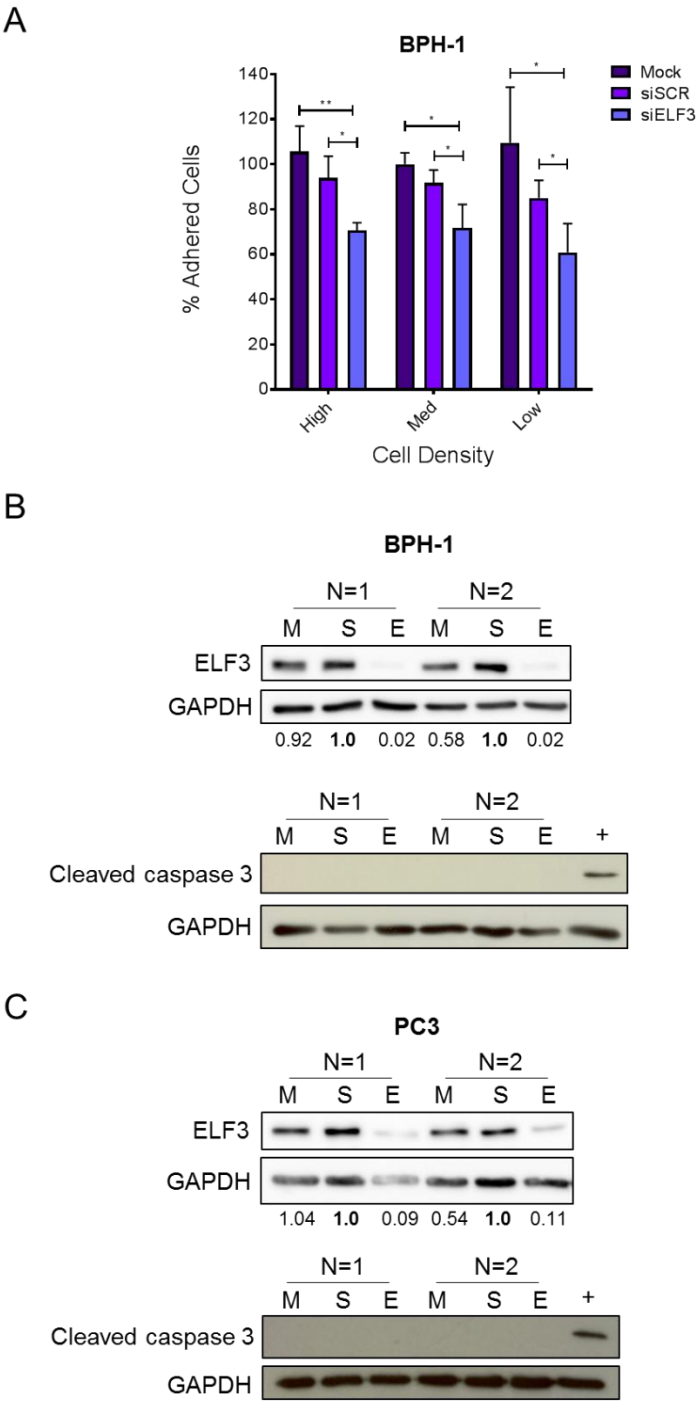

Figure 3.16. ELF3 knockdown reduces cell adhesion but does not cause cell death via apoptosis.
(A) An adhesion assay was performed on BPH-1 cells 48h following knockdown. Cells were trypsinised and re-plated at three different densities for 4 hours (High = 300,000 cells, Med = 100,000 cells, Low = 40,000 cells). Floating cells were washed off and adherent cells were counted using an automated cell counter. To assess cell death by apoptosis, lysates of (B) BPH-1 and (C) PC3 cells with ELF3 knockdown were probed for cleaved caspase 3. BPH-1 cells treated with 1µM Staurosporine for 24h were used as a positive control for apoptosis (+). 20µg of protein was loaded per lane onto a 10% SDS gel, transferred onto a PVDF membrane and probed for the indicated proteins. GAPDH was used as a loading control. Statistical significance was determined using a Student's T-test (unpaired, two-tailed).

3.4.3 ELF3 knockdown significantly decreases cell motility in prostate epithelial cell lines

The ability to migrate is a property of cancer cells and also a characteristic of SCs (Collins et al., 2005, Hanahan and Weinberg, 2000). Overexpression of ELF3 has previously been shown to increase the motility of PCa cell lines LNCaP and 22RV1 (Longoni et al., 2013). Cell motility was investigated using a wound healing assay whereby a wound is introduced to a confluent layer of cells. Images were taken at the starting point and after a time period to allow the cells to grow and migrate to close the wound. Width of the wound was measured at 10 points and compared to the width at the start point to determine % closure.

ELF3 knockdown significantly decreased the cell motility of both BPH-1 and PC3 cells (Figures 3.17 & 3.18). Whilst BPH-1 % wound closure was decreased by around 60%, PC3 cells had a more modest decrease of around 20%. This suggests PC3 cells have alternative mechanisms regulating migration which may be expected since cancer cells have increased migration capabilities.

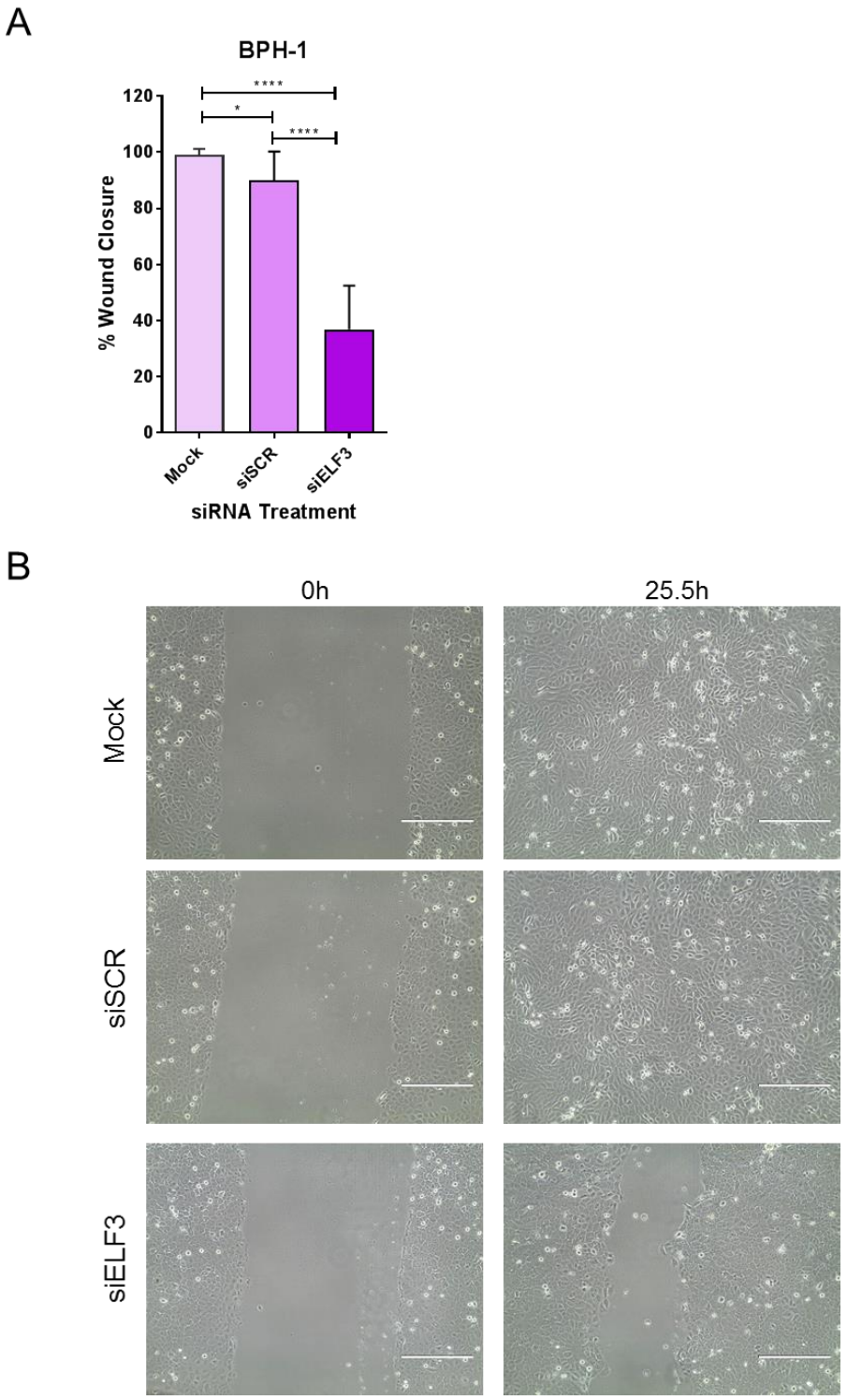

Figure 3.17. ELF3 knockdown decreases the migration of BPH-1 cells.

(A) Migration of BPH-1 cells following knockdown was calculated by % wound closure (n=3). A wound was introduced to a confluent monolayer of cells 24 hours post-transfection. The end point was determined by monitoring the wounds until the first triplicate set of one condition (mock, siSCR or siELF3) had closed. Image J software was used to determine the average width of the wounds between 10 points. Percent wound closure was calculated at the end point relative to zero hour images. (B) Representative images of wound closure at 25.5h post-injury. Scale bar = 400µm. Statistical significance was determined using a Student's T-test (unpaired, two-tailed).

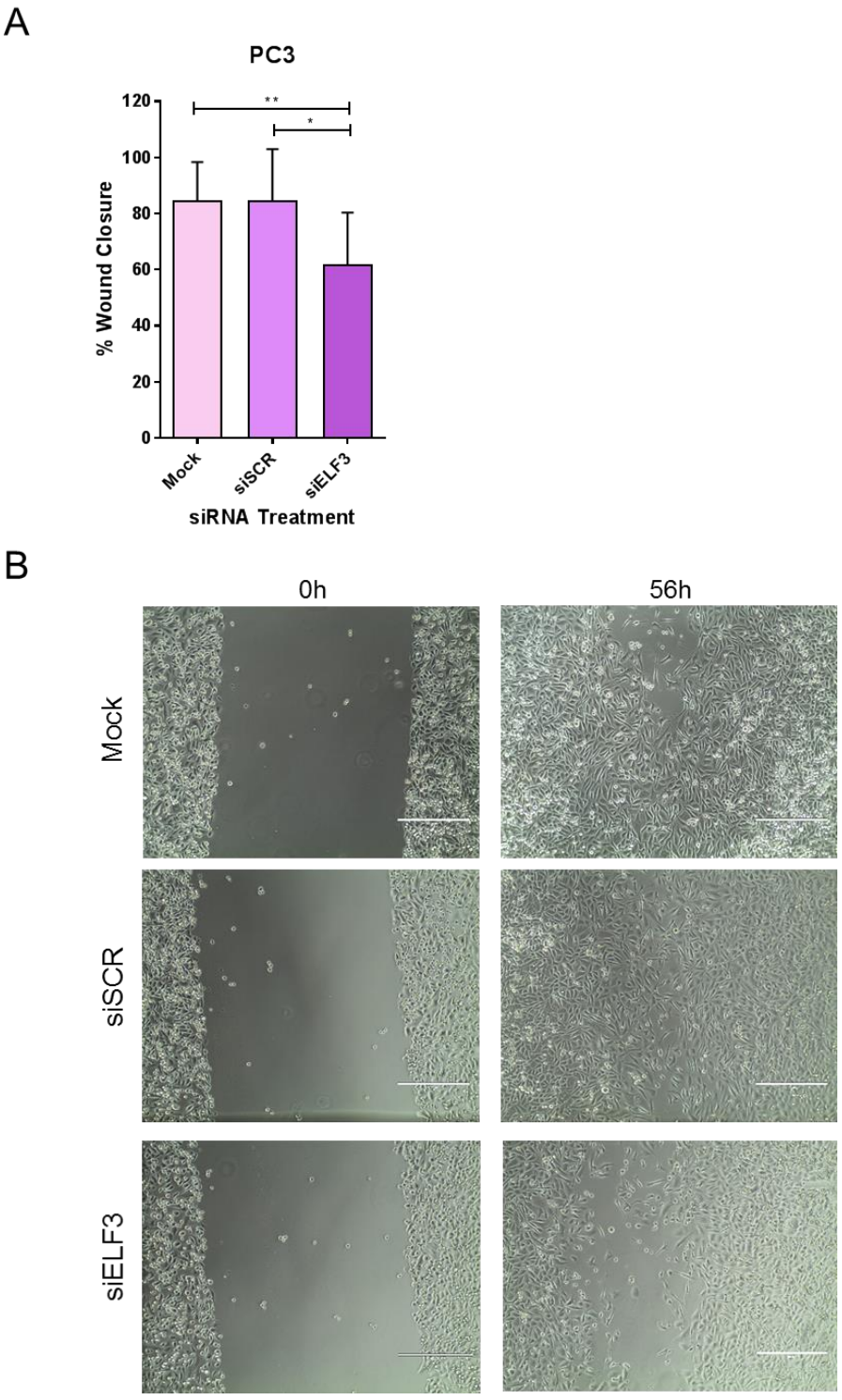

Figure 3.18. ELF3 knockdown reduces the migration of PC3 cells.

(A) Migration of PC3 cells following knockdown was calculated by % wound closure (n=3). A wound was introduced to a confluent monolayer of cells 24 hours post-transfection. The end point was determined by monitoring the wounds until the first triplicate set of one condition (mock, siSCR or siELF3) had closed. Image J software was used to determine the average width of the wounds between 10 points. Percent wound closure was calculated at the end point relative to zero hour images. (B) Representative images of wound closure at 56h post-injury. Scale bar = 400µm. Statistical significance was determined using a Student's T-test (unpaired, two-tailed).

3.4.4 ELF3 knockdown significantly decreases colony forming ability in prostate epithelial cell lines

Colony forming is the ability to grow from a single cell. This is challenging for a cell which usually requires a network of surrounding supportive cells for growth. Thus, colony forming ability is defined as a biological characteristic of SCs (Collins et al., 2005). A colony forming assay was carried out by plating 200 BPH-1 and PC3 cells into a 12 well plate in triplicate 24 hours post-transfection. Biological triplicates were also performed. Wells were stained with crystal violet and colonies over 32 cells were counted (5 population doublings defines an established colony (Puck and Marcus, 1956, Francipane et al., 2008) and the colony forming efficiency relative to mock transfected cells was calculated.

ELF3 knockdown significantly decreased the colony forming ability of prostate epithelial cell lines (Figure 3.19). BPH-1 cells with ELF3 knockdown had an 80% decrease in colonies formed, whilst PC3 cells had around a 65% decrease relative to mock transfected cells.

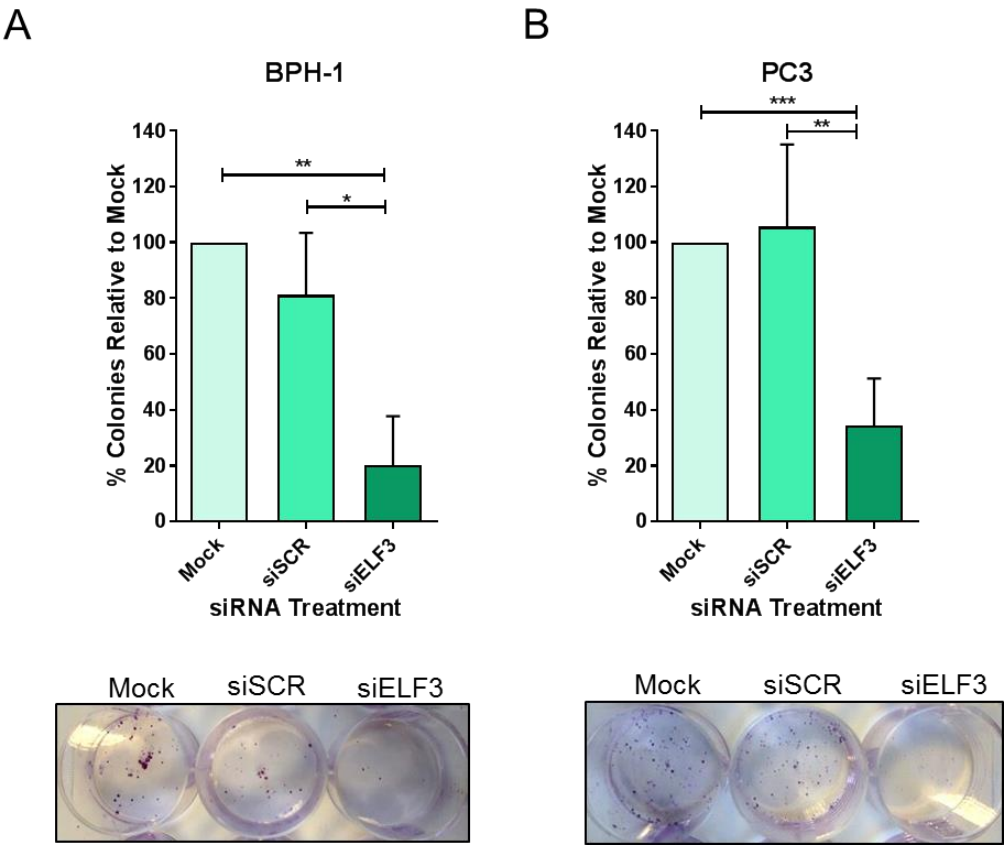

Figure 3.19. ELF3 knockdown decreases the colony forming ability of benign and cancer prostate epithelial cell lines.

Colony forming assays were performed on (A) BPH-1 cells (n=3) and (B) PC3 cells (n=3) 24 hours post-transfection. Top panel: Number of colonies >32 cells formed after seeding 200 cells in a 12 well plate following knockdown relative to mock. Bottom panel: representative images of colonies following crystal violet staining. Control samples were normalised to 100%. Statistical significance was determined using a Student's T-test (unpaired, two-tailed).

3.4.5 ELF3 knockdown alters the morphology and colony formation of prostate epithelial cells

Brightfield images of BPH-1 and PC3 cells with ELF3 knockdown were taken over a 6 day time course. Whilst there appeared to be no difference between conditions at the 24h time point, after replating the morphology and colony formation of each cell line was altered. BPH-1 cells tend to initially spread out at 24 hours after replating (24hRP) then form tight rounded colonies at 48hRP. However, with ELF3 knockdown, the cells were tightly packed together from 24hRP and the colonies were far more condensed at 48hRP and 72hRP compared to the mock and siSCR controls (Figure 3.20). Furthermore, it appeared that there were fewer cells present at 72hRP, which could be a combination of fewer cells adhering (as discussed in Section 3.4.2) and the cells being more tightly packed together.

Similarly there was no difference in PC3 cells at 24h post-transfection (Figure 3.21), but in contrast, unlike BPH-1 cells, PC3 cells tend to grow in a scattered manner and proceed to fill the gaps rather than grow in distinct colonies. There was no clear difference in cell morphology in the ELF3 knockdown PC3 cells after replating. However, there was again a noticeable decrease in cell number.

To further investigate the morphology of cells with ELF3 knockdown, BPH-1 and PC3 cells were stained with tubulin and phalloidin (Figures 3.22 and 3.23 respectively). In the mock and siSCR conditions of BPH-1 there were clear spaces between cells (white arrows). However, siELF3 cells were much closer together indicating an increase in cell-cell interactions. Furthermore, the pattern of tubulin and phalloidin expression was much more concentrated around the edges of the colony as a whole in siELF3 cells (red arrow), as opposed to individual cells seen in mock and siSCR cells. These changes were not as pronounced in PC3 cells, possibly due to differences in colony formation between PC3 and BPH-1 cells.

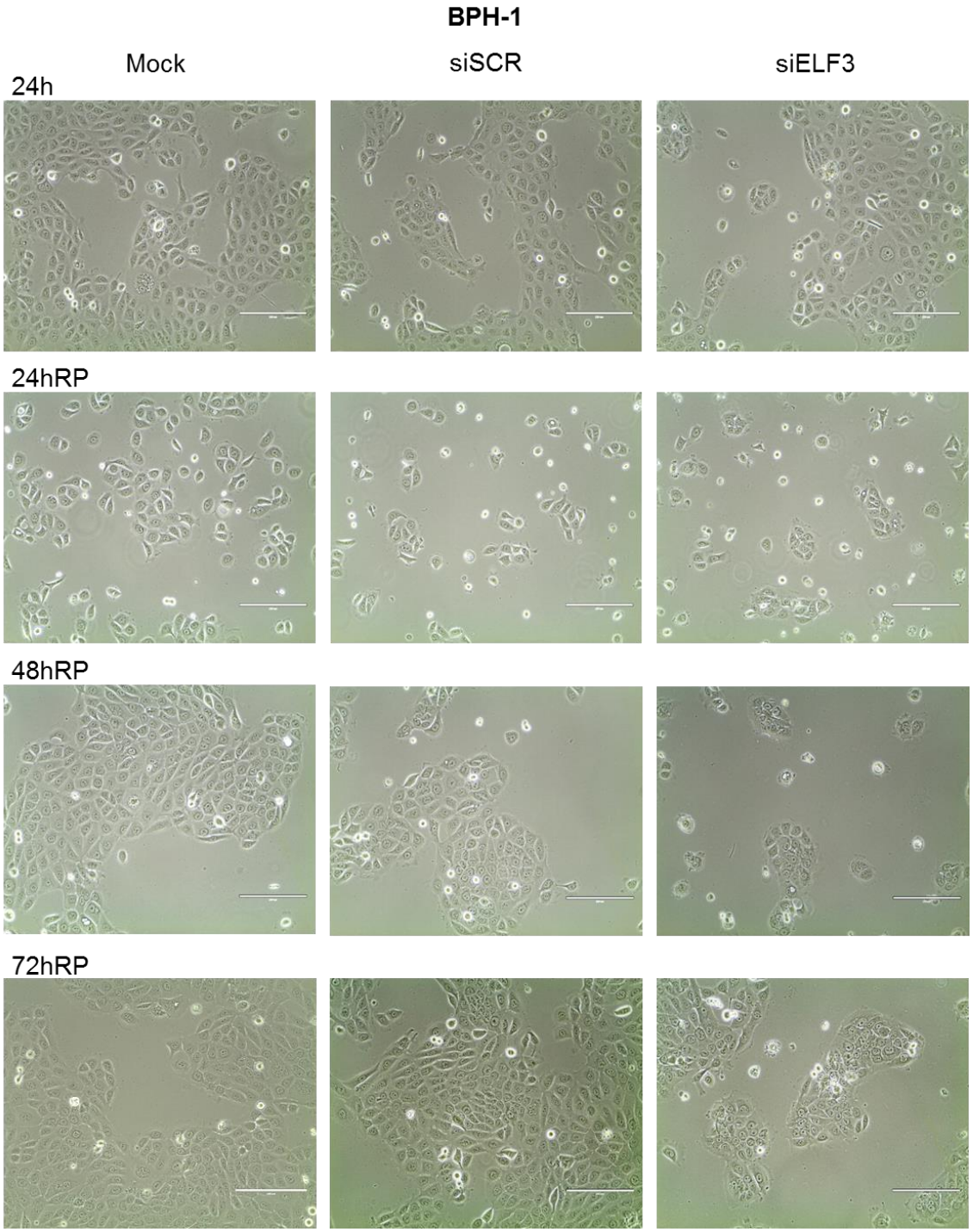

Figure 3.20. ELF3 knockdown alters the morphology of BPH-1 cells.

Brightfield images of BPH-1 cells following knockdown. The top row indicates cells 24h post-transfection. Cells were re-plated day 3 post-transfection and imaged for the following 72h. RP = re-plated. Scale bar = 200µM.

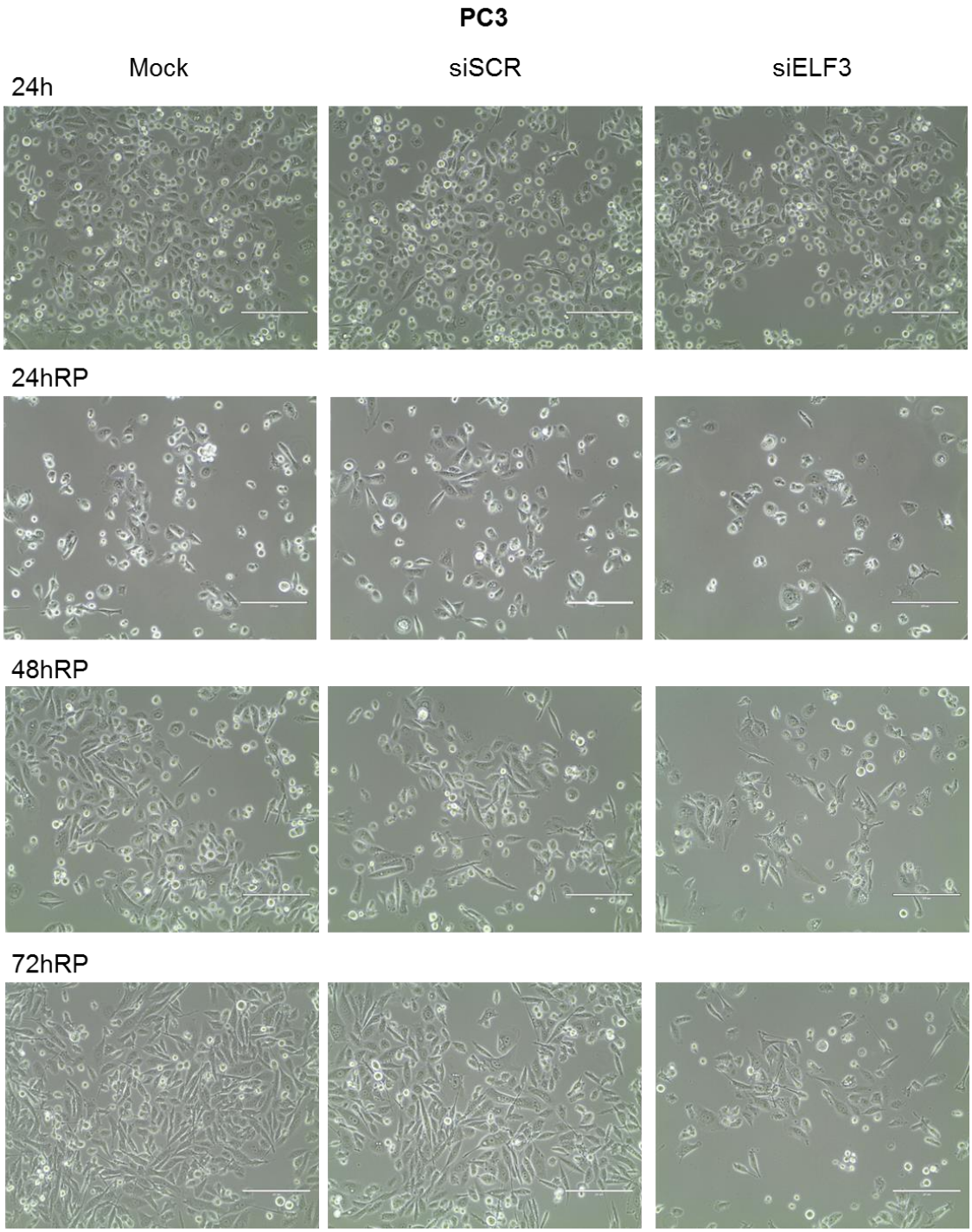

Figure 3.21. ELF3 knockdown alters the morphology of PC3 cells.

Brightfield images of PC3 cells following knockdown. The top row indicates cells 24h post-transfection. Cells were re-plated day 3 post-transfection and imaged for the following 72h. RP = re-plated. Scale bar = 200μM.

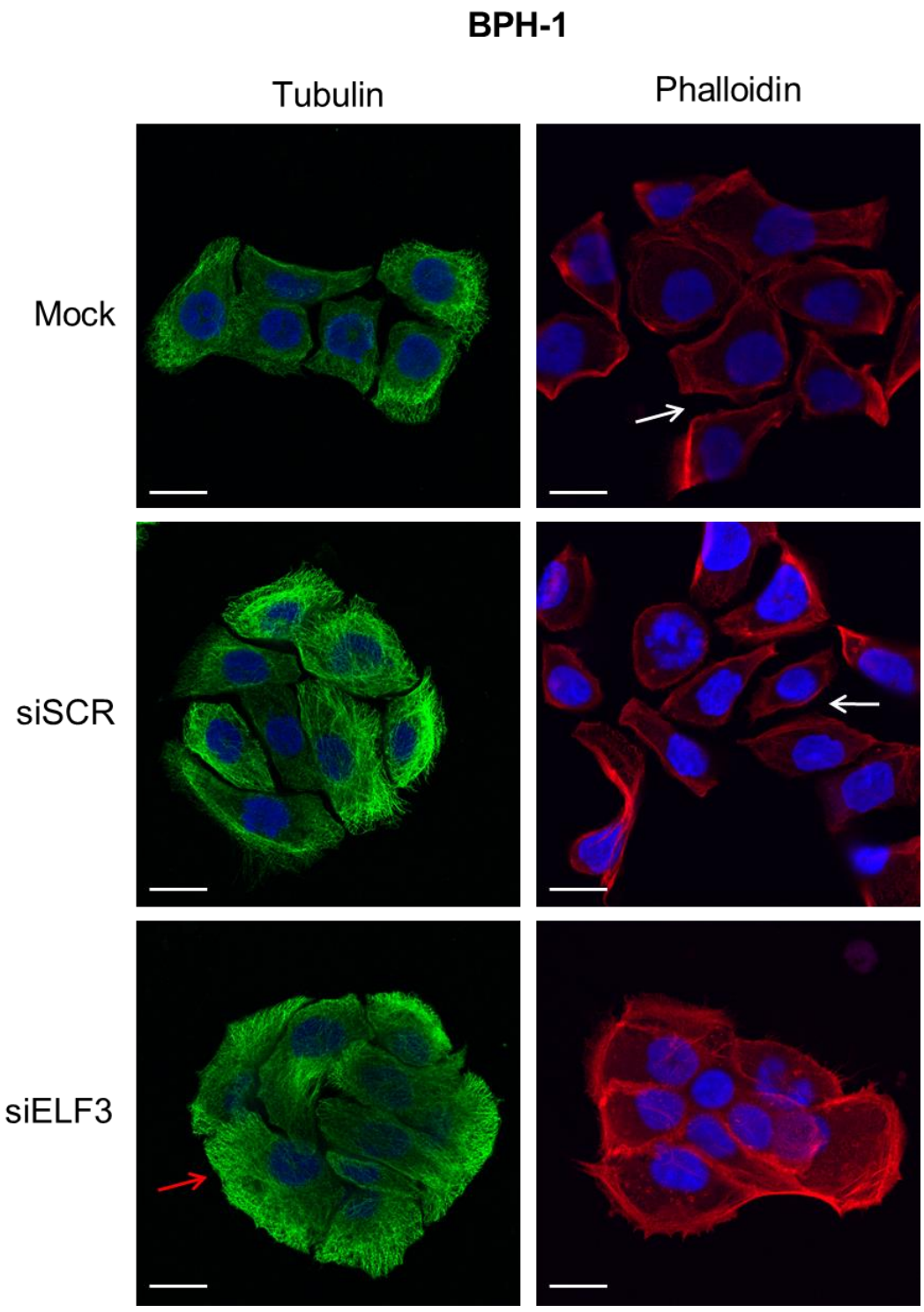

Figure 3.22. ELF3 knockdown alters colony formation in BPH-1 cells.

BPH-1 cells were transfected with ELF3 (siELF3) and scrambled siRNA (siSCR), fixed in 4% paraformaldehyde at day 3 post-transfection and stained with tubulin and phalloidin. The white arrows highlight spaces between cells in mock and siSCR cells. The red arrow highlights the location of tubulin at the colony periphery in siELF3 cells. Green = tubulin, red = phalloidin, blue = DAPI. Scale bar = 20µm.

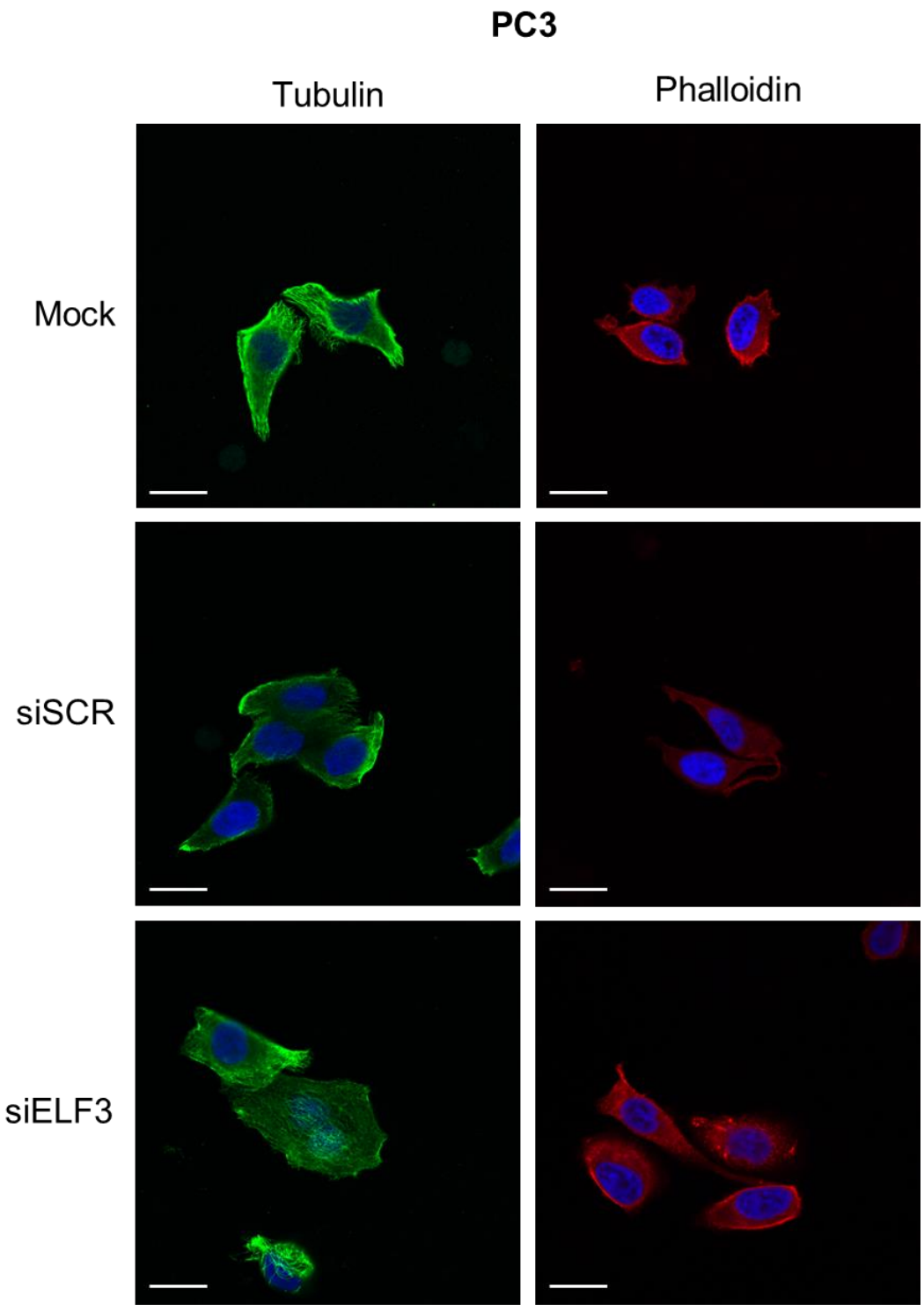

Figure 3.23. ELF3 knockdown does not alter colony formation in PC3 cells.

PC3 cells were transfected with ELF3 (siELF3) and scrambled siRNA (siSCR), fixed in 4% paraformaldehyde at day 3 post-transfection and stained with tubulin and phalloidin. Green = tubulin, red = phalloidin, blue = DAPI. Scale bar = 20µm.

3.4.6 ELF3 knockdown alters the expression of differentiation markers

The biological and morphological responses to ELF3 knockdown showed a significant change in phenotype. To determine the potential genes controlled by ELF3, the expression of differentiation and EMT markers were first investigated. CK5 is a basal cell marker whilst CK18 is a marker of luminal cells. BPH-1 cells are a good model as they grow as heterogeneous populations, like primary cultures, and so cells express varying levels of CK5 and CK18. E-cadherin is an epithelial cell marker whilst active β-catenin is a marker for EMT.

Western blot analysis was carried out on BPH-1 cells over a time course of 6 days after ELF3 knockdown (Figure 3.24A). At day 3 there was a modest increase in CK5 and decrease in CK18 expression, suggesting a more basal phenotype. There was an early and sustained increase of active β-catenin expression in ELF3 knockdown cells until day 3, however by day 5 this increase in expression had diminished, suggesting it was an early response to ELF3 knockdown. By day 5 there was also a sustained progressive increase in CK5 and E-cadherin expression and a decrease in CK18.

ICC was also carried out at the day 3 time point and showed an increase in CK5 and decrease in CK18, confirming the change to a more basal phenotype (Figure 3.24B). The colonies also appeared to be more condensed and there was less cytoplasmic space evident, compared to mock and siSCR cells, which correlates with the phalloidin and tubulin staining (Section 3.4.5). An increase in active β-catenin was also seen, however it was concentrated at the cell membrane. This suggests that rather than activating the Wnt signalling pathway and contributing to EMT, the active β-catenin is carrying out its alternative role as an adaptor to E-cadherin at the cell membrane. This corresponds to the increase in E-cadherin found by western blot.

In PC3 cells, western blot analysis detected a small decrease in CK18 expression at day 2 after ELF3 knockdown but this was not sustained until day 4 (Figure 3.25A). CK5 was not detected in any of the conditions or time points, even following repeats. This suggests the level of expression is below the limit of detection and these cells are not as basal as BPH-1 cells. There was also an increase in active β-catenin seen at later time points than the BPH-1 cells (day 4). There was little E-cadherin detected until days 4 and 5 in the ELF3 knockdown cells, which correlates with the results seen in BPH-1. The reduced response regarding differentiation and EMT markers in PC3 cells with ELF3 knockdown may reflect the reduced responses seen in some functional assays compared to BPH-1 cells. Furthermore, since only a few markers have been investigated, there may be more significant changes in other markers not studied.

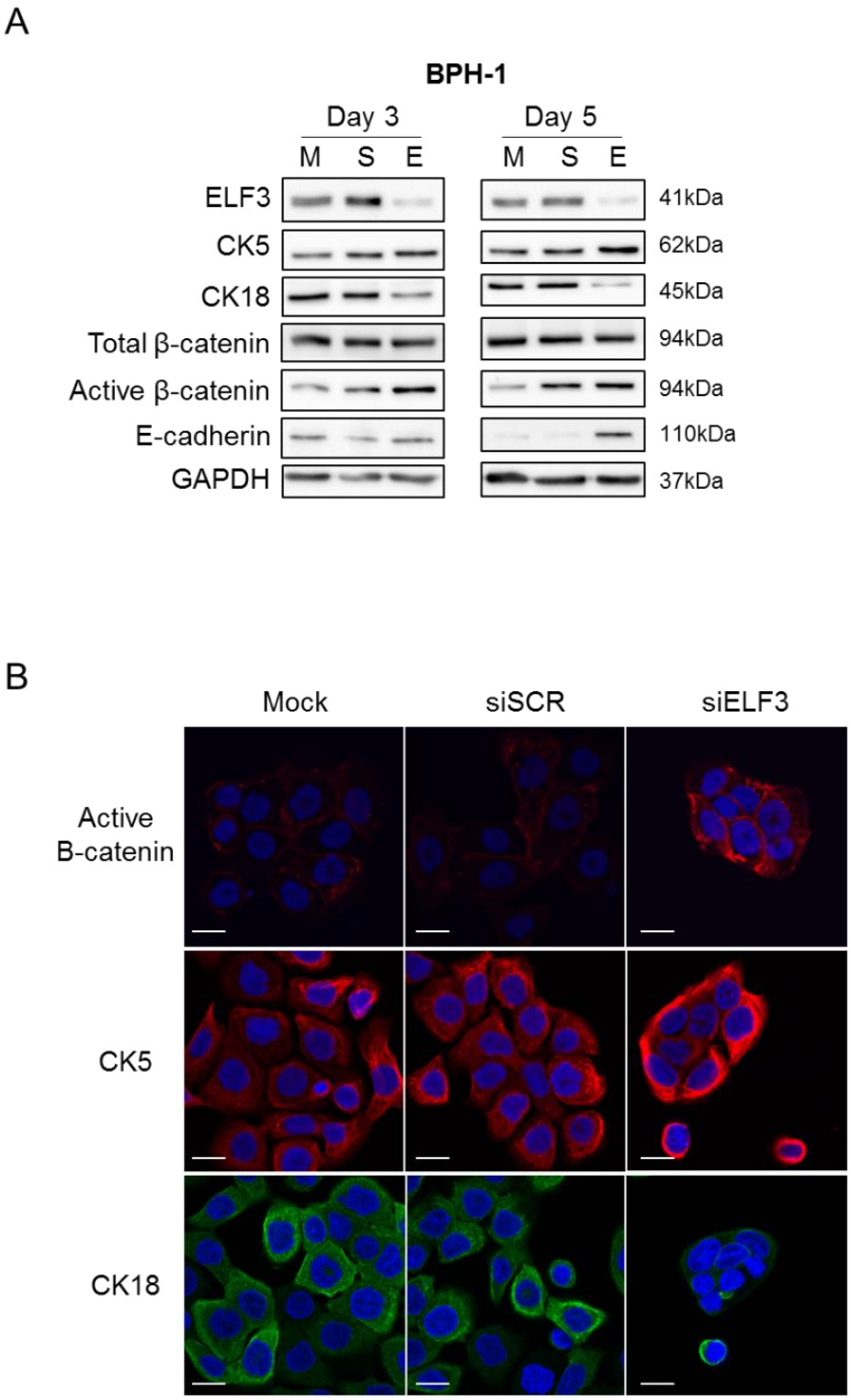

Figure 3.24. ELF3 knockdown alters the expression of differentiation markers in BPH-1 cells.

(A) Expression of differentiation markers was analysed by western blot in BPH-1 cells following ELF3 knockdown over a 6 day time course. Blots indicate protein expression at day 3 and day 5 post-transfection. 20µg of protein was loaded per lane onto a 10% SDS gel, transferred onto a PVDF membrane and probed for the indicated proteins. GAPDH was used as a loading control. M = Mock transfection, S = siSCR, E = siELF3. (B) BPH-1 cells were transfected with ELF3 (siELF3) and scrambled siRNA (siSCR), fixed in 4% paraformaldehyde at day 3 post-transfection and stained with the indicated antibodies. Scale bar = 20µm.

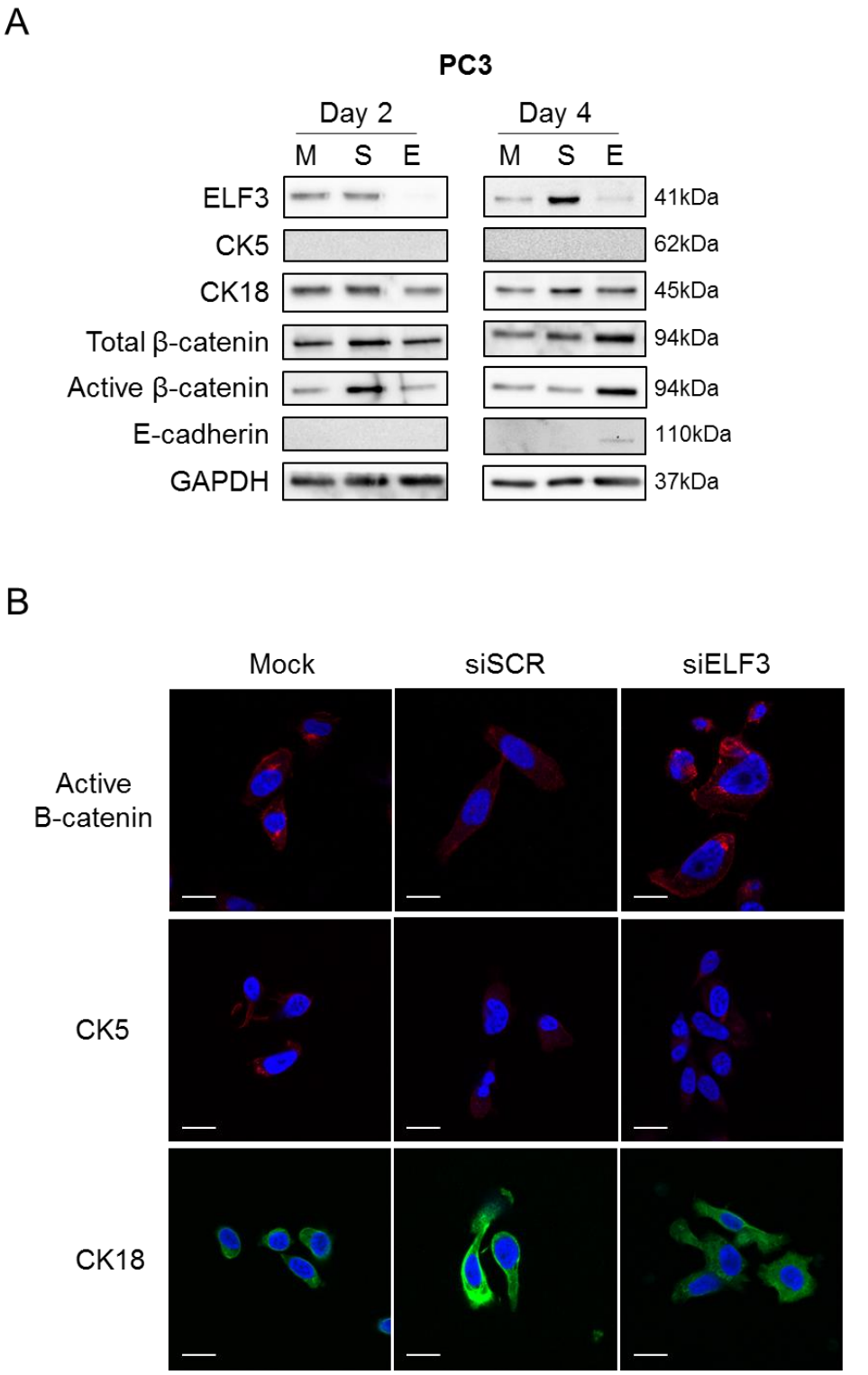

Figure 3.25. ELF3 knockdown alters the expression of differentiation markers in PC3 cells.

(A) Expression of differentiation markers was analysed by western blot in BPH-1 cells following ELF3 knockdown over a 6 day time course. Blots indicate protein expression at day 2 and day 4 post-transfection. 20µg of protein was loaded per lane onto a 10% SDS gel, transferred onto a PVDF membrane and probed for the indicated proteins. GAPDH was used as a loading control. M = Mock transfection, S = siSCR, E = siELF3. (B) BPH-1 cells were transfected with ELF3 (siELF3) and scrambled siRNA (siSCR), fixed in 4% paraformaldehyde at day 3 post-transfection and stained with the indicated antibodies. Scale bar = 20µm.

3.5 Generating lentiviral vectors for ELF3 overexpression studies

3.5.1 Invitrogen Gateway Cloning Technology strategy

Lentivirus transduction is an efficient method of manipulating gene expression in primary cells as they are more likely to die from treatment with traditional transfection reagents compared to cell lines. Lentiviruses were favoured over retroviruses as they are able to transduce quiescent cells such as SCs and more differentiated less proliferative cells, which are present in the primary cultures, whereas retroviruses are unable to do so. Furthermore lentiviruses also generally produce a better viral titre than retroviruses (Table 3.2) (Lewis and Emerman, 1994, Vannucci et al., 2013, Dufait et al., 2012, Howe et al., 2008).

The Invitrogen Gateway Cloning Technology (ThermoFisher Scientific) was used to generate lentiviral vectors to overexpress ELF3. The system is based on bacteriophage lambda *att* site recombination, where the phage genome can be integrated into the bacterial genome using specific sites and recombination enzymes (Katzen, 2007). The Gateway system is an efficient method of cloning, as one recombination reaction allows the gene of interest to be inserted into a "DONR" vector, resulting in the generation of an entry clone. The entry clone can then be used to generate a series of expression clones by recombination with a destination vector which has a desired expression characteristic, e.g. fluorescence, tag, antibiotic resistance, as well as the necessary sequences for lentivirus production. The entry and expression clones contain antibiotic resistance genes for selection.

For ELF3 to be integrated into the entry clone it was flanked with specific *attB* sequences by two rounds of PCR and gel extraction (Figure 3.26). The first set of primers contained the ends of the ELF3 sequence and the inner *attB* sequence, whilst the second set contained the outer *attB* sequence. A recombination reaction was carried out using BP Clonase™ in which the *attB* flanked ELF3 sequence was integrated into the DONR vector via *attP* sequences, resulting in the formation of *attL* sequences. Single clones were then selected on kanamycin agar plates following transformation in DH5α *E.coli* competent cells. Several entry clones were then validated by PCR, for the presence of ELF3, and then sequenced to ensure no mutations had been introduced during the recombination reaction. A second recombination reaction using LR Clonase™ was then carried out to incorporate ELF3 into two different destination vectors; one with GFP co-expressed with ELF3 under separate promoters (pDest298) and one with a Venus-tag at the N-terminal of ELF3 (pDest159). The *attL* sequences of the entry clone permit recombination with the specific destination vector which contain *attR* sequences via LR Clonase™. Single expression clones were selected following transformation using carbenicillin plates.

	Retrovirus	Lentivirus
Gene Expression	Stable & Transient	Stable & Transient
Transduce Dividing Cells	✓	✓
Transduce Non-Dividing Cells	X	✓
Integration into Target Cell Genome	✓	✓
Possible Insertional Mutagenesis	✓	✓
Relative Viral Titre	✓✓	✓✓✓

Table 3.2. Characteristics of retroviruses and lentiviruses as vectors for gene expression.

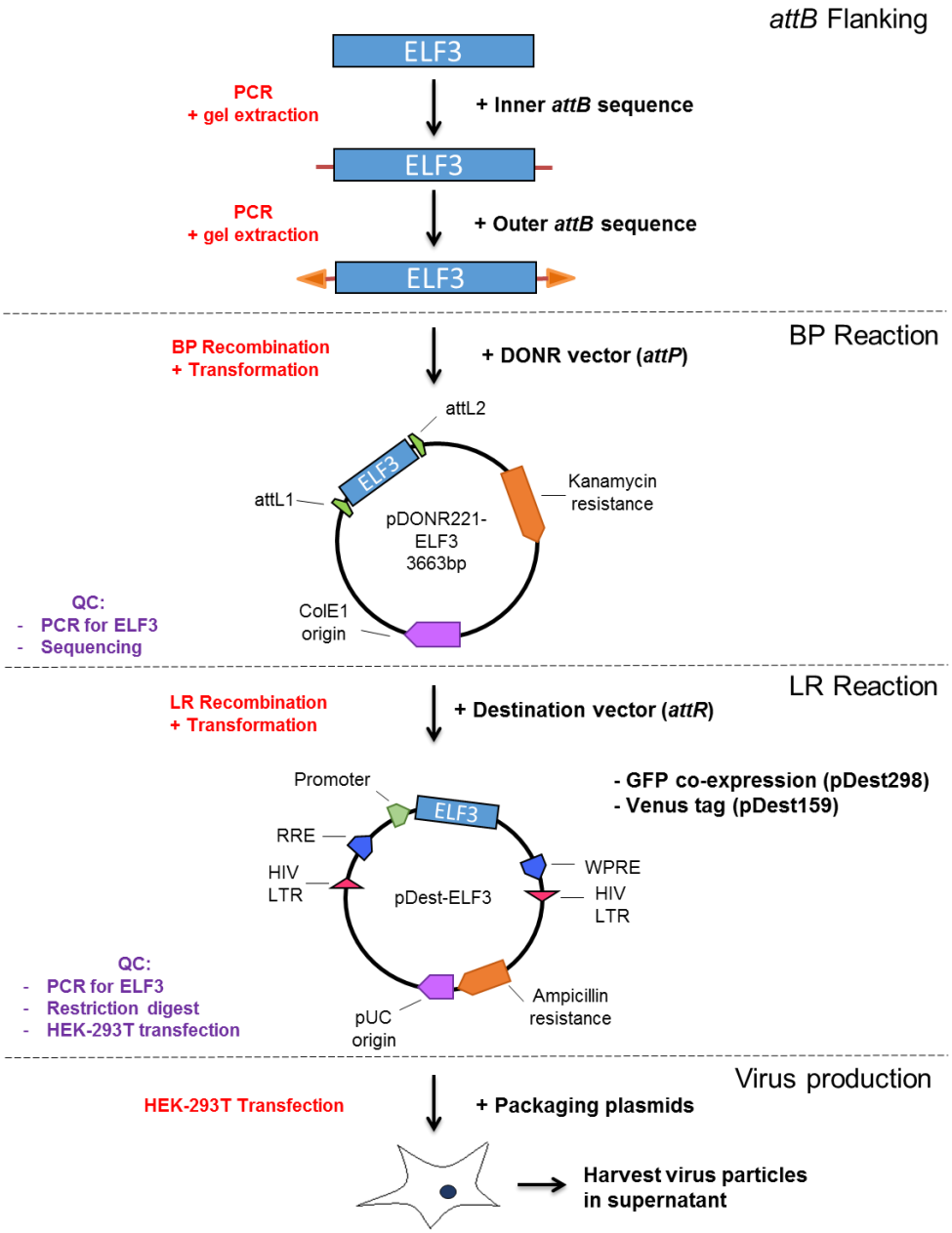

Figure 3.26. Lentivirus cloning strategy for ELF3 overexpression.

A summary of the steps involved in the production of ELF3-expressing lentiviral vectors using the Invitrogen Gateway Cloning Technology (ThermoFisher Scientific). ELF3 was first flanked with *attB* sequences by two rounds of PCR and gel extraction. This product was then inserted into a DONR vector by a BP recombination reaction. Following PCR and sequencing quality control checks, a second LR recombination reaction was carried out to incorporate ELF3 into two different destination vectors; one with GFP co-expressed with ELF3 under separate promoters (pDest298) and one with a Venus-tag at the N-terminal of ELF3 (pDest159). The destination vectors then underwent a series of quality control measures; PCR, restriction digest and HEK-293T transfection for the presence of the desired expression characteristic i.e. GFP/YFP expression. QC = quality control. RRE = Rev response element. LTR = long terminal repeats. WPRE = Woodchuck post-translational regulatory element.

3.5.2 Validation of ELF3 expression vectors

The described strategy (Figure 3.26) was performed using the wildtype (WT) ELF3 gene to create expression vectors pDest298-ELF3-WT and pDest159-ELF3-WT (Figure 3.27). The GFP co-expression vector (pDest298) was used for functional experiments, whilst the Venus-tag vector (pDest159) was used to determine the cellular localisation of ELF3. This was to eliminate any effects the tag may have on ELF3 functional assays.

In the literature, the cellular localisation of ELF3 has been described as both nuclear and cytoplasmic. Similarly, as demonstrated in Section 3.3, ELF3 is present in both the nucleus and cytoplasm of prostate epithelial cells. HEK-293T transfection of pDest159-ELF3-WT resulted in predominantly nuclear YFP, and therefore ELF3, expression (Figure 3.28B). To investigate any distinct functions ELF3 may have in the cytoplasm, an ELF3 mutant was acquired which contains a deletion of the AT-hook domain of ELF3 (obtained from Prof Arthur Gutierrez-Hartmann, University of Colorado) (Figure 3.29A). The AT-hook domain contains a nuclear localisation signal (NLS) and its deletion resulted in exclusively cytoplasmic expression (Figure 3.29C). This mutant therefore possesses no transcriptional activity.

The four resulting constructs (pDest298-ELF3-WT, pDest159-ELF3-WT, pDest298-ELF3-ΔAT and pDest159-ELF3-ΔAT) underwent several quality control processes (Figures 3.28 & 3.29). RT-PCR was carried out to determine which clones expressed ELF3 and a restriction digest was performed to ensure the ELF3-positive clones were complete expression vectors (as opposed to the entry vector). Finally, HEK-293T cells were transfected with each clone to examine the presence of either GFP or YFP and, in pDest159 vectors, the localisation of the YFP.

For functional studies, a control lentivirus construct was included in analysis. The control construct possessed the same lentiviral backbone (pDest298), however with the integration of a non-mammalian gene called β-glucoronidase (GUS). This therefore mimics the effects of lentiviral transduction, without the effects of specific gene expression.

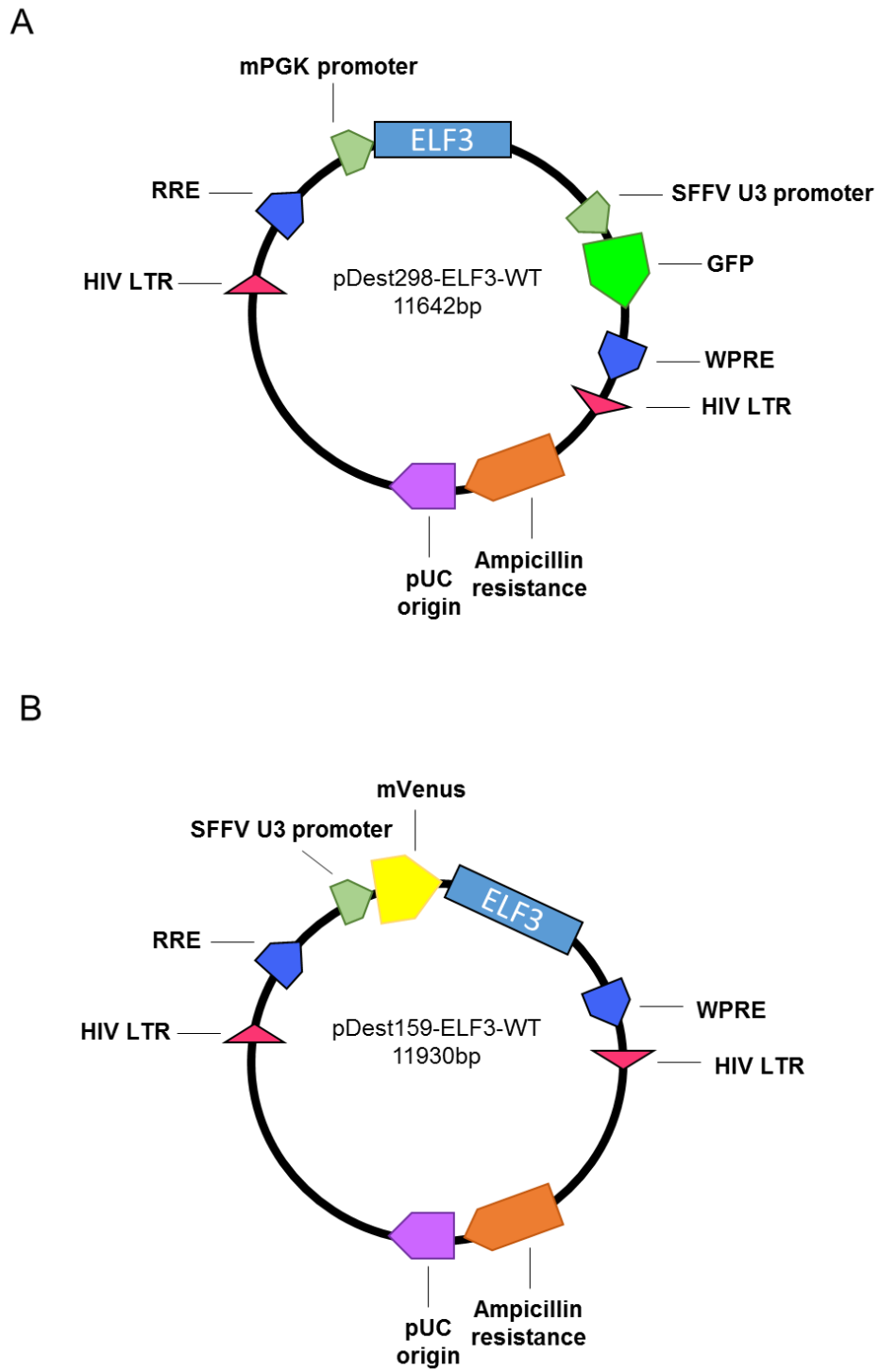

Figure 3.27. Vector maps of lentiviral ELF3 overexpression constructs.

Lentiviral vectors constructed for ELF3 overexpression using the Invitrogen Gateway Cloning Technology (ThermoFisher Scientific). (A) pDest298-ELF3-WT confers GFP co-expression with ELF3 under separate promoters. (B) pDest159-ELF3-WT confers a YFP-tag at the N-terminal of ELF3. Both vectors contain ampicillin resistance sequences for selection. RRE = Rev response element. LTR = Long terminal repeats. WPRE = Woodchuck post-transcription regulatory element.

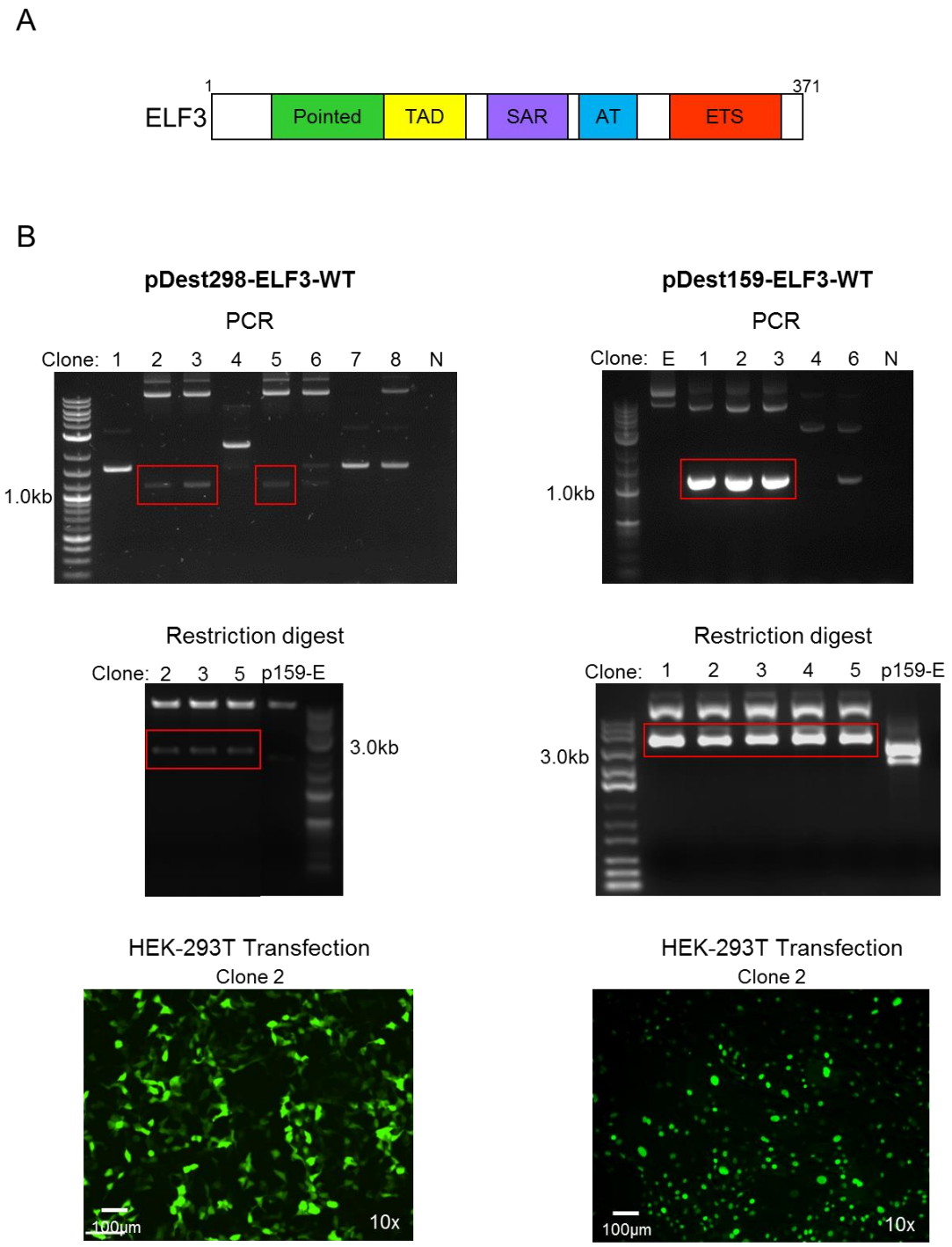

Figure 3.28. Validation of ELF3-WT lentiviral vectors.

(A) Schematic of the domain structure of wildtype (WT) ELF3 (371 amino acids long). (B) Lentiviral ELF3-WT overexpression vectors were validated by PCR for ELF3 expression (top panels), restriction digest to ensure the vectors were expression clones (middle panels) and HEK-293T transfection for GFP/YFP expression (bottom panels). pDest298-ELF3-WT (GFP co-expression), restriction enzyme = EcoRI. pDest159-ELF3-WT (Venus-tag), restriction enzyme = PvuII. N = no template control. p159-E = p159 empty vector.

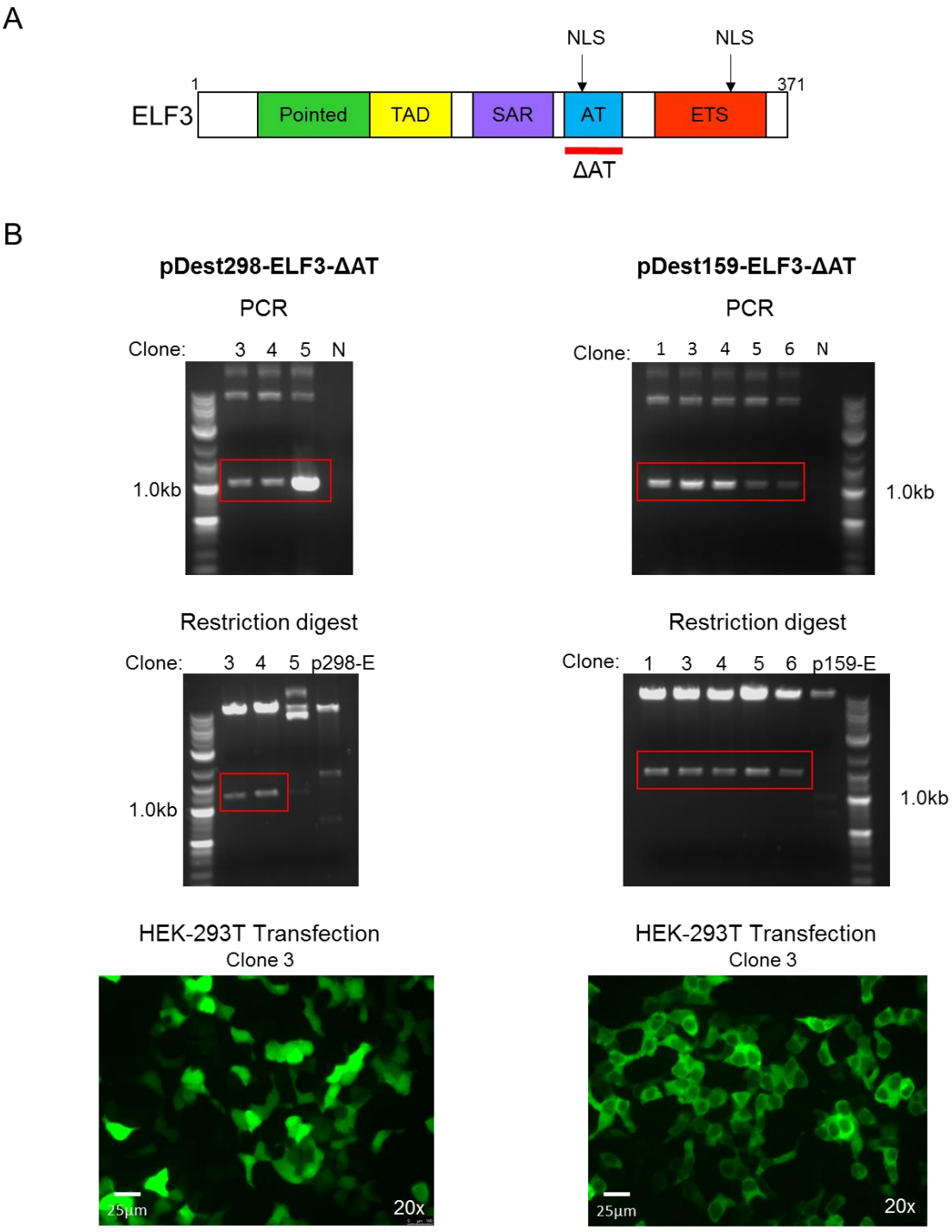

Figure 3.29. Validation of ELF3-ΔAT lentiviral vectors.

(A) Schematic of ELF3 domain structure indicating regions containing nuclear localisation signal (NLS) sequences. Red line indicates deletion in the ΔAT mutant. (B) Lentiviral ELF3-ΔAT overexpression vectors were validated by PCR for ELF3 expression (top panels), restriction digest to ensure the vectors were expression clones (middle panels) and HEK-293T transfection for GFP/YFP expression (bottom panels). pDest298-ELF3-ΔAT (GFP co-expression), restriction enzyme = BamHI. pDest159-ELF3-ΔAT (Venus-tag), restriction enzyme = BamHI. N = no template control. p298-E = p298 empty vector. p159-E = p159 empty vector.

3.5.3 Determining lentiviral titre of ELF3 overexpression vectors

Lentiviral titre was determined by GFP expression using flow cytometry analysis. Whilst several studies use easy to transduce cell lines such as HEK-293 to determine viral titre, it was important to use a model that related to the primary prostate epithelial cells, which were ultimately to be used in experiments and are more difficult to transduce. Since there is variability in transduction efficiency between different patient samples, it was also important to titre in a model which would produce a consistent and comparable titre between different batches of virus. For these reasons, P4E6 cells were chosen as an appropriate model to titre in as they were produced in this lab from a patient sample and are therefore closely related to the basal cultures that are routinely grown and have a similar transduction efficiency.

Viruses were concentrated using PEG-it solution and resuspended in PBS to avoid adding FCS containing media to primary cells as they are not ordinarily grown in this and would be induced to differentiate. A known number of P4E6 cells were transduced in suspension with 10-fold serial dilutions of concentrated virus between a range of 1:10 and 1:100,000. Cells were analysed at 48 hours post-transduction by flow cytometry on a CyAn ADP (Beckman Coulter). A summary of the gating strategy is shown in Figure 3.30. Viral titre was determined using dilutions which produced between 1 and 20% of GFP-positive P4E6 cells. Above 20% there may be an underestimation of the number of infectious particles, as cells may have been transduced more than once. The flow cytometer may also not be sensitive enough to detect the number of GFP-positive cells below 1%. pDest298 titres were in a range of $1.65x10^6$-$2.59x10^6$ whilst pDest159 titres were in a range of $1x10^6$-$1.2x10^7$ infectious particles/ml.

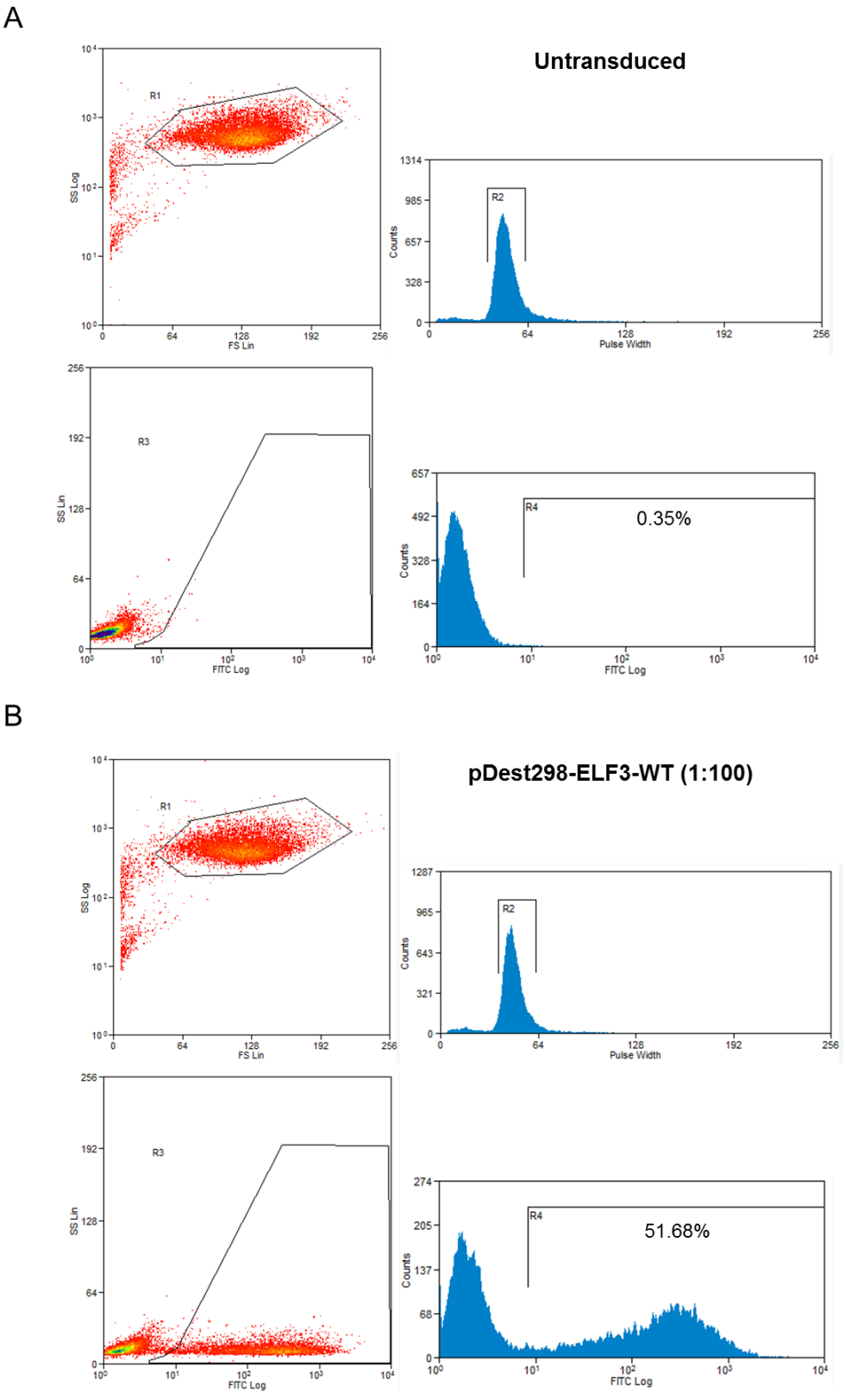

Figure 3.30. Gating strategy for lentiviral titration.

P4E6 cells were transduced with serial dilutions of generated lentivirus. Lentiviral titre was determined by GFP-expression at 48 hours post-transduction using flow cytometry. (A) Untransduced cells, (B) cells transduced with pDest298-ELF3-WT at a dilution of 1:100. Top panels show whole population (left) and singlets (right). Bottom panels indicate the GFP-positive population.

3.6 The effects of ELF3 overexpression on primary prostate epithelial cells

3.6.1 Localisation of ELF3 in lentiviral transduced primary prostate epithelial cells

Since reasonable ELF3 expression was present in all prostate cell lines tested (Section 3.1.1), investigation of the consequences of ELF3 overexpression was performed in primary prostate cells. As ELF3 was only expressed in the CB subpopulation of primary epithelial cultures (Section 3.2), the effects of ELF3 overexpression on the population as a whole was examined.

Primary prostate epithelial cells were transduced with pDest159-ELF3-WT and –ΔAT (in which the AT-hook domain containing a NLS has been deleted) vectors which possess a Venus-tag at the N-terminal of ELF3 to validate the cellular localisation of ELF3. Cells were transduced with each virus at a ratio of two infectious particles for every one cell. In cells transduced with ELF3-WT virus, ELF3 was present in the nucleus of cells, demonstrated by the co-localisation with DAPI (Figure 3.31). However, in cells transduced with ELF3-ΔAT virus, ELF3 was present in cytoplasm. This was the expected result and confirmed the ELF3-ΔAT virus could be used as a non-transcriptionally active control to identify any distinct cytoplasmic functions of ELF3 in primary prostate cells.

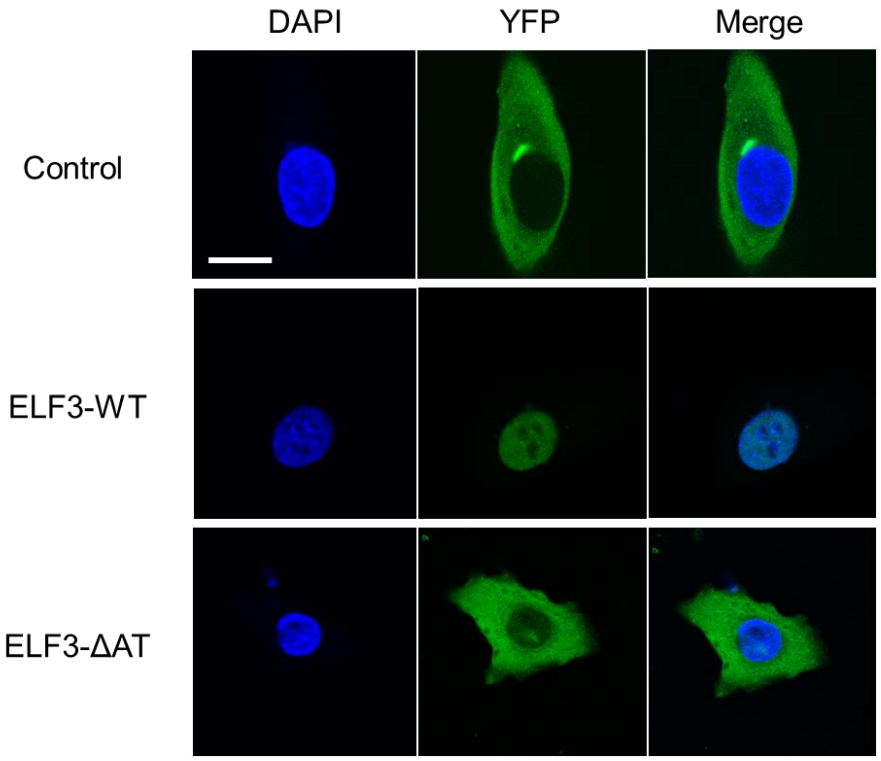

Figure 3.31. ELF3 localisation in primary prostate epithelial cells.

Lentiviral vectors conferring a YFP-tag at the N-terminal of ELF3 were used to determine the localisation of WT and mutant ELF3. Primary prostate cells were transduced with pDest159-GUS (control), pDest159-ELF3-WT (ELF3-WT) and pDest159-ELF3-ΔAT (ELF3-ΔAT) constructs at a ratio of two infectious particles for every individual cell. Representative confocal imaging of primary prostate cells. Blue = DAPI. Scale bar = 20μm.

3.6.2 ELF3 overexpression differentially alters the viability of primary normal and cancer prostate epithelial cells

ELF3 overexpression was carried out on two cancer samples and 3 normal and cancer matched pairs from the same patients. Cell viability was analysed by alamarBlue over a six day time course. Cells were replated at the original seeding density after the reading on day 3. Overexpression of nuclear ELF3 (ELF3-WT) in primary normal epithelial cells showed a trend of decreased viability, whilst in cancer samples there was an increase in viability (Figure 3.32). Although not significant, overexpression of cytoplasmic ELF3 (ELF3-ΔAT) showed a similar trend on the viability of both normal and cancer primary prostate samples as ELF3-WT.

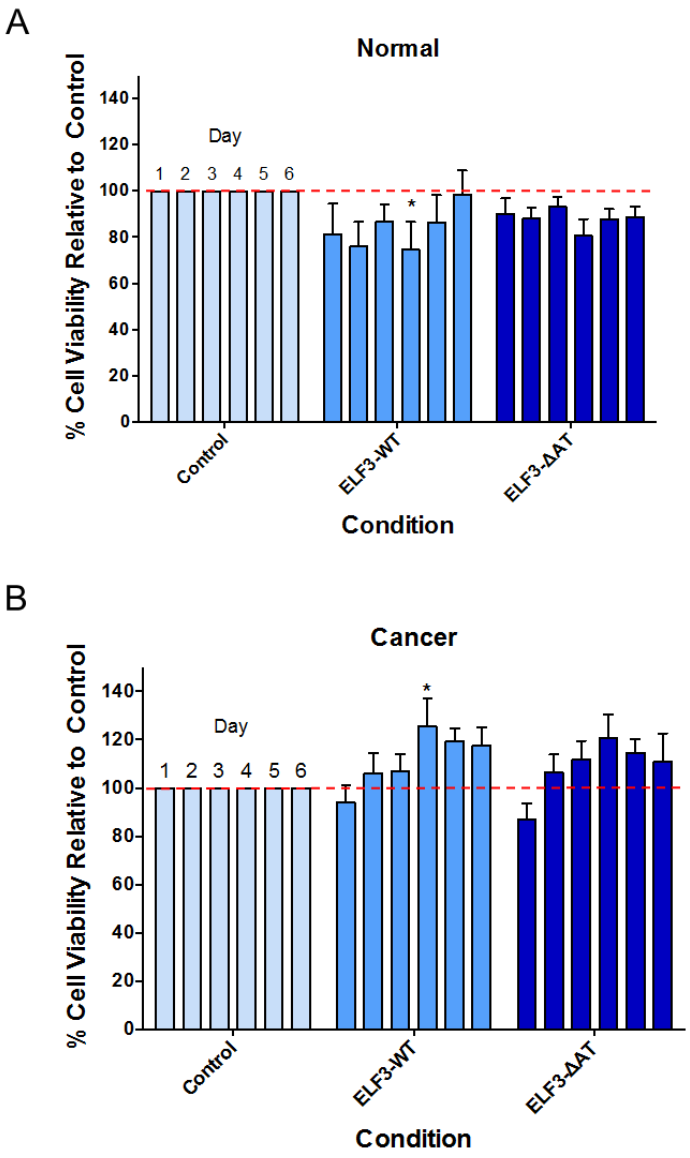

Figure 3.32. ELF3 overexpression differentially alters the viability of normal and cancer cells over time.

Two cancer and three normal/cancer matched primary prostate pairs were transduced with control, ELF3-WT and ELF3-ΔAT constructs at a ratio of two infectious particles for every individual cell. Cells were plated at 40% confluency on day 0 of alamarBlue assay and the fluorescence was read at days 1-6. Cells were replated at the original density on day 3. (A) Normal, n=3. (B) Cancer, n=5. Control samples were normalised to 100% viability. Statistical significance was determined using a 2-way ANOVA with Tukey's multiple comparison test.

3.6.3 ELF3 overexpression does not significantly alter primary prostate cell migration

To assess the effects of ELF3 overexpression on the migratory capacity of primary prostate cells, quantitative phase imaging was carried out on two normal and cancer matched pairs using a VL21 platform. An Ibidi insert was used to ensure the gap was consistent between all wells. Each condition was carried out in triplicate and each well contained three regions of interest (ROI). Sample H681/17 L (cancer) does not have a control transduced condition in this instance as the culture became infected, however ELF3-WT and ELF3-ΔAT were compared. Full time lapse videos are shown in Appendix 3.1 (see attached CD). There is no consistent trend between samples. The control wound closed significantly faster in samples H681/17 R (normal) and H682/17 L (cancer), whereas the ELF3 overexpressing conditions closed faster than the control in sample H682/17 R (normal) (Figure 3.33). There was no significant difference between ELF3-WT and ELF3-ΔAT in any of the samples. The inconsistency in wound closure highlights the heterogeneity between patients. More patients would have to be tested in order to draw a clear conclusion.

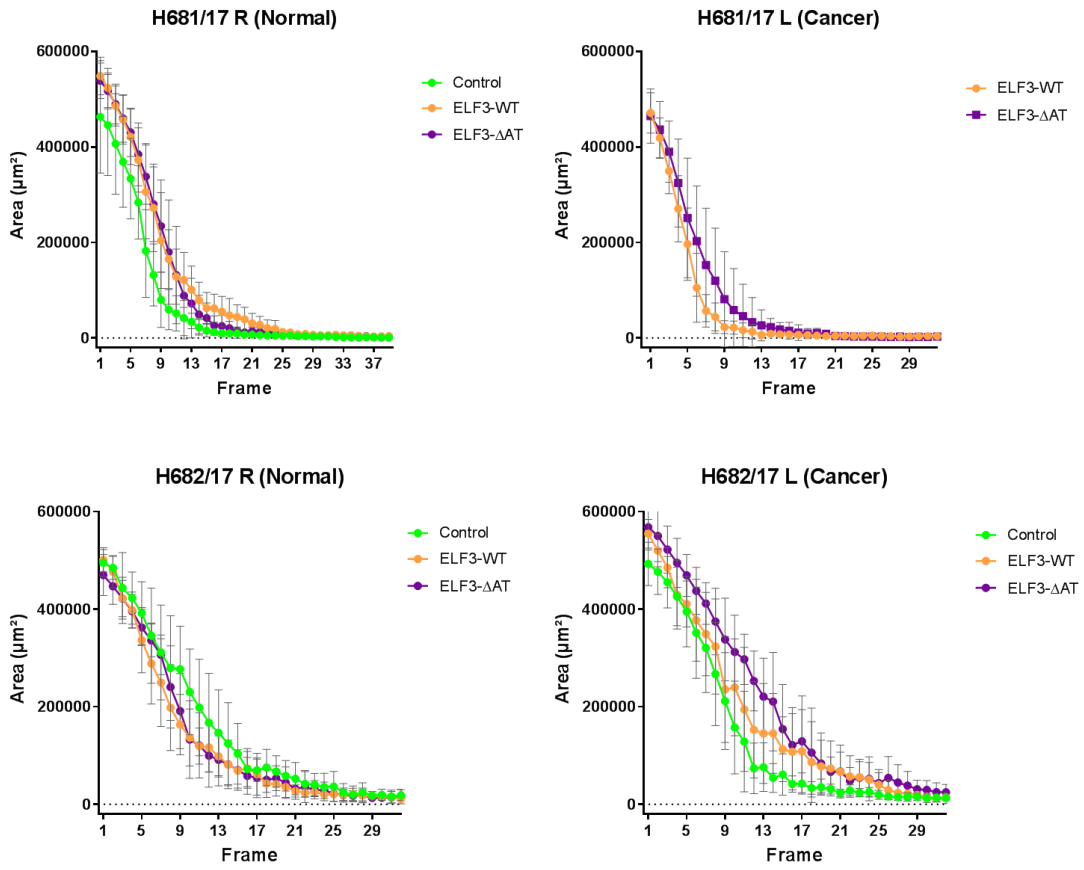

Figure 3.33. The effects of ELF3 overexpression on primary prostate cell migration.

Two normal/cancer matched primary prostate pairs were transduced with control, ELF3-WT and ELF3-ΔAT viruses at a ratio of two infectious particles for every individual cell. Cells were plated into Ibidi inserts to create a consistent gap in the centre and placed on a VL21 microscope to track wound closure at 35 minute intervals. The data was processed by Amanda Noble using Cell Analysis Toolbox (CAT) software and analysed and presented by myself. Graphs show area of the wounds at each 35 minute time frame. Accompanying videos found in Appendix 3.1. Statistical significance was determined using a 2-way ANOVA with Tukey's multiple comparison test.

3.6.4 ELF3 overexpression alters the differentiation state of primary prostate epithelial cells

The videos obtained from the migration analysis using quantitative phase imaging indicated there may be a change in cell subpopulation proportions with ELF3 overexpression (Figure 3.34). TA cells are generally smaller and fast moving, whilst CB cells are larger and more spread out (Frame et al., 2017). Therefore, in general, TA cells have a smaller median cell area and perimeter than CB cells. The quantitative phase imaging tracked each individual cell and recorded the median cell area and median cell perimeter for the duration of the time course.

Figure 3.37 summarises the significance and trend of the data shown in Figures 3.35 (median cell area) and 3.36 (median cell perimeter). Cell numbers ranged from 781 to 1640 for each individual ROI. The three ROIs from each well were combined as replicates and plotted. With the exception of sample H681/17 L (cancer) which did not have a control, results show that ELF3-WT cells tended to be smaller than control cells and ELF3-ΔAT cells. This indicates that ELF3-WT cells may have a larger proportion of TA cells. Furthermore, corresponding to this, ELF3-ΔAT cells tended to be larger than the control cells and ELF3-WT cells, thus indicating a larger proportion of CB cells. These findings were irrespective of diagnosis.

To further investigate this observation, the two matched pairs from the imaging experiment together with a third matched pair, were stained with CD49b and analysed by flow cytometry. TA cells have high expression of CD49b ($\alpha_2\beta_1$ integrin), whilst CB cells have low expression. Since the cells show a range of expression, median fluorescence was used to compare subpopulation proportions. In both the normal and cancer samples, there was a significant increase in CD49b expression in ELF3-WT cells relative to control cells and ELF3-ΔAT cells, indicative of a higher proportion of more primitive TA cells (Figure 3.38). There was no significant difference in CD49b expression in ELF3-ΔAT cells relative to control cells in both normal and cancer samples. However, two out of the three cancer samples did show a decrease in median fluorescence.

Collectively, these data show that ELF3-WT transduced cells have a higher proportion of TA cells and ELF3-ΔAT transduced cells have a higher proportion of CB cells, regardless of whether the cells where derived from normal or cancer regions.

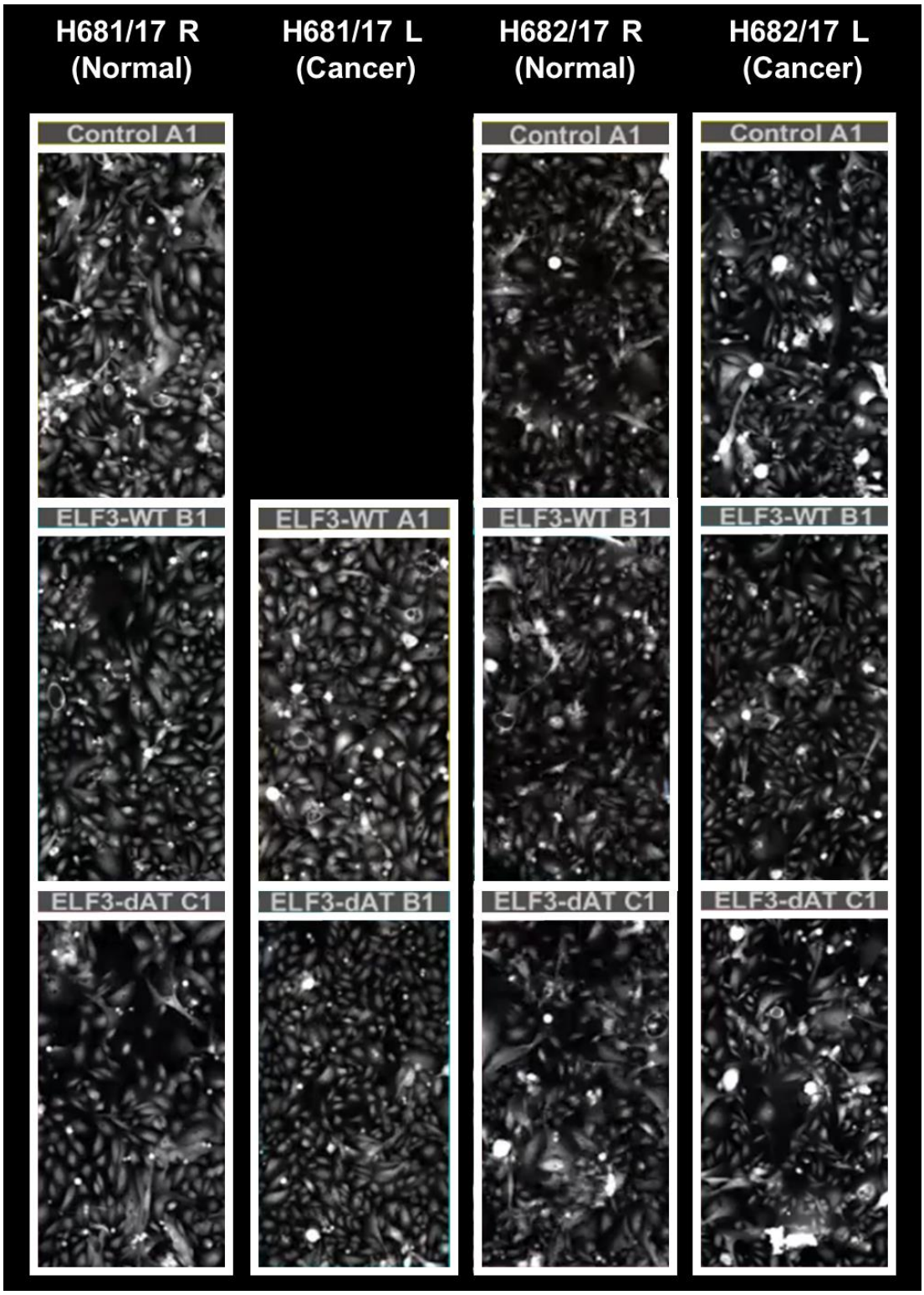

Figure 3.34. Heterogeneity of primary prostate epithelial cells with ELF3 overexpression.

Two normal/cancer matched primary prostate pairs were transduced with control, ELF3-WT and ELF3-ΔAT constructs at a ratio of two infectious particles for every individual cell. Panels show still frames of the quantitative phase imaging from a VL21 microscope. The data was processed by Amanda Noble using Cell Analysis Toolbox (CAT) software and analysed and presented by myself. A1, B1, C1 merely represents which well from the 6-well plate is in the image.

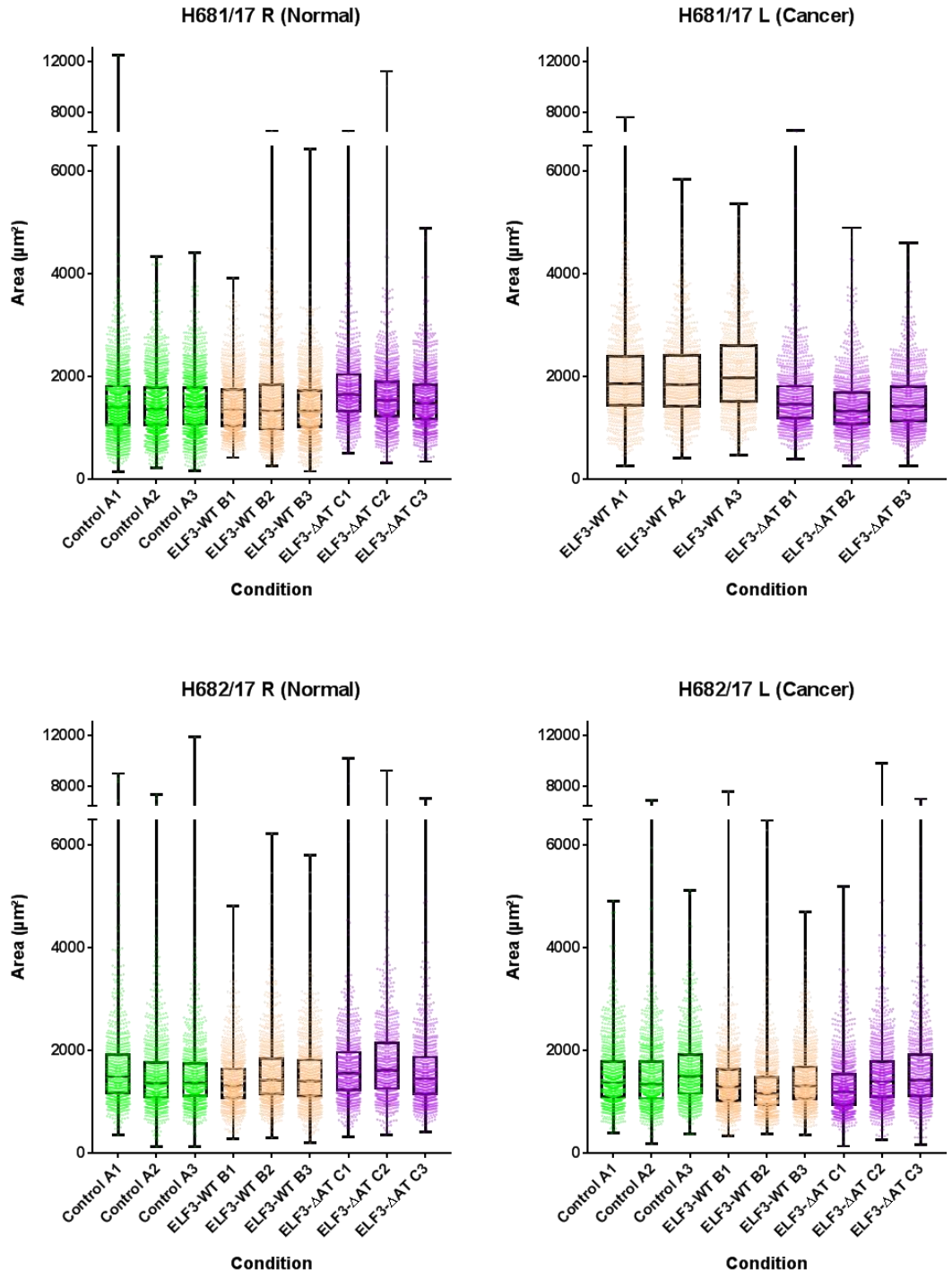

Figure 3.35. ELF3 overexpression significantly alters the median cell area of primary prostate epithelial cells.

Two normal/cancer matched primary prostate pairs were transduced with control, ELF3-WT and ELF3-ΔAT constructs at a ratio of two infectious particles for every individual cell. Quantitative phase imaging on a VL21 microscope was used to track individual cells. The data was processed by Amanda Noble using Cell Analysis Toolbox (CAT) software and analysed and presented by myself. Graphs show the median cell area where each data point is a single cell. Each condition was carried out in triplicate (denoted A1, A2 and A3 etc.) and each bar represents data from three regions of interest (ROI) within each replicate. Statistical significance is shown in Figure 3.37.

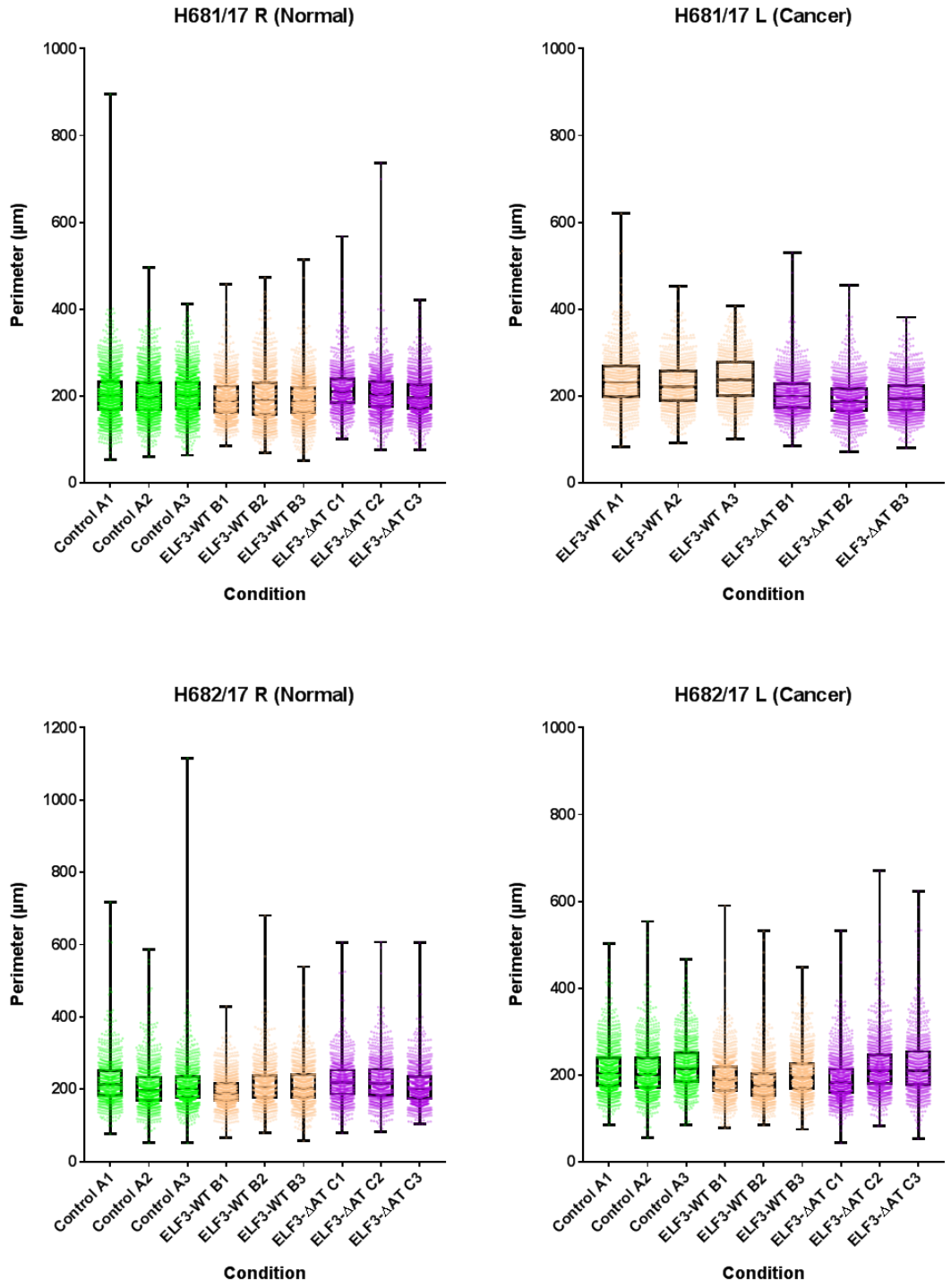

Figure 3.36. ELF3 overexpression significantly alters the median cell perimeter of primary prostate epithelial cells.

Two normal/cancer matched primary prostate pairs were transduced with control, ELF3-WT and ELF3-ΔAT constructs at a ratio of two infectious particles for every individual cell. Quantitative phase imaging on a VL21 microscope was used to track individual cells. The data was processed by Amanda Noble using Cell Analysis Toolbox (CAT) software and analysed and presented by myself. Graphs show the median cell perimeter where each data point is a single cell. Each condition was carried out in triplicate (denoted A1, A2 and A3 etc.) and each bar represents data from three regions of interest (ROI) within each replicate. Statistical significance is shown in Figure 3.37.

H681/17 R (Normal)			
Comparison	**Median cell area significance / direction**	**Median cell perimeter significance / direction**	**Trend**
Cont:ELF3-WT			
A1:B1	NS	**** / ↓	Control cells larger than ELF3-WT
A2:B2	NS	** / ↓	
A3:B3	** / ↓	**** / ↓	
Cont:ELF3-ΔAT			
A1:C1	**** / ↑	**** / ↑	ELF3-ΔAT cells larger than control
A2:C2	**** / ↑	** / ↑	
A3:C3	*** / ↑	NS	
ELF3-WT:ELF3-ΔAT			
B1:C1	**** / ↑	**** / ↑	ELF3-ΔAT cells larger than ELF3-WT
B2:C2	**** / ↑	**** / ↑	
B3:C3	**** / ↑	**** / ↑	

H681/17 L (Cancer)			
Comparison	**Median cell area significance / direction**	**Median cell perimeter significance / direction**	**Trend**
ELF3-WT:ELF3-ΔAT			
A1:B1	**** / ↓	**** / ↓	ELF3-WT cells larger than ELF3-ΔAT
A2:B2	**** / ↓	**** / ↓	
A3:B3	**** / ↓	**** / ↓	

H682/17 R (Normal)			
Comparison	**Median cell area significance / direction**	**Median cell perimeter significance / direction**	**Trend**
Cont:ELF3-WT			
A1:B1	**** / ↓	**** / ↓	Control cells similar to ELF3-WT
A2:B2	** / ↑	** / ↑	
A3:B3	NS	NS	
Cont:ELF3-ΔAT			
A1:C1	* / ↑	NS	ELF3-ΔAT cells larger than control
A2:C2	**** / ↑	**** / ↑	
A3:C3	** / ↑	NS	
ELF3-WT:ELF3-ΔAT			
B1:C1	**** / ↑	**** / ↑	ELF3-ΔAT cells larger than ELF3-WT
B2:C2	**** / ↑	**** / ↑	
B3:C3	* / ↑	NS	

H682/17 L (Cancer)			
Comparison	**Median cell area significance / direction**	**Median cell perimeter significance / direction**	**Trend**
Cont:ELF3-WT			
A1:B1	**** / ↓	**** / ↓	Control cells larger than ELF3-WT
A2:B2	**** / ↓	**** / ↓	
A3:B3	**** / ↓	**** / ↓	
Cont:ELF3-ΔAT			
A1:C1	**** / ↓	**** / ↓	Control cells similar to ELF3-ΔAT
A2:C2	NS	*** / ↑	
A3:C3	NS	NS	
ELF3-WT:ELF3-ΔAT			
B1:C1	*** / ↓	** / ↓	ELF3-ΔAT cells larger than ELF3-WT
B2:C2	**** / ↑	**** / ↑	
B3:C3	**** / ↑	**** / ↑	

Figure 3.37. Statistical analysis of median cell area and median cell perimeter of primary prostate cells with ELF3 overexpression.

Tables show statistical significance and trend of each primary sample from Figures 3.35 (median cell area) and 3.36 (median cell perimeter). For simplicity, only corresponding triplicate wells for each condition were compared. Statistical significance was analysed using the Mann-Whitney test.

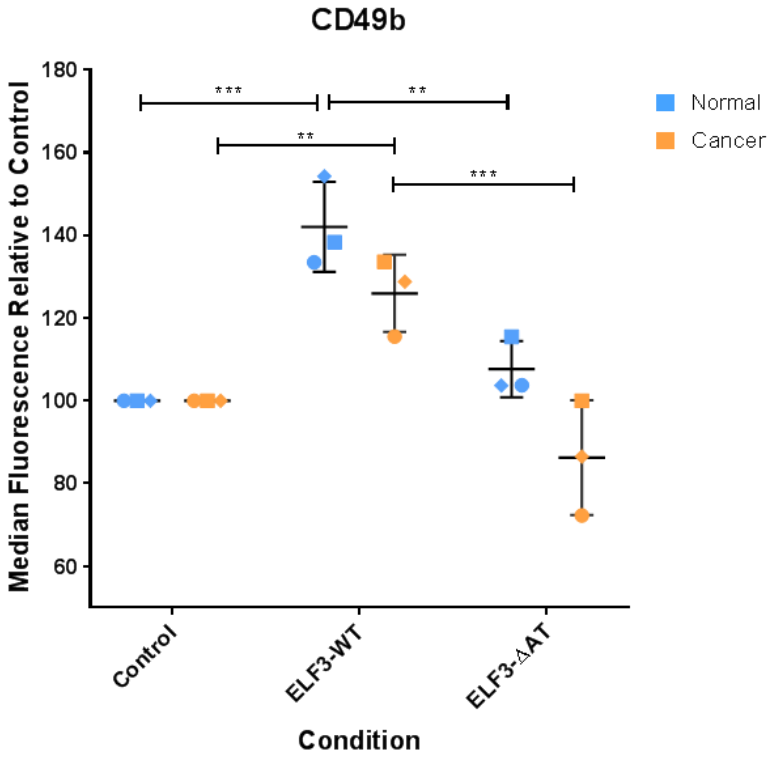

Figure 3.38. ELF3 overexpression alters the differentiation state of primary prostate cells.

Three normal/cancer matched primary prostate pairs were transduced with control, ELF3-WT and ELF3-ΔAT constructs at a ratio of two infectious particles for every individual cell. Relative median fluorescence of CD49b staining was analysed by flow cytometry. Control cells were normalised to a median fluorescence of 100. Matching symbols indicate cells from the same patient. Statistical significance was determined using a 2-way ANOVA with Tukey's multiple comparison test.

3.7 ELF3 regulatory networks

3.7.1 ELF3 expression is upregulated by histone deacetylase inhibitor Vorinostat in primary prostate epithelial cells but does not induce a neuroendocrine phenotype

Given that prostate tissue homogenate lysates did not express ELF3, and ELF3 was only expressed in CB, not TA cells, it was hypothesised that ELF3 may be epigenetically silenced in TA cells. To investigate this, primary prostate epithelial cell cultures were treated with three different doses of the HDAC inhibitor vorinostat (low = 0.625μM, medium = 2.5μM and high = 10μM) (Frame et al., 2017). Cells were harvested at 4 hours and 24 hours post-treatment for protein analysis by western blot. Compared to the untreated controls, ELF3 expression was induced by vorinostat treatment in both primary samples tested (Figure 3.39A). ELF3 expression increased both with increasing concentration and duration of treatment with vorinostat.

To determine in which cell populations ELF3 was upregulated, vorinostat treatment was administered to the selected TA and CB cell subpopulations as well as the whole population of patient sample H609/17 (Gleason 3+4). The medium dose of 2.5μM for 24 hours was selected as the optimal treatment for significant ELF3 upregulation. Whilst ELF3 was expressed at low levels in the untreated whole population or TA cells, there was significant ELF3 expression in the untreated CB population, confirming the expression pattern described in section 3.2.3. However, following vorinostat treatment, ELF3 was upregulated in all three cell populations (Figure 3.39B).

HDAC inhibitors are known to induce a NE phenotype in PCa (Frigo and McDonnell, 2008). Furthermore, it has been demonstrated by a previous PhD student that treatment with HDAC inhibitors can result in the upregulation of NE cell markers in our primary prostate epithelial cell cultures (Oldridge E., unpublished data). Given the previous finding that ELF3 was expressed in a subset of high grade (Gleason >7) PCa's shown by tissue microarray, it was hypothesised that this may be due to the emergence of a NE phenotype in some less differentiated PCa's (Section 3.3.2). Whilst NE cells are present in the normal prostate, evidence shows the emergence of a NE phenotype in more advanced PCa (Terry and Beltran, 2014). Neuron specific enolase (NSE) was used as a marker of NE differentiation. Whilst there was an increase in NSE expression in sample H591/17 at the 24 hour time point with the high vorinostat dose, there was no increase in sample H598/17 with vorinostat treatment. However, a more elongated morphology was present following treatment (Figure 3.39C), as well as the formation of processes which is characteristic of NE cells (Abrahamsson, 1999).

A

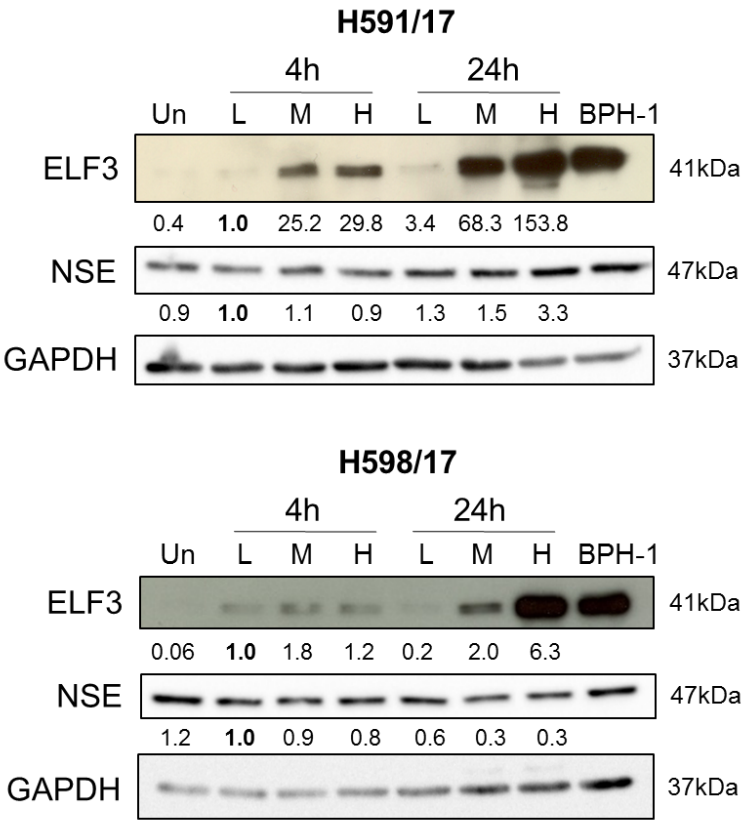
H591/17
4h
24h
Un L M H L M H BPH-1
ELF3
41kDa
0.4 1.0 25.2 29.8 3.4 68.3 153.8
NSE
47kDa
0.9 1.0 1.1 0.9 1.3 1.5 3.3
GAPDH
37kDa
H598/17
4h
24h
Un L M H L M H BPH-1
ELF3
41kDa
0.06 1.0 1.8 1.2 0.2 2.0 6.3
NSE
47kDa
1.2 1.0 0.9 0.8 0.6 0.3 0.3
GAPDH
37kDa

B

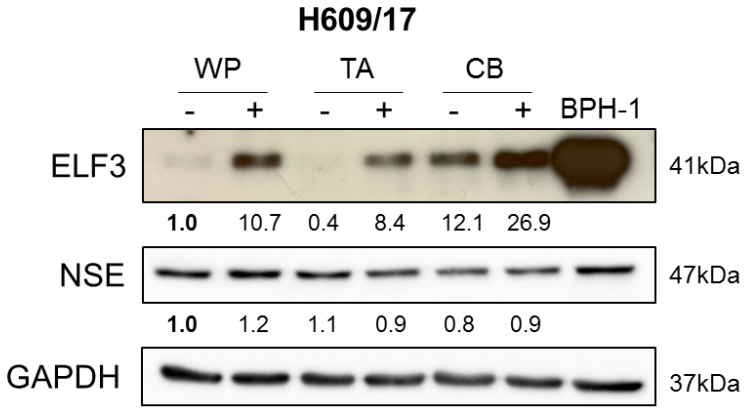
H609/17
WP
TA
CB
- + - + - + BPH-1
ELF3
41kDa
1.0 10.7 0.4 8.4 12.1 26.9
NSE
47kDa
1.0 1.2 1.1 0.9 0.8 0.9
GAPDH
37kDa

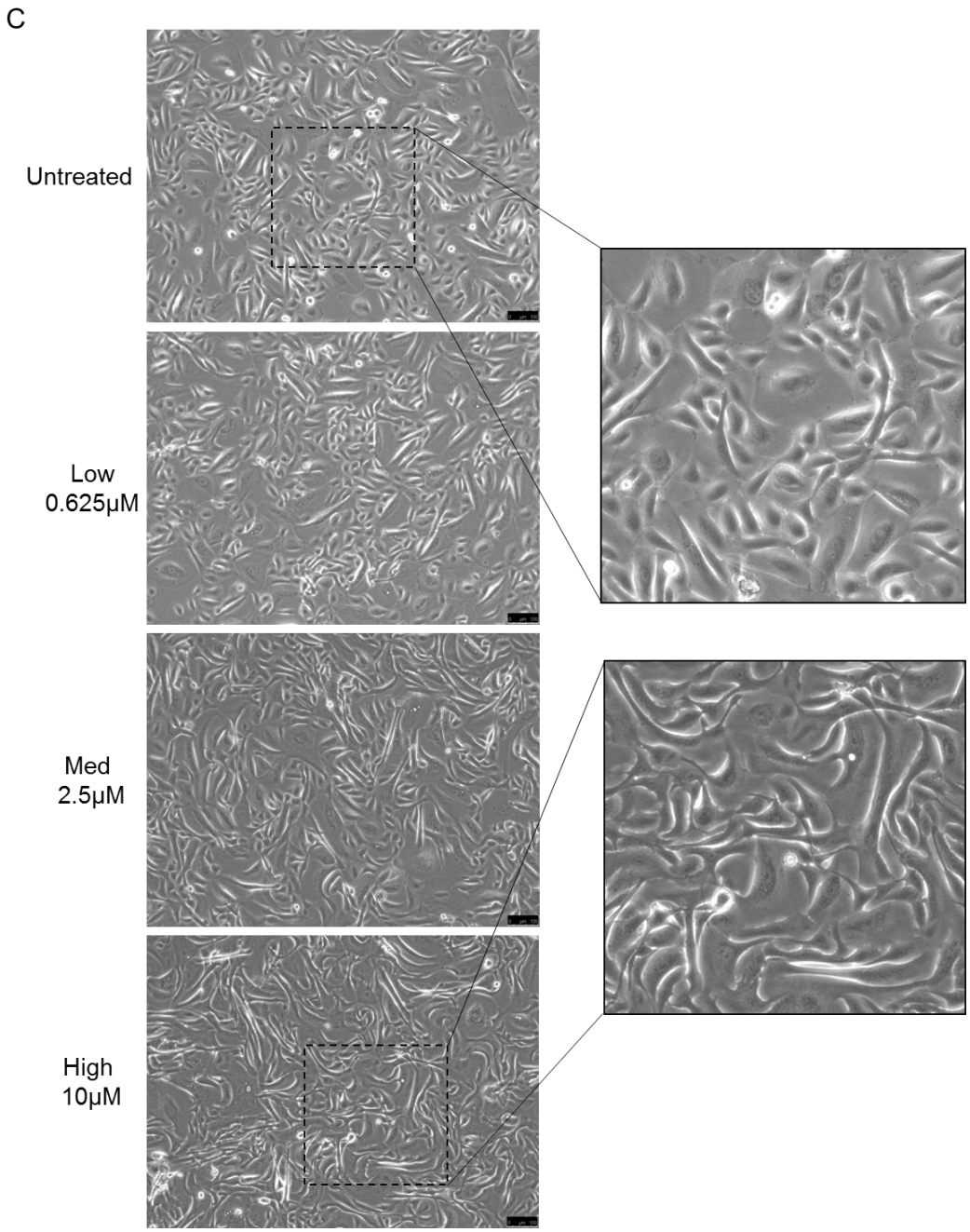

Figure 3.39. ELF3 expression is upregulated in primary prostate epithelial cells following vorinostat treatment.

(A) Primary prostate epithelial cell cultures were treated with three different doses of HDAC inhibitor vorinostat (L = 0.625µM, M = 2.5µM and H = 10µM). Cells were harvested at 4 hours and 24 hours after treatment for protein analysis. 30µg of protein was loaded per lane onto a 10% SDS gel, transferred onto a PVDF membrane and probed for the indicated proteins. GAPDH was used a loading control. Densitometry was carried out using Image J software. Numbers below blots indicate expression of ELF3 and NSE relative to the low dose (L) which was normalised to 1. (B) The TA and CB enriched subpopulations were treated with 2.5µM vorinostat for 24 hours before harvesting for protein analysis. WP = whole population. Numbers below blots indicate expression of ELF3 and NSE normalised to the low dose, 4 hour vorinostat treatment. (C) Brightfield images of sample H598/17 24 hours after vorinostat treatment. Scale bar = 100µm.

3.7.2 Global gene expression changes following ELF3 knockdown in prostate epithelial cell lines

In order to assess the global effects of ELF3 knockdown, an Affymetrix Clariom D gene expression microarray was carried out (Eurofins Genomics, Wolverhampton UK). This next generation Affymetrix array can detect around 200,000 known transcripts from Ensembl. Sample sets consisted of BPH-1 and PC3 cells in biological triplicate (siSCR and siELF3). Each set was carried out in duplicate in order to extract both RNA for the microarray and also protein for validation of ELF3 knockdown and to also validate any differentially expressed genes of interest from the array at the protein level.

The array data was analysed using TAC 4.0 software. The differential gene expression between siSCR and siELF3 samples of BPH-1 and PC3 cells was analysed both individually and collectively with a significance threshold of 2-fold increase or decrease and a p-value <0.05 (Table 3.3). Whilst the RNA expression of ELF3 was not significantly altered (Table 3.4), there was a significant downregulation of ELF3 at the protein level in all samples (Figure 3.40). PC3 cells had the most appreciable response to ELF3 knockdown, with a total of 2779 differentially expressed genes (including putative unannotated transcripts), compared with 1440 genes in BPH-1 cells (Table 3.3). 675 genes were differentially expressed between siSCR and siELF3 samples regardless of cell type, implying that ELF3 is involved in similar pathways in both cell lines (Table 3.3) (Figure 3.41).

Analysis	Total genes	Upregulated	Downregulated
BPH-1: siSCR (3) vs siELF3 (3)	1440	776	664
PC3: siSCR (3) vs siELF3 (3)	2779	1848	931
Both: siSCR (6) vs siELF3 (6)	675	355	320

Table 3.3. Number of differentially expressed genes in each gene expression microarray analysis.

GO analyses were carried out using DAVID and visualised using REVIGO. GO analysis of all sets revealed multiple terms associated with cell cycle-related processes and histone regulated processes (Figure 3.40) (Appendix 3.3). In agreement with this, several of the most significantly altered genes in both cell lines following ELF3 knockdown included cell cycle-related genes and histone genes. Most notably, the serine-threonine protein kinase PLK1 was downregulated 7.5-fold in siELF3 samples compared to siSCR in both BPH-1 and PC3 cells combined. Furthermore, when BPH-1 and PC3 cells were analysed in separate analyses, PLK1 was downregulated 15.5-fold in BPH-1 cells and over 5.5-fold in PC3 cells. A list of differentially expressed cell-cycle related genes are shown in Appendix 3.4.

The transcription of histone genes is regulated during the cell cycle, with a 35-fold increase during S phase and a subsequent 35-fold decrease upon entering G2 (Marzluff et al., 2002, Harris et al., 1991). This may explain the observed bias towards histone regulated processes in the GO analyses. PLK1 is involved in

several stages of the cell cycle, most notably during G2 and cytokinesis (de Gooijer et al., 2017, Petronczki et al., 2008). Other significantly altered genes from the microarray were also linked to G2 cell cycle phase and the PLK1 pathway, such as CDC25C and p21 (Appendix 3.4).

The expression of other ETS transcription factors was assessed following ELF3 knockdown (Table 3.4). Here, there was a differential response between BPH-1 and PC3 cells. In BPH-1 cells, there was a 2-fold upregulation of ETS1 and ELF1, whilst in PC3 cells there was a 7-fold upregulation of ESE3 and a 2.5 fold upregulation of ETS2. PC3 cells also showed an almost 5-fold downregulation of ETV4. This indicates there may be distinct compensatory mechanisms for the loss of ELF3 between the cell lines.

ETS Transcription Factors		**BPH-1**		**PC3**		**Both**	
Gene	**ETS Subfamily**	**Fold Change**	**P-Val**	**Fold Change**	**P-Val**	**Fold Change**	**P-Val**
ELF3	ESE	-1.78	0.09	-1.06	0.8396	-1.2	0.4737
ESE3	ESE	1.32	3.18E-02	6.94	7.29E-06	2.77	0.4516
ELF5	ESE	-1.11	0.8197	1.28	0.2094	-1.01	0.8739
ELF1	ELF	2.06	0.0345	1.51	0.0549	1.61	0.2949
ELF2	ELF	1.06	0.7253	1.13	0.4599	1.08	0.8173
ELF4	ELF	-1.18	0.2635	-1.1	0.906	-1.31	0.0788
ERG	ERG	-1.04	0.1453	1.01	0.9114	1.1	0.4003
FLI1	ERG	-1.1	0.3314	-1.66	0.3058	-1.23	0.2653
FEV	ERG	1.01	0.9598	1.24	0.2396	1.06	0.6011
ERF	ERF	-1.27	0.0994	1.1	0.1774	-1.04	0.6698
ETV3	ERF	1.36	0.015	1.73	0.0007	1.65	0.0073
ETS1	ETS	2.21	4.78E-05	1.15	0.5584	1.46	0.0851
ETS2	ETS	1.72	0.0287	2.54	0.0002	2.12	0.1448
GABPA	ELG	1.49	0.0142	1.76	0.0075	1.65	0.0331
SPDEF	PDEF	-1.11	0.4906	1.41	0.0774	1.58	0.769
ETV6	TEL	1.16	0.2277	1.01	0.867	1.29	0.6859

ETV7	TEL	1.49	0.1247	1.04	0.825	1.66	0.663
SPI1	SPI	-1.03	0.6846	1.16	0.985	-1.03	0.7397
SPIB	SPI	1	0.6875	1.01	0.9574	1.05	0.5418
SPIC	SPI	1.21	0.6362	-1.66	0.0256	-1.15	0.2898
ELK1	TCF	-1.46	0.0439	-1.07	0.72	-1.25	0.3695
ELK3	TCF	3.53	0.1319	-1.18	0.0939	1.76	0.7782
ELK4	TCF	1.19	0.06	1.4	0.0384	1.28	0.1032
ETV4	PEA3	-1.45	0.0468	-4.91	4.84E-05	-2.88	0.1632
ETV5	PEA3	-1.36	0.8792	-1.52	0.0496	-1.38	0.6811
ETV1	PEA3	-1.1	0.6199	-1.06	0.3914	-1.46	0.8467
ETV2	PEA3	-1.25	0.0958	-1.19	0.1595	-1.21	0.0525

Table 3.4. Expression changes of ETS transcription factors following ELF3 knockdown. Highlighted boxes indicate genes with a significance threshold of 2-fold increase or decrease and a p-value <0.05.

Other networks of interest identified by functional studies (Sections 3.4 and 3.6) were also investigated, including differentiation and EMT-associated genes (Table 3.5). PC3 cells showed an upregulation of the mesenchymal cell marker fibronectin and its receptor, integrin α5. However, there was also a 2-fold upregulation of epithelial cell marker E-cadherin. Both PC3 and BPH-1 cells exhibited an upregulation of the neuroendocrine cell marker NSE. There were no significant changes in gene expression found in basal/luminal cell markers or EMT-associated transcription factors in either cell line (Tables 3.5 and 3.6).

Genes associated with the SC phenotype were also examined. However, the only significant change was a modest upregulation of CD49b in BPH-1 cells (Table 3.7).

Differentiation			BPH-1		PC3		Both	
Gene	Description	Group	Fold Change	P-Val	Fold Change	P-Val	Fold Change	P-Val
CDH1	E-cadherin	E	1.13	0.2709	2.34	0.005	1.79	0.6553
CTNNA1	Alpha 1 catenin	E	-1.04	0.5768	-1.06	0.6651	-1.07	0.9748
CTNNA2	Alpha 2 catenin	E	-1.16	0.6181	-1.56	0.2072	-1.98	0.0083
SDC1	Syndecan-1	E	-1.2	0.4455	-1.31	0.0872	-1.25	0.4876
CTNNB1	Beta catenin	E/M	-1.25	0.1436	1.04	0.9653	-1.06	0.7317
VIM	Vimentin	M	-1.4	0.9851	1.21	0.1469	1.02	0.9857
CDH2	N-Cadherin	M	-2.79	0.0781	1.62	0.0077	-1.03	0.9682
ITGA5	Integrin α5	M	1.81	0.0935	2.84	0.001	2.33	0.0239
FN1	Fibronectin	M	-2.58	0.5795	3.64	0.0002	2.86	0.3618
TP63	p63	B	1.09	0.6889	1.11	0.9957	1.13	0.9416
KRT5	Cytokeratin 5	B	-1.12	0.4817	-1.08	0.4656	-1.11	0.9766
KRT14	Cytokeratin 14	B	2.08	0.2539	1.02	0.6336	1.6	0.7718
KRT8	Cytokeratin 8	L	-1.21	0.6864	1.2	0.034	1.26	0.6874
KRT18	Cytokeratin 18	L	-1.54	0.8863	-1.14	0.7831	-1.05	0.7718
AR	Androgen Receptor	L	-1.46	0.0801	-1.11	0.8565	-1.23	0.2166
KLK3	PSA	L	-1.17	0.1616	1.03	0.6645	-1.09	0.5905
NKX3-1	NK3 homeobox 1	L	1.5	0.0304	1.27	0.1129	1.46	0.3081
ENO2	Neurone specific enolase	NE	2.6	0.0436	7.21	2.09E-05	3.53	0.0158
SYP	Synaptophysin	NE	-1.01	0.9912	-1.05	0.5319	1	0.8678

CHGA	Chromogranin A	NE	-1.28	0.0722	-1.46	0.0984	-1.13	0.1963

Table 3.5. Expression changes of genes involved in differentiation following ELF3 knockdown. E = epithelial, M = mesenchymal, B = basal, L = luminal, NE = neuroendocrine. Highlighted boxes indicate genes with significance threshold of 2-fold increase or decrease and a p-value <0.05.

EMT Transcription Factors		BPH-1		PC3		Both	
Gene	**Description**	**Fold Change**	**P-Val**	**Fold Change**	**P-Val**	**Fold Change**	**P-Val**
SNAI1	Snail	1.24	0.1636	1.27	0.1237	1.19	0.089
SNAI2	Slug	-1.11	0.3626	2.3	0.0915	1.39	0.553
TWIST1	Twist Family BHLH Transcription Factor 1	-1.04	0.5925	1.66	0.0873	-1.11	0.5819
TWIST2	Twist Family BHLH Transcription Factor 2	1.21	0.0886	1.32	0.1515	1.23	0.1012
ZEB1	Zinc Finger E-Box Binding Homeobox 1	1.25	0.4184	-1.06	0.9053	1.19	0.9248
ZEB2	Zinc Finger E-Box Binding Homeobox 2	-1.05	0.675	-1.07	0.7297	1.02	0.7351
FOXC2	Forkhead Box C2	-1.08	0.5417	1.34	0.474	1.09	0.8927

Table 3.6. Expression changes of transcription factors involved in epithelial-to-mesenchymal transition (EMT) following ELF3 knockdown.

Stem Cell Markers		BPH-1		PC3		Both	
Gene	**Description**	**Fold Change**	**P-Val**	**Fold Change**	**P-Val**	**Fold Change**	**P-Val**
PSCA	Prostate stem cell antigen	1.46	0.0804	1.24	0.3098	1.32	0.0466
NANOG	Nanog homeobox	-1.01	0.7987	1.1	0.9167	1.07	0.2411
ALDH1A1	Aldehyde dehydrogenase 1 family, member A1	1.52	0.4134	1.13	0.8367	1.03	0.9889
ALDH1A3	Aldehyde dehydrogenase 1 family, member A3	1.26	0.4657	1.19	0.4469	1.01	0.8824
SOX2	SRY box 2	1.17	0.7479	-1.06	0.4364	-1.07	0.968
POU5F1	POU class 5 homeobox 1	-1.04	0.7425	1	0.8813	1.09	0.82
NES	Nestin	1.1	0.2663	-1.01	0.2414	1.14	0.9003
MYC	V-myc avian myelocytomatosis viral oncogene homolog	1.14	0.394	-1.25	0.2376	-1.02	0.989
ITGA2	Integrin, alpha 2 (CD49B)	2.89	0.0047	1.48	0.3968	1.7	0.0613
CD44		1.01	0.8094	1.04	0.2241	-1.04	0.7694
ABCG2	ATP binding cassette subfamily G member 2	-1.54	0.557	-1.02	0.9041	1.14	0.9082

Table 3.7. Expression changes of stem cell markers following ELF3 knockdown. Highlighted boxes indicate genes with significance threshold of 2-fold increase or decrease and a p-value <0.05.

Further analysis was carried out by Dr Alastair Droop to determine whether there was a differential response to ELF3 knockdown between BPH-1 and PC3 cells. Twelve known genes showed differential behaviour upon knockdown between the two cell lines (Table 3.8). Expression graphs are shown in Appendix 3.5 (generated by Dr Alastair Droop). The analysis shows that there are a subset of genes which have comparable levels of expression between BPH-1 siSCR and PC3 siSCR, but with ELF3 knockdown there is a significant increase of expression in PC3 cells but not BPH-1. The most significant differentially expressed gene was LXN, which showed a small decrease in BPH-1 siELF3 cells but showed a significant increase PC3 siELF3 cells compared to their respective siSCR counterparts. An exception to this is ESE3 (also known as EHF) which has very high levels of expression in both BPH-1 siSCR and siELF3, whereas PC3 siSCR cells have relatively low expression with a significant increase in PC3 siELF3 cells.

Gene	Description	Log Fold Change	P value
LXN	Zinc-dependent metallocarboxypeptidases inhibitor	-2.28	7.88E-08
GHR	Growth hormone receptor	-2.11	2.14E-07
FBN1	Extracellular matrix glycoprotein	-2.13	3.85E-07
PDGFA	Platelet-derived growth factor subunit A	-1.61	7.31E-07
CSPG5	Proteoglycan that may function as a neural growth and differentiation factor	-2.44	3.25E-06
CADM2	Cell adhesion molecule	-3.17	4.64E-06
ESE3	Epithelial-specific ETS transcription factor	-1.48	5.91E-06
TMEM117	Transmembrane protein 117 involved in stress-induced cell death pathway	-2.41	7.40E-06
SFMBT2	Transcriptional repressor by binding to methylated lysines in histones	-1.48	7.55E-06
PDK4	Mitochondrial protein involved in glucose metabolism	-1.66	8.82E-06
STC1	Calcium and phosphate regulator	-2.13	1.54E-05
TNFSF4	Cytokine which mediates adhesion of activated T cells to endothelial cells	-1.99	1.62E-05

Table 3.8. Genes that show different behaviour upon ELF3 knockdown between BPH-1 and PC3 cells.

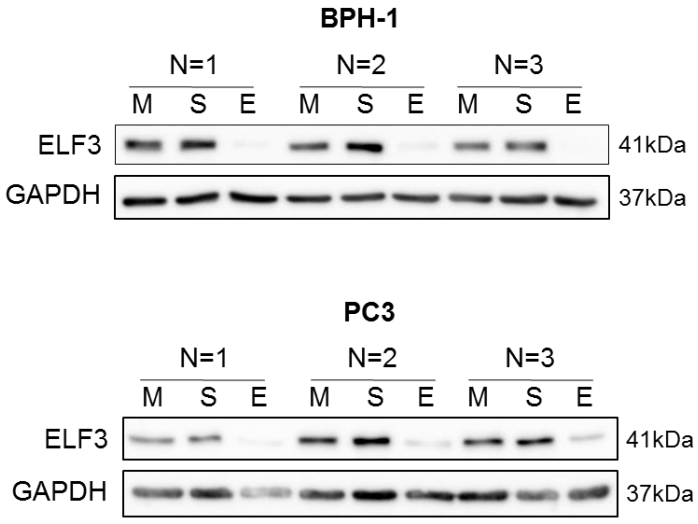

Figure 3.40. Validation of ELF3 knockdown at the protein level in array samples.

Western blot indicating ELF3 protein expression 72 hours following ELF3 knockdown. 25µg of protein was loaded per lane onto a 10% SDS gel, transferred onto a PVDF membrane and probed for the indicated proteins. GAPDH was used a loading control. RNA extracted from duplicate samples were sent for Affymetrix gene expression microarray. M = mock, S = siSCR, E = siELF3.

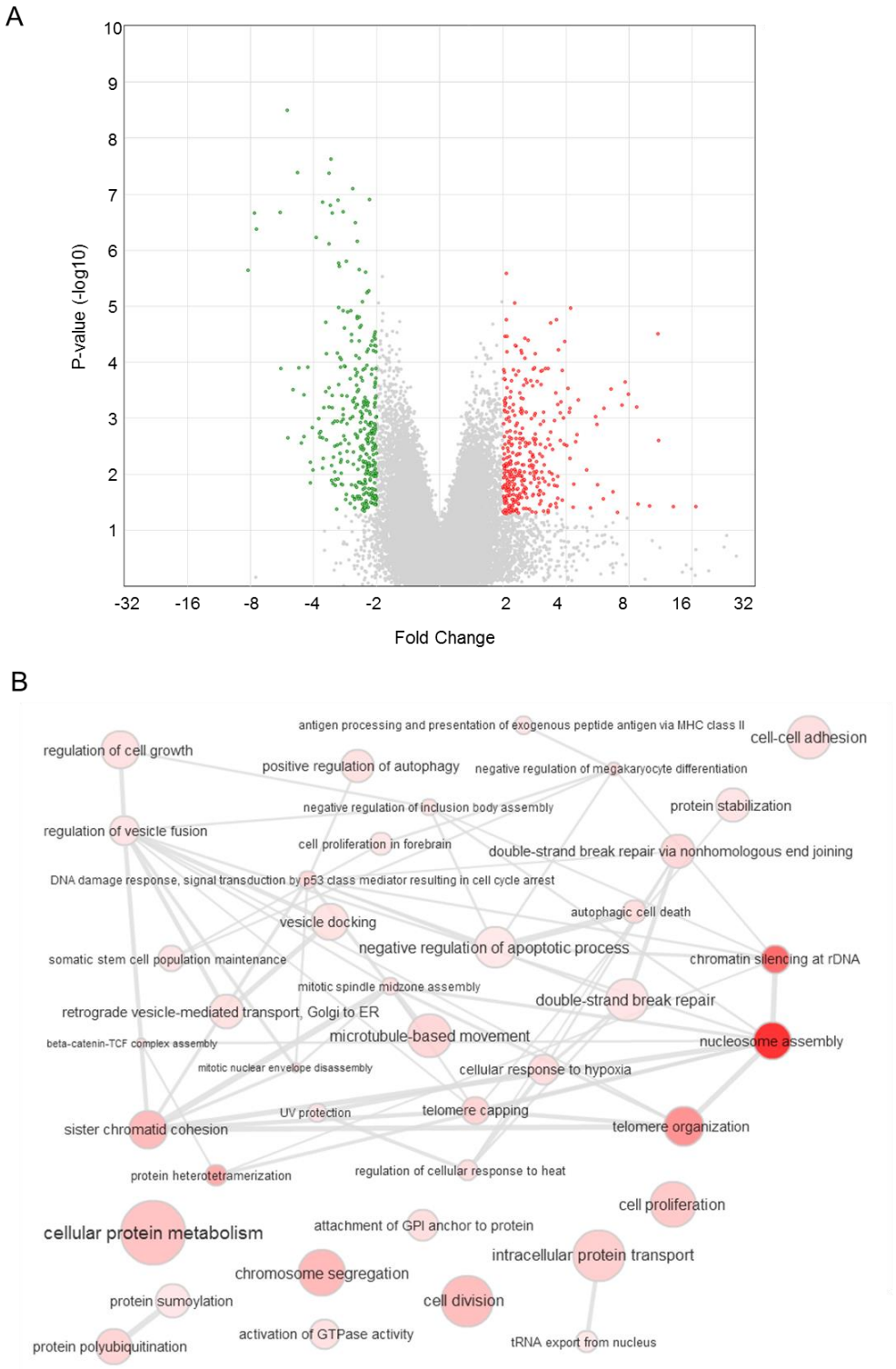

Figure 3.41. Gene expression changes and gene ontology in prostate epithelial cells following ELF3 knockdown.

Differential gene expression of BPH-1 and PC3 cells with ELF3 knockdown was determined by an Affymetrix Clariom D microarray. (A) Volcano plot indicating gene expression changes of siSCR vs siELF3 BPH-1 and PC3 cells collectively. Significance threshold included genes with a 2-fold increase or decrease and a p-value <0.05. Red = increased expression, green = decreased expression. (B) Gene ontology terms associated with significant differential gene expression changes between siSCR and siELF3 cells. Generated via the Database for Annotation, Visualization and Integrated Discovery (DAVID) and visualised using REVIGO.

3.7.3 ELF3 knockdown alters the expression of key cell cycle regulatory genes in prostate epithelial cell lines at the protein level and results in a block at the G2 phase

To validate results found in the gene expression microarray, several G2 phase proteins were tested by western blot using lysates from the BPH-1 and PC3 siELF3 cells (Figure 3.42). PLK1 and CDC25C were downregulated in both PC3 and BPH-1 cells at the protein level. The cyclin-dependent kinase (CDK) inhibitor p21 was also increased. These changes correlated with an arrest at the G2 checkpoint which was shown by a progressive accumulation of cells in the G2 phase during cell cycle analysis (Figure 3.43). Phospho-histone H3 (PHH3) ICC staining was also carried out on BPH-1 cells to determine the number of cells in mitosis with siELF3 compared to siSCR. Representative images indicating the different stages of mitosis is shown in Figure 3.44A. Whilst 9% of mock and siSCR cells were positive for PHH3, only 3.8% of siELF3 cells were undergoing mitosis, further indicating cell cycle arrest (Figure 3.44B).

A

(i)

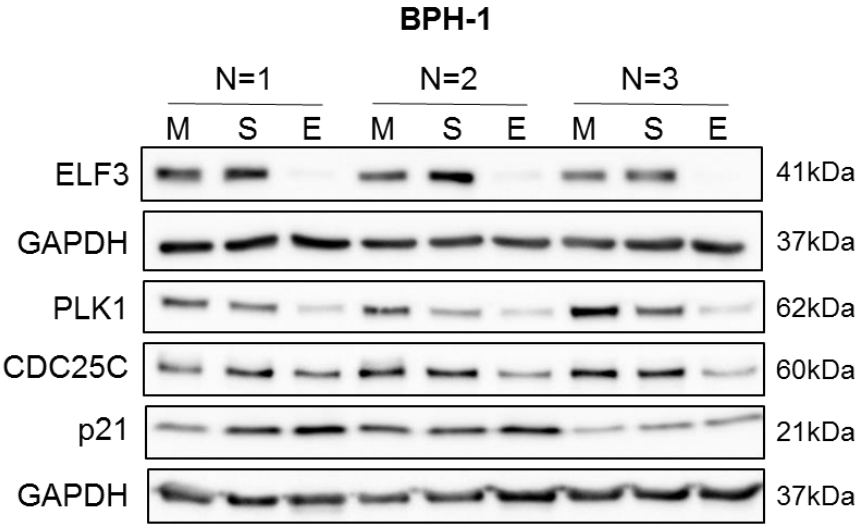
BPH-1
N=1
N=2
N=3
M S E M S E M S E
ELF3
GAPDH
PLK1
CDC25C
p21
GAPDH
41kDa
37kDa
62kDa
60kDa
21kDa
37kDa

(ii)

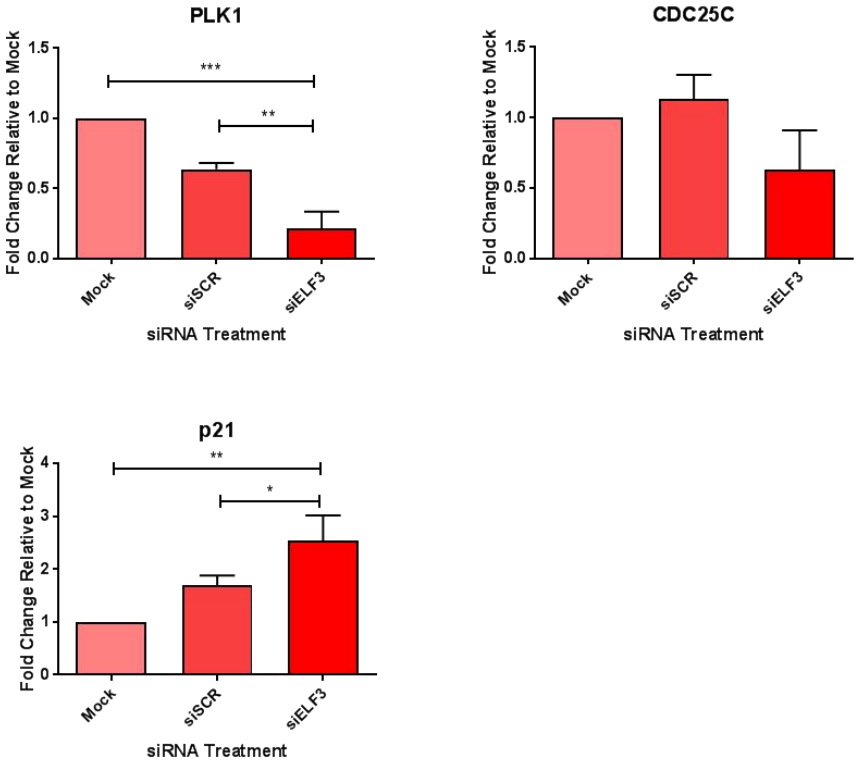
PLK1
Fold Change Relative to Mock
1.5
1.0
0.5
0.0
***
**
Mock
siSCR
siELF3
siRNA Treatment
CDC25C
Fold Change Relative to Mock
1.5
1.0
0.5
0.0
Mock
siSCR
siELF3
siRNA Treatment
p21
Fold Change Relative to Mock
4
3
2
1
0
**
*
Mock
siSCR
siELF3
siRNA Treatment

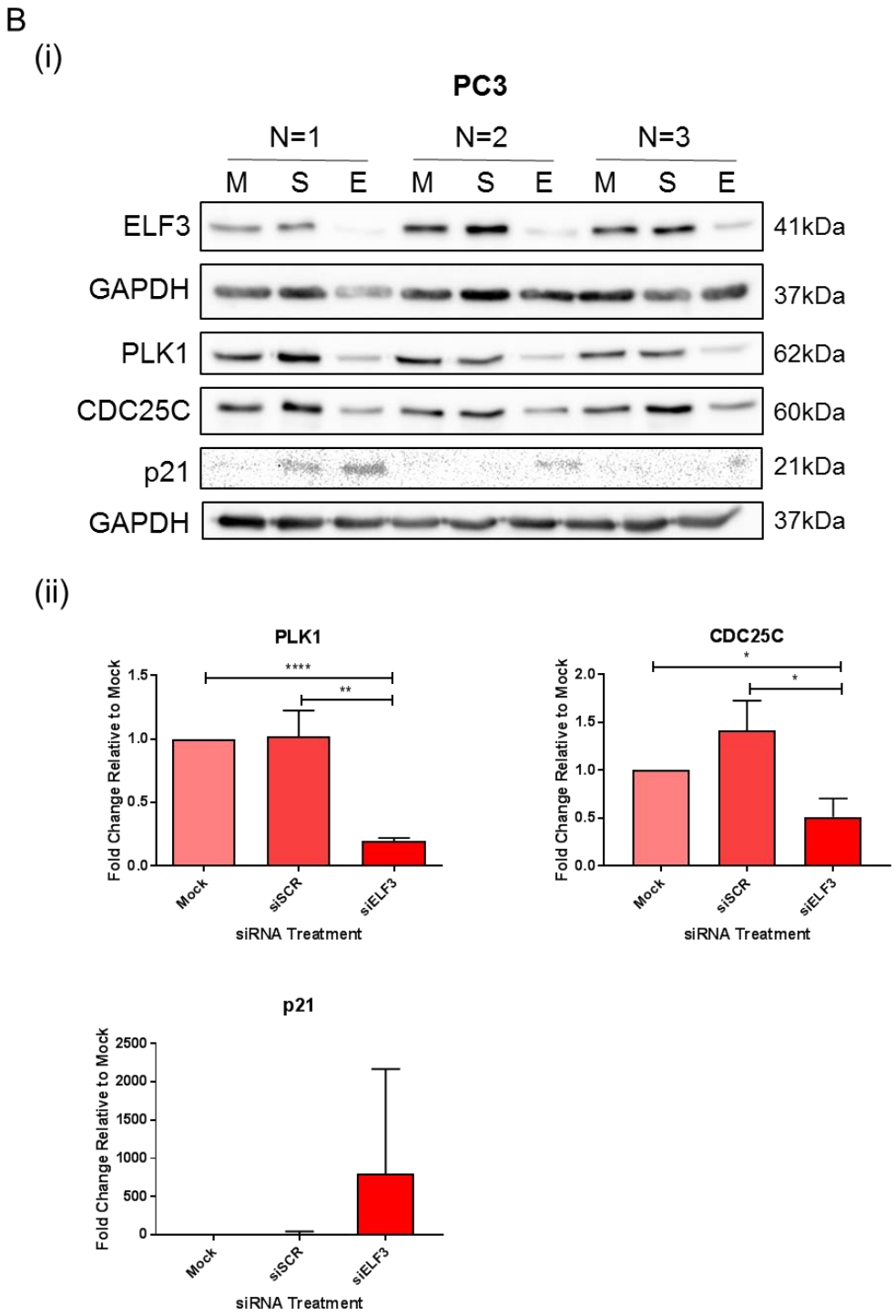

Figure 3.42. ELF3 knockdown alters the expression of key cell cycle regulator genes.

Protein expression (i) and densitometry analysis (ii) of G2 phase cell cycle-related genes in (A) BPH-1 cells and (B) PC3 cells 72 hours following ELF3 knockdown. 25µg of protein was loaded per lane onto a 10% SDS gel, transferred onto a PVDF membrane and probed for the indicated proteins. GAPDH was used a loading control. Densitometry was carried out using Image J software. M = mock, S = siSCR, E = siELF3. Statistical significance was determined using a Student's T-test (unpaired, two-tailed).

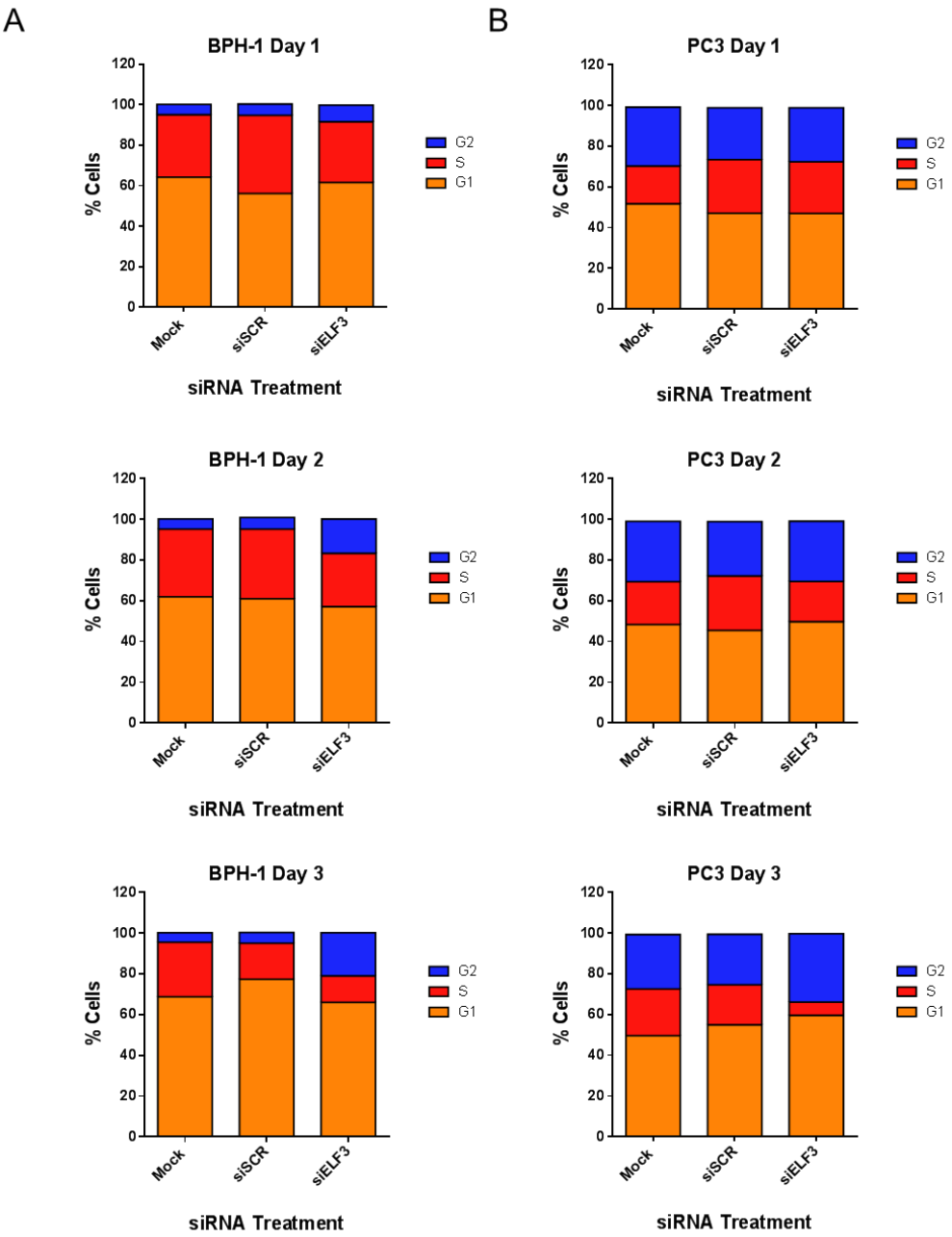

Figure 3.43. ELF3 knockdown causes a progressive accumulation of cells in the G2 phase of the cell cycle.

Cell cycle analysis was carried out on (A) BPH-1 and (B) PC3 cells 24 hours post-transfection with mock, siSCR or siELF3 for three consecutive days. Cells were treated with EdU for 4 hours and harvested and stained with propidium iodide before analysing by flow cytometry. Graphs represent the average of three biological replicates.

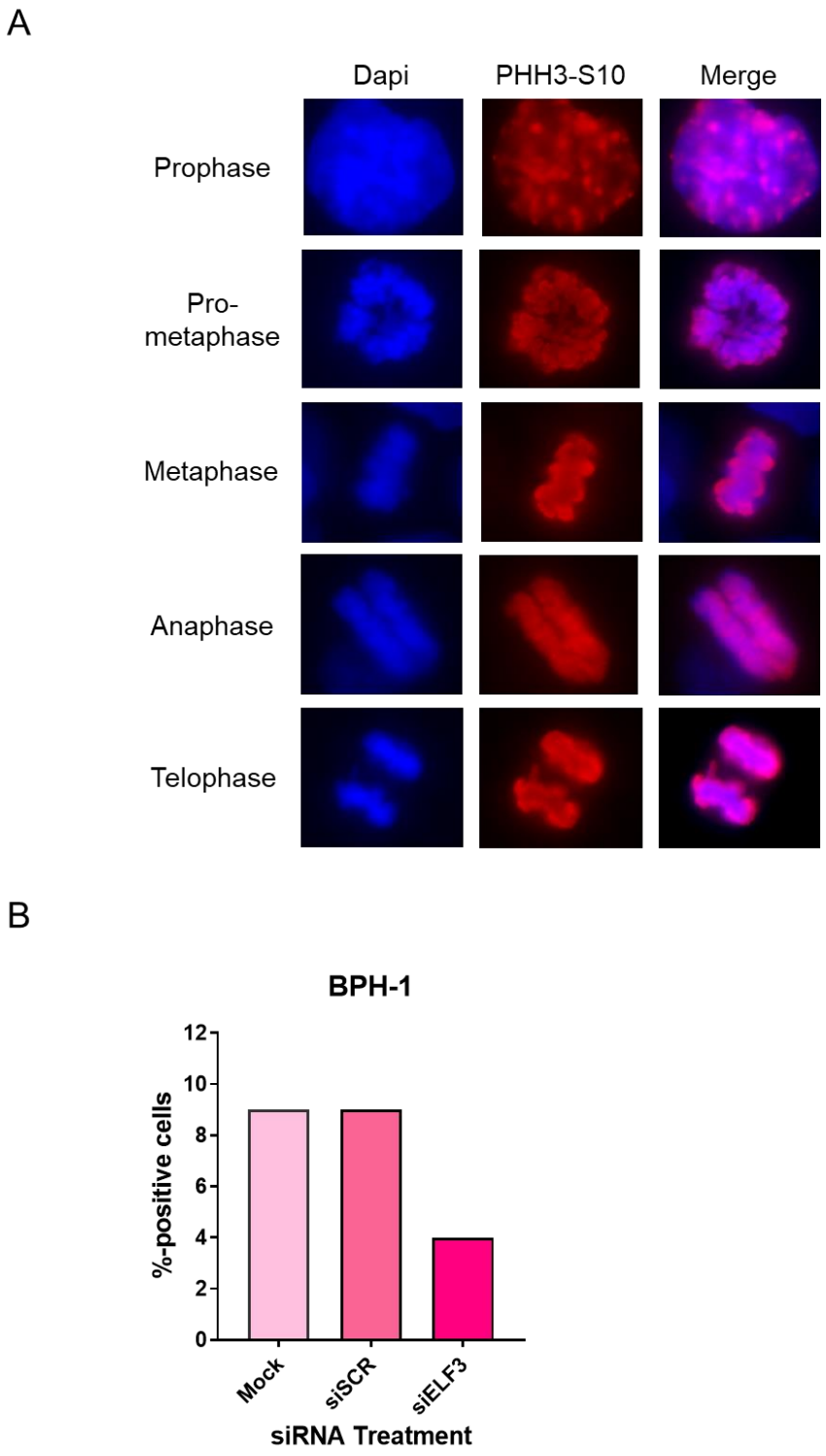

Figure 3.44. ELF3 knockdown reduces the number of BPH-1 cells in mitosis.

BPH-1 cells were transfected with ELF3 (siELF3) and scrambled siRNA (siSCR), fixed in 4% paraformaldehyde at day 3 post-transfection and stained with phospho-histone 3 (PHH3-S10) as a marker of mitosis. Blue = DAPI, red = PHH3-S10. (A) Representative images of cells in each stage of mitosis. (B) 220 cells were counted in each condition and presented as a percent PHH3-S10-positive.

3.7.4 ELF3 knockdown does not significantly alter the cell cycle in primary prostate epithelial cells

To investigate whether the effects seen in prostate epithelial cell lines with ELF3 knockdown are mirrored in primary cells, ELF3 knockdown was optimised in primary prostate epithelial cells. Primary prostate samples were selected for CB cells as this is the subpopulation which expresses highest ELF3 protein (Section 3.2.3) CB cells were counted and plated onto 6 well plates for knockdown. Cells were harvested 72 hours post-transfection for western blot analysis. A range of 70-99% knockdown was achieved in all samples tested (Figure 3.45). The same G2 cell cycle proteins were probed for in each knockdown sample as had been tested with the cell lines (Section 3.7.3) and also cyclin B1 and phosphorylated cyclin B1 (p-cyclin B1) as it is a substrate for PLK1. PLK1 was only detected in one sample (H589/17), and did decrease in siELF3 cells in this sample (Figure 3.46). CDC25C and p-cyclin B1 were not detected, however p21 was detected in all samples and treatments. This suggests that the cells are arresting and not reaching G2 phase of the cell cycle. An explanation for this could be that the primary cell density required for transfection meant that at 72 hours, when the cells were harvested, the cells were confluent and may have ceased to proliferate. This was also reflected in the cell cycle analysis, where there was no change between siRNA treatments and few cells in G2 (Figure 3.46D).

Colony forming assays were also set up but the cells did not form colonies in any treatment, indicating that the selection of CB cells was robust since they are less proliferative in the primary cultures (Collins et al., 2001). Therefore, ELF3 knockdown does not promote de-differentiation into SC/TA cells which are more capable of forming colonies.

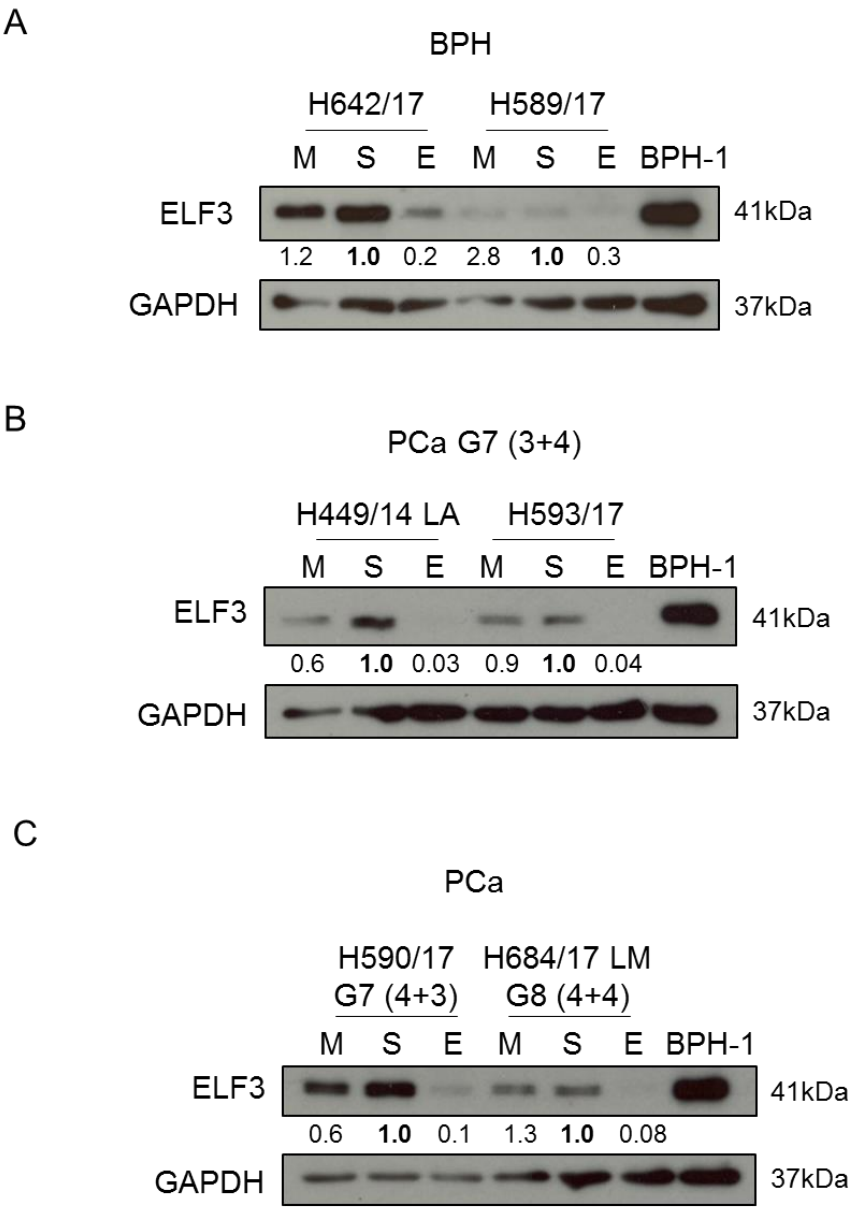

Figure 3.45. Efficiency of ELF3 knockdown in primary prostate committed basal cells.

ELF3 knockdown was optimised in primary prostate epithelial cell cultures. CB cells were first enriched for by lack of adhesion to collagen-I coated plates after 20 minutes incubation. Cells were then plated at a density of 200,000 cells per well in a collagen-I coated 6-well plate. siRNA was transfected into cells using Oligofectamine transfection reagent (Invitrogen). Cells were harvested 72 hours post-transfection for protein analysis. 30µg of protein was loaded per lane onto a 10% SDS gel, transferred onto a PVDF membrane and probed for the indicated proteins. GAPDH was used a loading control. Densitometry was carried out using Image J software. Samples included those derived from (A) BPH, (B) Gleason 3+4 and (C) High Gleason (4+3 and 4+4) samples. M = mock, S = siSCR, E = siELF3, G = Gleason score.

A

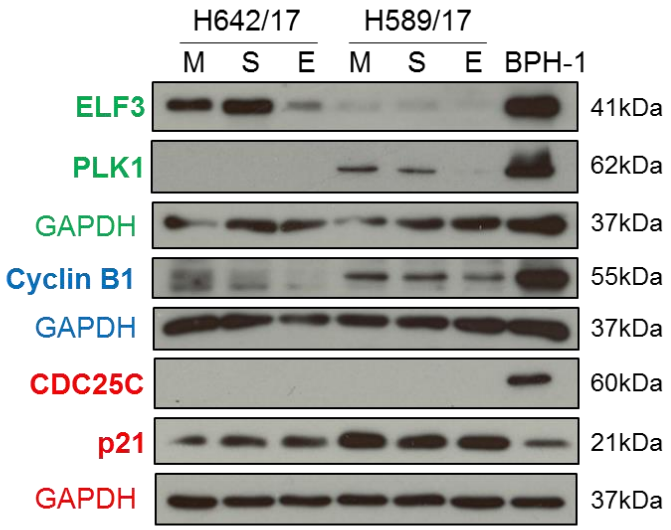
H642/17
H589/17
M S E M S E BPH-1
ELF3
41kDa
PLK1
62kDa
GAPDH
37kDa
Cyclin B1
55kDa
GAPDH
37kDa
CDC25C
60kDa
p21
21kDa
GAPDH
37kDa

B

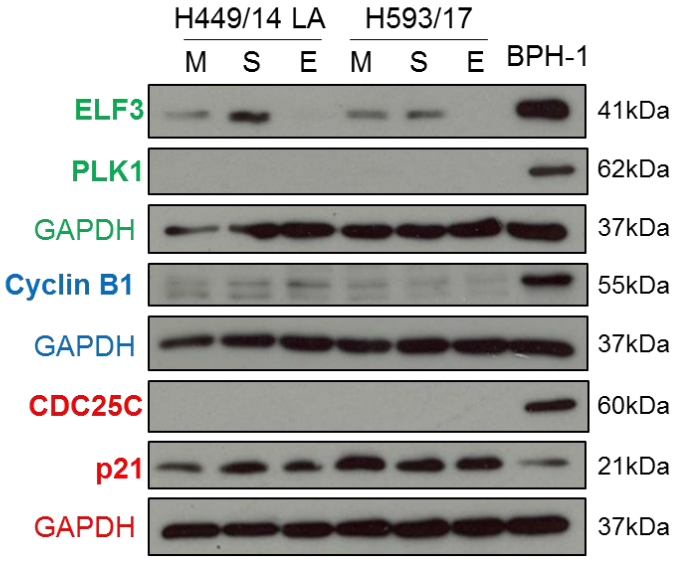
H449/14 LA
H593/17
M S E M S E BPH-1
ELF3
41kDa
PLK1
62kDa
GAPDH
37kDa
Cyclin B1
55kDa
GAPDH
37kDa
CDC25C
60kDa
p21
21kDa
GAPDH
37kDa

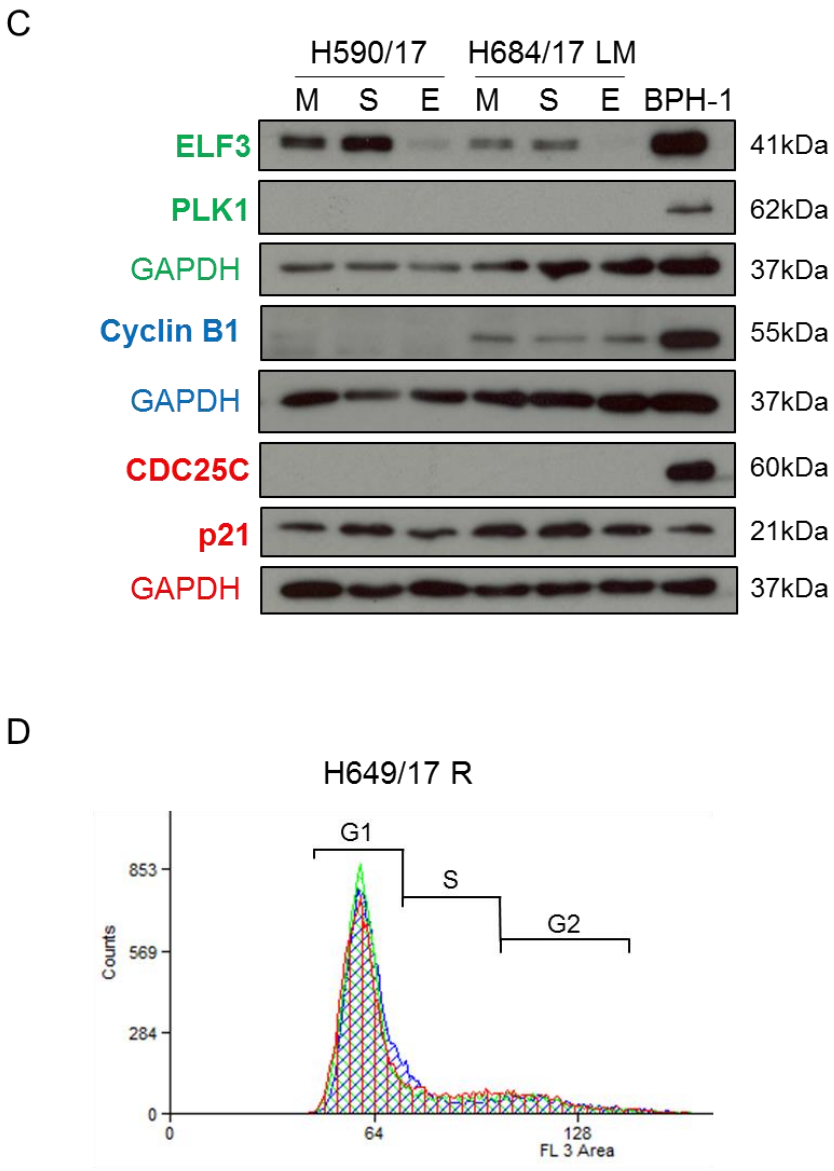

Figure 3.46. ELF3 knockdown does not alter the cell cycle in primary prostate committed basal cells. Protein expression of G2 phase cell cycle-related genes in primary prostate committed basal cell cultures 72 hours post transfection with mock (M), siSCR (S) and siELF3 (E). 30µg of protein was loaded per lane onto a 10% SDS gel, transferred onto a PVDF membrane and probed for the indicated proteins. GAPDH was used a loading control. Densitometry was carried out using Image J software. Samples were derived from (A) BPH, (B) Gleason 3+4 and (C) High Gleason (4+3 and 4+4) samples. (D) Representative histogram of cell cycle analysis 72 hours post-transfection. Red = mock, green = siSCR, blue = siELF3.

3.7.5 ELF3 overexpression has no effect on the cell cycle of primary prostate epithelial cells

Since ELF3 knockdown has been shown to arrest prostate epithelial cells in G2, a complementary study using lentiviral ELF3 overexpression was next carried out. A normal/cancer matched pair was transduced with control, ELF3-WT and ELF3-ΔAT lentiviruses. A pulse-chase cell cycle analysis was carried out using EdU and propidium iodide staining to assess progression through the cell cycle. At the 24h time point a larger proportion of cells progressed to the G2 phase compared to 4h in all conditions (Figure 3.47). However, there was no clear difference in cell cycle phases *between* the control, ELF3-WT and ELF3-ΔAT conditions.

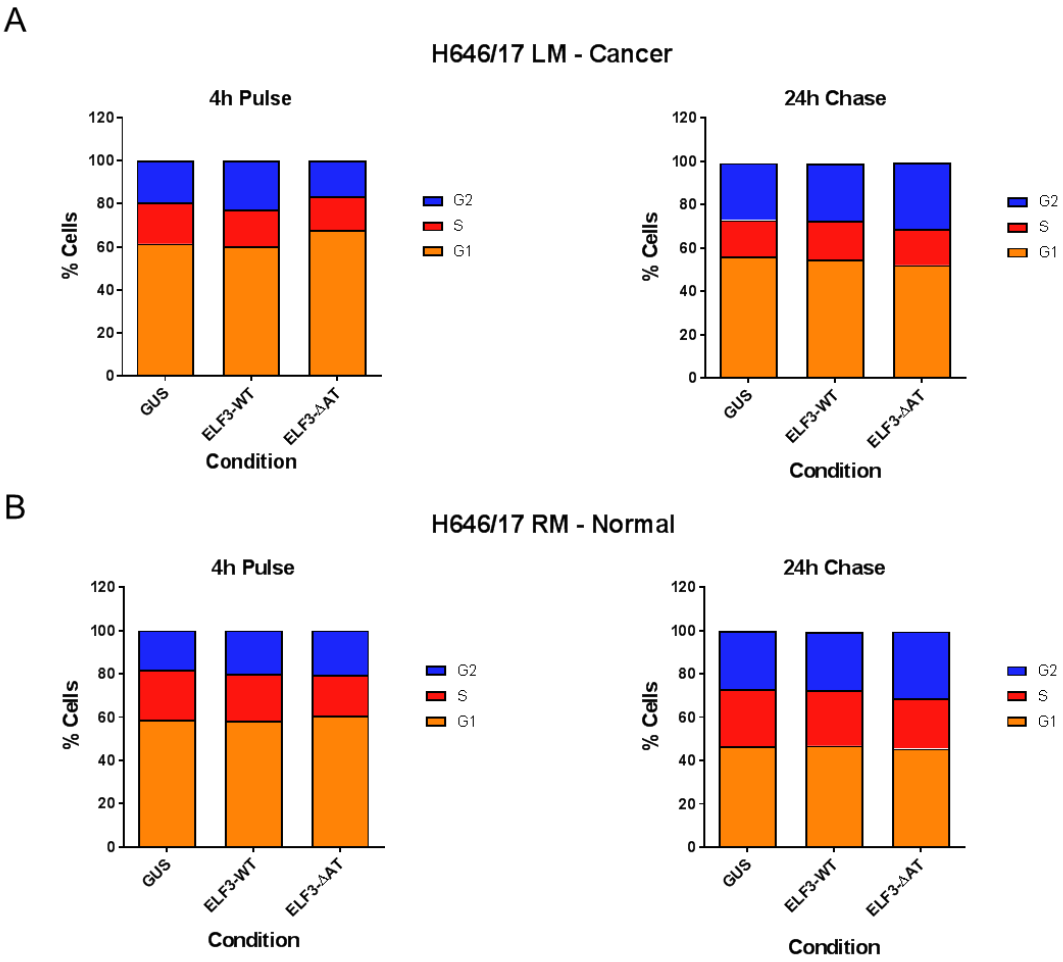

Figure 3.47. ELF3 overexpression does not have a distinct effect on cell cycle.

Cell cycle analysis was carried out on a (A) cancer and (B) normal primary matched pair with ELF3 overexpression by flow cytometry. Cells were treated with EdU for 4 hours (pulse) and medium was then replaced in duplicate wells with normal growth medium and cells were harvested at 24 hours (chase) to assess progression through the cell cycle.

4. Discussion

Deregulation of the ETS transcription factor family members is now recognised as a common feature in multiple cancers; with aberrant expression, loss of tumour suppressor function, inactivating mutations and the formation of fusion genes observed (Seth and Watson, 2005). Most notably, the TMPRSS2-ERG gene fusion is present in approximately 50% of PCas and in prostate CSCs (Tomlins et al., 2005, Polson et al., 2013). However, the role of other ETS transcription factors in PCa is less well understood. Notably, there is now mounting evidence that the epithelial-specific ETS factors ELF3, ESE3, and PDEF play a role in PCa. Furthermore, these ETS factors also play a role in epithelial cell differentiation and consequently may be important regulators of the SC (and CSC) phenotype in the prostate (Archer et al., 2017).

Existing literature at the beginning of this study was conflicting in terms of the role of ELF3 in the prostate. This consisted of one study which identified ELF3 as a driver of PCa and one which proposed it as a suppressor. In order to identify the genuine function of ELF3 it was important to consider the multiple cell populations present in the prostate. A gene expression microarray was previously carried out assessing the differential gene expression between prostate SCs and the more differentiated CB cells derived from benign and cancerous prostate tissue (Birnie et al., 2008). ELF3 was identified as significantly upregulated in the more differentiated CB cells of the prostate epithelium compared to SCs irrespective of diagnosis. This current study has been an in depth investigation into the expression pattern of ELF3 as well as its potential function in different cellular compartments of both normal and malignant prostate basal epithelial cells.

4.1 Expression pattern of ELF3 in prostate cells and tissue

This study details the most comprehensive ELF3 expression profile to date in prostate cell lines and primary prostate epithelial cell subpopulations. Longoni et al. described LNCaP, 22RV1 and Du145 cells as possessing low, intermediate and high ELF3 expression, respectively (Longoni et al., 2013), which agrees with our findings. In section 3.1.1, ELF3 expression was also determined in multiple other prostate cell lines, including those derived from normal and benign prostate, as well as primary and metastatic PCa. Whilst ELF3 was expressed in all cell lines tested, there was no clear pattern correlating with diagnoses. A study in colon cancer also observed a similar range of ELF3 expression amongst a panel of colon cell lines of normal, primary cancer and metastatic origin (Wang et al., 2014). Furthermore, we found no distinct correlation between ELF3 expression and prostate cell lines considered more basal/intermediate or more luminal.

To determine the expression of ELF3 in the primary prostate, IHC staining of benign prostate tissue sections was carried out. This revealed that ELF3 expression was restricted to the basal epithelial cells of glands and was absent from luminal epithelial cells and the surrounding stroma (Section 3.3.2). As well as tissue IHC, ELF3 was not detected in lysates derived from the stromal cells of several patients (Section 3.2.2). This is unsurprising as ELF3 is described as an epithelial-specific transcription factor and is generally expressed in tissue with high epithelial cell content (Tymms et al., 1997). ELF3 expression however, can be induced in

several stromal-like cell lines following treatment with inflammatory stimuli (Rudders et al., 2001). Nevertheless, this does not appear to occur in the inflammatory setting of BPH. A study of the bladder found ELF3 to be expressed in the epithelial cells of human urothelium (Bock et al., 2014). In contrast to the prostate, ELF3 expression progressively increased as cells differentiated from the basal layer to the most superficial, differentiated cells. However, in the normal oral mucosa, like prostate, ELF3 is most highly expressed in the basal epithelium (AbdulMajeed et al., 2013).

Western blot analysis was also carried out on enriched TA and CB epithelial subpopulations, which showed that ELF3 was consistently expressed in the CB subpopulation, with little or no detection in the TA cells (Section 3.2.2). This was evident in cells derived from both benign and cancerous tissue and there was no significant difference in expression between the two diagnoses. This agreed with the gene expression microarray which showed ELF3 was more highly expressed in CBs vs SCs at the RNA level irrespective of diagnosis (Section 3.2.1). Analysis of two independent breast cancer data sets also found ELF3 expression to be significantly lower in the CSC population compared to more differentiated subpopulations (Merino et al., 2016), suggesting its expression is linked to differentiation in both tissue types.

Analysis of benign prostate tissue TMA's showed that ELF3 protein was expressed in all sections that contained epithelial glands (Section 3.3.2), confirming the pattern of expression seen previously in individual patient sections. There were several patterns of expression observed in the PCa TMA analysed. Many cancer sections either showed no ELF3 staining, or high ELF3 expression in non-cancerous, AMACR-negative glands, regardless of Gleason grade. Some more advanced, less differentiated cancers of Gleason grade ≥7 were positive for ELF3 expression. Longoni et al. showed that a subset of prostate tumours expressed higher ELF3 than normal prostate by qRT-PCR and IHC (Longoni et al., 2013). However, there was no further distinction between Gleason grades in that study. Analysis of two independent datasets also found increased ELF3 expression in metastatic tumours compared to primary prostate tumours, indicating that ELF3 expression may be associated with more advanced tumours (Longoni et al., 2013). Results from other tissues vary. In the colon, liver and lung, ELF3 expression appears to be associated with cancer progression and metastases (Wang et al., 2014, Nakarai et al., 2012, Zheng et al., 2018, Wang et al., 2018). In contrast, in oral and ovarian tissue, development of cancer is associated with a loss of ELF3 expression (AbdulMajeed et al., 2013, Yeung et al., 2017).

Breast cancers can be classified into different subtypes according to molecular marker expression, including luminal and basal-like subtypes. Analysis from a genomic and transcriptomic study of 52 commonly used breast cancer cell lines divided the basal-like subgroup into two categories; basal A and basal B (Kao, 2009). Basal A cell lines were found to associate with ETS transcription factor pathways and expressed genes related to basal-like tumours. Basal B cell lines expressed genes related to mesenchymal and SC/progenitor cell properties and EMT. Notably, re-analysis of this data in a later study found that ELF3 was highly expressed in the basal A cell lines, with little or no expression in the basal B cell lines (Kar and Gutierrez-Hartmann, 2017). This pattern of expression resembles what we have found in the prostate with regards to high ELF3 expression in CB cells but low in the SC/TA subpopulation. It should also be noted that basal-

like breast cancers are associated with poor prognosis, further suggesting that ELF3 expression could be linked to more advanced disease.

Whilst both similar and conflicting ELF3 expression patterns have been found in other tissues, multiple techniques have confirmed that ELF3 expression is restricted to the basal layer of the prostate epithelium. A larger patient cohort would be required to determine if there was a significant difference in ELF3 expression with increasing Gleason grade in PCa. With regards to metastases, which has been discussed in other studies, tissue is difficult to obtain as prostate metastases are primarily to the bone and are therefore not readily available for study.

4.2 Subcellular localisation of ELF3

Determining the cellular localisation of a protein is important for understanding its function. A number of publications have examined the localisation of ELF3 in various tissues including bladder, colon, liver, breast and prostate tissues as well as cell lines. However, each has proposed differing cellular localisations (cytoplasmic, nuclear or pan-cellular), and subsequently roles, for ELF3. Whilst in urothelium, lung and ovarian epithelial cells ELF3 is almost exclusively nuclear (Bock et al., 2014, Wang et al., 2018, Yeung et al., 2017), there is evidence of cytoplasmic expression in other tissues. Abdulmajeed et al. found ELF3 to be exclusively cytoplasmic in the basal epithelium of oral mucosa tissue and cell lines, and in the colon tissue ELF3 appears to be pancellular (AbdulMajeed et al., 2013, Wang et al., 2014).

We have shown by fractionated western blot that ELF3 is expressed in both the nucleus and cytoplasm of prostate epithelial cell lines of normal, benign and cancerous origin (Section 3.3.1). Furthermore, in prostate tissue sections, some patients exhibited exclusively cytoplasmic staining, whilst others showed expression in both the cytoplasm and nucleus (Section 3.3.2). In accordance with this, Longoni et al detected ELF3 in both the cytoplasm and nucleus of normal prostate and cancer tissue (Longoni et al., 2013). The authors also carried out immunofluorescence on DU145 and 22RV1 PCa cell lines. Whilst DU145 cells presented with a clear nuclear localisation, 22RV1 cells showed a more pan-cellular appearance, however no nuclear co-stain was carried out with these cells so this is difficult to determine.

As a transcription factor, ELF3 requires efficient transport to the nucleus, which can be mediated through classical NLS (Gorlich and Kutay, 1999). Through deletions and mutations, multiple NLS motifs were identified within the AT-hook and ETS DNA-binding domains in the murine homologue of ELF3 (mElf3) (Do et al., 2006). This was further defined in human ELF3 by Prescott et al., who identified that a single NLS motif in the AT-hook domain was sufficient for nuclear translocation, as its deletion resulted in exclusively cytoplasmic expression in breast cell lines (Prescott et al., 2004, Prescott et al., 2011). Furthermore, two nuclear export signals (NES) were also found, suggesting that ELF3 is capable of translocating both to and from the nucleus. In fact, a study in colorectal cancer showed that treatment of HT-29 cells with TNF-α, a known upregulator of ELF3, resulted in the translocation of ELF3 from the cytoplasm to the nucleus (Brown

et al., 2004, Wu et al., 2008, Li et al., 2015). This process is true of many other transcription factors such as NF-κB and NFAT as well as fellow ETS factor ETS1 (Tsao et al., 2013).

Collectively the data indicates that ELF3 can be expressed in both the nucleus and cytoplasm of prostate epithelial cells and could therefore carry out distinct functions in both cellular compartments. Appropriately, the effects of ELF3 overexpression was investigated using two lentiviral constructs which resulted in expression in the separate cellular compartments to distinguish any overt distinct functions and will be discussed further in Section 4.4.

4.3 ELF3 and the neuroendocrine phenotype

The analysis of a PCa TMA showed that ELF3 was expressed in a subset of PCa's with Gleason grade ≥7. However, ELF3 was not expressed in AMACR-positive regions of Gleason 6 PCa's, likely due to the characteristic loss of the basal cell population in the development of PCa tumours (Parimi et al., 2014). As mentioned previously, ELF3 has been linked to the progression of advanced cancers of other tissues (Wang et al., 2014, Zheng et al., 2018, Wang et al., 2018). Additionally, the ETS factor ETS1 has been linked to Gleason grade and time to progression of CRPC (Li et al., 2012).

Adenocarcinomas are the most common malignancy of the prostate. However, a subset of NE prostate neoplasms exist, which include carcinoid tumours, small cell carcinomas and large cell carcinomas. These classes of prostate tumours are generally very rare and are associated with poor prognosis (Parimi et al., 2014). Several studies have shown that NE differentiation also occurs in conventional prostate adenocarcinomas, in association with more advanced disease. In particular, an increase in NE cells has been observed following ADT and has been suggested as a mechanism of treatment resistance and therefore linked to the emergence of CRPC (Hirano et al., 2004, Berruti et al., 2007, Sasaki et al., 2005, Terry and Beltran, 2014).

The increase of NE cells following ADT is thought to occur via a process called NE transdifferentiation, whereby prostate epithelial adenocarcinoma cells acquire NE markers and properties. This phenomenon has been shown experimentally *in vitro* most extensively in LNCaP cells, but also PC3 cells (Bang et al., 1994, Shen et al., 1997, Wright et al., 2003).

HDAC inhibitors have been proposed as a potential PCa therapy due to the induction of cell death in AR-positive cell lines (Rokhlin et al., 2006). However, they have also been shown to reduce AR expression and induce a NE phenotype in LNCaP and LAPC4 cells (Frigo and McDonnell, 2008). To determine whether ELF3 was associated with a NE phenotype in PCa we treated primary prostate epithelial cultures derived from tumours with the HDAC inhibitor vorinostat. Vorinostat upregulated ELF3 in a concentration and time-dependent manner in TA, CB and whole populations of basal epithelial cells (Section 3.7.1). Whilst the NE cell marker NSE increased with vorinostat treatment in one sample, this induction was not consistent in all samples tested. However, there was a distinct change in cell morphology following treatment, even in samples with no change in NSE levels, with the presence of dendritic-like processes characteristic of NE

cells (Abrahamsson, 1999). Literature shows that chromogranin A (ChrA) and synaptophysin are more specific markers of NE cells (Parimi et al., 2014), and whilst an antibody was tested for ChrA, it was found to be unsuitable for western blot.

The origin of NE cells in prostate adenocarcinoma is not fully understood. Evidence suggests that the NE cells in the normal prostate likely arise from the same SC population that forms the epithelial cell hierarchy (Hudson, 2004). NE cells found in prostate adenocarcinomas have been proposed to be of cancerous luminal cell origin due to their expression of luminal CKs (Yuan et al., 2007). However, NE cells present in adenocarcinomas do not express AR or PSA and have also been shown to express the basal cell marker CK5 as well as luminal CKs (Hudson, 2004). Given the proliferative capabilities, differentiation and plasticity of prostate basal cells, as shown by their ability to undergo EMT, it is not unreasonable to assume they could also undergo transdifferentiation to NE cells. It should also be noted that transdifferentiation can be mediated *in vitro* by IL-1β (Spiotto and Chung, 2000, Chiao et al., 1999), which is a known activator of ELF3 (Grall et al., 2005, Rudders et al., 2001, Longoni et al., 2013, Wu et al., 2008).

In conclusion, despite our demonstration of ELF3-positivity in a subset of high Gleason grade PCa's, there is currently not enough evidence to determine if ELF3 expression is associated with the NE phenotype. Of note, the treatment status of patients in the tested TMA is unknown. Obtaining more high grade, CRPC tissue sections, as well as investigation of additional markers, namely ChrA and synaptophysin, would be beneficial. However, CRPC patients generally do not undergo routine biopsies and tissue is only available from channel TURPs, which are rare.

4.4 The role of ELF3 in the prostate and prostate cancer

4.4.1 ELF3 and the stem cell phenotype

When investigating a gene whose function is not fully elucidated, and its potential role in cancer initiation and progression, it is important to also consider what occurs in the non-cancer, normal setting. Appropriate prostate epithelial cell line models were chosen to initially investigate the role of ELF3 by considering the basal expression pattern found in primary prostate cells (Sections 3.2.2 and 3.3.2) and the levels of ELF3 expression across the panel of prostate cell lines tested (Section 3.1.1). PC3 and BPH-1 cells were chosen because they are androgen-independent and do not have features of terminally differentiated luminal cells. They are typically called intermediate cells, having several basal epithelial markers, with some markers associated with more differentiated cells, but no androgen receptor expression. They also express significant but modifiable levels of ELF3 and are derived from benign and cancer patients respectively.

Since ELF3 is expressed in the CB population of primary prostate basal cells and absent from SC and luminal cell populations and also taking into consideration that ELF3 has been ascribed both tumour suppressive and oncogenic roles in literature, we therefore originally hypothesised that knockdown of ELF3 could either: 1) cause de-differentiation and initiate SC-like characteristics, or 2) promote differentiation and reduce SC-like characteristics. We found that ELF3 knockdown significantly reduced the colony forming

ability of BPH-1 cells by 80% and PC3 cells by 65%. (Section 3.4.4). There was also a significant decrease in cell viability (Section 3.4.2) and migration (Section 3.4.3). These findings demonstrate that cells with ELF3 knockdown display a less malignant phenotype, do not acquire SC characteristics, and are therefore unlikely to be undergoing de-differentiation.

The findings from the loss of function studies of ELF3 raised the possibility that induction of ELF3 expression could drive the opposite and promote a malignant cell phenotype, as described in the prostate by Longoni et al. One study has proposed that ELF3 expression specifically promotes a SC phenotype in lung adenocarcinoma cell lines (Ali et al., 2016). They showed that ELF3 is activated by protein kinase C-iota via phosphorylation in its PNT domain, which promoted nuclear localisation and activation of the NOTCH3 promoter. ELF3 knockdown reduced oncosphere growth and cell viability and decreased the number of asymmetric divisions characteristic of SC/CSCs.

To study the overexpression of ELF3 in prostate cells we wanted to address the complex nature of its cellular localisation. The data showed that ELF3 was expressed in both the cytoplasm and nucleus of prostate epithelial cells (discussed in Section 4.2). Furthermore, other studies have shown that ELF3 carries out functions other than conventional transcriptional regulation in the nucleus. Prescott et al. used a series of deletion mutants of ELF3 to investigate its cellular localisation (Prescott et al., 2004, Prescott et al., 2011). Cytoplasmic localisation of ELF3 resulted in transformation of the non-tumorigenic breast cell line MCF-12A. This was found to be mediated by the SAR domain of ELF3, suggesting this is a non-transcriptional function. These effects were also eliminated by tagging a NLS onto the cytoplasmic ELF3 mutant. Prof Gutierrez-Hartmann kindly gifted us the ELF3-ΔAT plasmid which expressed full length ELF3 with an AT-hook domain deletion which resulted in cytoplasmic expression due to the deletion of an essential NLS. ELF-ΔAT (cytoplasmic) and ELF3-WT (nuclear) were cloned into lentiviral constructs to investigate the function of ELF3 in the distinct cellular compartments in primary prostate epithelial cells (Sections 3.5 and 3.6.1). ELF3 is the sole ETS factor containing an AT-hook domain, which is primarily found in a subset of high mobility group proteins which are regulators of chromatin structure (Reeves, 2000). To date, the AT-hook domain has been ascribed functions only within the nucleus and has been shown to be important in ELF3-mediated transcriptional activation in a promoter-dependent manner (Kopp et al., 2007). Therefore, deletion of this domain should not interfere with any function ELF3 could potentially carry out in the cytoplasm.

Overexpression of ELF3 in primary prostate basal cells showed inconclusive findings. In wound closure assays, two samples, one cancer and one normal derived from different patients, the control wound closed faster than the ELF-WT and ELF3-ΔAT wounds, whilst the third sample showed the opposite. Further samples would have to be tested in order to deduce what effect overexpression of ELF3 has on the migratory potential of primary cells. Longoni et al. showed that ELF3 overexpression in the PCa cell lines LNCaP and 22RV1 induced a more malignant phenotype including increased colony formation and migration (Longoni et al., 2013). However, these cell lines possess a luminal phenotype (Table 3.1) and our data has shown that ELF3 is not endogenously expressed in luminal cells in primary prostate tissue (Section 3.3.2). Data of Longoni et al. may therefore not be representative of what occurs *in vivo*. To distinguish induction of SC

characteristics, colony forming assays were attempted, however due to interference of non-transduced cells the data was deemed unreliable. Transduced GFP-positive cells could have been selected using fluorescence-activated cell sorting (FACS), however colony forming ability has been shown to be negatively affected following this procedure in our lab. An antibiotic selection marker would have been a more suitable set up for colony forming assays in this instance.

To explore the wider consequences of lack of ELF3 expression, an Affymetrix Clariom D microarray was carried out on BPH-1 and PC3 cells with ELF3 knockdown in triplicate (Section 3.7.2). Data was analysed by individual cell line and also collectively, to identify ELF3-regulated pathways which are important in both cell lines. The expression of a number of classical SC/CSC markers were investigated, however there was no significant difference in expression with ELF3 knockdown in either cell line. There was an approximately 3-fold increase of CD49b in BPH-1 cells, but this alone is insufficient to suggest induction of a SC phenotype, particularly considering the outcomes of functional assays.

Collectively, the data suggests that whilst ELF3 knockdown inhibits a malignant cell phenotype, there is no decrease in classical SC markers to suggest ELF3 is involved in promoting such a phenotype. Furthermore, more studies on the consequences of ELF3 overexpression would have to be performed to distinguish true SC biological characteristics, such as colony formation.

4.4.2 ELF3 as a regulator of the cell cycle

Since we found that ELF3 knockdown did not cause cleaved caspase-3-induced apoptosis, this suggested that the observed decrease in viable cell number may be due to reduced proliferation (Section 3.4.2). Previous studies have highlighted ELF3 as a cell cycle regulator in breast and non-small cell lung carcinoma (NSCLC) cell lines. ELF3 knockdown resulted in an accumulation of cells in the G1 phase and, in breast cancer cells, a reduction in cyclin D1 (Kar and Gutierrez-Hartmann, 2017, Wang et al., 2018). GO analysis from the microarray revealed that the differentially expressed genes were involved in processes related to the cell cycle and histone regulation. PLK1 was one of the most significantly differentially expressed genes, and was amongst the highest fold changes in all three analyses (BPH-1, PC3 and combined), suggesting it may be highly regulated by ELF3. PLK1 is involved in G2 and cytokinesis stages of the cell cycle, both of which were highlighted in the GO anaylsis, (de Gooijer et al., 2017, Petronczki et al., 2008). As mentioned previously, histone gene expression is highly regulated during the cell cycle, and this may account for the bias towards histone-regulated processes in the GO analysis. There were also significant changes in expression of genes upstream and downstream of the PLK1 pathway, including CDC25C, cyclin B1, p21 and FOXM1.

Of note, increased PLK1 expression has been detected in PCa (Weichert et al., 2004). Moreover, there is a correlation of increased PLK1 in PCa tumours with NE differentiation (Grobholz et al., 2005), further suggesting there could be a link between ELF3 expression and NE differentiation as discussed in Section 4.3. Contradictory to this, both cell lines in this study showed a significant increase in NSE expression following ELF3 knockdown, particularly PC3 cells which showed an over 7-fold induction. However, there

was no change in other NE markers such as ChrA or synaptophysin. PC3 cells represent aggressive PCa and are known to inherently express some NE markers (Tai et al., 2011). Nevertheless, this increase in NE phenotype does not coincide with results from functional studies, as siELF3 cells showed a decrease in malignant phenotype.

Multiple candidate G2 cell cycle proteins were validated at the protein level (Section 3.7.3). There was a significant decrease in PLK1 and CDC25C as well as an increase in CDK inhibitor p21 with ELF3 knockdown. This was also validated at the functional level, where there was an accumulation of BPH-1 and PC3 siELF3 cells in the G2 phase over time. Furthermore, PHH3-S10 staining confirmed there were fewer siELF3 cells undergoing mitosis compared to mock and siSCR. This conclusively validates ELF3 as a cell cycle regulator in prostate epithelial cell lines regardless of diagnosis. It would be interesting to determine whether ELF3 is a direct regulator of PLK1, either transcriptionally, which could be observed using a luciferase-reporter assay, chromatin immunoprecipitation (ChIP) or electrophoretic mobility shift assay (EMSA), or at the protein level by co-immunoprecipitation (co-IP). In relation to this, PDEF (another epithelial-specific ETS factor), can bind to and inhibit the FOXM1 promoter in TRAMP mouse cells (Cheng et al., 2014). PLK1 is a FOXM1 target gene and was also showed decreased expression in the ELF3 knockdown microarray.

ELF3 knockdown was optimised in primary prostate cultures enriched for CB cells to determine the effects on cell cycle. However, whilst significant knockdown in this challenging model was achieved, there was no significant, consistent effect on cell cycle phase or the expression of G2 cell cycle proteins (Section 3.7.4). This could largely be due to unsuitable experimental set up for cell cycle analysis. The cells were virtually fully confluent at the 72h time point following transfection and cells were therefore not rapidly proliferating, as indicated by the high levels of p21 across all samples. A stable knockdown via lentivirus transduction and selection may be more suited in this instance as the starting cell density for experiments can be optimised more readily than following transient transfection.

4.4.3 The differential role of ELF3 in benign and cancerous prostate

In the overexpression studies, ELF3-ΔAT and ELF3-WT showed the same trend in effects on the cell viability of both normal and cancer primary prostate samples, although this was only significant at one time point in the ELF3-WT and further samples would be beneficial to confirm this (Section 3.6.2). The trend showed an increase in cell viability of cancer samples and decreased cell viability of normal samples. This could suggest that ELF3 differentially affects cell proliferation between the normal and cancer setting. In accordance with this, Prescott et al. found that transiently overexpressing ELF3 in breast cell lines resulted in nuclear localisation and exerted differential effects on normal and cancer cell lines (Prescott et al., 2004). Specifically, nuclear ELF3 promoted apoptosis in normal breast cell lines but not cancer. Whilst we found no change in expression of the apoptosis marker cleaved caspase-3 in cells with ELF3 knockdown, this has not been tested in primary prostate cells with ELF3 overexpression. Some studies have linked ELF3 expression to apoptosis, particularly in the inflammatory setting (Feng et al., 2016, Li et al., 2015). Other

studies have also shown that nuclear translocation of ELF3 induces apoptosis in a transcription-dependent manner (Lee et al., 2008, Longoni et al., 2013), which suggests ELF3 may require specific stimuli to promote apoptosis.

In the microarray, PC3 cells possessed almost double the number of significantly altered genes (1848 upregulated, 931 downregulated) compared to BPH-1 (776 upregulated, 664 downregulated). This is interesting as PC3 cells showed a more modest response in colony forming and migration assays compared to BPH-1 cells. Given that the degree of knockdown was similar in both cell lines, this result further implies that PC3 cells may be upregulating compensatory pathways to cope with ELF3 knockdown, which in turn suggests that ELF3 may be an important regulator in cancer.

Following the unbiased analysis of GO terms, changes in expression of other ETS factors were also assessed. Interestingly, PC3 cells showed a significant 7-fold upregulation of ESE3. ETS factors are known to display redundancy among their functions (Oikawa and Yamada, 2003, Hollenhorst et al., 2007). Therefore ESE3 upregulation may represent one compensatory mechanism for PC3 cells. As mentioned in Section 1.8.3.3, ESE3 is an epithelial-specific ETS factor belonging to the same subfamily as ELF3 and they share 84% homology within their ETS DNA-binding domain (Kas et al., 2000). However, each has a distinct PNT domain, suggesting that whilst they may bind to similar target genes, their effects could ultimately vary, depending on the protein-protein interactions achieved via their PNT domains. In the prostate, ESE3 has been found to possess tumour suppressor functions. One study demonstrated that ESE3 can upregulate the expression of Nkx3.1; a tumour-suppressor commonly lost in PCa partly by heterozygous deletion of the gene located at chromosome 8p21.2 (Bowen et al., 2000, Vocke et al., 1996, Kunderfranco et al., 2010). Further studies by the same group have identified that loss of ESE3 promotes a SC phenotype due in part to its repression of IL-6 and the STAT3 pathway (Albino et al., 2012, Albino et al., 2016). ESE3 expression is also lost in cancers of other tissues (Tugores et al., 2001). Given these observations, it is surprising that PC3 cells would upregulate ESE3 in response to ELF3 knockdown. However, ESE3 displays a similar expression pattern to ELF3 in the normal prostate and is therefore most highly expressed in basal epithelial cells (Tugores et al., 2001). Given the homology between ELF3 and ESE3 and the plethora of regulation that ETS factors exhibit, ESE3 could potentially alter its function in this context to partially restore colony forming and migratory abilities.

4.4.4 The role of ELF3 in differentiation and EMT

BPH-1 siELF3 cells showed a more overt morphological change when compared to PC3 siELF3 cells. BPH-1 cells were more tightly packed together which was evident in brightfield images and IF of tubulin and phalloidin (Section 3.4.5). There was also a progressive increase of basal marker CK5 and decrease of luminal marker CK18 shown by western blot and ICC, indicating cells were becoming more basal. On the other hand, PC3 cells showed an initial decrease in CK18, however this was not sustained, and CK5 was only detected at low levels in all conditions by ICC. This shift in CK expression could be due to death of the more differentiated CK18 positive cells that cease to divide.

Differentiation status was also investigated in primary prostate cells after ELF3 overexpression. Using two methods, quantitative phase imaging and flow cytometry, we showed that irrespective of diagnosis, ELF3-WT cultures had a higher proportion of more primitive TA cells compared to ELF3-ΔAT cultures, which had a higher proportion of CB cells (Figure 4.1). This indicates that nuclear ELF3 may be required to maintain prostate epithelial cells in the basal state, and downregulation of expression may contribute to CB cell commitment of differentiation to luminal cells. Knockout of murine Elf3 results in 30% lethality, highlighting its importance in development (Ng et al., 2002). Furthermore, the surviving mice displayed several abnormalities of the epithelial cell-rich small intestine, including the inability to undergo proper terminal differentiation. ELF3 has also been linked to differentiation in many human studies. For instance, Brembeck et al. showed ELF3 repressed the basal keratin 4 and upregulated the late differentiation marker SPRR2A in oesophageal squamous carcinoma cell lines (Brembeck et al., 2000). In the bladder, ELF3 has been shown to be a regulator of differentiation in the urothelium, as knockdown of ELF3 prevents differentiation and expression of late differentiation marker uroplakin3a (Bock et al., 2014). Several studies have also showed that ELF3 is upregulated in primitive cell lines following induced differentiation by retinoic acid (Park et al., 2014, Cheong et al., 2010, Kim and Lotan, 2004). This also coincides with the expression pattern of ELF3 we have found in prostate basal subpopulations, whereby SCs express low ELF3 which is upregulated upon basal cell differentiation. Our findings indicate that a delicate balance of ELF3 expression is required to maintain the proper differentiation and homeostasis of the prostate epithelial hierarchy and increased ELF3 may feedback to increase progenitor cell numbers.

E-cadherin and active β-catenin expression were also examined as epithelial and EMT markers, respectively. Both cell lines showed an increase in E-cadherin and active β-catenin, albeit they were upregulated in PC3 siELF3 cells at a later time point than BPH-1 siELF3 cells. Active β-catenin was localised to the cell membrane in both cell types. In the nucleus, β-catenin can activate the Wnt signalling pathway and promote EMT. However, the observed localisation indicates that rather than acting as a driver of EMT, it was likely acting as an adaptor to E-cadherin in the cell membrane adhesion complex (Shin et al., 2010, Tian et al., 2011). This coincides with the increased cell-cell contacts and compact colony formation observed in BPH-1 cells with ELF3 knockdown. ELF3 has been shown to bind and co-localise with β-catenin in the cytoplasm of colon cancer cells via its ETS domain (Yang and Lee, 2016). This raises the possibility that ELF3 sequesters β-catenin in the cytoplasm of prostate epithelial cells and therefore loss of ELF3 liberates the protein.

From findings in the functional assays and literature, other pathways of interest were also investigated from the gene expression microarray, such as EMT. PC3 cells with ELF3 knockdown showed an upregulation of fibronectin and its receptor integrin α5, which are associated with mesenchymal cells. PC3 cells have an invasive cell phenotype and inherently express markers of EMT such as vimentin to a certain degree (Singh et al., 2003). However, there was no change in mesenchymal cell marker expression in BPH-1 cells. There was also a 2-fold upregulation of E-cadherin in PC3 cells, which agrees with the previous western blot findings. There was also no significant change in EMT transcription factor expression. Several recent studies

have explored the role of ELF3 in EMT with conflicting findings. In colorectal and breast cancer, ELF3 has been shown to negatively regulate ZEB1, a key driver of EMT (Liu et al., 2018, Sinh et al., 2017). Studies in ovarian cancer and NSCLC have also found ELF3 expression to negatively regulate EMT by decreasing cell proliferation, anchorage independent growth, migration and invasion, as well as reducing expression of classical EMT markers such as vimentin and Snail (Yeung et al., 2017, Lou et al., 2018). Conflicting studies in breast, NSCLC and hepatocellular carcinoma have shown ELF3 to promote EMT. In hepatocellular carcinoma, ELF3 promotes ZEB1 expression by binding to miR-141-3p and repressing its action on ZEB1 (Zheng et al., 2018). In NSCLC, ELF3 promotes EMT marker expression through activation of the PI3K/Akt and ERK signalling pathways (Wang et al., 2018). Finally, a study by Schedin et al. showed that overexpression of ELF3 in a normal breast cell line resulted in sphere formation which resembled tumours with an EMT phenotype compared to normal glandular spheres formed by control cells (Schedin et al., 2004).

Whilst ELF3 knockdown reduced colony formation, cell viability and migration, there was no overt differential expression of EMT transcription factors or mesenchymal cell markers in the microarray. Though, there was an increase in E-cadherin and active β-catenin at the cell membrane, demonstrating that cells are becoming more epithelial. The experimental and gene expression data shows that ELF3 knockdown induces functional changes which were in part due to reduced cell proliferation via cell cycle arrest at G2. However, EMT is a dynamic process, and fluctuation of ELF3 expression levels clearly influences the epithelial phenotype. Therefore, it would be interesting to investigate the expression of EMT markers at the protein level to fully confirm whether ELF3 is a regulator of EMT in prostate epithelial cells.

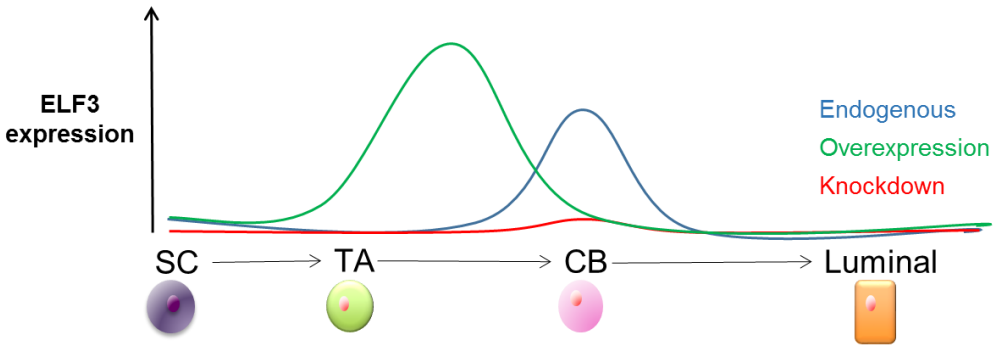

Figure 4.1. ELF3 expression in the prostate epithelial hierarchy.

A summary of ELF3 expression manipulation carried out in prostate epithelial cells. ELF3 is endogenously expressed in the CB subpopulation (blue), whilst ELF3-WT overexpression via lentiviruses induces a proportional shift towards the TA subpopulation (green).

4.5 Targeting ETS factors in cancer

4.5.1. Direct targeting of ETS factors

Various methods of targeting ETS factors have been investigated either at the transcriptional, mRNA or protein levels. For instance, triplex-forming oligonucleotides (TFOs) are single-stranded oligonucleotides that bind to specific sequences in DNA and form triple helices, interrupting the transcription of the targeted gene. They bind to long homopurine sequences, which are commonly found in gene promoter regions and enhance both the specificity and stability of the interaction. A TFO targeted to ETS2 resulted in decreased colony forming ability and induced apoptosis in DU145 cells (Carbone et al., 2004). Since ETS2 is a regulator of telomerase activation in breast cancer cells (Dwyer and Liu, 2010), this type of therapy could potentially abrogate the self-renewal capacity of CSCs. The control experiments in this study revealed that the ETS2 TFO was highly target gene-specific and presented an appealing prospect for future gene-targeted therapies (Carbone et al., 2003). However, a suitable delivery method and the potential for long-term mutagenic effects are significant limitations.

A small molecule inhibitor of ETS factor fusion protein EWS-FLI1 in Ewing's sarcoma has been tested on ERG-fusion positive VCaP cells and ETV1-fusion positive LNCaP cells (Rahim et al., 2011). The inhibitor, YK-4-279, decreased the migratory and invasive properties associated with ERG and ETV1 overexpression in PCa, without altering their protein levels in vitro. The fusion negative cell line (PC3) was unresponsive to treatment, suggesting the inhibitor is selectively targeting the overexpressed ETS factors. Whether YK-4-279 will also target essential ETS factors and cause off-target toxic effects in vivo still needs to be investigated.

A major consideration is that direct targeting of a transcription factor is likely to result in off-target side effects, especially given the wide variety of functions ETS factors perform in different types of cells and tissues (Figure 4.2). ETS factor knockouts in mice generally result in at best detrimental effects or even lethality (Bartel et al., 2000). As only a limited number of target genes are likely to cause the oncogenic effects, or alternatively block tumour suppressors, the toxicity induced by blocking transcription factors must therefore be carefully monitored. Targeting unique cancer-associated molecules such as TMPRSS2-ERG mRNA would avoid such complications and specifically target cancer cells. A good example of this in practice is imatinib, a small molecule inhibitor of the BCR-ABL fusion protein which has revolutionised the treatment of fusion positive chronic myeloid leukaemia (CML) as well as other cancers (Nadal and Olavarria, 2004). TMPRSS2-ERG is a complex target since the mRNA presents as multiple different splice variants in each patient and the translated protein formed only consists of ERG. Shao et al. designed siRNA molecules specific for the unique junctions of two isoforms of TMPRSS2-ERG mRNA, including the most common isoform TMPRSS2 exon 1-ERG exon 4 and TMPRSS2 exon 2-ERG exon 4 which is associated with aggressive disease (Shao et al., 2012). The efficiency in knocking down the fusion gene was tested in vivo via liposomal nanovectors, which have also been successfully tested in murine models of breast and ovarian cancer (Landen et al., 2005, Halder et al., 2006). The siRNAs were able to reduce growth of established

VCaP xenograft tumours with no effect on normal ERG levels and no toxicity observed in the mice. Since prostate CSCs express TMPRSS2-ERG, knocking it down might inhibit cell growth. Whilst this approach is appealing, its effect on the function and longevity of fusion positive prostate CSCs would need to be monitored before it could be considered curative. Furthermore, CSC liposome uptake into every tumour cell and their potential to degrade the siRNA through resistance mechanisms would also need to be investigated.

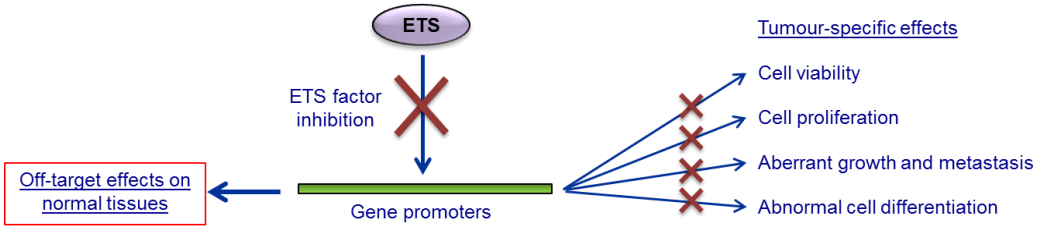

Figure 4.2. The benefits and disadvantages of inhibiting ETS factors in cancer.
The inhibition of aberrantly expressed ETS transcription factors in cancer would prevent their binding to the promoter regions of target genes. This would subsequently lead to the repression of cancer-associated target genes normally upregulated by said ETS factor in cancer. Alternatively, this may also alleviate the suppression of repressed tumour suppressor genes. This will lead to many beneficial, tumour-specific effects. However, given the importance of ETS factors in normal tissue homeostasis, there will also be toxic, off-target effects to normal cells. Taken from (Archer et al., 2017).

4.5.2. Indirect targeting of ETS factors

An alternative and almost certainly less toxic method of preventing the aberrant effects of ETS factors in cancer is to indirectly target the specific factor and thus target the oncogenic effect. ETS factors are known to regulate gene expression via interactions with co-regulatory proteins (Li et al., 2000). Since multiple ETS factors are able to bind to the same target genes, targeting the protein-protein interactions should be a more selective way of inhibiting their effects in cancer without interfering with the normal binding of other ETS factors. Several synthetic molecules have been constructed which interfere with the interaction between ELF3 and one of its co-activators, Sur2 (Shimogawa et al., 2004, Asada et al., 2003, Lee et al., 2009). The ELF3-Sur2 interaction is required for the activation of the growth factor HER2 (Moasser, 2007). The use of ELF3-Sur2 inhibitors downregulated HER2 expression with a concomitant decrease in cell proliferation and increase in apoptosis in cell line models of breast cancer, gastric cancer and HNSCC. Furthermore, the ELF3-Sur2 inhibitors sensitised breast cancer cell lines to tamoxifen and also worked synergistically with the currently used treatments for gastric cancer and HNSCC (Nam et al., 2013, Kim et al., 2012, Zhang et al., 2013). Thus, determining the interacting partners of ETS factors which are important in driving tumour progression may be a more viable route for cancer therapeutics.

In order to inhibit the negative effects of a specific ETS factor in cancer without hindering its normal roles in target and surrounding tissues, the induced transcriptome of the factor is an essential tool. The ability to evaluate precisely which target genes are important for cancer initiation and progression, and identifying key co-regulators would be instrumental in developing ETS factor targeting therapies. Although time-

consuming, this is the only way, short of finding a cancer-specific and targetable molecule, to maintain the equilibrium between positive and negative ETS factor function. ChIP-chip technology, where whole genome analysis can identify all the binding sites of a specific ETS factor within the genome in different types of cells would be a primary tool for this analysis (Buck and Lieb, 2004).

4.5.3. Expression of suppressive ETS factors

With regards to PCa, PDEF and ESE3 are candidate tumour suppressors that could be exploited for gene therapy. The classical example of a tumour suppressor is transcription factor p53, which is mutated in over 50% of all human cancers, making it an attractive therapy target. Re-introduction of wildtype p53 has been investigated using non-replicative adenoviruses in multiple cancers including prostate (Hong et al., 2014, Stegh, 2012, Yang et al., 1995). Clinical trials have produced promising results in different cancers particularly in combination with conventional chemotherapy and radiotherapy (Xie et al., 2010, Li et al., 2009). Notably, loss of functional p53 has also been linked to enhancement of the CSC phenotype (Prabhu et al., 2012). Therefore, reintroduction of p53 may abrogate the CSC population and could explain the success of the viral transduction approach in combination with traditional cancer therapies. Re-expression of PDEF or ESE3 would only be beneficial for the subtype of PCas that have lost PDEF or ESE3 expression. If PDEF and ESE3 loss are truly maintaining cells in a de-differentiated state then their re-expression, e.g. via a viral vector, could promote differentiation of the tumour cells. This should also differentiate the CSCs into a cell type that is more susceptible to conventional treatments.

4.5.4 Differentiation therapy

In order to cure PCa, we must take into account the cellular heterogeneity of the disease, a challenge which current therapy strategies have been unable to surmount. This is reflected in the limited survival rates of patients prescribed the next-generation drugs which typically only target luminal cells. The effects of the aberrantly expressed epithelial-specific ETS factors in PCa appear to maintain the cancer cells in a more SC-like state (Archer et al., 2017). We and others have observed this stem-like phenotype in advanced metastatic tumours (Rane et al., 2015, Pellacani et al., 2014, Smith et al., 2015). This will confer drug-resistance mechanisms and inevitably tumour recurrence following treatment, as these cells retain their proliferative potential and hence tumour renewal potency. The premise of differentiation therapy is to manipulate CSCs and progenitor cells to drive them towards differentiation and lose their stem-like abilities, resulting in differentiated cells with limited proliferative capacity characteristic of the bulk of a prostate tumour. Although an attractive theory, the design of effective differentiation therapies has been limited (Rane et al., 2012). The most notable success has been with acute promyelotic leukaemia (APL) which is characterised by an accumulation of progenitor cells caused by a block in differentiation (de The et al., 1991, Grignani et al., 1993). Differentiation is restored in APL via all-trans retinoic acid treatment which is now part of the standard APL therapy regime (Huang et al., 1988, Sanz et al., 2009). If differentiation therapy were to be successful in PCa it would have to be combined with conventional cytotoxic treatments to kill the bulk

tumour cells as well as the differentiated and now vulnerable CSCs, which would eradicate all tumour cells and prevent recurrence.

4.6 Concluding remarks

The regulatory potential of ETS factors most likely explains the conflicting findings in literature of ELF3 biological functions such as tumour suppressor vs. oncogene or even more specifically activation vs. repression of the same gene. This could involve interaction with various co-factors, or under specific stimuli. The possible redundancy found between ETS factors adds an additional layer of complexity when studying these proteins. Studies in ELF3 and other discussed ETS factors have also shown that function is extremely context-dependent, with regards to tissue type, cell type and pathology. Consequently, defining the correct cell type to study ELF3 expression was integral to determining its genuine function in the prostate.

Whilst established cell lines are easily manipulated and provide a suitable means to explore mechanisms and theories, they do not fully represent the complexity of a tumour and how the cells interact and differentiate. To illustrate this, multidimensional scaling of cell lines and primary cells shows distinct clustering, demonstrating that they are very different, and both should be employed appropriately within a study (Figure 4.3). By utilising the fractionated cell populations from primary patient tumours, this study has for the first time provided a comprehensive account of ELF3 expression in the prostate, including individual subpopulations. Furthermore, we have described a novel role for ELF3 as a regulator of the cell cycle in prostate basal cells as well as generating an effective tool for studying ELF3 overexpression. We have generated data that implies that ELF3 almost certainly carries out additional functions in the prostate, of which we could only begin to unravel in the duration of this study. This includes the regulation of primary prostate epithelial cell differentiation, potential regulation of β-catenin function, and providing a survival benefit in cancer vs. normal cells and a possible link to advanced prostate tumours.

Collectively, these findings suggest ELF3 may be an oncogene in the PCa setting. However, given ELF3 is also a regulator of the cell cycle and potentially differentiation in normal prostate epithelial cells, this would need to be taken into consideration in the context of developing therapies. The gene expression microarray of cells with ELF3 knockdown provided a useful repository of information and a similar investigation into the genome-wide changes caused by ELF3 overexpression would be invaluable in defining further roles and unveiling important signalling pathways regulated by ELF3, and whether it or its downstream effectors could ultimately be manipulated to improve PCa treatment.

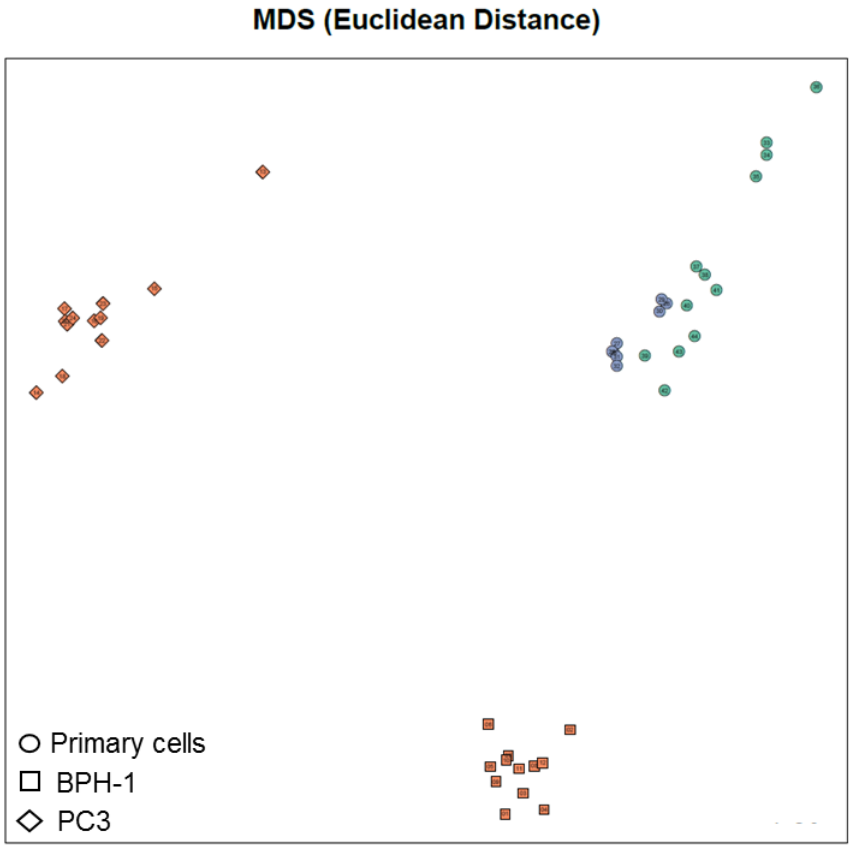

Figure 4.3. Multidimensional scaling of prostate epithelial cells.

Multidimensional scaling (MDS) of prostate primary cells, BPH-1 and PC3 cell lines. Cell line sample sets were in biological triplicate and included untransfected, mock transfected, siSCR and siELF3 of BPH-1 and PC3 cells. Primary cells represent several individual patients. Produced by Alastair Droop.

Appendices

Appendix 3.1: Videos of migration assay of primary prostate cells with ELF3 overexpression (see attached CD).

Appendix 3.2: ELF3 knockdown does not induce apoptosis in primary prostate committed basal cells.

Primary prostate committed basal cell lysates harvested 72 hours post-transfection were probed for cleaved caspase 3 as a marker of apoptosis. S = staurosporine-treated BPH-1 cells (1μM for 24 hours).

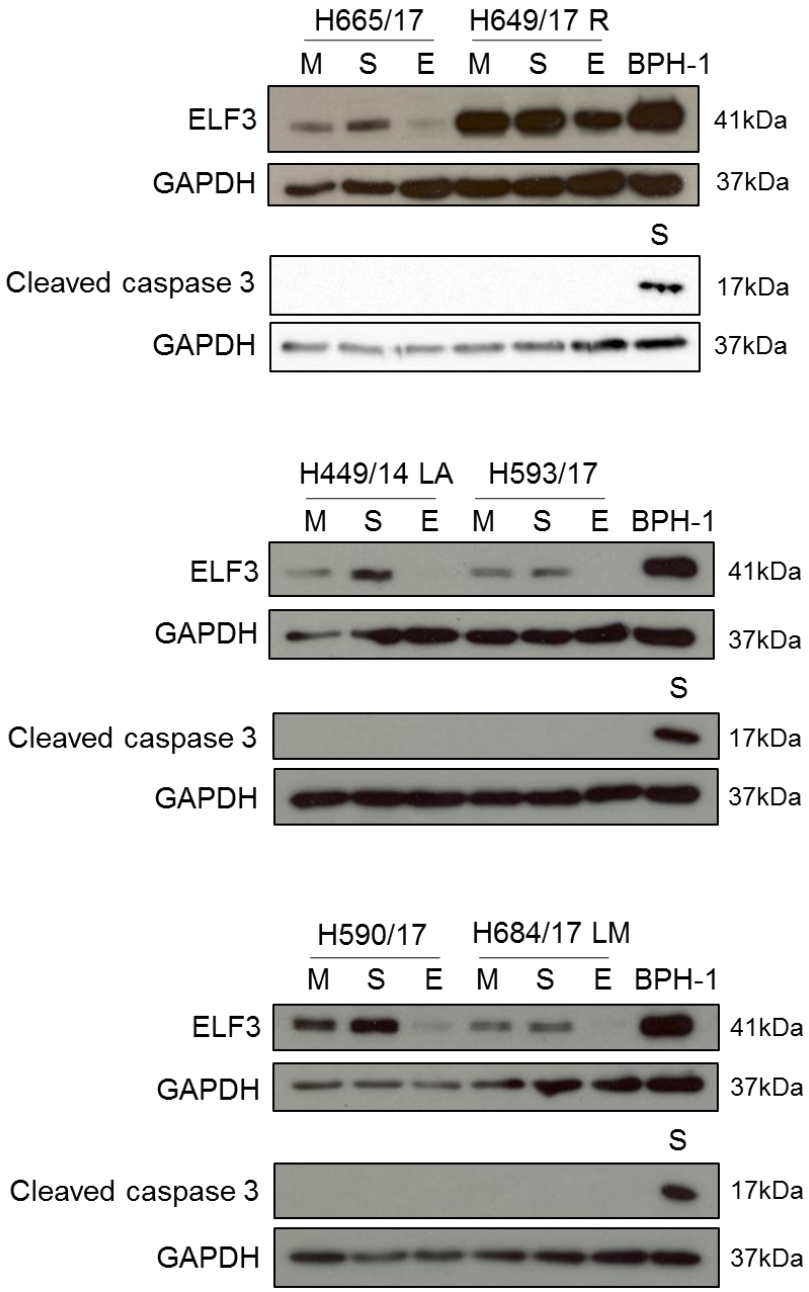

Appendix 3.3: Gene ontology (GO) terms associated with siSCR vs siELF3 in BPH-1 and PC3 cells combined. Top 35 terms with highest p-values shown.

Term	P-value	Genes
GO:0006334 Nucleosome assembly	3.75E-13	HIST2H3A, HIST1H3J, HIST1H1E, HIST1H1D, HIST1H2BF, HIST2H3C, HIST1H2BM, HIST1H1T, HIST1H2BN, HIST1H4A, HIST1H2BL, HIST1H2BJ, NAA60, HIST1H3A, HIST1H3B, HIST1H4E, HIST1H3C, HIST1H4C, H2AFX, HIST1H3F, ASF1B, HIST2H3PS2, HIST1H4J
GO:0000183 Chromatin silencing at rDNA	1.45E-09	HIST2H3A, HIST1H3J, HIST1H4A, HIST1H3A, HIST1H3B, SUV39H1, HIST1H4E, HIST1H3C, HIST1H4C, HIST1H3F, HIST1H4J, HIST2H3C
GO:0006335 DNA replication-dependent nucleosome assembly	4.76E-09	HIST1H3J, HIST1H4A, IPO4, HIST1H3A, HIST1H3B, HIST1H4E, HIST1H3C, HIST1H4C, ASF1B, HIST1H3F, HIST1H4J
GO:0006342 Chromatin silencing	1.74E-07	HIST1H2AB, HIST2H2AB, HIST1H2AG, HIST1H2AE, MORF4L2, HIST1H2AI, H2AFX, HIST1H2AJ, HIST1H2AM, HIST1H2AL, BAHD1
GO:0032200 Telomere organization	2.74E-07	HIST1H3J, HIST1H4A, HIST1H3A, HIST1H3B, HIST1H4E, HIST1H3C, HIST1H4C, HIST1H3F, HIST1H4J
GO:0045815 Positive regulation of gene expression, epigenetic	4.81E-07	HIST2H3A, HIST1H3J, POLR2F, HIST1H4A, HIST1H3A, HIST1H3B, HIST1H4E, HIST1H3C, HIST1H4C, HIST1H3F, HIST1H4J, HIST2H3C
GO:0045814 Negative regulation of gene expression, epigenetic	4.99E-07	HIST2H3A, HIST1H3J, HIST1H4A, HIST1H3A, HIST1H3B, HIST1H4E, HIST1H3C, HIST1H4C, HIST1H3F, HIST1H4J, HIST2H3C
GO:0031047 Gene silencing by RNA	1.06E-06	HIST2H3A, HIST1H3J, NUP133, POLR2F, POM121, HIST1H4A, NUP210, HIST1H3A, HIST1H3B, HIST1H4E, HIST1H3C, HIST1H4C, HIST1H3F, HIST1H4J, HIST2H3C
GO:0051290 Protein heterotetramerization	1.04E-05	HIST1H3J, HIST1H4A, HIST1H3A, HIST1H3B, HIST1H4E, HIST1H3C, HIST1H4C, HIST1H3F, HIST1H4J
GO:0007059 Chromosome segregation	6.16E-05	KIF11, SPAG5, INCENP, NAA60, CENPF, SKA3, CENPW, CENPE, NDC80, RCC1
GO:0007062 Sister chromatid cohesion	7.29E-05	ITGB3BP, KIF22, NUP133, MAD2L1, PLK1, INCENP, CENPF, CENPE, NDC80, AURKB, CDCA5, CENPI
GO:0007067 Mitotic nuclear division	8.57E-05	ITGB3BP, KIF22, KIF11, KIF15, CENPF, NDC80, AURKB, RCC1, HMGA2, CDC25C, REEP4, CCNB2, PLK1, INCENP, SKA3, CENPW, MAD2L2, CDCA5, TUBB3

GO:0051301 Cell division	1.24E-04	ITGB3BP, KIF14, CKS1B, KIF11, PSRC1, KIF18B, CENPF, NDC80, CENPE, RCC1, HMGA2, CDC25C, REEP4, CCNB1, NCAPH, MAD2L1, CCNB2, NCAPG, SPAG5, CENPW, SKA3, MAD2L2, CDCA5
GO:0060968 Regulation of gene silencing	1.27E-04	HIST1H3J, HIST1H3A, HIST1H3B, HIST1H3C, HIST1H3F
GO:0044267 Cellular protein metabolic process	2.47E-04	HIST2H3A, HIST1H3J, HIST1H4A, GSN, HIST1H3A, HIST1H3B, HIST1H4E, HIST1H3C, HIST1H4C, HIST1H3F, HIST1H4J, HIST2H3C
GO:0051726 Regulation of cell cycle	3.80E-04	CCNB1, ADARB1, CCNB2, TSC1, DTL, PLK1, FOXM1, SKP2, CENPF, BOP1, CDC25C, MYBL2
GO:0006336 DNA replication-independent nucleosome assembly	4.78E-04	HIST1H4A, IPO4, HIST1H4E, HIST1H4C, ASF1B, HIST1H4J
GO:0008283 Cell proliferation	5.95E-04	CKS1B, TSPAN1, KIF15, MET, HDGF, PIM1, SKP2, CENPF, PRKDC, BOP1, AURKB, PIM2, CDC25C, MXD1, ISG20, TGFB2, LRP1, PLK1, NAA60, MELK, ERCC1, USP13
GO:0034080 CENP-A containing nucleosome assembly	7.90E-04	ITGB3BP, HIST1H4A, HIST1H4E, CENPW, HIST1H4C, HIST1H4J, CENPI
GO:0006886 Intracellular protein transport	0.001300515	STX3, TBC1D3G, TBC1D3H, COPZ1, CTSA, TBC1D3B, BCAP31, AP1S3, STX12, IPO4, TBC1D13, RHOB, TOMM22, STX11, TBC1D3, VPS39
GO:0007080 Mitotic metaphase plate congression	0.002509116	KIF14, CCNB1, KIF22, PSRC1, CENPE, CDCA5
GO:0016233 Telomere capping	0.002660512	HIST1H4A, HIST1H4E, PRKDC, HIST1H4C, HIST1H4J
GO:0000086 G2/M transition of mitotic cell cycle	0.003025545	CCNB1, CCNB2, CEP250, PLK1, FOXM1, SKP2, CALM3, OPTN, CDC25C, MELK, HMMR
GO:0000209 Protein polyubiquitination	0.003113594	WSB1, PSMB4, C18ORF25, DTL, RNF165, TRIM69, TPP2, SKP2, RBCK1, RNF24, RNF181, RNF213, CBFB
GO:0051310 Metaphase plate congression	0.003190695	KIF22, CENPF, CENPE, NDC80
GO:0000070 Mitotic sister chromatid segregation	0.003648786	MAD2L1, PLK1, SPAG5, KIF18B, NDC80

GO:0000278 Mitotic cell cycle	0.003964187	E2F4, CEP250, CENPF, KIF18B, CENPW, CENPE
GO:0007018 Microtubule-based movement	0.004995467	KIF23, KIF14, KIF22, KIF4A, KIF11, KIF15, KIF18B, CENPE
GO:0006977 DNA damage response, signal transduction by p53 class mediator resulting in cell cycle arrest	0.005278038	CCNB1, E2F1, CDKN1B, E2F4, E2F7, ARID3A, CDC25C
GO:0007077 Mitotic nuclear envelope disassembly	0.005392878	CCNB1, NUP133, POM121, CCNB2, PLK1, NUP210
GO:0006303 Double-strand break repair via nonhomologous end joining	0.005709232	HIST1H4A, C7ORF49, HIST1H4E, PRKDC, H2AFX, HIST1H4C, HIST1H4J
GO:0045653 Negative regulation of megakaryocyte differentiation	0.010547239	HIST1H4A, HIST1H4E, HIST1H4C, HIST1H4J
GO:0098609 Cell-cell adhesion	0.011251182	HSP90AB1, HIST1H3J, DIAPH3, WASF2, HSPA1A, GIPC1, ESYT2, EPB41L1, HNRNPK, CCNB2, HIST1H3A, HIST1H3B, HIST1H3C, NDRG1, HIST1H3F
GO:0071456 Cellular response to hypoxia	0.01233504	CCNB1, E2F1, STC2, CPEB2, SUV39H1, BNIP3, NDRG1, ADAM8
GO:0016255 Attachment of GPI anchor to protein	0.012898059	PIGK, GPAA1, PIGT

Appendix 3.4: Expression changes of cell cycle-related genes following ELF3 knockdown from gene expression microarray. Highlighted boxes indicate genes with significance threshold of 2-fold increase or decrease and a p-value <0.05. NS = not significant.

Cell Cycle - significant only		BPH-1		PC3		Both	
Gene	Description	Fold Change	P-Val	Fold Change	P-Val	Fold Change	P-Val
PLK1	Polo-like kinase 1	-15.56	0.0001	-5.59	1.16E-06	-7.53	4.24E-07
CCNB2	Cyclin B2	-13.21	0.0001	-8.27	9.34E-07	-8.22	2.27E-06
SKP2	S-phase kinase-associated protein 2	-5.07	2.62E-06	-6.2	5.65E-05	-5.32	0.0022
CDCA5	Cell cycle division associated 5	-2.36	0.0036	-3.17	0.007	-2.98	0.0062
CKS1BP7	CDC28 protein kinase regulatory subunit 1B pseudogene 7	-2.3	0.0366	-2.09	0.0014	-2.91	0.0154
CKS1B	CDC28 protein kinase regulatory subunit 1B	-2.7	0.0202	-2.4	0.0002	-2.79	0.0232
CENPF	Centromere protein F	-3.8	0.0024	-2.15	0.0036	-2.83	0.0024
CDC25C	Cell division cycle 25C	-2.34	0.0008	-2.27	0.0006	-2.42	2.39E-05
AURKB	Aurora kinase B	-2.68	0.0046	-2.55	0.009	-2.23	0.0045
CCNB2	Cyclin B2	-13.21	0.0001	-8.27	9.34E-07	-8.22	2.27E-06
CDCA5	Soronin	-2.36	0.0036	-3.17	0.007	-2.98	0.0062
MAD2L2	MAD2 mitotic arrest deficient-like 2 (yeast)	-2.9	8.80E-06	-3.96	9.56E-06	-3.31	2.35E-08

CENPW	Centromere protein W	-2.22	0.0334	-2.04	0.0222	-2.03	0.0095
FOXM1	Forkhead box M1	-2.27	0.0125	NS	NS	-2.4	0.0141
CEP128	Centrosomal protein 128kDa	-2.6	0.0014	NS	NS	-2.98	0.0029
CENPE	Centromere protein E	-3.62	0.0044	NS	NS	-2.15	0.0013
INCENP	Inner centromere protein	-2.62	0.0011	NS	NS	-2.36	0.001
CCNC	Cyclin C	2.69	0.0028	NS	NS	2.29	0.0086
CKS1BP3	CDC28 protein kinase regulatory subunit 1B pseudogene 3	NS	NS	-2.21	0.0004	-2.3	0.0453
SKA3	Spindle and kinetochore associated complex subunit 3	NS	NS	-2.38	0.0008	-2.06	0.0019
PPP2R1B	Protein phosphatase 2, regulatory subunit A, beta	NS	NS	2.74	1.65E-05	2.87	6.97E-05
CDKN1B	Cyclin-dependent kinase inhibitor 1B	NS	NS	3.84	7.47E-06	2.13	0.0368
PPP2R5B	Protein phosphatase 2, regulatory subunit B, beta	4.75	0.0207	3.04	0.0002	NS	NS
CDKL5	Cyclin-dependent kinase-like 5	2.21	0.0173	2.22	0.0007	NS	NS

CKS1B	CDC28 protein kinase regulatory subunit 1B	-2.7	0.0202	-2.4	0.0002	NS	NS
NDC80	Kinetochore complex component	NS	NS	NS	NS	-2.19	0.0098
PRC1	Protein regulator of cytokinesis 1	NS	NS	NS	NS	-2.02	0.001
CCNB1	Cyclin B1	NS	NS	NS	NS	-2.59	0.004
CENPI	Centromere protein I	NS	NS	NS	NS	-2.13	0.0093
CDK6	Cyclin-dependent kinase 6	-5.26	3.41E-05	NS	NS	NS	NS
BUB1B	mitotic checkpoint ser/thr kinase B	-2.56	0.0067	NS	NS	NS	NS
CDKN3	Cyclin-dependent kinase inhibitor 3	-2	0.0284	NS	NS	NS	NS
CCNY	Cyclin Y	-2.5	0.0008	NS	NS	NS	NS
ANAPC11	Anaphase promoting complex subunit 11	-2.16	0.0005	NS	NS	NS	NS
MKI67	Ki67	-2.04	0.0374	NS	NS	NS	NS
CCNJL	cyclin J-like	2.13	0.0338	NS	NS	NS	NS
PAK4	p21 protein (Cdc42/Rac)-activated kinase 4	-2.05	0.0005	NS	NS	NS	NS
CDCA7	cell division cycle associated 7	-2.22	0.0008	NS	NS	NS	NS
CDCA2	cell division cycle associated 2	-2.48	0.0006	NS	NS	NS	NS

CDCA3	cell division cycle associated 3	-2.75	0.0143	NS	NS	NS	NS
CDK5	Cyclin-dependent kinase 5	NS	NS	-2.78	0.0003	NS	NS
CDKN1A	Cyclin-dependent kinase inhibitor 1A (p21, Cip1)	NS	NS	6.94	8.41E-06	NS	NS
ANAPC1	Anaphase promoting complex subunit 1	NS	NS	-2.5	0.0015	NS	NS
BRCA1	Breast cancer type 1 susceptibility protein	NS	NS	-2.7	0.0013	NS	NS
CDK2	Cyclin-dependent kinase 2	NS	NS	-3.08	0.0315	NS	NS
PLK4	Polo-like kinase 4	NS	NS	-2.83	0.0037	NS	NS
CENPM	Centromere protein M	NS	NS	-2.2	0.0049	NS	NS
DSCC1	DNA replication and sister chromatid cohesion 1	NS	NS	-2.27	0.0311	NS	NS
CCNG2	Cyclin G2	NS	NS	5.14	0.0019	NS	NS
CDKN2C	Cyclin-dependent kinase inhibitor 2C	NS	NS	2.51	0.0032	NS	NS
CDKL4	cyclin-dependent kinase-like 4	NS	NS	2.36	0.0025	NS	NS
CDK19	cyclin-dependent kinase 19	NS	NS	2.18	0.0431	NS	NS
CDKL1	cyclin-dependent kinase-like 1	NS	NS	-2.47	0.0001	NS	NS

	(CDC2-related kinase)						
CDK5	cyclin-dependent kinase 5	NS	NS	-2.78	0.0003	NS	NS
CDCA4	cell division cycle associated 4	NS	NS	-2.92	0.0065	NS	NS
CENPB	centromere protein B	NS	NS	-2.02	0.0153	NS	NS
CENPN	centromere protein N	NS	NS	-2.16	0.0081	NS	NS
CENPP	centromere protein P	NS	NS	-2.23	0.0001	NS	NS

Appendix 3.5: Expression graphs of genes that show different behaviour upon ELF3 knockdown between BPH-1 and PC3 cells from gene expression microarray. Norm = siSCR, kd = siELF3. Graphs generated by Alastair Droop.

A

(i)

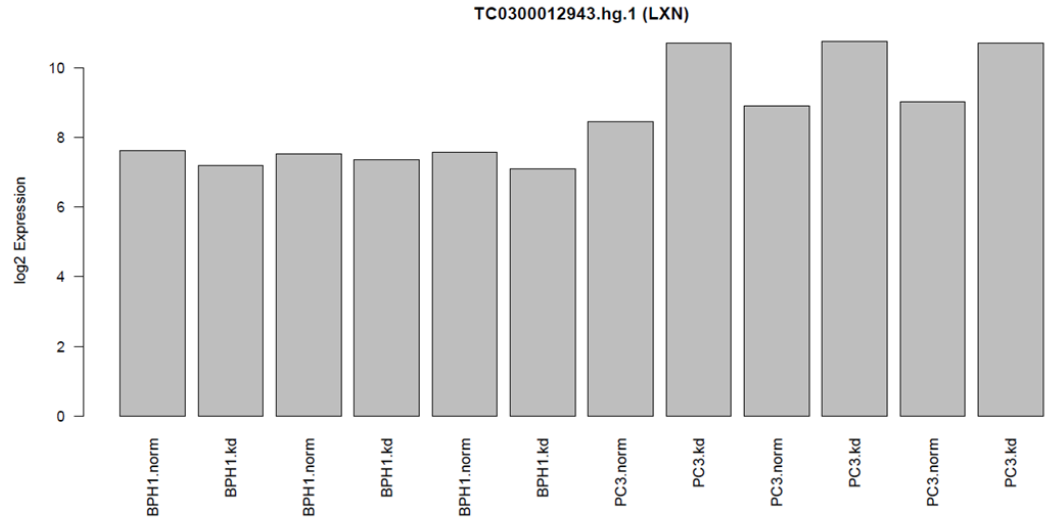

(ii)

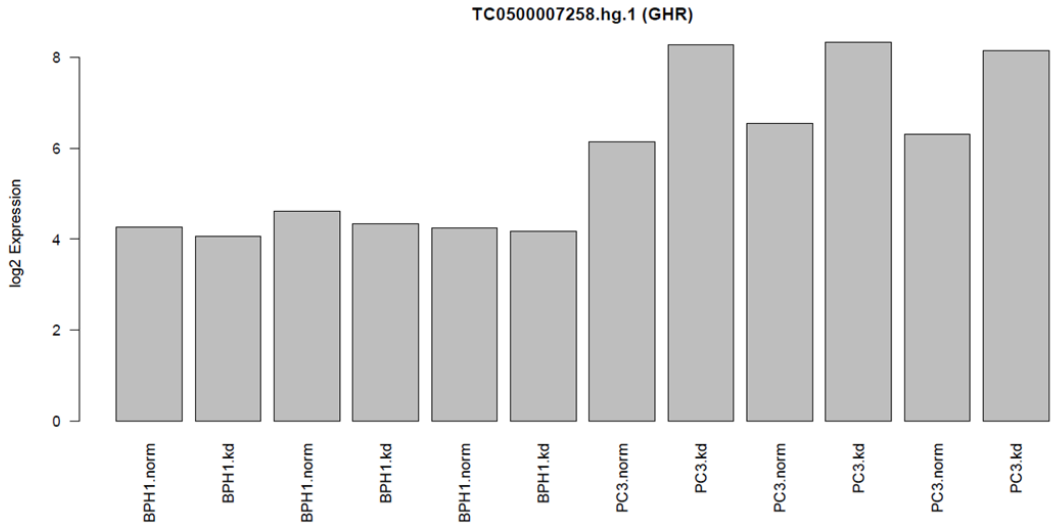

(iii)

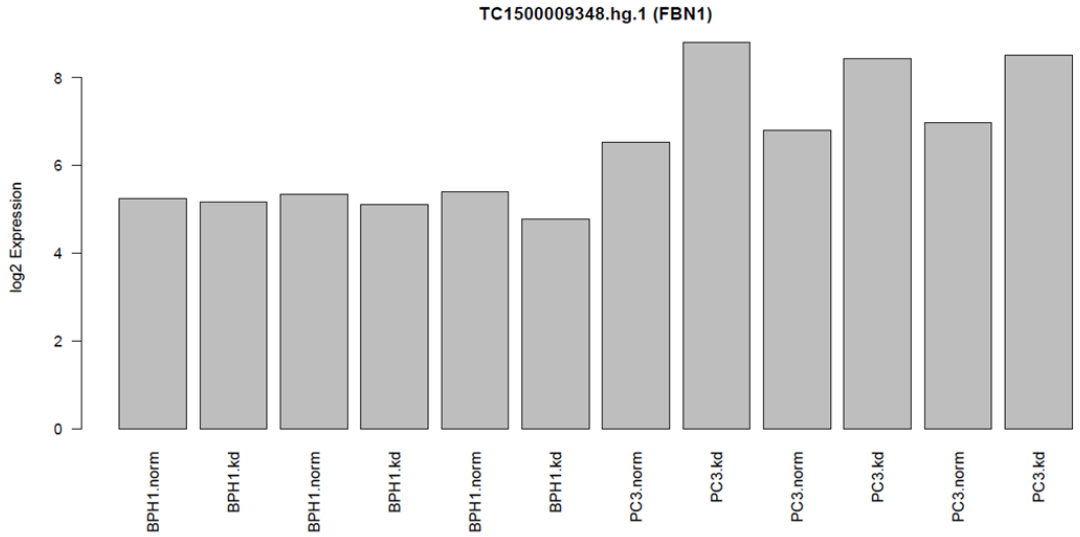
TC1500009348.hg.1 (FBN1)
log2 Expression
0
2
4
6
8
BPH1.norm
BPH1.kd
BPH1.norm
BPH1.kd
BPH1.norm
BPH1.kd
PC3.norm
PC3.kd
PC3.norm
PC3.kd
PC3.norm
PC3.kd

(iv)

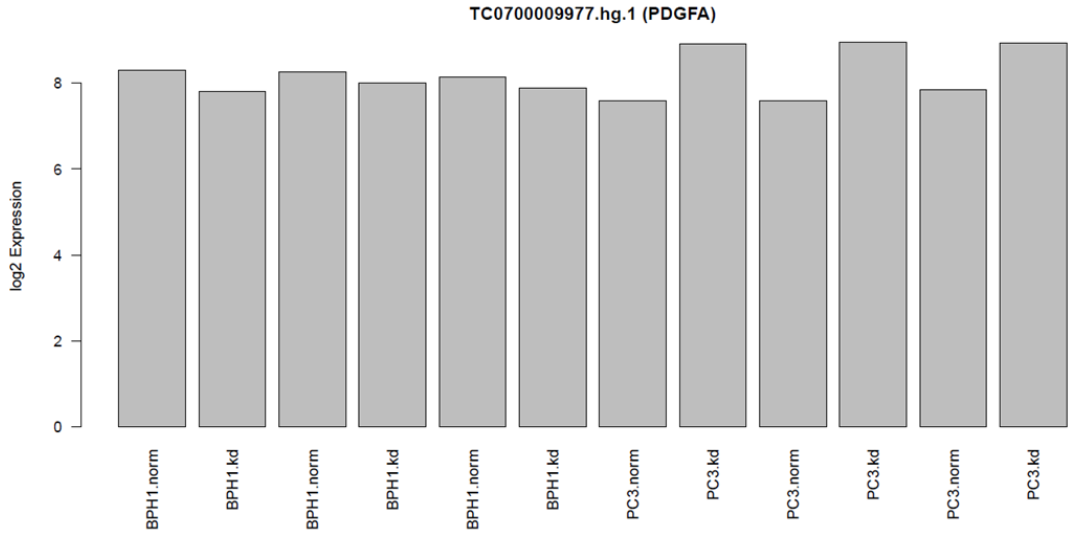
TC0700009977.hg.1 (PDGFA)
log2 Expression
0
2
4
6
8
BPH1.norm
BPH1.kd
BPH1.norm
BPH1.kd
BPH1.norm
BPH1.kd
PC3.norm
PC3.kd
PC3.norm
PC3.kd
PC3.norm
PC3.kd

(v)

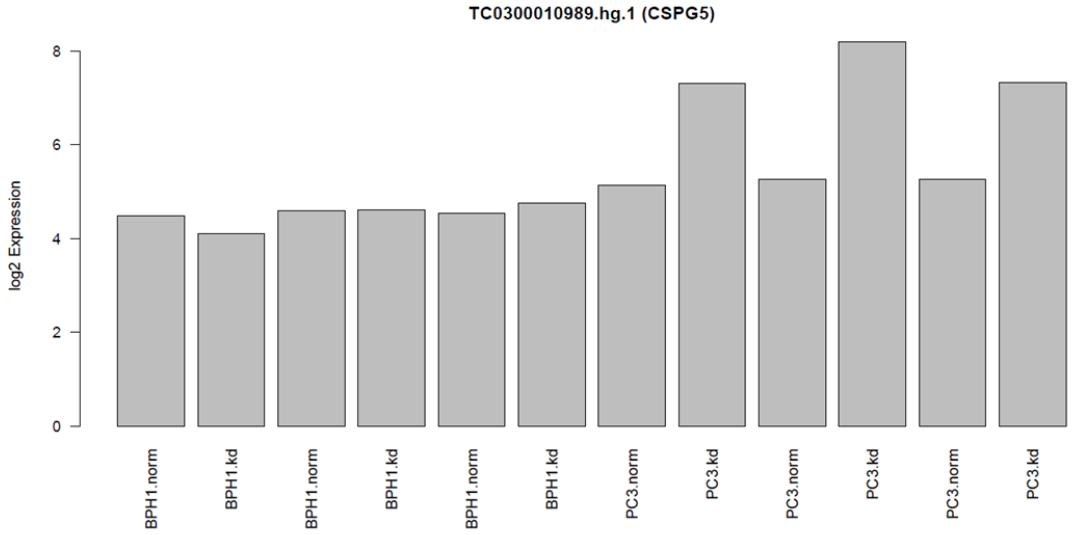
TC0300010989.hg.1 (CSPG5)
log2 Expression
0
2
4
6
8
BPH1.norm
BPH1.kd
BPH1.norm
BPH1.kd
BPH1.norm
BPH1.kd
PC3.norm
PC3.kd
PC3.norm
PC3.kd
PC3.norm
PC3.kd

(vi)

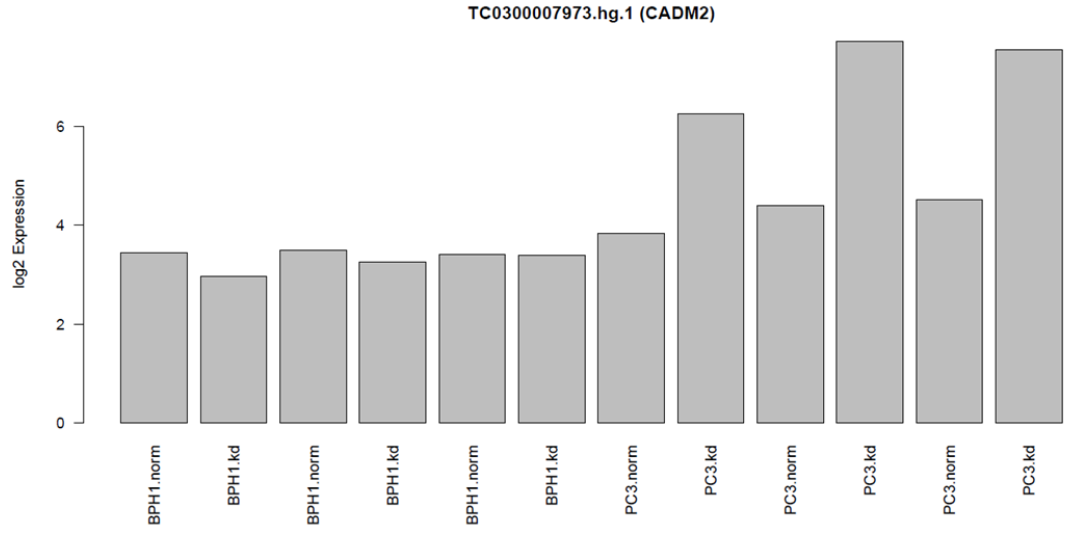
TC0300007973.hg.1 (CADM2)
log2 Expression
0
2
4
6
BPH1.norm
BPH1.kd
BPH1.norm
BPH1.kd
BPH1.norm
BPH1.kd
PC3.norm
PC3.kd
PC3.norm
PC3.kd
PC3.norm
PC3.kd

(vii)

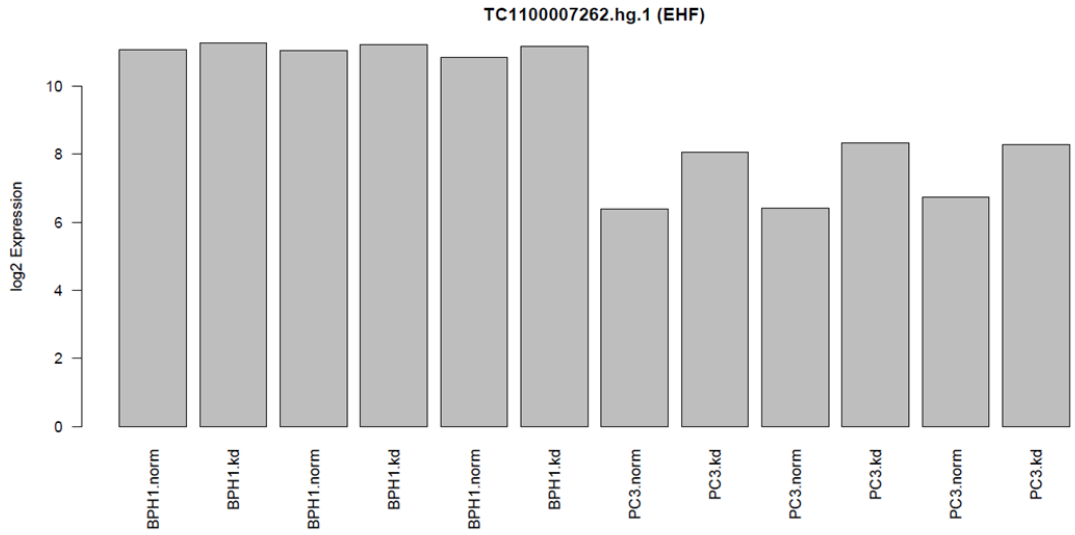
TC1100007262.hg.1 (EHF)
log2 Expression
0
2
4
6
8
10
BPH1.norm
BPH1.kd
BPH1.norm
BPH1.kd
BPH1.norm
BPH1.kd
PC3.norm
PC3.kd
PC3.norm
PC3.kd
PC3.norm
PC3.kd

(viii)

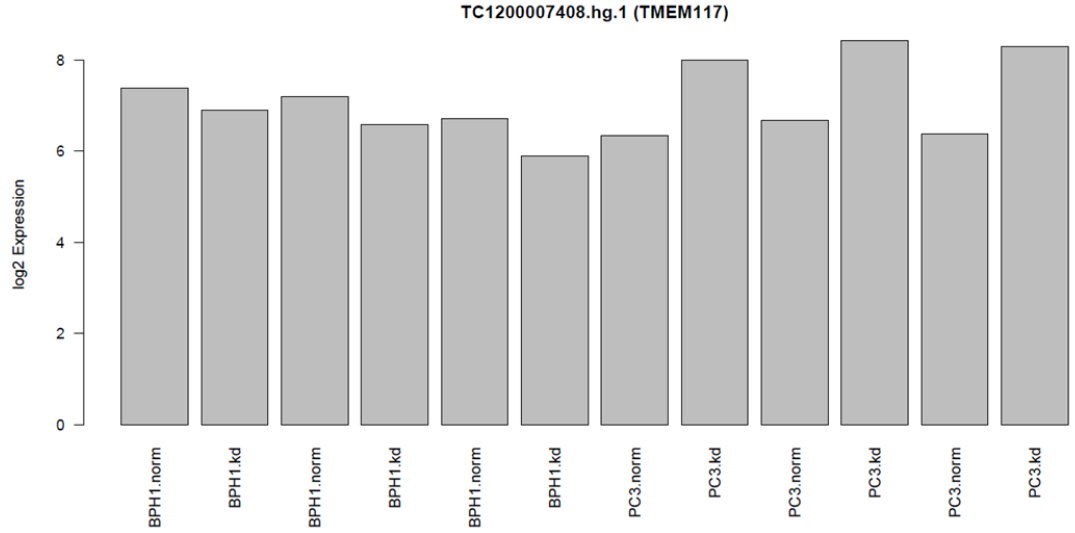
TC1200007408.hg.1 (TMEM117)
log2 Expression
0
2
4
6
8
BPH1.norm
BPH1.kd
BPH1.norm
BPH1.kd
BPH1.norm
BPH1.kd
PC3.norm
PC3.kd
PC3.norm
PC3.kd
PC3.norm
PC3.kd

(ix)

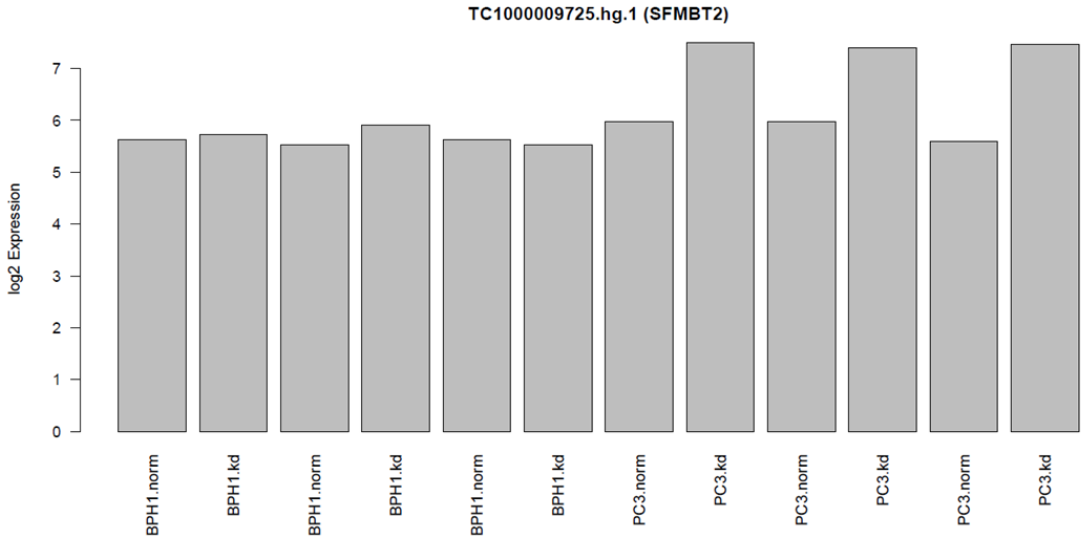
TC1000009725.hg.1 (SFMBT2)
log2 Expression
0
1
2
3
4
5
6
7
BPH1.norm
BPH1.kd
BPH1.norm
BPH1.kd
BPH1.norm
BPH1.kd
PC3.norm
PC3.kd
PC3.norm
PC3.kd
PC3.norm
PC3.kd

(x)

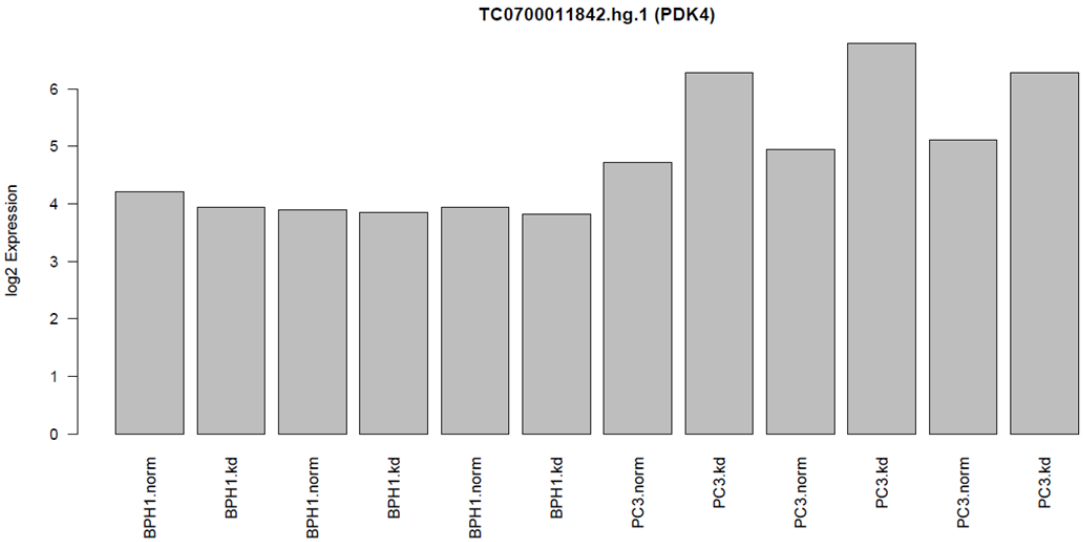
TC0700011842.hg.1 (PDK4)
log2 Expression
0
1
2
3
4
5
6
BPH1.norm
BPH1.kd
BPH1.norm
BPH1.kd
BPH1.norm
BPH1.kd
PC3.norm
PC3.kd
PC3.norm
PC3.kd
PC3.norm
PC3.kd

(xi)

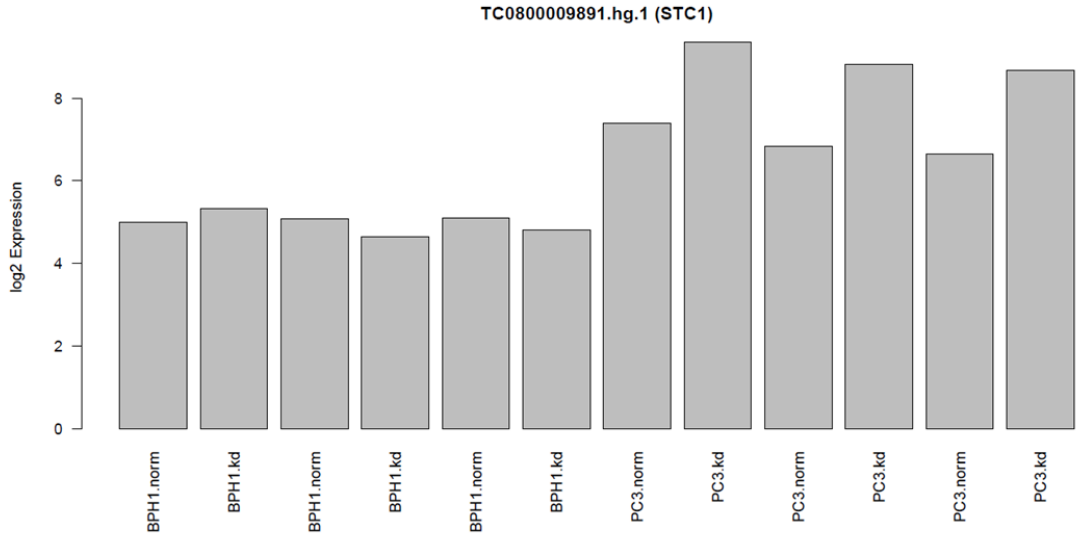
TC0800009891.hg.1 (STC1)
log2 Expression
0
2
4
6
8
BPH1.norm
BPH1.kd
BPH1.norm
BPH1.kd
BPH1.norm
BPH1.kd
PC3.norm
PC3.kd
PC3.norm
PC3.kd
PC3.norm
PC3.kd

(xii)

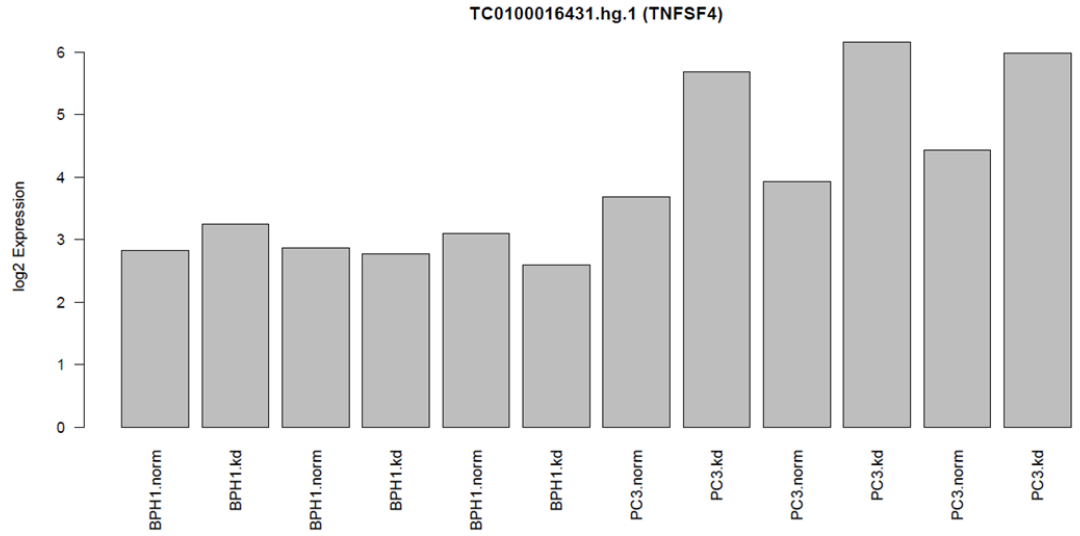
TC0100016431.hg.1 (TNFSF4)
log2 Expression
0
1
2
3
4
5
6
BPH1.norm
BPH1.kd
BPH1.norm
BPH1.kd
BPH1.norm
BPH1.kd
PC3.norm
PC3.kd
PC3.norm
PC3.kd
PC3.norm
PC3.kd

Abbreviations

3D-CRT	Three-dimensional conformal radiation therapy
ADT	Androgen-deprivation therapy
AML	Acute myeloid leukaemia
APL	Acute promyelotic leukaemia
AR	Androgen receptor
ARB	Angiotensin II type I receptor blocker
ARE	Androgen response elements
BCA	Bicinchoninic acid assay
BM	Basement membrane
bp	Base pairs
BPE	Bovine pituitary extract
BPH	Benign prostatic hyperplasia
BSA	Bovine serum albumin
CAF	Cancer-associated fibroblasts
CARN	Castration-resistant Nkx3.1-expressing cells
CB	Committed basal
cDNA	Complementary DNA
ChIP	Chromatin immunoprecipitation
ChrA	Chromogranin A
CK	Cytokeratin
CML	Chronic myeloid leukaemia
Co-IP	Co-immunoprecipitation
CPPS	Chronic pelvic pain syndrome
CRC	Colorectal cancer
CRPC	Castration-resistant prostate cancer
CSC	Cancer stem cell

C_T	Threshold cycle
D10	DMEM + 10% FCS + 2 mM L-Glutamine
DAB	Diaminobenzidene
DAPI	4',6-diamidino-2-phenylindole
DAVID	Database for Annotation, Visualization and Integrated Discovery
DDT	Dithiothreitol
DES	Diethylstilbestrol
DHT	Dihydrotestosterone
DMEM	Dulbecco's Modified Eagle's Medium
DMSO	Dimethyl sulfoxide
DNA	Deoxyribonucleic acid
dNTP	Deoxyribonucleotide triphosphate
E.coli	Escherichia coli
EBRT	External beam radiation therapy
ECL	Enhanced chemiluminescence
EDTA	Ethylenediaminetetraacetic acid
EGF	Epidermal growth factor
EGTA	Ethylene glycol-bis(β-aminoethyl ether
EMSA	Electrophoretic mobility shift assay
EMT	Epithelial-to-mesenchymal transition
ER	Oestrogen receptor
ETS	E26 transformation-specific
FACS	Fluorescence activated cell sorting
FCS	Foetal calf serum
FDA	U.S. Food and Drug Administration
FISH	Fluorescent in situ hybridisation
g	Gram

GnRH	Gonadotrophin-releasing hormone
GO	Gene ontology
GUS	β-glucoronidase
H7	Ham's F-12 + 7% FCS + 2 mM L-Glutamine
HDAC	Histone deacetylase
HIER	Heat-induced epitope retrieval
HIFU	High-intensity focused ultrasound
HMW-CK	High molecular weight cytokeratin
HNSCC	Head and neck squamous cell carcinoma
Hr	Hour
HRP	Horseradish peroxidase
IAP	Inhibitor of apoptosis
ICC	Immunocytochemistry
IHC	Immunohistochemistry
IMRT	Image-guided intensity-modulated radiation therapy
K2	KSFM media + 2% FCS + 2 mM L-Glutamine + BPE + EGF
kDa	Kilo Dalton
KSFM	Keratinocyte Serum-Free Medium
L	Left lobe (in relation to primary samples)
LB	Lysogeny broth
MACS	Magnetic-activated cell sorting
MDS	Multidimensional scaling
mElf3	Murine ELF3 homologue
MET	Mesenchymal-to-epithelial transition
mg	Milligram
$MgCl_2$	Magnesium chloride
ml	Millilitre

mM	Millimolar
MRI	Magnetic resonance imaging
mRNA	Messenger RNA
$Na_4P_2O_7$	Sodium pyrophosphate tetrabasic
NaCl	Sodium chloride
NaF	Sodium fluoride
$NaVO_4$	Sodium orthovanadate
NE	Neuroendocrine
NES	Nuclear export signal
ng	Nanogram
NLS	Nuclear localisation signal
nm	Nanometre
NSCLC	Non-small cell lung cancer
NSE	Neurone specific enolase
PAGE	Polyacrylamide gel electrophoresis
PAP	Prostatic acid phosphatase
PBS	Phosphate buffered saline
PCa	Prostate cancer
PCR	Polymerase chain reaction
PDEF	Prostate-derived ETS factor
PDT	Photodynamic therapy
PFA	Paraformaldehyde
PHH3	Phospho-histone H3
PIN	Prostatic intraepithelial neoplasia
PNT	Pointed domain
PrECs	Normal prostate epithelial cells (cell line)
PSA	Prostate specific antigen

qRT-PCR	Quantitative reverse-transcriptase PCR
R	Right lobe (in relation to primary samples)
R10	RPMI + 10% FCS + 2 mM L-Glutamine
R5	RPMI + 5% FCS + 2 mM L-Glutamine
RIPA	Radioimmunoprecipitation assay buffer
RNA	Ribonucleic acid
ROS	reactive oxygen species
RP	radical prostatectomy
RP	Replated
RPM	Revolutions per minute
RPMI	Roswell Park Memorial Institute medium
RT	Reverse transcriptase
SC	Stem cell
SCM	Stem cell media
SDS	Sodium dodecyl sulfate
siELF3	ELF3 siRNA
siRNA	Small interfering RNA
siSCR	Scrambled siRNA
T-25	25cm^2 tissue culture flask
T-75	75cm^2 tissue culture flask
TA	Transit amplifying
TAC	Transcriptome analysis software
TAE	Tris base + acetic acid + EDTA buffer
TBP	TATA-binding protein
TBS	Tris-buffered saline
TBST	TBS + Tween-20
TFO	Triplex-forming oligonucleotides

TMA	Tissue microarray
TRUS	Transrectal ultrasound
TURP	Transurethral resection of the prostate
v/v	Volume per volume
w/v	Weight per volume
WHTH	Winged-helix-turn-helix
WT	Wildtype
µg	Microgram
µl	Microlitre
µm	Micrometre
µM	Micromolar

References

ABDULMAJEED, A. A., DALLEY, A. J. & FARAH, C. S. 2013. Loss of ELF3 immunoexpression is useful for detecting oral squamous cell carcinoma but not for distinguishing between grades of epithelial dysplasia. *Ann Diagn Pathol,* 17**,** 331-40.

ABRAHAMSSON, P. A. 1999. Neuroendocrine cells in tumour growth of the prostate. *Endocr Relat Cancer,* 6**,** 503-19.

ADAMO, P. & LADOMERY, M. R. 2015. The oncogene ERG: a key factor in prostate cancer. *Oncogene*.

AGARWAL, S., HYNES, P. G., TILLMAN, H. S., LAKE, R., ABOU-KHEIR, W. G., FANG, L., CASEY, O. M., AMERI, A. H., MARTIN, P. L., YIN, J. J., IAQUINTA, P. J., KARTHAUS, W. R., CLEVERS, H. C., SAWYERS, C. L. & KELLY, K. 2015. Identification of Different Classes of Luminal Progenitor Cells within Prostate Tumors. *Cell Rep*.

AKASHI, T., KOIZUMI, K., TSUNEYAMA, K., SAIKI, I., TAKANO, Y. & FUSE, H. 2008. Chemokine receptor CXCR4 expression and prognosis in patients with metastatic prostate cancer. *Cancer Sci,* 99**,** 539-42.

ALBINO, D., CIVENNI, G., ROSSI, S., MITRA, A., CATAPANO, C. V. & CARBONE, G. M. 2016. The ETS factor ESE3/EHF represses IL-6 preventing STAT3 activation and expansion of the prostate cancer stem-like compartment. *Oncotarget,* 7**,** 76756-76768.

ALBINO, D., LONGONI, N., CURTI, L., MELLO-GRAND, M., PINTON, S., CIVENNI, G., THALMANN, G., D'AMBROSIO, G., SARTI, M., SESSA, F., CHIORINO, G., CATAPANO, C. V. & CARBONE, G. M. 2012. ESE3/EHF controls epithelial cell differentiation and its loss leads to prostate tumors with mesenchymal and stem-like features. *Cancer Res,* 72**,** 2889-900.

ALI, S. A., JUSTILIEN, V., JAMIESON, L., MURRAY, N. R. & FIELDS, A. P. 2016. Protein Kinase Ciota Drives a NOTCH3-dependent Stem-like Phenotype in Mutant KRAS Lung Adenocarcinoma. *Cancer Cell,* 29**,** 367-78.

ALIPOV, G., NAKAYAMA, T., ITO, M., KAWAI, K., NAITO, S., NAKASHIMA, M., NIINO, D. & SEKINE, I. 2005. Overexpression of Ets-1 proto-oncogene in latent and clinical prostatic carcinomas. *Histopathology,* 46**,** 202-8.

ALISON, M. R., LIN, W. R., LIM, S. M. & NICHOLSON, L. J. 2012. Cancer stem cells: in the line of fire. *Cancer Treat Rev,* 38**,** 589-98.

ALVERO, A. B., FU, H. H., HOLMBERG, J., VISINTIN, I., MOR, L., MARQUINA, C. C., OIDTMAN, J., SILASI, D. A. & MOR, G. 2009. Stem-like ovarian cancer cells can serve as tumor vascular progenitors. *Stem Cells,* 27**,** 2405-13.

ANASSI, E. & NDEFO, U. A. 2011. Sipuleucel-T (provenge) injection: the first immunotherapy agent (vaccine) for hormone-refractory prostate cancer. *P t,* 36**,** 197-202.

ANDRIOLE, G. L., BOSTWICK, D. G., BRAWLEY, O. W., GOMELLA, L. G., MARBERGER, M., MONTORSI, F., PETTAWAY, C. A., TAMMELA, T. L., TELOKEN, C., TINDALL, D. J., SOMERVILLE, M. C., WILSON, T. H., FOWLER, I. L. & RITTMASTER, R. S. 2010. Effect of dutasteride on the risk of prostate cancer. *N Engl J Med,* 362**,** 1192-202.

ARCHER, L. K., FRAME, F. M. & MAITLAND, N. J. 2017. Stem cells and the role of ETS transcription factors in the differentiation hierarchy of normal and malignant prostate epithelium. *J Steroid Biochem Mol Biol,* 166**,** 68-83.

ARORA, R., KOCH, M. O., EBLE, J. N., ULBRIGHT, T. M., LI, L. & CHENG, L. 2004. Heterogeneity of Gleason grade in multifocal adenocarcinoma of the prostate. *Cancer,* 100**,** 2362-6.

ASADA, S., CHOI, Y. & UESUGI, M. 2003. A gene-expression inhibitor that targets an alpha-helix-mediated protein interaction. *J Am Chem Soc,* 125**,** 4992-3.

ATTARD, G., BORRE, M., GURNEY, H., LORIOT, Y., ANDRESEN-DANIIL, C., KALLEDA, R., PHAM, T. & TAPLIN, M. E. 2018. Abiraterone Alone or in Combination With Enzalutamide in Metastatic Castration-Resistant Prostate Cancer With Rising Prostate-Specific Antigen During Enzalutamide Treatment. *J Clin Oncol,* 36**,** 2639-2646.

ATTARD, G., CLARK, J., AMBROISINE, L., FISHER, G., KOVACS, G., FLOHR, P., BERNEY, D., FOSTER, C. S., FLETCHER, A., GERALD, W. L., MOLLER, H., REUTER, V., DE BONO, J. S., SCARDINO, P., CUZICK, J. & COOPER, C. S. 2008. Duplication of the fusion of TMPRSS2 to ERG sequences identifies fatal human prostate cancer. *Oncogene,* 27**,** 253-63.

AUMULLER, G. 1991. Postnatal development of the prostate. *Bull Assoc Anat (Nancy),* 75**,** 39-42.

BAHL, A., OUDARD, S., TOMBAL, B., OZGUROGLU, M., HANSEN, S., KOCAK, I., GRAVIS, G., DEVIN, J., SHEN, L., DE BONO, J. S. & SARTOR, A. O. 2013. Impact of cabazitaxel on 2-year survival and palliation of tumour-related pain in men with metastatic castration-resistant prostate cancer treated in the TROPIC trial. *Ann Oncol,* 24**,** 2402-8.

BANG, Y. J., PIRNIA, F., FANG, W. G., KANG, W. K., SARTOR, O., WHITESELL, L., HA, M. J., TSOKOS, M., SHEAHAN, M. D., NGUYEN, P., NIKLINSKI, W. T., MYERS, C. E. & TREPEL, J. B. 1994. Terminal neuroendocrine differentiation of human prostate carcinoma cells in response to increased intracellular cyclic AMP. *Proc Natl Acad Sci U S A,* 91**,** 5330-4.

BAO, S., WU, Q., MCLENDON, R. E., HAO, Y., SHI, Q., HJELMELAND, A. B., DEWHIRST, M. W., BIGNER, D. D. & RICH, J. N. 2006. Glioma stem cells promote radioresistance by preferential activation of the DNA damage response. *Nature,* 444**,** 756-60.

BARRON, D. A. & ROWLEY, D. R. 2012. The reactive stroma microenvironment and prostate cancer progression. *Endocr Relat Cancer,* 19**,** R187-204.

BARROS-SILVA, J. D., PAULO, P., BAKKEN, A. C., CERVEIRA, N., LOVF, M., HENRIQUE, R., JERONIMO, C., LOTHE, R. A., SKOTHEIM, R. I. & TEIXEIRA, M. R. 2013. Novel 5' fusion partners of ETV1 and ETV4 in prostate cancer. *Neoplasia,* 15**,** 720-6.

BARTEL, F. O., HIGUCHI, T. & SPYROPOULOS, D. D. 2000. Mouse models in the study of the Ets family of transcription factors. *Oncogene,* 19**,** 6443-54.

BAUMAN, G., RUMBLE, R. B., CHEN, J., LOBLAW, A. & WARDE, P. 2012. Intensity-modulated radiotherapy in the treatment of prostate cancer. *Clin Oncol (R Coll Radiol),* 24**,** 461-73.

BECK, B., DRIESSENS, G., GOOSSENS, S., YOUSSEF, K. K., KUCHNIO, A., CAAUWE, A., SOTIROPOULOU, P. A., LOGES, S., LAPOUGE, G., CANDI, A., MASCRE, G., DROGAT, B., DEKONINCK, S., HAIGH, J. J., CARMELIET, P. & BLANPAIN, C. 2011. A vascular niche and a VEGF-Nrp1 loop regulate the initiation and stemness of skin tumours. *Nature,* 478**,** 399-403.

BELLARDITA, L., VALDAGNI, R., VAN DEN BERGH, R., RANDSDORP, H., REPETTO, C., VENDERBOS, L. D., LANE, J. A. & KORFAGE, I. J. 2014. How Does Active Surveillance for Prostate Cancer Affect Quality of Life? A Systematic Review. *Eur Urol*.

BELTRAN, H., BEER, T. M., CARDUCCI, M. A., DE BONO, J., GLEAVE, M., HUSSAIN, M., KELLY, W. K., SAAD, F., STERNBERG, C., TAGAWA, S. T. & TANNOCK, I. F. 2011. New therapies for castration-resistant prostate cancer: efficacy and safety. *Eur Urol,* 60**,** 279-90.

BERRUTI, A., MOSCA, A., PORPIGLIA, F., BOLLITO, E., TUCCI, M., VANA, F., CRACCO, C., TORTA, M., RUSSO, L., CAPPIA, S., SAINI, A., ANGELI, A., PAPOTTI, M., SCARPA, R. M. & DOGLIOTTI, L. 2007. Chromogranin A expression in patients with hormone naive prostate cancer predicts the development of hormone refractory disease. *J Urol,* 178**,** 838-43; quiz 1129.

BERRY, P. A., MAITLAND, N. J. & COLLINS, A. T. 2008. Androgen receptor signalling in prostate: effects of stromal factors on normal and cancer stem cells. *Mol Cell Endocrinol,* 288**,** 30-7.

BERTHON, P., CUSSENOT, O., HOPWOOD, L., LEDUC, A. & MAITLAND, N. 1995. Functional expression of sv40 in normal human prostatic epithelial and fibroblastic cells - differentiation pattern of nontumorigenic cell-lines. *Int J Oncol,* 6**,** 333-43.

BIRNIE, R., BRYCE, S. D., ROOME, C., DUSSUPT, V., DROOP, A., LANG, S. H., BERRY, P. A., HYDE, C. F., LEWIS, J. L., STOWER, M. J., MAITLAND, N. J. & COLLINS, A. T. 2008. Gene expression profiling of human prostate cancer stem cells reveals a pro-inflammatory phenotype and the importance of extracellular matrix interactions. *Genome Biology,* 9.

BISSON, I. & PROWSE, D. M. 2009. WNT signaling regulates self-renewal and differentiation of prostate cancer cells with stem cell characteristics. *Cell Res,* 19**,** 683-97.

BOCK, M., HINLEY, J., SCHMITT, C., WAHLICHT, T., KRAMER, S. & SOUTHGATE, J. 2014. Identification of ELF3 as an early transcriptional regulator of human urothelium. *Dev Biol,* 386**,** 321-30.

BOSTANCI, Y., KAZZAZI, A., MOMTAHEN, S., LAZE, J. & DJAVAN, B. 2013. Correlation between benign prostatic hyperplasia and inflammation. *Curr Opin Urol,* 23**,** 5-10.

BOSTWICK, D. G., LIU, L., BRAWER, M. K. & QIAN, J. 2004. High-grade prostatic intraepithelial neoplasia. *Rev Urol,* 6**,** 171-9.

BOSTWICK, D. G., SHAN, A., QIAN, J., DARSON, M., MAIHLE, N. J., JENKINS, R. B. & CHENG, L. 1998. Independent origin of multiple foci of prostatic intraepithelial neoplasia: comparison with matched foci of prostate carcinoma. *Cancer,* 83**,** 1995-2002.

BOWEN, C., BUBENDORF, L., VOELLER, H. J., SLACK, R., WILLI, N., SAUTER, G., GASSER, T. C., KOIVISTO, P., LACK, E. E., KONONEN, J., KALLIONIEMI, O. P. & GELMANN, E. P. 2000. Loss of NKX3.1 expression in human prostate cancers correlates with tumor progression. *Cancer Res,* 60**,** 6111-5.

BOYLE, P. 1994. New insights into the epidemiology and natural history of benign prostatic hyperplasia. *Prog Clin Biol Res,* 386**,** 3-18.

BRACARDA, S., LOGOTHETIS, C., STERNBERG, C. N. & OUDARD, S. 2011. Current and emerging treatment modalities for metastatic castration-resistant prostate cancer. *BJU Int,* 107 Suppl 2**,** 13-20.

BREMBECK, F. H., OPITZ, O. G., LIBERMANN, T. A. & RUSTGI, A. K. 2000. Dual function of the epithelial specific ets transcription factor, ELF3, in modulating differentiation. *Oncogene,* 19**,** 1941-9.

BROWN, C., GASPAR, J., PETTIT, A., LEE, R., GU, X., WANG, H., MANNING, C., VOLAND, C., GOLDRING, S. R., GOLDRING, M. B., LIBERMANN, T. A., GRAVALLESE, E. M. & OETTGEN, P. 2004. ESE-1 is a novel transcriptional mediator of angiopoietin-1 expression in the setting of inflammation. *J Biol Chem,* 279**,** 12794-803.

BUBENDORF, L., SCHOPFER, A., WAGNER, U., SAUTER, G., MOCH, H., WILLI, N., GASSER, T. C. & MIHATSCH, M. J. 2000. Metastatic patterns of prostate cancer: an autopsy study of 1,589 patients. *Hum Pathol,* 31**,** 578-83.

BUCHWALTER, G., HICKEY, M. M., CROMER, A., SELFORS, L. M., GUNAWARDANE, R. N., FRISHMAN, J., JESELSOHN, R., LIM, E., CHI, D., FU, X., SCHIFF, R., BROWN, M. & BRUGGE, J. S. 2013. PDEF promotes luminal differentiation and acts as a survival factor for ER-positive breast cancer cells. *Cancer Cell,* 23**,** 753-67.

BUCK, M. J. & LIEB, J. D. 2004. ChIP-chip: considerations for the design, analysis, and application of genome-wide chromatin immunoprecipitation experiments. *Genomics,* 83**,** 349-60.

BUL, M., ZHU, X., VALDAGNI, R., PICKLES, T., KAKEHI, Y., RANNIKKO, A., BJARTELL, A., VAN DER SCHOOT, D. K., CORNEL, E. B., CONTI, G. N., BOEVE, E. R., STAERMAN, F., VIS-MATERS, J. J., VERGUNST, H., JASPARS, J. J., STROLIN, P., VAN MUILEKOM, E., SCHRODER, F. H., BANGMA, C. H. & ROOBOL, M. J. 2013. Active surveillance for low-risk prostate cancer worldwide: the PRIAS study. *Eur Urol,* 63**,** 597-603.

CABRAL, A., FISCHER, D. F., VERMEIJ, W. P. & BACKENDORF, C. 2003. Distinct functional interactions of human Skn-1 isoforms with Ese-1 during keratinocyte terminal differentiation. *J Biol Chem,* 278**,** 17792-9.

CAI, J., KANDAGATLA, P., SINGAREDDY, R., KROPINSKI, A., SHENG, S., CHER, M. L. & CHINNI, S. R. 2010. Androgens Induce Functional CXCR4 through ERG Factor Expression in TMPRSS2-ERG Fusion-Positive Prostate Cancer Cells. *Transl Oncol,* 3**,** 195-203.

CAI, T., MAZZOLI, S., MEACCI, F., BODDI, V., MONDAINI, N., MALOSSINI, G. & BARTOLETTI, R. 2011. Epidemiological features and resistance pattern in uropathogens isolated from chronic bacterial prostatitis. *J Microbiol,* 49**,** 448-54.

CANCER RESEARCH UK. 2016. *Prostate cancer statistics* [Online]. Available: https://www.cancerresearchuk.org/health-professional/cancer-statistics/statistics-by-cancer-type/prostate-cancer#heading-Zero [Accessed 11th Sept 2018].

CARBONE, G. M., MCGUFFIE, E. M., COLLIER, A. & CATAPANO, C. V. 2003. Selective inhibition of transcription of the Ets2 gene in prostate cancer cells by a triplex-forming oligonucleotide. *Nucleic Acids Res,* 31**,** 833-43.

CARBONE, G. M., NAPOLI, S., VALENTINI, A., CAVALLI, F., WATSON, D. K. & CATAPANO, C. V. 2004. Triplex DNA-mediated downregulation of Ets2 expression results in growth inhibition and apoptosis in human prostate cancer cells. *Nucleic Acids Res,* 32**,** 4358-67.

CARVER, B. S., TRAN, J., CHEN, Z., CARRACEDO-PEREZ, A., ALIMONTI, A., NARDELLA, C., GOPALAN, A., SCARDINO, P. T., CORDON-CARDO, C., GERALD, W. & PANDOLFI, P. P. 2009a. ETS rearrangements and prostate cancer initiation. *Nature,* 457**,** E1; discussion E2-3.

CARVER, B. S., TRAN, J., GOPALAN, A., CHEN, Z., SHAIKH, S., CARRACEDO, A., ALIMONTI, A., NARDELLA, C., VARMEH, S., SCARDINO, P. T., CORDON-CARDO, C., GERALD, W. & PANDOLFI, P. P. 2009b. Aberrant ERG expression cooperates with loss of PTEN to promote cancer progression in the prostate. *Nat Genet,* 41**,** 619-24.

CASEY, O. M., FANG, L., HYNES, P. G., ABOU-KHEIR, W. G., MARTIN, P. L., TILLMAN, H. S., PETROVICS, G., AWWAD, H. O., WARD, Y., LAKE, R., ZHANG, L. & KELLY, K. 2012. TMPRSS2- driven ERG expression in vivo increases self-renewal and maintains expression in a castration resistant subpopulation. *PLoS One,* 7**,** e41668.

CASTRO, E., GOH, C., LEONGAMORNLERT, D., SAUNDERS, E., TYMRAKIEWICZ, M., DADAEV, T., GOVINDASAMI, K., GUY, M., ELLIS, S., FROST, D., BANCROFT, E., COLE, T., TISCHKOWITZ, M., KENNEDY, M. J., EASON, J., BREWER, C., EVANS, D. G., DAVIDSON, R., ECCLES, D., PORTEOUS, M. E., DOUGLAS, F.,

ADLARD, J., DONALDSON, A., ANTONIOU, A. C., KOTE-JARAI, Z., EASTON, D. F., OLMOS, D. & EELES, R. 2015. Effect of BRCA Mutations on Metastatic Relapse and Cause-specific Survival After Radical Treatment for Localised Prostate Cancer. *Eur Urol,* 68**,** 186-93.

CHANG, C. C., SHIEH, G. S., WU, P., LIN, C. C., SHIAU, A. L. & WU, C. L. 2008. Oct-3/4 expression reflects tumor progression and regulates motility of bladder cancer cells. *Cancer Res,* 68**,** 6281-91.

CHANG, H. H., CHEN, B. Y., WU, C. Y., TSAO, Z. J., CHEN, Y. Y., CHANG, C. P., YANG, C. R. & LIN, D. P. 2011. Hedgehog overexpression leads to the formation of prostate cancer stem cells with metastatic property irrespective of androgen receptor expression in the mouse model. *J Biomed Sci,* 18**,** 6.

CHEN, C., OUYANG, W., GRIGURA, V., ZHOU, Q., CARNES, K., LIM, H., ZHAO, G. Q., ARBER, S., KURPIOS, N., MURPHY, T. L., CHENG, A. M., HASSELL, J. A., CHANDRASHEKAR, V., HOFMANN, M. C., HESS, R. A. & MURPHY, K. M. 2005. ERM is required for transcriptional control of the spermatogonial stem cell niche. *Nature,* 436**,** 1030-4.

CHEN, X., MENG, Q., ZHAO, Y., LIU, M., LI, D., YANG, Y., SUN, L., SUI, G., CAI, L. & DONG, X. 2013. Angiotensin II type 1 receptor antagonists inhibit cell proliferation and angiogenesis in breast cancer. *Cancer Lett,* 328**,** 318-24.

CHENG, X. H., BLACK, M., USTIYAN, V., LE, T., FULFORD, L., SRIDHARAN, A., MEDVEDOVIC, M., KALINICHENKO, V. V., WHITSETT, J. A. & KALIN, T. V. 2014. SPDEF inhibits prostate carcinogenesis by disrupting a positive feedback loop in regulation of the Foxm1 oncogene. *PLoS Genet,* 10**,** e1004656.

CHEONG, H. S., LEE, H. C., PARK, B. L., KIM, H., JANG, M. J., HAN, Y. M., KIM, S. Y., KIM, Y. S. & SHIN, H. D. 2010. Epigenetic modification of retinoic acid-treated human embryonic stem cells. *BMB Rep,* 43**,** 830-5.

CHESS, A. 2012. Mechanisms and consequences of widespread random monoallelic expression. *Nat Rev Genet,* 13**,** 421-8.

CHETRAM, M. A., ODERO-MARAH, V. & HINTON, C. V. 2011. Loss of PTEN permits CXCR4-mediated tumorigenesis through ERK1/2 in prostate cancer cells. *Mol Cancer Res,* 9**,** 90-102.

CHIAO, J. W., HSIEH, T. C., XU, W., SKLAREW, R. J. & KANCHERLA, R. 1999. Development of human prostate cancer cells to neuroendocrine-like cells by interleukin-1. *Int J Oncol,* 15**,** 1033-7.

CHNG, K. R., CHANG, C. W., TAN, S. K., YANG, C., HONG, S. Z., SNG, N. Y. & CHEUNG, E. 2012. A transcriptional repressor co-regulatory network governing androgen response in prostate cancers. *Embo j,* 31**,** 2810-23.

CHUA, C. W., SHIBATA, M., LEI, M., TOIVANEN, R., BARLOW, L. J., BERGREN, S. K., BADANI, K. K., MCKIERNAN, J. M., BENSON, M. C., HIBSHOOSH, H. & SHEN, M. M. 2014. Single luminal epithelial progenitors can generate prostate organoids in culture. *Nat Cell Biol,* 16**,** 951-61, 1-4.

CLARK, J., ATTARD, G., JHAVAR, S., FLOHR, P., REID, A., DE-BONO, J., EELES, R., SCARDINO, P., CUZICK, J., FISHER, G., PARKER, M. D., FOSTER, C. S., BERNEY, D., KOVACS, G. & COOPER, C. S. 2008. Complex patterns of ETS gene alteration arise during cancer development in the human prostate. *Oncogene,* 27**,** 1993-2003.

CLARK, J., MERSON, S., JHAVAR, S., FLOHR, P., EDWARDS, S., FOSTER, C. S., EELES, R., MARTIN, F. L., PHILLIPS, D. H., CRUNDWELL, M., CHRISTMAS, T., THOMPSON, A., FISHER, C., KOVACS, G. & COOPER, C. S. 2007. Diversity of TMPRSS2-ERG fusion transcripts in the human prostate. *Oncogene,* 26**,** 2667-73.

COHEN, J. K. & MILLER, R. J. 1994. Thermal protection of urethra during cryosurgery of prostate. *Cryobiology,* 31**,** 313-6.

COLLINS, A. T., BERRY, P. A., HYDE, C., STOWER, M. J. & MAITLAND, N. J. 2005. Prospective identification of tumorigenic prostate cancer stem cells. *Cancer Res,* 65**,** 10946-51.

COLLINS, A. T., HABIB, F. K., MAITLAND, N. J. & NEAL, D. E. 2001. Identification and isolation of human prostate epithelial stem cells based on alpha(2)beta(1)-integrin expression. *J Cell Sci,* 114**,** 3865-72.

COOPER, C. S., EELES, R., WEDGE, D. C. & VAN LOO, P. 2015. Analysis of the genetic phylogeny of multifocal prostate cancer identifies multiple independent clonal expansions in neoplastic and morphologically normal prostate tissue. 47**,** 367-72.

CORDEIRO, E. R., CATHELINEAU, X., THUROFF, S., MARBERGER, M., CROUZET, S. & DE LA ROSETTE, J. J. 2012. High-intensity focused ultrasound (HIFU) for definitive treatment of prostate cancer. *BJU Int,* 110**,** 1228-42.

CROOK, J. 2011. The role of brachytherapy in the definitive management of prostate cancer. *Cancer Radiother,* 15**,** 230-7.

CUSSENOT, O., BERTHON, P., BERGER, R., MOWSZOWICZ, I., FAILLE, A., HOJMAN, F., TEILLAC, P., LE DUC, A. & CALVO, F. 1991. Immortalization of human adult normal prostatic epithelial cells by liposomes containing large T-SV40 gene. *J Urol,* 146**,** 881-6.

DAKHOVA, O., OZEN, M., CREIGHTON, C. J., LI, R., AYALA, G., ROWLEY, D. & ITTMANN, M. 2009. Global gene expression analysis of reactive stroma in prostate cancer. *Clin Cancer Res,* 15**,** 3979-89.

DE BONO, J. S., LOGOTHETIS, C. J., MOLINA, A., FIZAZI, K., NORTH, S., CHU, L., CHI, K. N., JONES, R. J., GOODMAN, O. B., JR., SAAD, F., STAFFURTH, J. N., MAINWARING, P., HARLAND, S., FLAIG, T. W., HUTSON, T. E., CHENG, T., PATTERSON, H., HAINSWORTH, J. D., RYAN, C. J., STERNBERG, C. N., ELLARD, S. L., FLECHON, A., SALEH, M., SCHOLZ, M., EFSTATHIOU, E., ZIVI, A., BIANCHINI, D., LORIOT, Y., CHIEFFO, N., KHEOH, T., HAQQ, C. M. & SCHER, H. I. 2011. Abiraterone and increased survival in metastatic prostate cancer. *N Engl J Med,* 364**,** 1995-2005.

DE FELICE, F., TOMBOLINI, V., MARAMPON, F., MUSELLA, A. & MARCHETTI, C. 2017. Defective DNA repair mechanisms in prostate cancer: impact of olaparib. *Drug Des Devel Ther,* 11**,** 547-552.

DE GOOIJER, M. C., VAN DEN TOP, A., BOCKAJ, I., BEIJNEN, J. H., WURDINGER, T. & VAN TELLINGEN, O. 2017. The G2 checkpoint-a node-based molecular switch. *FEBS Open Bio,* 7**,** 439-455.

DE LA TAILLE, A., HAYEK, O., BENSON, M. C., BAGIELLA, E., OLSSON, C. A., FATAL, M. & KATZ, A. E. 2000. Salvage cryotherapy for recurrent prostate cancer after radiation therapy: the Columbia experience. *Urology,* 55**,** 79-84.

DE MARZO, A. M., PLATZ, E. A., SUTCLIFFE, S., XU, J., GRONBERG, H., DRAKE, C. G., NAKAI, Y., ISAACS, W. B. & NELSON, W. G. 2007. Inflammation in prostate carcinogenesis. *Nat Rev Cancer,* 7**,** 256-69.

DE NIGRIS, F., MEGA, T., BERGER, N., BARONE, M. V., SANTORO, M., VIGLIETTO, G., VERDE, P. & FUSCO, A. 2001. Induction of ETS-1 and ETS-2 transcription factors is required for thyroid cell transformation. *Cancer Res,* 61**,** 2267-75.

DE THE, H., LAVAU, C., MARCHIO, A., CHOMIENNE, C., DEGOS, L. & DEJEAN, A. 1991. The PML-RAR alpha fusion mRNA generated by the t(15;17) translocation in acute promyelocytic leukemia encodes a functionally altered RAR. *Cell,* 66**,** 675-84.

DENG, G., MA, L., MENG, Q., JU, X., JIANG, K., JIANG, P. & YU, Z. 2016. Notch signaling in the prostate: critical roles during development and in the hallmarks of prostate cancer biology. *J Cancer Res Clin Oncol,* 142**,** 531-47.

DESHAYES, E., ROUMIGUIE, M., THIBAULT, C., BEUZEBOC, P., CACHIN, F., HENNEQUIN, C., HUGLO, D., ROZET, F., KASSAB-CHAHMI, D., REBILLARD, X. & HOUEDE, N. 2017. Radium 223 dichloride for prostate cancer treatment. *Drug Des Devel Ther,* 11**,** 2643-2651.

DI SANT'AGNESE, P. A. 1998. Neuroendocrine cells of the prostate and neuroendocrine differentiation in prostatic carcinoma: a review of morphologic aspects. *Urology,* 51**,** 121-4.

DIEHN, M., CHO, R. W., LOBO, N. A., KALISKY, T., DORIE, M. J., KULP, A. N., QIAN, D., LAM, J. S., AILLES, L. E., WONG, M., JOSHUA, B., KAPLAN, M. J., WAPNIR, I., DIRBAS, F. M., SOMLO, G., GARBEROGLIO, C., PAZ, B., SHEN, J., LAU, S. K., QUAKE, S. R., BROWN, J. M., WEISSMAN, I. L. & CLARKE, M. F. 2009. Association of reactive oxygen species levels and radioresistance in cancer stem cells. *Nature,* 458**,** 780-3.

DO, H. J., SONG, H., YANG, H. M., KIM, D. K., KIM, N. H., KIM, J. H., CHA, K. Y., CHUNG, H. M. & KIM, J. H. 2006. Identification of multiple nuclear localization signals in murine Elf3, an ETS transcription factor. *FEBS Lett,* 580**,** 1865-71.

DU, Z., JIA, D., LIU, S., WANG, F., LI, G., ZHANG, Y., CAO, X., LING, E. A. & HAO, A. 2009. Oct4 is expressed in human gliomas and promotes colony formation in glioma cells. *Glia,* 57**,** 724-33.

DUBRIDGE, R. B., TANG, P., HSIA, H. C., LEONG, P. M., MILLER, J. H. & CALOS, M. P. 1987. Analysis of mutation in human cells by using an Epstein-Barr virus shuttle system. *Mol Cell Biol,* 7**,** 379-87.

DUFAIT, I., LIECHTENSTEIN, T., LANNA, A., BRICOGNE, C., LARANGA, R., PADELLA, A., BRECKPOT, K. & ESCORS, D. 2012. Retroviral and lentiviral vectors for the induction of immunological tolerance. *Scientifica (Cairo),* 2012.

DUTTA, A., LE MAGNEN, C., MITROFANOVA, A., OUYANG, X., CALIFANO, A. & ABATE-SHEN, C. 2016. Identification of an NKX3.1-G9a-UTY transcriptional regulatory network that controls prostate differentiation. *Science,* 352**,** 1576-80.

DWYER, J. M. & LIU, J. P. 2010. Ets2 transcription factor, telomerase activity and breast cancer. *Clin Exp Pharmacol Physiol,* 37**,** 83-7.

DYLLA, S. J., BEVIGLIA, L., PARK, I. K., CHARTIER, C., RAVAL, J., NGAN, L., PICKELL, K., AGUILAR, J., LAZETIC, S., SMITH-BERDAN, S., CLARKE, M. F., HOEY, T., LEWICKI, J. & GURNEY, A. L. 2008. Colorectal cancer stem cells are enriched in xenogeneic tumors following chemotherapy. *PLoS One,* 3**,** e2428.

EELES, R. A., OLAMA, A. A., BENLLOCH, S., SAUNDERS, E. J., LEONGAMORNLERT, D. A., TYMRAKIEWICZ, M., GHOUSSAINI, M., LUCCARINI, C., DENNIS, J., JUGURNAUTH-LITTLE, S., DADAEV, T., NEAL, D. E., HAMDY, F. C., DONOVAN, J. L., MUIR, K., GILES, G. G., SEVERI, G., WIKLUND, F., GRONBERG, H., HAIMAN, C. A., SCHUMACHER, F., HENDERSON, B. E., LE MARCHAND, L., LINDSTROM, S., KRAFT, P., HUNTER, D. J., GAPSTUR, S., CHANOCK, S. J., BERNDT, S. I., ALBANES, D., ANDRIOLE, G., SCHLEUTKER, J., WEISCHER, M., CANZIAN, F., RIBOLI, E., KEY, T. J., TRAVIS, R. C., CAMPA, D., INGLES, S. A., JOHN, E. M., HAYES, R. B., PHAROAH, P. D., PASHAYAN, N., KHAW, K. T., STANFORD, J. L., OSTRANDER, E. A., SIGNORELLO, L. B., THIBODEAU, S. N., SCHAID, D., MAIER, C., VOGEL, W., KIBEL, A. S., CYBULSKI, C., LUBINSKI, J., CANNON-ALBRIGHT, L., BRENNER, H., PARK, J. Y., KANEVA, R., BATRA, J., SPURDLE, A. B., CLEMENTS, J. A., TEIXEIRA, M. R., DICKS, E., LEE, A., DUNNING, A. M., BAYNES, C., CONROY, D., MARANIAN, M. J., AHMED, S., GOVINDASAMI, K., GUY, M., WILKINSON, R. A., SAWYER, E. J., MORGAN, A., DEARNALEY, D. P., HORWICH, A., HUDDART, R. A., KHOO, V. S., PARKER, C. C., VAN AS, N. J., WOODHOUSE, C. J., THOMPSON, A., DUDDERIDGE, T., OGDEN, C., COOPER, C. S., LOPHATANANON, A., COX, A., SOUTHEY, M. C., HOPPER, J. L., ENGLISH, D. R., ALY, M., ADOLFSSON, J., XU, J., ZHENG, S. L., YEAGER, M., KAAKS, R., DIVER, W. R., GAUDET, M. M., STERN, M. C., CORRAL, R., et al. 2013. Identification of 23 new prostate cancer susceptibility loci using the iCOGS custom genotyping array. *Nat Genet,* 45**,** 385-91, 391e1-2.

EGGENER, S., SALOMON, G., SCARDINO, P. T., DE LA ROSETTE, J., POLASCIK, T. J. & BREWSTER, S. 2010. Focal therapy for prostate cancer: possibilities and limitations. *Eur Urol,* 58**,** 57-64.

ENGLISH, H. F., SANTEN, R. J. & ISAACS, J. T. 1987. Response of glandular versus basal rat ventral prostatic epithelial cells to androgen withdrawal and replacement. *Prostate,* 11**,** 229-42.

EPSTEIN, J. I. 2010. An update of the Gleason grading system. *J Urol,* 183**,** 433-40.

EPSTEIN, J. I., ZELEFSKY, M. J., SJOBERG, D. D., NELSON, J. B., EGEVAD, L., MAGI-GALLUZZI, C., VICKERS, A. J., PARWANI, A. V., REUTER, V. E., FINE, S. W., EASTHAM, J. A., WIKLUND, P., HAN, M., REDDY, C. A., CIEZKI, J. P., NYBERG, T. & KLEIN, E. A. 2016. A Contemporary Prostate Cancer Grading System: A Validated Alternative to the Gleason Score. *Eur Urol,* 69**,** 428-35.

FDA. 2011. *FDA drug safety communication: 5α reductase inhibitors (5-ARIs) may increase the risk of a more serious form of prostate cancer* [Online]. Available: http://www.fda.gov/Drugs/DrugSafety/ucm258314.htm [Accessed Dec 2014].

FELDMAN, R. J., SEMENTCHENKO, V. I., GAYED, M., FRAIG, M. M. & WATSON, D. K. 2003. Pdef expression in human breast cancer is correlated with invasive potential and altered gene expression. *Cancer Res,* 63**,** 4626-31.

FENG, Y., XUE, H., ZHU, J., YANG, L., ZHANG, F., QIAN, R., LIN, W. & WANG, Y. 2016. ESE1 is Associated with Neuronal Apoptosis in Lipopolysaccharide Induced Neuroinflammation. *Neurochem Res,* 41**,** 2752-2762.

FIBBI, B., PENNA, G., MORELLI, A., ADORINI, L. & MAGGI, M. 2010. Chronic inflammation in the pathogenesis of benign prostatic hyperplasia. *Int J Androl,* 33**,** 475-88.

FINE, S. W., GOPALAN, A., LEVERSHA, M. A., AL-AHMADIE, H. A., TICKOO, S. K., ZHOU, Q., SATAGOPAN, J. M., SCARDINO, P. T., GERALD, W. L. & REUTER, V. E. 2010. TMPRSS2-ERG gene fusion is associated with low Gleason scores and not with high-grade morphological features. *Mod Pathol,* 23**,** 1325-33.

FLETCHER, J. I., HABER, M., HENDERSON, M. J. & NORRIS, M. D. 2010. ABC transporters in cancer: more than just drug efflux pumps. *Nat Rev Cancer,* 10**,** 147-56.

FRAME, F. M. & MAITLAND, N. J. 2011. Cancer stem cells, models of study and implications of therapy resistance mechanisms. *Advances in Experimental Medicine and Biology.*

FRAME, F. M., NOBLE, A. R., KLEIN, S., WALKER, H. F., SUMAN, R., KASPROWICZ, R., MANN, V. M., SIMMS, M. S. & MAITLAND, N. J. 2017. Tumor heterogeneity and therapy resistance - implications for future treatments of prostate cancer. *Journal of Cancer Metastasis and Treatment,* 3**,** 302-14.

FRAME, F. M., PELLACANI, D., COLLINS, A. T. & MAITLAND, N. J. 2016. Harvesting Human Prostate Tissue Material and Culturing Primary Prostate Epithelial Cells. *Methods Mol Biol,* 1443**,** 181-201.

FRAME, F. M., PELLACANI, D., COLLINS, A. T., SIMMS, M. S., MANN, V. M., JONES, G. D., MEUTH, M., BRISTOW, R. G. & MAITLAND, N. J. 2013. HDAC inhibitor confers radiosensitivity to prostate stem-like cells. *Br J Cancer,* 109**,** 3023-33.

FRANCIPANE, M. G., ALEA, M. P., LOMBARDO, Y., TODARO, M., MEDEMA, J. P. & STASSI, G. 2008. Crucial role of interleukin-4 in the survival of colon cancer stem cells. *Cancer Res,* 68**,** 4022-5.

FREITAS, D. P., TEIXEIRA, C. A., SANTOS-SILVA, F., VASCONCELOS, M. H. & ALMEIDA, G. M. 2014. Therapy-induced enrichment of putative lung cancer stem-like cells. *Int J Cancer,* 134**,** 1270-8.

FRIGO, D. E. & MCDONNELL, D. P. 2008. Differential effects of prostate cancer therapeutics on neuroendocrine transdifferentiation. *Mol Cancer Ther,* 7**,** 659-69.

GAO, N., ISHII, K., MIROSEVICH, J., KUWAJIMA, S., OPPENHEIMER, S. R., ROBERTS, R. L., JIANG, M., YU, X., SHAPPELL, S. B., CAPRIOLI, R. M., STOFFEL, M., HAYWARD, S. W. & MATUSIK, R. J. 2005. Forkhead box A1 regulates prostate ductal morphogenesis and promotes epithelial cell maturation. *Development,* 132**,** 3431-43.

GERMANN, M., WETTERWALD, A., GUZMAN-RAMIREZ, N., VAN DER PLUIJM, G., CULIG, Z., CECCHINI, M. G., WILLIAMS, E. D. & THALMANN, G. N. 2012. Stem-like cells with luminal progenitor phenotype survive castration in human prostate cancer. *Stem Cells,* 30**,** 1076-86.

GHADERSOHI, A., SHARMA, S., ZHANG, S., AZRAK, R. G., WILDING, G. E., MANJILI, M. H. & LI, F. 2011. Prostate-derived Ets transcription factor (PDEF) is a potential prognostic marker in patients with prostate cancer. *Prostate,* 71**,** 1178-88.

GLEASON, D. F. 1966. Classification of prostatic carcinomas. *Cancer Chemother Rep,* 50**,** 125-8.

GOLDSTEIN, A. S., HUANG, J., GUO, C., GARRAWAY, I. P. & WITTE, O. N. 2010. Identification of a cell of origin for human prostate cancer. *Science,* 329**,** 568-71.

GOLUB, T. R., GOGA, A., BARKER, G. F., AFAR, D. E., MCLAUGHLIN, J., BOHLANDER, S. K., ROWLEY, J. D., WITTE, O. N. & GILLILAND, D. G. 1996. Oligomerization of the ABL tyrosine kinase by the Ets protein TEL in human leukemia. *Mol Cell Biol,* 16**,** 4107-16.

GORLICH, D. & KUTAY, U. 1999. Transport between the cell nucleus and the cytoplasm. *Annu Rev Cell Dev Biol,* 15**,** 607-60.

GRALL, F. T., PRALL, W. C., WEI, W., GU, X., CHO, J. Y., CHOY, B. K., ZERBINI, L. F., INAN, M. S., GOLDRING, S. R., GRAVALLESE, E. M., GOLDRING, M. B., OETTGEN, P. & LIBERMANN, T. A. 2005. The Ets transcription factor ESE-1 mediates induction of the COX-2 gene by LPS in monocytes. *Febs j,* 272**,** 1676-87.

GREAVES, M. 2010. Cancer stem cells: back to Darwin? *Semin Cancer Biol,* 20**,** 65-70.

GREAVES, M. & MALEY, C. C. 2012. Clonal evolution in cancer. *Nature,* 481**,** 306-13.

GREENBERG, N. M., DEMAYO, F., FINEGOLD, M. J., MEDINA, D., TILLEY, W. D., ASPINALL, J. O., CUNHA, G. R., DONJACOUR, A. A., MATUSIK, R. J. & ROSEN, J. M. 1995. Prostate cancer in a transgenic mouse. *Proc Natl Acad Sci U S A,* 92**,** 3439-43.

GREGORIEFF, A., STANGE, D. E., KUJALA, P., BEGTHEL, H., VAN DEN BORN, M., KORVING, J., PETERS, P. J. & CLEVERS, H. 2009. The ets-domain transcription factor Spdef promotes maturation of goblet and paneth cells in the intestinal epithelium. *Gastroenterology,* 137**,** 1333-45.e1-3.

GRIGNANI, F., FERRUCCI, P. F., TESTA, U., TALAMO, G., FAGIOLI, M., ALCALAY, M., MENCARELLI, A., GRIGNANI, F., PESCHLE, C., NICOLETTI, I. & ET AL. 1993. The acute promyelocytic leukemia-specific PML-RAR alpha fusion protein inhibits differentiation and promotes survival of myeloid precursor cells. *Cell,* 74**,** 423-31.

GROBHOLZ, R., GRIEBE, M., SAUER, C. G., MICHEL, M. S., TROJAN, L. & BLEYL, U. 2005. Influence of neuroendocrine tumor cells on proliferation in prostatic carcinoma. *Hum Pathol,* 36**,** 562-70.

GU, X., ZERBINI, L. F., OTU, H. H., BHASIN, M., YANG, Q., JOSEPH, M. G., GRALL, F., ONATUNDE, T., CORREA, R. G. & LIBERMANN, T. A. 2007. Reduced PDEF expression increases invasion and expression of mesenchymal genes in prostate cancer cells. *Cancer Res,* 67**,** 4219-26.

GUENECHEA, G., GAN, O. I., DORRELL, C. & DICK, J. E. 2001. Distinct classes of human stem cells that differ in proliferative and self-renewal potential. *Nat Immunol,* 2**,** 75-82.

GUNAWARDANE, R. N., SGROI, D. C., WROBEL, C. N., KOH, E., DALEY, G. Q. & BRUGGE, J. S. 2005. Novel role for PDEF in epithelial cell migration and invasion. *Cancer Res,* 65**,** 11572-80.

GUNDEM, G., VAN LOO, P., KREMEYER, B., ALEXANDROV, L. B., TUBIO, J. M., PAPAEMMANUIL, E., BREWER, D. S., KALLIO, H. M., HOGNAS, G., ANNALA, M., KIVINUMMI, K., GOODY, V., LATIMER, C., O'MEARA, S., DAWSON, K. J., ISAACS, W., EMMERT-BUCK, M. R., NYKTER, M., FOSTER, C., KOTE-JARAI, Z., EASTON, D., WHITAKER, H. C., NEAL, D. E., COOPER, C. S., EELES, R. A., VISAKORPI, T., CAMPBELL, P. J., MCDERMOTT, U., WEDGE, D. C. & BOVA, G. S. 2015. The evolutionary history of lethal metastatic prostate cancer. *Nature,* 520**,** 353-7.

GUPTA, G. P. & MASSAGUE, J. 2006. Cancer metastasis: building a framework. *Cell,* 127**,** 679-95.

GUPTA, S., ILJIN, K., SARA, H., MPINDI, J. P., MIRTTI, T., VAINIO, P., RANTALA, J., ALANEN, K., NEES, M. & KALLIONIEMI, O. 2010. FZD4 as a mediator of ERG oncogene-induced WNT signaling and epithelial-to-mesenchymal transition in human prostate cancer cells. *Cancer Res,* 70**,** 6735-45.

GUZEL, E., KARATAS, O. F., DUZ, M. B., SOLAK, M., ITTMANN, M. & OZEN, M. 2014. Differential expression of stem cell markers and ABCG2 in recurrent prostate cancer. *Prostate,* 74**,** 1498-505.

HAFFNER, M. C., MOSBRUGER, T., ESOPI, D. M., FEDOR, H., HEAPHY, C. M., WALKER, D. A., ADEJOLA, N., GUREL, M., HICKS, J., MEEKER, A. K., HALUSHKA, M. K., SIMONS, J. W., ISAACS, W. B., DE MARZO, A. M., NELSON, W. G. & YEGNASUBRAMANIAN, S. 2013. Tracking the clonal origin of lethal prostate cancer. *J Clin Invest,* 123**,** 4918-22.

HALDER, J., KAMAT, A. A., LANDEN, C. N., JR., HAN, L. Y., LUTGENDORF, S. K., LIN, Y. G., MERRITT, W. M., JENNINGS, N. B., CHAVEZ-REYES, A., COLEMAN, R. L., GERSHENSON, D. M., SCHMANDT, R., COLE, S. W., LOPEZ-BERESTEIN, G. & SOOD, A. K. 2006. Focal adhesion kinase targeting using in vivo short interfering

RNA delivery in neutral liposomes for ovarian carcinoma therapy. *Clin Cancer Res,* 12**,** 4916-24.

HALL, J. A., MAITLAND, N. J., STOWER, M. & LANG, S. H. 2002. Primary prostate stromal cells modulate the morphology and migration of primary prostate epithelial cells in type 1 collagen gels. *Cancer Res,* 62**,** 58-62.

HAMDY, F. C., DONOVAN, J. L., LANE, J. A., MASON, M., METCALFE, C., HOLDING, P., DAVIS, M., PETERS, T. J., TURNER, E. L., MARTIN, R. M., OXLEY, J., ROBINSON, M., STAFFURTH, J., WALSH, E., BOLLINA, P., CATTO, J., DOBLE, A., DOHERTY, A., GILLATT, D., KOCKELBERGH, R., KYNASTON, H., PAUL, A., POWELL, P., PRESCOTT, S., ROSARIO, D. J., ROWE, E. & NEAL, D. E. 2016. 10-Year Outcomes after Monitoring, Surgery, or Radiotherapy for Localized Prostate Cancer. *N Engl J Med,* 375**,** 1415-1424.

HANAHAN, D. & WEINBERG, R. A. 2000. The hallmarks of cancer. *Cell,* 100**,** 57-70.

HANAHAN, D. & WEINBERG, R. A. 2011. Hallmarks of cancer: the next generation. *Cell,* 144**,** 646-74.

HARRIS, M. E., BOHNI, R., SCHNEIDERMAN, M. H., RAMAMURTHY, L., SCHUMPERLI, D. & MARZLUFF, W. F. 1991. Regulation of histone mRNA in the unperturbed cell cycle: evidence suggesting control at two posttranscriptional steps. *Mol Cell Biol,* 11**,** 2416-24.

HAYWARD, S. W., DAHIYA, R., CUNHA, G. R., BARTEK, J., DESHPANDE, N. & NARAYAN, P. 1995. Establishment and characterization of an immortalized but non-transformed human prostate epithelial cell line: BPH-1. *In Vitro Cell Dev Biol Anim,* 31**,** 14-24.

HEIDENREICH, A., BASTIAN, P. J., BELLMUNT, J., BOLLA, M., JONIAU, S., VAN DER KWAST, T., MASON, M., MATVEEV, V., WIEGEL, T., ZATTONI, F. & MOTTET, N. 2014a. EAU guidelines on prostate cancer. part 1: screening, diagnosis, and local treatment with curative intent-update 2013. *Eur Urol,* 65**,** 124-37.

HEIDENREICH, A., BASTIAN, P. J., BELLMUNT, J., BOLLA, M., JONIAU, S., VAN DER KWAST, T., MASON, M., MATVEEV, V., WIEGEL, T., ZATTONI, F. & MOTTET, N. 2014b. EAU guidelines on prostate cancer. Part II: Treatment of advanced, relapsing, and castration-resistant prostate cancer. *Eur Urol,* 65**,** 467-79.

HEINLEIN, C. A. & CHANG, C. 2004. Androgen receptor in prostate cancer. *Endocr Rev,* 25**,** 276-308.

HELGESON, B. E., TOMLINS, S. A., SHAH, N., LAXMAN, B., CAO, Q., PRENSNER, J. R., CAO, X., SINGLA, N., MONTIE, J. E., VARAMBALLY, S., MEHRA, R. & CHINNAIYAN, A. M. 2008. Characterization of TMPRSS2:ETV5 and SLC45A3:ETV5 gene fusions in prostate cancer. *Cancer Res,* 68**,** 73-80.

HELLSTEN, R., JOHANSSON, M., DAHLMAN, A., STERNER, O. & BJARTELL, A. 2011. Galiellalactone inhibits stem cell-like ALDH-positive prostate cancer cells. *PLoS One,* 6**,** e22118.

HIRANO, D., OKADA, Y., MINEI, S., TAKIMOTO, Y. & NEMOTO, N. 2004. Neuroendocrine differentiation in hormone refractory prostate cancer following androgen deprivation therapy. *Eur Urol,* 45**,** 586-92; discussion 592.

HIYAMA, E. & HIYAMA, K. 2002. Clinical utility of telomerase in cancer. *Oncogene,* 21**,** 643-9.

HOCK, H., MEADE, E., MEDEIROS, S., SCHINDLER, J. W., VALK, P. J., FUJIWARA, Y. & ORKIN, S. H. 2004. Tel/Etv6 is an essential and selective regulator of adult hematopoietic stem cell survival. *Genes Dev,* 18**,** 2336-41.

HOLLENHORST, P. C., SHAH, A. A., HOPKINS, C. & GRAVES, B. J. 2007. Genome-wide analyses reveal properties of redundant and specific promoter occupancy within the ETS gene family. *Genes Dev,* 21**,** 1882-94.

HONG, B., VAN DEN HEUVEL, A. P., PRABHU, V. V., ZHANG, S. & EL-DEIRY, W. S. 2014. Targeting tumor suppressor p53 for cancer therapy: strategies, challenges and opportunities. *Curr Drug Targets,* 15**,** 80-9.

HONG, M. K., MACINTYRE, G., WEDGE, D. C. & VAN LOO, P. 2015. Tracking the origins and drivers of subclonal metastatic expansion in prostate cancer. 6**,** 6605.

HOROSZEWICZ, J. S., LEONG, S. S., KAWINSKI, E., KARR, J. P., ROSENTHAL, H., CHU, T. M., MIRAND, E. A. & MURPHY, G. P. 1983. LNCaP model of human prostatic carcinoma. *Cancer Res,* 43**,** 1809-18.

HOWE, S. J., MANSOUR, M. R., SCHWARZWAELDER, K., BARTHOLOMAE, C., HUBANK, M., KEMPSKI, H., BRUGMAN, M. H., PIKE-OVERZET, K., CHATTERS, S. J., DE RIDDER, D., GILMOUR, K. C., ADAMS, S., THORNHILL, S. I., PARSLEY, K. L., STAAL, F. J., GALE, R. E., LINCH, D. C., BAYFORD, J., BROWN, L., QUAYE, M., KINNON, C., ANCLIFF, P., WEBB, D. K., SCHMIDT, M., VON KALLE, C., GASPAR, H. B. & THRASHER, A. J. 2008. Insertional mutagenesis combined with acquired somatic mutations causes leukemogenesis following gene therapy of SCID-X1 patients. *J Clin Invest,* 118**,** 3143-50.

HUANG, K. C., DOLPH, M., DONNELLY, B. & BISMAR, T. A. 2014. ERG expression is associated with increased risk of biochemical relapse following radical prostatectomy in early onset prostate cancer. *Clin Transl Oncol,* 16**,** 973-9.

HUANG, M. E., YE, Y. C., CHEN, S. R., CHAI, J. R., LU, J. X., ZHOA, L., GU, L. J. & WANG, Z. Y. 1988. Use of all-trans retinoic acid in the treatment of acute promyelocytic leukemia. *Blood,* 72**,** 567-72.

HUDSON, D. L. 2004. Epithelial stem cells in human prostate growth and disease. *Prostate Cancer Prostatic Dis,* 7**,** 188-94.

HUDSON, D. L., GUY, A. T., FRY, P., O'HARE, M. J., WATT, F. M. & MASTERS, J. R. 2001. Epithelial cell differentiation pathways in the human prostate: identification of intermediate phenotypes by keratin expression. *J Histochem Cytochem,* 49**,** 271-8.

HUMPHREY, P. A. 2004. Gleason grading and prognostic factors in carcinoma of the prostate. *Mod Pathol,* 17**,** 292-306.

HUMPHREY, P. A. 2007. Diagnosis of adenocarcinoma in prostate needle biopsy tissue. *J Clin Pathol,* 60**,** 35-42.

ISAACS, J. T. & COFFEY, D. S. 1989. Etiology and disease process of benign prostatic hyperplasia. *Prostate Suppl,* 2**,** 33-50.

ISHII, H., IWATSUKI, M., IETA, K., OHTA, D., HARAGUCHI, N., MIMORI, K. & MORI, M. 2008. Cancer stem cells and chemoradiation resistance. *Cancer Sci,* 99**,** 1871-7.

ISHIZAWA, K., RASHEED, Z. A., KARISCH, R., WANG, Q., KOWALSKI, J., SUSKY, E., PEREIRA, K., KARAMBOULAS, C., MOGHAL, N., RAJESHKUMAR, N. V., HIDALGO, M., TSAO, M., AILLES, L., WADDELL, T. K., MAITRA, A., NEEL, B. G. & MATSUI, W. 2010. Tumor-initiating cells are rare in many human tumors. *Cell Stem Cell,* 7**,** 279-82.

IVERSEN, P. 2003. Bicalutamide monotherapy for early stage prostate cancer: an update. *J Urol,* 170**,** S48-52; discussion S52-4.

IVERSEN, P., TYRRELL, C. J., KAISARY, A. V., ANDERSON, J. B., VAN POPPEL, H., TAMMELA, T. L., CHAMBERLAIN, M., CARROLL, K. & MELEZINEK, I. 2000. Bicalutamide monotherapy compared with castration in patients with nonmetastatic locally advanced prostate cancer: 6.3 years of followup. *J Urol,* 164**,** 1579-82.

IWATA, T., SCHULTZ, D., HICKS, J., HUBBARD, G. K., MUTTON, L. N., LOTAN, T. L., BETHEL, C., LOTZ, M. T., YEGNASUBRAMANIAN, S., NELSON, W. G., DANG, C. V., XU, M., ANELE, U., KOH, C. M., BIEBERICH, C. J. & DE MARZO, A. M. 2010. MYC overexpression induces prostatic intraepithelial neoplasia and loss of Nkx3.1 in mouse luminal epithelial cells. *PLoS ONE,* 5.

IZADPANAH, R., KAUSHAL, D., KRIEDT, C., TSIEN, F., PATEL, B., DUFOUR, J. & BUNNELL, B. A. 2008. Long-term in vitro expansion alters the biology of adult mesenchymal stem cells. *Cancer Res,* 68**,** 4229-38.

JAMES, N. D., DE BONO, J. S., SPEARS, M. R., CLARKE, N. W., MASON, M. D., DEARNALEY, D. P., RITCHIE, A. W. S., AMOS, C. L., GILSON, C., JONES, R. J., MATHESON, D., MILLMAN, R., ATTARD, G., CHOWDHURY, S., CROSS, W. R., GILLESSEN, S., PARKER, C. C., RUSSELL, J. M., BERTHOLD, D. R., BRAWLEY, C., ADAB, F., AUNG, S., BIRTLE, A. J., BOWEN, J., BROCK, S., CHAKRABORTI, P., FERGUSON, C., GALE, J., GRAY, E., HINGORANI, M., HOSKIN, P. J., LESTER, J. F., MALIK, Z. I., MCKINNA, F., MCPHAIL, N., MONEY-KYRLE, J., O'SULLIVAN, J., PARIKH, O., PROTHEROE, A., ROBINSON, A., SRIHARI, N. N., THOMAS, C., WAGSTAFF, J., WYLIE, J., ZARKAR, A., PARMAR, M. K. B. & SYDES, M. R. 2017. Abiraterone for Prostate Cancer Not Previously Treated with Hormone Therapy. *N Engl J Med,* 377**,** 338-351.

JAMES, N. D., SYDES, M. R., CLARKE, N. W., MASON, M. D., DEARNALEY, D. P., SPEARS, M. R., RITCHIE, A. W., PARKER, C. C., RUSSELL, J. M., ATTARD, G., DE BONO, J., CROSS, W., JONES, R. J., THALMANN, G., AMOS, C., MATHESON, D., MILLMAN, R., ALZOUEBI, M., BEESLEY, S., BIRTLE, A. J., BROCK, S., CATHOMAS, R., CHAKRABORTI, P., CHOWDHURY, S., COOK, A., ELLIOTT, T., GALE, J., GIBBS, S., GRAHAM, J. D., HETHERINGTON, J., HUGHES, R., LAING, R., MCKINNA, F., MCLAREN, D. B., O'SULLIVAN, J. M., PARIKH, O., PEEDELL, C., PROTHEROE, A., ROBINSON, A. J., SRIHARI, N.,

SRINIVASAN, R., STAFFURTH, J., SUNDAR, S., TOLAN, S., TSANG, D., WAGSTAFF, J. & PARMAR, M. K. 2016. Addition of docetaxel, zoledronic acid, or both to first-line long-term hormone therapy in prostate cancer (STAMPEDE): survival results from an adaptive, multiarm, multistage, platform randomised controlled trial. *Lancet,* 387**,** 1163-77.

JOHNSON, T. R., KOUL, S., KUMAR, B., KHANDRIKA, L., VENEZIA, S., MARONI, P. D., MEACHAM, R. B. & KOUL, H. K. 2010. Loss of PDEF, a prostate-derived Ets factor is associated with aggressive phenotype of prostate cancer: regulation of MMP 9 by PDEF. *Mol Cancer,* 9**,** 148.

JOSSON, S., MATSUOKA, Y., CHUNG, L. W., ZHAU, H. E. & WANG, R. 2010. Tumor-stroma co-evolution in prostate cancer progression and metastasis. *Semin Cell Dev Biol,* 21**,** 26-32.

JOUSSET, C., CARRON, C., BOUREUX, A., QUANG, C. T., OURY, C., DUSANTER-FOURT, I., CHARON, M., LEVIN, J., BERNARD, O. & GHYSDAEL, J. 1997. A domain of TEL conserved in a subset of ETS proteins defines a specific oligomerization interface essential to the mitogenic properties of the TEL-PDGFR beta oncoprotein. *Embo j,* 16**,** 69-82.

KAIGHN, M. E., NARAYAN, K. S., OHNUKI, Y., LECHNER, J. F. & JONES, L. W. 1979. Establishment and characterization of a human prostatic carcinoma cell line (PC-3). *Invest Urol,* 17**,** 16-23.

KANTOFF, P. W., HIGANO, C. S., SHORE, N. D., BERGER, E. R., SMALL, E. J., PENSON, D. F., REDFERN, C. H., FERRARI, A. C., DREICER, R., SIMS, R. B., XU, Y., FROHLICH, M. W. & SCHELLHAMMER, P. F. 2010. Sipuleucel-T immunotherapy for castration-resistant prostate cancer. *N Engl J Med,* 363**,** 411-22.

KAR, A. & GUTIERREZ-HARTMANN, A. 2013. Molecular mechanisms of ETS transcription factor-mediated tumorigenesis. *Crit Rev Biochem Mol Biol,* 48**,** 522-43.

KAR, A. & GUTIERREZ-HARTMANN, A. 2017. ESE-1/ELF3 mRNA expression associates with poor survival outcomes in HER2(+) breast cancer patients and is critical for tumorigenesis in HER2(+) breast cancer cells. *Oncotarget,* 8**,** 69622-69640.

KAS, K., FINGER, E., GRALL, F., GU, X., AKBARALI, Y., BOLTAX, J., WEISS, A., OETTGEN, P., KAPELLER, R. & LIBERMANN, T. A. 2000. ESE-3, a novel member of an epithelium-specific ets transcription factor subfamily, demonstrates different target gene specificity from ESE-1. *J Biol Chem,* 275**,** 2986-98.

KASPER, S., SHEPPARD, P. C., YAN, Y., PETTIGREW, N., BOROWSKY, A. D., PRINS, G. S., DODD, J. G., DUCKWORTH, M. L. & MATUSIK, R. J. 1998. Development, progression, and androgen-dependence of prostate tumors in probasin-large T antigen transgenic mice: a model for prostate cancer. *Lab Invest,* 78**,** 319-33.

KASTNER, P. & CHAN, S. 2008. PU.1: a crucial and versatile player in hematopoiesis and leukemia. *Int J Biochem Cell Biol,* 40**,** 22-7.

KATZEN, F. 2007. Gateway((R)) recombinational cloning: a biological operating system. *Expert Opin Drug Discov,* 2**,** 571-89.

KAWAI, J., HIROSE, K., FUSHIKI, S., HIROTSUNE, S., OZAWA, N., HARA, A., HAYASHIZAKI, Y. & WATANABE, S. 1994. Comparison of DNA methylation patterns among mouse cell lines by restriction landmark genomic scanning. *Mol Cell Biol,* 14**,** 7421-7.

KELLOKUMPU-LEHTINEN, P., SANTTI, R. & PELLINIEMI, L. J. 1979. Early cytodifferentiation of human prostatic urethra and Leydig cells. *Anat Rec,* 194**,** 429-43.

KELLY, K. & YIN, J. J. 2008. Prostate cancer and metastasis initiating stem cells. *Cell Res,* 18**,** 528-37.

KIM, H. J. & LOTAN, R. 2004. Identification of retinoid-modulated proteins in squamous carcinoma cells using high-throughput immunoblotting. *Cancer Res,* 64**,** 2439-48.

KIM, H. L., JEON, K. H., JUN, K. Y., CHOI, Y., KIM, D. K., NA, Y. & KWON, Y. 2012. A-62176, a potent topoisomerase inhibitor, inhibits the expression of human epidermal growth factor receptor 2. *Cancer Lett,* 325**,** 72-9.

KIM, Y. S., KANG, M. J. & CHO, Y. M. 2013. Low production of reactive oxygen species and high DNA repair: mechanism of radioresistance of prostate cancer stem cells. *Anticancer Res,* 33**,** 4469-74.

KING, J. C., XU, J., WONGVIPAT, J., HIERONYMUS, H., CARVER, B. S., LEUNG, D. H., TAYLOR, B. S., SANDER, C., CARDIFF, R. D., COUTO, S. S., GERALD, W. L. & SAWYERS, C. L. 2009. Cooperativity of TMPRSS2-ERG with PI3-kinase pathway activation in prostate oncogenesis. *Nat Genet,* 41**,** 524-6.

KLARMANN, G. J., HURT, E. M., MATHEWS, L. A., ZHANG, X., DUHAGON, M. A., MISTREE, T., THOMAS, S. B. & FARRAR, W. L. 2009. Invasive prostate cancer cells are tumor initiating cells that have a stem cell-like genomic signature. *Clin Exp Metastasis,* 26**,** 433-46.

KLEZOVITCH, O., RISK, M., COLEMAN, I., LUCAS, J. M., NULL, M., TRUE, L. D., NELSON, P. S. & VASIOUKHIN, V. 2008. A causal role for ERG in neoplastic transformation of prostate epithelium. *Proc Natl Acad Sci U S A,* 105**,** 2105-10.

KLOTZ, L. 2006. Active surveillance versus radical treatment for favorable-risk localized prostate cancer. *Curr Treat Options Oncol,* 7**,** 355-62.

KLOTZ, L., BOCCON-GIBOD, L., SHORE, N. D., ANDREOU, C., PERSSON, B. E., CANTOR, P., JENSEN, J. K., OLESEN, T. K. & SCHRODER, F. H. 2008. The efficacy and safety of degarelix: a 12-month, comparative, randomized, open-label, parallel-group phase III study in patients with prostate cancer. *BJU Int,* 102**,** 1531-8.

KOLLMEIER, M. A. & ZELEFSKY, M. J. 2012. How to select the optimal therapy for early-stage prostate cancer. *Crit Rev Oncol Hematol,* 84 Suppl 1**,** e6-e15.

KONOPLEVA, M., ZHAO, S., HU, W., JIANG, S., SNELL, V., WEIDNER, D., JACKSON, C. E., ZHANG, X., CHAMPLIN, R., ESTEY, E., REED, J. C. & ANDREEFF, M. 2002. The anti-apoptotic genes Bcl-X(L) and Bcl-2 are over-expressed and contribute to chemoresistance of non-proliferating leukaemic CD34+ cells. *Br J Haematol,* 118**,** 521-34.

KOPP, J. L., WILDER, P. J., DESLER, M., KINARSKY, L. & RIZZINO, A. 2007. Different domains of the transcription factor ELF3 are required in a promoter-specific manner and multiple domains control its binding to DNA. *J Biol Chem,* 282**,** 3027-41.

KORSTEN, H., ZIEL-VAN DER MADE, A., MA, X., VAN DER KWAST, T. & TRAPMAN, J. 2009. Accumulating progenitor cells in the luminal epithelial cell layer are candidate tumor initiating cells in a Pten knockout mouse prostate cancer model. *PLoS One,* 4**,** e5662.

KOSAKA, T., MIYAJIMA, A., SHIROTAKE, S., KIKUCHI, E., HASEGAWA, M., MIKAMI, S. & OYA, M. 2010. Ets-1 and hypoxia inducible factor-1alpha inhibition by angiotensin II type-1 receptor blockade in hormone-refractory prostate cancer. *Prostate,* 70**,** 162-9.

KOUDINOVA, N. V., PINTHUS, J. H., BRANDIS, A., BRENNER, O., BENDEL, P., RAMON, J., ESHHAR, Z., SCHERZ, A. & SALOMON, Y. 2003. Photodynamic therapy with Pd-Bacteriopheophorbide (TOOKAD): successful in vivo treatment of human prostatic small cell carcinoma xenografts. *Int J Cancer,* 104**,** 782-9.

KRAMER, G., MITTEREGGER, D. & MARBERGER, M. 2007. Is benign prostatic hyperplasia (BPH) an immune inflammatory disease? *Eur Urol,* 51**,** 1202-16.

KRIEGER, J. N. 2004. Classification, epidemiology and implications of chronic prostatitis in North America, Europe and Asia. *Minerva Urol Nefrol,* 56**,** 99-107.

KROON, P., BERRY, P. A., STOWER, M. J., RODRIGUES, G., MANN, V. M., SIMMS, M., BHASIN, D., CHETTIAR, S., LI, C., LI, P. K., MAITLAND, N. J. & COLLINS, A. T. 2013. JAK-STAT blockade inhibits tumor initiation and clonogenic recovery of prostate cancer stem-like cells. *Cancer Research,* 73**,** 5288-5298.

KUNDERFRANCO, P., MELLO-GRAND, M., CANGEMI, R., PELLINI, S., MENSAH, A., ALBERTINI, V., MALEK, A., CHIORINO, G., CATAPANO, C. V. & CARBONE, G. M. 2010. ETS transcription factors control transcription of EZH2 and epigenetic silencing of the tumor suppressor gene Nkx3.1 in prostate cancer. *PLoS One,* 5**,** e10547.

KUPELIAN, P., KUBAN, D., THAMES, H., LEVY, L., HORWITZ, E., MARTINEZ, A., MICHALSKI, J., PISANSKY, T., SANDLER, H., SHIPLEY, W., ZELEFSKY, M. & ZIETMAN, A. 2005. Improved biochemical relapse-free survival with increased external radiation doses in patients with localized prostate cancer: the combined experience of nine institutions in patients treated in 1994 and 1995. *Int J Radiat Oncol Biol Phys,* 61**,** 415-9.

LANDEN, C. N., JR., CHAVEZ-REYES, A., BUCANA, C., SCHMANDT, R., DEAVERS, M. T., LOPEZ-BERESTEIN, G. & SOOD, A. K. 2005. Therapeutic EphA2 gene targeting in vivo using neutral liposomal small interfering RNA delivery. *Cancer Res,* 65**,** 6910-8.

LANG, S. H., SHARRARD, R. M., STARK, M., VILLETTE, J. M. & MAITLAND, N. J. 2001a. Prostate epithelial cell lines form spheroids with evidence of glandular differentiation in three-dimensional Matrigel cultures. *Br J Cancer,* 85**,** 590-9.

LANG, S. H., SMITH, J., HYDE, C., MACINTOSH, C., STOWER, M. & MAITLAND, N. J. 2006. Differentiation of prostate epithelial cell cultures by matrigel/ stromal cell glandular reconstruction. *In Vitro Cell Dev Biol Anim,* 42**,** 273-80.

LANG, S. H., STARK, M., COLLINS, A., PAUL, A. B., STOWER, M. J. & MAITLAND, N. J. 2001b. Experimental prostate epithelial morphogenesis in response to stroma and three-dimensional matrigel culture. *Cell Growth Differ,* 12**,** 631-40.

LAPIDOT, T., SIRARD, C., VORMOOR, J., MURDOCH, B., HOANG, T., CACERES-CORTES, J., MINDEN, M., PATERSON, B., CALIGIURI, M. A. & DICK, J. E. 1994. A cell initiating human acute myeloid leukaemia after transplantation into SCID mice. *Nature,* 367**,** 645-8.

LAUDET, V., NIEL, C., DUTERQUE-COQUILLAUD, M., LEPRINCE, D. & STEHELIN, D. 1993. Evolution of the ets gene family. *Biochem Biophys Res Commun,* 190**,** 8-14.

LAWRENCE, M. G., TAYLOR, R. A., TOIVANEN, R., PEDERSEN, J., NORDEN, S., POOK, D. W., FRYDENBERG, M., PAPARGIRIS, M. M., NIRANJAN, B., RICHARDS, M. G., WANG, H., COLLINS, A. T., MAITLAND, N. J. & RISBRIDGER, G. P. 2013. A preclinical xenograft model of prostate cancer using human tumors. *Nature Protocols,* 8**,** 836-848.

LAWSON, D. A., ZONG, Y., MEMARZADEH, S., XIN, L., HUANG, J. & WITTE, O. N. 2010. Basal epithelial stem cells are efficient targets for prostate cancer initiation. *Proc Natl Acad Sci U S A,* 107**,** 2610-5.

LEAV, I. & LING, G. V. 1968. Adenocarcinoma of the canine prostate. *Cancer,* 22**,** 1329-45.

LEE, C. H., AKIN-OLUGBADE, O. & KIRSCHENBAUM, A. 2011. Overview of prostate anatomy, histology, and pathology. *Endocrinol Metab Clin North Am,* 40**,** 565-75, viii-ix.

LEE, J., KOTLIAROVA, S., KOTLIAROV, Y., LI, A., SU, Q., DONIN, N. M., PASTORINO, S., PUROW, B. W., CHRISTOPHER, N., ZHANG, W., PARK, J. K. & FINE, H. A. 2006. Tumor stem cells derived from glioblastomas cultured in bFGF and EGF more closely mirror the phenotype and genotype of primary tumors than do serum-cultured cell lines. *Cancer Cell,* 9**,** 391-403.

LEE, L. W., TAYLOR, C. E., DESAULNIERS, J. P., ZHANG, M., HOJFELDT, J. W., PAN, Q. & MAPP, A. K. 2009. Inhibition of ErbB2(Her2) expression with small molecule transcription factor mimics. *Bioorg Med Chem Lett,* 19**,** 6233-6.

LEE, S. H., BAHN, J. H., CHOI, C. K., WHITLOCK, N. C., ENGLISH, A. E., SAFE, S. & BAEK, S. J. 2008. ESE-1/EGR-1 pathway plays a role in tolfenamic acid-induced apoptosis in colorectal cancer cells. *Mol Cancer Ther,* 7**,** 3739-50.

LEONG, K. G. & GAO, W. Q. 2008. The Notch pathway in prostate development and cancer. *Differentiation,* 76**,** 699-716.

LESHEM, O., MADAR, S., KOGAN-SAKIN, I., KAMER, I., GOLDSTEIN, I., BROSH, R., COHEN, Y., JACOB-HIRSCH, J., EHRLICH, M., BEN-SASSON, S., GOLDFINGER, N., LOEWENTHAL, R., GAZIT, E., ROTTER, V. & BERGER, R.

2011. TMPRSS2/ERG promotes epithelial to mesenchymal transition through the ZEB1/ZEB2 axis in a prostate cancer model. *PLoS One,* 6**,** e21650.

LEWIS, P. F. & EMERMAN, M. 1994. Passage through mitosis is required for oncoretroviruses but not for the human immunodeficiency virus. *J Virol,* 68**,** 510-6.

LI, B., SHIMIZU, Y., KOBAYASHI, T., TERADA, N., YOSHIMURA, K., KAMBA, T., MIKAMI, Y., INOUE, T., NISHIYAMA, H. & OGAWA, O. 2012. Overexpression of ETS-1 is associated with malignant biological features of prostate cancer. *Asian J Androl,* 14**,** 860-3.

LI, L., MIAO, X., NI, R., MIAO, X., WANG, L., GU, X., YAN, L., TANG, Q. & ZHANG, D. 2015. Epithelial-specific ETS-1 (ESE1/ELF3) regulates apoptosis of intestinal epithelial cells in ulcerative colitis via accelerating NF-kappaB activation. *Immunol Res,* 62**,** 198-212.

LI, L. & XIE, T. 2005. Stem cell niche: structure and function. *Annu Rev Cell Dev Biol,* 21**,** 605-31.

LI, R., PEI, H. & WATSON, D. K. 2000. Regulation of Ets function by protein - protein interactions. *Oncogene,* 19**,** 6514-23.

LI, X., LEWIS, M. T., HUANG, J., GUTIERREZ, C., OSBORNE, C. K., WU, M. F., HILSENBECK, S. G., PAVLICK, A., ZHANG, X., CHAMNESS, G. C., WONG, H., ROSEN, J. & CHANG, J. C. 2008. Intrinsic resistance of tumorigenic breast cancer cells to chemotherapy. *J Natl Cancer Inst,* 100**,** 672-9.

LI, Y., LI, L. J., ZHANG, S. T., WANG, L. J., ZHANG, Z., GAO, N., ZHANG, Y. Y. & CHEN, Q. M. 2009. In vitro and clinical studies of gene therapy with recombinant human adenovirus-p53 injection for oral leukoplakia. *Clin Cancer Res,* 15**,** 6724-31.

LINJA, M. J., SAVINAINEN, K. J., SARAMAKI, O. R., TAMMELA, T. L., VESSELLA, R. L. & VISAKORPI, T. 2001. Amplification and overexpression of androgen receptor gene in hormone-refractory prostate cancer. *Cancer Res,* 61**,** 3550-5.

LINN, D. E., YANG, X., SUN, F., XIE, Y., CHEN, H., JIANG, R., CHEN, H., CHUMSRI, S., BURGER, A. M. & QIU, Y. 2010. A Role for OCT4 in Tumor Initiation of Drug-Resistant Prostate Cancer Cells. *Genes Cancer,* 1**,** 908-16.

LIU, A. Y., COREY, E., VESSELLA, R. L., LANGE, P. H., TRUE, L. D., HUANG, G. M., NELSON, P. S. & HOOD, L. 1997a. Identification of differentially expressed prostate genes: increased expression of transcription factor ETS-2 in prostate cancer. *Prostate,* 30**,** 145-53.

LIU, A. Y., TRUE, L. D., LATRAY, L., NELSON, P. S., ELLIS, W. J., VESSELLA, R. L., LANGE, P. H., HOOD, L. & VAN DEN ENGH, G. 1997b. Cell-cell interaction in prostate gene regulation and cytodifferentiation. *Proc Natl Acad Sci U S A,* 94**,** 10705-10.

LIU, D., SKOMOROVSKA, Y., SONG, J., BOWLER, E., HARRIS, R., RAVASZ, M., BAI, S., AYATI, M., TAMAI, K., KOYUTURK, M., YUAN, X., WANG, Z., WANG, Y. & EWING, R. M. 2018. ELF3 is an antagonist of oncogenic-signalling-induced expression of EMT-TF ZEB1. *Cancer Biol Ther***,** 1-11.

LIU, G., YUAN, X., ZENG, Z., TUNICI, P., NG, H., ABDULKADIR, I. R., LU, L., IRVIN, D., BLACK, K. L. & YU, J. S. 2006. Analysis of gene expression and chemoresistance of CD133+ cancer stem cells in glioblastoma. *Mol Cancer,* 5**,** 67.

LIU, J., PASCAL, L. E., ISHARWAL, S., METZGER, D., RAMOS GARCIA, R., PILCH, J., KASPER, S., WILLIAMS, K., BASSE, P. H., NELSON, J. B., CHAMBON, P. & WANG, Z. 2011. Regenerated luminal epithelial cells are derived from preexisting luminal epithelial cells in adult mouse prostate. *Mol Endocrinol,* 25**,** 1849-57.

LONGONI, N., SARTI, M., ALBINO, D., CIVENNI, G., MALEK, A., ORTELLI, E., PINTON, S., MELLO-GRAND, M., OSTANO, P., D'AMBROSIO, G., SESSA, F., GARCIA-ESCUDERO, R., THALMANN, G. N., CHIORINO, G., CATAPANO, C. V. & CARBONE, G. M. 2013. ETS transcription factor ESE1/ELF3 orchestrates a positive feedback loop that constitutively activates NF-κB and drives prostate cancer progression. *Cancer Research,* 73**,** 4533-4547.

LOU, Z., LEE, B. S., HA, T., XU, Y., KIM, H. J., KIM, C. H. & LEE, S. H. 2018. ESE1 suppresses the growth, invasion and migration of human NSCLC cells and tumor formation in vivo. *Oncol Rep,* 40**,** 1734-1742.

MACKERETH, C. D., SCHARPF, M., GENTILE, L. N., MACINTOSH, S. E., SLUPSKY, C. M. & MCINTOSH, L. P. 2004. Diversity in structure and function of the Ets family PNT domains. *J Mol Biol,* 342**,** 1249-64.

MADJD, Z., MEHRJERDI, A. Z., SHARIFI, A. M., MOLANAEI, S., SHAHZADI, S. Z. & ASADI-LARI, M. 2009. CD44+ cancer cells express higher levels of the anti-apoptotic protein Bcl-2 in breast tumours. *Cancer Immun,* 9**,** 4.

MAITLAND, N. J. & COLLINS, A. T. 2008. Prostate cancer stem cells: A new target for therapy. *Journal of Clinical Oncology,* 26**,** 2862-2870.

MAITLAND, N. J. & COLLINS, A. T. 2014. The Hallmarks of Prostate Cancer Stem Cells. *In:* RAJASEKHAR, V. K. (ed.) *Cancer Stem Cells.* John Wiley & Sons, Inc.

MAITLAND, N. J., FRAME, F. M., POLSON, E. S., LEWIS, J. L. & COLLINS, A. T. 2011. Prostate Cancer Stem Cells: Do They Have a Basal or Luminal Phenotype? *Hormones and Cancer,* 2**,** 47-61.

MAITLAND, N. J., MACINTOSH, C. A., HALL, J., SHARRARD, M., QUINN, G. & LANG, S. 2001. In vitro models to study cellular differentiation and function in human prostate cancers. *Radiat Res,* 155**,** 133-142.

MARCATO, P., DEAN, C. A., PAN, D., ARASLANOVA, R., GILLIS, M., JOSHI, M., HELYER, L., PAN, L., LEIDAL, A., GUJAR, S., GIACOMANTONIO, C. A. & LEE, P. W. 2011. Aldehyde dehydrogenase activity of breast cancer stem cells is primarily due to isoform ALDH1A3 and its expression is predictive of metastasis. *Stem Cells,* 29**,** 32-45.

MARZLUFF, W. F., GONGIDI, P., WOODS, K. R., JIN, J. & MALTAIS, L. J. 2002. The human and mouse replication-dependent histone genes. *Genomics,* 80**,** 487-98.

MAUGERI-SACCA, M., BARTUCCI, M. & DE MARIA, R. 2012. DNA damage repair pathways in cancer stem cells. *Mol Cancer Ther,* 11**,** 1627-36.

MAY, W. A., LESSNICK, S. L., BRAUN, B. S., KLEMSZ, M., LEWIS, B. C., LUNSFORD, L. B., HROMAS, R. & DENNY, C. T. 1993. The Ewing's sarcoma EWS/FLI-1 fusion gene encodes a more potent transcriptional activator and is a more powerful transforming gene than FLI-1. *Mol Cell Biol,* 13**,** 7393-8.

MCCULLOCH, D. R., OPESKIN, K., THOMPSON, E. W. & WILLIAMS, E. D. 2005. BM18: A novel androgen-dependent human prostate cancer xenograft model derived from a bone metastasis. *Prostate,* 65**,** 35-43.

MCDONNELL, T. J., TRONCOSO, P., BRISBAY, S. M., LOGOTHETIS, C., CHUNG, L. W., HSIEH, J. T., TU, S. M. & CAMPBELL, M. L. 1992. Expression of the protooncogene bcl-2 in the prostate and its association with emergence of androgen-independent prostate cancer. *Cancer Res,* 52**,** 6940-4.

MCGRATH, S., CHRISTIDIS, D., PERERA, M., HONG, S. K., MANNING, T., VELA, I. & LAWRENTSCHUK, N. 2016. Prostate cancer biomarkers: Are we hitting the mark? *Prostate Int,* 4**,** 130-135.

MCLEOD, D. G. 2003. Hormonal therapy: historical perspective to future directions. *Urology,* 61**,** 3-7.

MCNEAL, J. E. 1981. The zonal anatomy of the prostate. *Prostate,* 2**,** 35-49.

MEHRA, R., HAN, B., TOMLINS, S. A., WANG, L., MENON, A., WASCO, M. J., SHEN, R., MONTIE, J. E., CHINNAIYAN, A. M. & SHAH, R. B. 2007. Heterogeneity of TMPRSS2 gene rearrangements in multifocal prostate adenocarcinoma: molecular evidence for an independent group of diseases. *Cancer Res,* 67**,** 7991-5.

MEHRA, R., TOMLINS, S. A., YU, J., CAO, X., WANG, L., MENON, A., RUBIN, M. A., PIENTA, K. J., SHAH, R. B. & CHINNAIYAN, A. M. 2008. Characterization of TMPRSS2-ETS gene aberrations in androgen-independent metastatic prostate cancer. *Cancer Res,* 68**,** 3584-90.

MEISSNER, A., MIKKELSEN, T. S., GU, H., WERNIG, M., HANNA, J., SIVACHENKO, A., ZHANG, X., BERNSTEIN, B. E., NUSBAUM, C., JAFFE, D. B., GNIRKE, A., JAENISCH, R. & LANDER, E. S. 2008. Genome-scale DNA methylation maps of pluripotent and differentiated cells. *Nature,* 454**,** 766-70.

MERINO, V. F., NGUYEN, N., JIN, K., SADIK, H., CHO, S., KORANGATH, P., HAN, L., FOSTER, Y. M., ZHOU, X. C., ZHANG, Z., CONNOLLY, R. M., STEARNS, V., ALI, S. Z., ADAMS, C., CHEN, Q., PAN, D., HUSO, D. L., ORDENTLICH, P., BRODIE, A. & SUKUMAR, S. 2016. Combined Treatment with Epigenetic, Differentiating, and Chemotherapeutic Agents Cooperatively Targets Tumor-Initiating Cells in Triple-Negative Breast Cancer. *Cancer Res*.

MITCHELL, S., ABEL, P., WARE, M., STAMP, G. & LALANI, E. 2000. Phenotypic and genotypic characterization of commonly used human prostatic cell lines. *BJU Int,* 85**,** 932-44.

MOASSER, M. M. 2007. Targeting the function of the HER2 oncogene in human cancer therapeutics. *Oncogene,* 26**,** 6577-92.

MOGNETTI, B., LA MONTAGNA, G., PERRELLI, M. G., PAGLIARO, P. & PENNA, C. 2013. Bone marrow mesenchymal stem cells increase motility of prostate cancer

cells via production of stromal cell-derived factor-1alpha. *J Cell Mol Med,* 17**,** 287-92.

MOITRA, K., LOU, H. & DEAN, M. 2011. Multidrug efflux pumps and cancer stem cells: insights into multidrug resistance and therapeutic development. *Clin Pharmacol Ther,* 89**,** 491-502.

MOORE, C. M., PENDSE, D. & EMBERTON, M. 2009. Photodynamic therapy for prostate cancer--a review of current status and future promise. *Nat Clin Pract Urol,* 6**,** 18-30.

MORGANTI, G., GIANFERRARI, L., CRESSERI, A., ARRIGONI, G. & LOVATI, G. 1956. [Clinico-statistical and genetic research on neoplasms of the prostate]. *Acta Genet Stat Med,* 6**,** 304-5.

MORRISON, R., SCHLEICHER, S. M., SUN, Y., NIERMANN, K. J., KIM, S., SPRATT, D. E., CHUNG, C. H. & LU, B. 2011. Targeting the mechanisms of resistance to chemotherapy and radiotherapy with the cancer stem cell hypothesis. *J Oncol,* 2011**,** 941876.

MORRISSEY, C. & VESSELLA, R. L. 2007. The role of tumor microenvironment in prostate cancer bone metastasis. *J Cell Biochem,* 101**,** 873-86.

MOTTET, N., BELLMUNT, J., BOLLA, M., BRIERS, E., CUMBERBATCH, M. G., DE SANTIS, M., FOSSATI, N., GROSS, T., HENRY, A. M., JONIAU, S., LAM, T. B., MASON, M. D., MATVEEV, V. B., MOLDOVAN, P. C., VAN DEN BERGH, R. C. N., VAN DEN BROECK, T., VAN DER POEL, H. G., VAN DER KWAST, T. H., ROUVIERE, O., SCHOOTS, I. G., WIEGEL, T. & CORNFORD, P. 2017. EAU-ESTRO-SIOG Guidelines on Prostate Cancer. Part 1: Screening, Diagnosis, and Local Treatment with Curative Intent. *Eur Urol,* 71**,** 618-629.

MOUSSA, O., TURNER, D. P., FELDMAN, R. J., SEMENTCHENKO, V. I., MCCARRAGHER, B. D., DESOUKI, M. M., FRAIG, M. & WATSON, D. K. 2009. PDEF is a negative regulator of colon cancer cell growth and migration. *J Cell Biochem,* 108**,** 1389-98.

MURPHY, A. B., MACEJKO, A., TAYLOR, A. & NADLER, R. B. 2009. Chronic prostatitis: management strategies. *Drugs,* 69**,** 71-84.

NADAL, E. & OLAVARRIA, E. 2004. Imatinib mesylate (Gleevec/Glivec) a molecular-targeted therapy for chronic myeloid leukaemia and other malignancies. *Int J Clin Pract,* 58**,** 511-6.

NAKARAI, C., OSAWA, K., MATSUBARA, N., IKEUCHI, H., YAMANO, T., OKAMURA, S., KAMOSHIDA, S., TSUTOU, A., TAKAHASHI, J., EJIRI, K., HIROTA, S., TOMITA, N. & KIDO, Y. 2012. Significance of ELF3 mRNA expression for detection of lymph node metastases of colorectal cancer. *Anticancer Res,* 32**,** 3753-8.

NAKAYAMA, T., ITO, M., OHTSURU, A., NAITO, S. & SEKINE, I. 2001. Expression of the ets-1 proto-oncogene in human colorectal carcinoma. *Mod Pathol,* 14**,** 415-22.

NAM, J. M., JEON, K. H., KWON, H., LEE, E., JUN, K. Y., JIN, Y. B., LEE, Y. S., NA, Y. & KWON, Y. 2013. Dithiiranylmethyloxy azaxanthone shows potent anti-tumor activity via suppression of HER2 expression and HER2-mediated signals in HER2-overexpressing breast cancer cells. *Eur J Pharm Sci,* 50**,** 181-90.

NAPOLI, A., ANZIDEI, M., DE NUNZIO, C., CARTOCCI, G., PANEBIANCO, V., DE DOMINICIS, C., CATALANO, C., PETRUCCI, F. & LEONARDO, C. 2013. Real-time magnetic resonance-guided high-intensity focused ultrasound focal therapy for localised prostate cancer: preliminary experience. *Eur Urol,* 63**,** 395-8.

NG, A. Y., WARING, P., RISTEVSKI, S., WANG, C., WILSON, T., PRITCHARD, M., HERTZOG, P. & KOLA, I. 2002. Inactivation of the transcription factor Elf3 in mice results in dysmorphogenesis and altered differentiation of intestinal epithelium. *Gastroenterology,* 122**,** 1455-66.

NICKEL, J. C., DOWNEY, J., YOUNG, I. & BOAG, S. 1999. Asymptomatic inflammation and/or infection in benign prostatic hyperplasia. *BJU Int,* 84**,** 976-81.

NICKEL, J. C., ROEHRBORN, C. G., O'LEARY, M. P., BOSTWICK, D. G., SOMERVILLE, M. C. & RITTMASTER, R. S. 2008. The relationship between prostate inflammation and lower urinary tract symptoms: examination of baseline data from the REDUCE trial. *Eur Urol,* 54**,** 1379-84.

NOAH, T. K., KAZANJIAN, A., WHITSETT, J. & SHROYER, N. F. 2010. SAM pointed domain ETS factor (SPDEF) regulates terminal differentiation and maturation of intestinal goblet cells. *Exp Cell Res,* 316**,** 452-65.

NOMURA, T. & MIMATA, H. 2012. Focal therapy in the management of prostate cancer: an emerging approach for localized prostate cancer. *Adv Urol,* 2012**,** 391437.

NOWESKI, A., ROOSEN, A., LEBDAI, S., BARRET, E., EMBERTON, M., BENZAGHOU, F., APFELBECK, M., GAILLAC, B., GRATZKE, C., STIEF, C. & AZZOUZI, A. R. 2018. Medium-term Follow-up of Vascular-targeted Photodynamic Therapy of Localized Prostate Cancer Using TOOKAD Soluble WST-11 (Phase II Trials). *Eur Urol Focus*.

OBORT, A. S., AJADI, M. B. & AKINLOYE, O. 2013. Prostate-specific antigen: any successor in sight? *Rev Urol,* 15**,** 97-107.

OETTGEN, P., ALANI, R. M., BARCINSKI, M. A., BROWN, L., AKBARALI, Y., BOLTAX, J., KUNSCH, C., MUNGER, K. & LIBERMANN, T. A. 1997. Isolation and characterization of a novel epithelium-specific transcription factor, ESE-1, a member of the ets family. *Mol Cell Biol,* 17**,** 4419-33.

OETTGEN, P., FINGER, E., SUN, Z., AKBARALI, Y., THAMRONGSAK, U., BOLTAX, J., GRALL, F., DUBE, A., WEISS, A., BROWN, L., QUINN, G., KAS, K., ENDRESS, G., KUNSCH, C. & LIBERMANN, T. A. 2000. PDEF, a novel prostate epithelium-specific ets transcription factor, interacts with the androgen receptor and activates prostate-specific antigen gene expression. *J Biol Chem,* 275**,** 1216-25.

OIKAWA, T. & YAMADA, T. 2003. Molecular biology of the Ets family of transcription factors. *Gene,* 303**,** 11-34.

OLDRIDGE, E. E., PELLACANI, D., COLLINS, A. T. & MAITLAND, N. J. 2012. Prostate cancer stem cells: Are they androgen-responsive? *Molecular and Cellular Endocrinology,* 360**,** 14-24.

ONCOMED PHARMACEUTICALS. 2016. *OncoMed Provides Update on Tarextumab Phase 2 Pancreatic Cancer ALPINE Trial* [Online]. Available:

https://globenewswire.com/news-release/2016/01/25/804294/0/en/OncoMed-Provides-Update-on-Tarextumab-Phase-2-Pancreatic-Cancer-ALPINE-Trial.html [Accessed 11th Sept 2018].

ONCOMED PHARMACEUTICALS. 2017. *OncoMed's Phase 2 Trial Of Tarextumab In Small Cell Lung Cancer Does Not Meet Endpoints* [Online]. Available: https://www.clinicalleader.com/doc/oncomed-s-phase-trial-tarextumab-in-small-cell-lung-cancer-meet-endpoints-0001 [Accessed 11th Sept 2018].

PANAGOPOULOS, I., AMAN, P., FIORETOS, T., HOGLUND, M., JOHANSSON, B., MANDAHL, N., HEIM, S., BEHRENDTZ, M. & MITELMAN, F. 1994. Fusion of the FUS gene with ERG in acute myeloid leukemia with t(16;21)(p11;q22). *Genes Chromosomes Cancer,* 11**,** 256-62.

PARIMI, V., GOYAL, R., POROPATICH, K. & YANG, X. J. 2014. Neuroendocrine differentiation of prostate cancer: a review. *Am J Clin Exp Urol,* 2**,** 273-85.

PARK, P. C., SELVARAJAH, S., BAYANI, J., ZIELENSKA, M. & SQUIRE, J. A. 2007. Stem cell enrichment approaches. *Semin Cancer Biol,* 17**,** 257-64.

PARK, S. W., DO, H. J., HA, W. T., HAN, M. H., YANG, H. M., LEE, S. H., SONG, H., KIM, N. H. & KIM, J. H. 2014. Transcriptional regulation of OCT4 by the ETS transcription factor ESE-1 in NCCIT human embryonic carcinoma cells. *Biochem Biophys Res Commun,* 450**,** 984-90.

PASCAL, L. E., OUDES, A. J., PETERSEN, T. W., GOO, Y. A., WALASHEK, L. S., TRUE, L. D. & LIU, A. Y. 2007. Molecular and cellular characterization of ABCG2 in the prostate. *BMC Urol,* 7**,** 6.

PATRAWALA, L., CALHOUN, T., SCHNEIDER-BROUSSARD, R., LI, H., BHATIA, B., TANG, S., REILLY, J. G., CHANDRA, D., ZHOU, J., CLAYPOOL, K., COGHLAN, L. & TANG, D. G. 2006. Highly purified CD44+ prostate cancer cells from xenograft human tumors are enriched in tumorigenic and metastatic progenitor cells. *Oncogene,* 25**,** 1696-708.

PEAR, W. S., NOLAN, G. P., SCOTT, M. L. & BALTIMORE, D. 1993. Production of high-titer helper-free retroviruses by transient transfection. *Proc Natl Acad Sci U S A,* 90**,** 8392-6.

PEELING, W. B. 1989. Phase III studies to compare goserelin (Zoladex) with orchiectomy and with diethylstilbestrol in treatment of prostatic carcinoma. *Urology,* 33**,** 45-52.

PELLACANI, D., KESTORAS, D., DROOP, A. P., FRAME, F. M., BERRY, P. A., LAWRENCE, M. G., STOWER, M. J., SIMMS, M. S., MANN, V. M., COLLINS, A. T., RISBRIDGER, G. P. & MAITLAND, N. J. 2014. DNA hypermethylation in prostate cancer is a consequence of aberrant epithelial differentiation and hyperproliferation. *Cell Death and Differentiation,* 21**,** 761-773.

PERNER, S., DEMICHELIS, F., BEROUKHIM, R., SCHMIDT, F. H., MOSQUERA, J. M., SETLUR, S., TCHINDA, J., TOMLINS, S. A., HOFER, M. D., PIENTA, K. G., KUEFER, R., VESSELLA, R., SUN, X. W., MEYERSON, M., LEE, C., SELLERS, W. R., CHINNAIYAN, A. M. & RUBIN, M. A. 2006. TMPRSS2:ERG fusion-

associated deletions provide insight into the heterogeneity of prostate cancer. *Cancer Res,* 66**,** 8337-41.

PETRONCZKI, M., LENART, P. & PETERS, J. M. 2008. Polo on the Rise-from Mitotic Entry to Cytokinesis with Plk1. *Dev Cell,* 14**,** 646-59.

PEZARO, C. J., OMLIN, A. G., ALTAVILLA, A., LORENTE, D., FERRALDESCHI, R., BIANCHINI, D., DEARNALEY, D., PARKER, C., DE BONO, J. S. & ATTARD, G. 2014. Activity of cabazitaxel in castration-resistant prostate cancer progressing after docetaxel and next-generation endocrine agents. *Eur Urol,* 66**,** 459-65.

POLSON, E. S., LEWIS, J. L., CELIK, H., MANN, V. M., STOWER, M. J., SIMMS, M. S., RODRIGUES, G., COLLINS, A. T. & MAITLAND, N. J. 2013. Monoallelic expression of TMPRSS2/ERG in prostate cancer stem cells. *Nat Commun,* 4**,** 1623.

POLYAK, K. & WEINBERG, R. A. 2009. Transitions between epithelial and mesenchymal states: acquisition of malignant and stem cell traits. *Nat Rev Cancer,* 9**,** 265-73.

PONTEN, J. & MACINTYRE, E. H. 1968. Long term culture of normal and neoplastic human glia. *Acta Pathol Microbiol Scand,* 74**,** 465-86.

POTTER, S. R. & PARTIN, A. W. 2000. Hereditary and familial prostate cancer: biologic aggressiveness and recurrence. *Rev Urol,* 2**,** 35-6.

PRABHU, V. V., ALLEN, J. E., HONG, B., ZHANG, S., CHENG, H. & EL-DEIRY, W. S. 2012. Therapeutic targeting of the p53 pathway in cancer stem cells. *Expert Opin Ther Targets,* 16**,** 1161-74.

PRESCOTT, J. D., KOTO, K. S., SINGH, M. & GUTIERREZ-HARTMANN, A. 2004. The ETS transcription factor ESE-1 transforms MCF-12A human mammary epithelial cells via a novel cytoplasmic mechanism. *Mol Cell Biol,* 24**,** 5548-64.

PRESCOTT, J. D., POCZOBUTT, J. M., TENTLER, J. J., WALKER, D. M. & GUTIERREZ-HARTMANN, A. 2011. Mapping of ESE-1 subdomains required to initiate mammary epithelial cell transformation via a cytoplasmic mechanism. *Mol Cancer,* 10**,** 103.

PUCK, T. T. & MARCUS, P. I. 1956. Action of x-rays on mammalian cells. *J Exp Med,* 103**,** 653-66.

QUINN, M. & BABB, P. 2002. Patterns and trends in prostate cancer incidence, survival, prevalence and mortality. Part I: international comparisons. *BJU Int,* 90**,** 162-73.

QUINTANA, E., SHACKLETON, M., SABEL, M. S., FULLEN, D. R., JOHNSON, T. M. & MORRISON, S. J. 2008. Efficient tumour formation by single human melanoma cells. *Nature,* 456**,** 593-8.

R CORE TEAM. 2014. *R: A language and environment for statistical computing.* [Online]. R Foundation for Statistical Computing, Vienna, Austria. Available: http://www.R-project.org/. [Accessed].

RAHIM, S., BEAUCHAMP, E. M., KONG, Y., BROWN, M. L., TORETSKY, J. A. & UREN, A. 2011. YK-4-279 inhibits ERG and ETV1 mediated prostate cancer cell invasion. *PLoS One,* 6**,** e19343.

RAJPUT, A. B., MILLER, M. A., DE LUCA, A., BOYD, N., LEUNG, S., HURTADO-COLL, A., FAZLI, L., JONES, E. C., PALMER, J. B., GLEAVE, M. E., COX, M. E. & HUNTSMAN, D. G. 2007. Frequency of the TMPRSS2:ERG gene fusion is increased in moderate to poorly differentiated prostate cancers. *J Clin Pathol,* 60**,** 1238-43.

RAMSAY, C. R., ADEWUYI, T. E., GRAY, J., HISLOP, J., SHIRLEY, M. D., JAYAKODY, S., MACLENNAN, G., FRASER, C., MACLENNAN, S., BRAZZELLI, M., N'DOW, J., PICKARD, R., ROBERTSON, C., ROTHNIE, K., RUSHTON, S. P., VALE, L. & LAM, T. B. 2015. Ablative therapy for people with localised prostate cancer: a systematic review and economic evaluation. *Health Technol Assess,* 19**,** 1-490.

RANE, J. K., PELLACANI, D. & MAITLAND, N. J. 2012. Advanced prostate cancer - A case for adjuvant differentiation therapy. *Nature Reviews Urology,* 9**,** 595-602.

RANE, J. K., SCARAVILLI, M., YLIPAA, A., PELLACANI, D., MANN, V. M., SIMMS, M. S., NYKTER, M., COLLINS, A. T., VISAKORPI, T. & MAITLAND, N. J. 2015. MicroRNA expression profile of primary prostate cancer stem cells as a source of biomarkers and therapeutic targets. *Eur Urol,* 67**,** 7-10.

REEVES, R. 2000. Structure and function of the HMGI(Y) family of architectural transcription factors. *Environ Health Perspect,* 108 Suppl 5**,** 803-9.

RICHARDSON, G. D., ROBSON, C. N., LANG, S. H., NEAL, D. E., MAITLAND, N. J. & COLLINS, A. T. 2004. CD133, a novel marker for human prostatic epithelial stem cells. *J Cell Sci,* 117**,** 3539-45.

RITCHIE, M. E., PHIPSON, B., WU, D., HU, Y., LAW, C. W., SHI, W. & SMYTH, G. K. 2015. limma powers differential expression analyses for RNA-sequencing and microarray studies. *Nucleic Acids Res,* 43**,** e47.

ROEHRBORN, C. G. 2008. Pathology of benign prostatic hyperplasia. *Int J Impot Res,* 20 Suppl 3**,** S11-8.

ROKHLIN, O. W., GLOVER, R. B., GUSEVA, N. V., TAGHIYEV, A. F., KOHLGRAF, K. G. & COHEN, M. B. 2006. Mechanisms of cell death induced by histone deacetylase inhibitors in androgen receptor-positive prostate cancer cells. *Mol Cancer Res,* 4**,** 113-23.

ROMERO OTERO, J., GARCIA GOMEZ, B., CAMPOS JUANATEY, F. & TOUIJER, K. A. 2014. Prostate cancer biomarkers: an update. *Urol Oncol,* 32**,** 252-60.

RUDDERS, S., GASPAR, J., MADORE, R., VOLAND, C., GRALL, F., PATEL, A., PELLACANI, A., PERRELLA, M. A., LIBERMANN, T. A. & OETTGEN, P. 2001. ESE-1 is a novel transcriptional mediator of inflammation that interacts with NF-kappa B to regulate the inducible nitric-oxide synthase gene. *J Biol Chem,* 276**,** 3302-9.

RUMPOLD, H., HEINRICH, E., UNTERGASSER, G., HERMANN, M., PFISTER, G., PLAS, E. & BERGER, P. 2002. Neuroendocrine differentiation of human prostatic primary epithelial cells in vitro. *Prostate,* 53**,** 101-8.

RUSSELL, L. & GARRETT-SINHA, L. A. 2010. Transcription factor Ets-1 in cytokine and chemokine gene regulation. *Cytokine,* 51**,** 217-26.

SANZ, M. A., GRIMWADE, D., TALLMAN, M. S., LOWENBERG, B., FENAUX, P., ESTEY, E. H., NAOE, T., LENGFELDER, E., BUCHNER, T., DOHNER, H., BURNETT, A. K. & LO-COCO, F. 2009. Management of acute promyelocytic leukemia: recommendations from an expert panel on behalf of the European LeukemiaNet. *Blood,* 113**,** 1875-91.

SASAKI, T., KOMIYA, A., SUZUKI, H., SHIMBO, M., UEDA, T., AKAKURA, K. & ICHIKAWA, T. 2005. Changes in chromogranin a serum levels during endocrine therapy in metastatic prostate cancer patients. *Eur Urol,* 48**,** 224-9; discussion 229-30.

SATHIANATHEN, N. J., KONETY, B. R., CROOK, J., SAAD, F. & LAWRENTSCHUK, N. 2018. Landmarks in prostate cancer. *Nat Rev Urol*.

SCHALKEN, J. A. & VAN LEENDERS, G. 2003. Cellular and molecular biology of the prostate: stem cell biology. *Urology,* 62**,** 11-20.

SCHEDIN, P. J., ECKEL-MAHAN, K. L., MCDANIEL, S. M., PRESCOTT, J. D., BRODSKY, K. S., TENTLER, J. J. & GUTIERREZ-HARTMANN, A. 2004. ESX induces transformation and functional epithelial to mesenchymal transition in MCF-12A mammary epithelial cells. *Oncogene,* 23**,** 1766-79.

SCHEEL, C. & WEINBERG, R. A. 2011. Phenotypic plasticity and epithelial-mesenchymal transitions in cancer and normal stem cells? *Int J Cancer,* 129**,** 2310-4.

SCHER, H. I., FIZAZI, K., SAAD, F., TAPLIN, M. E., STERNBERG, C. N., MILLER, K., DE WIT, R., MULDERS, P., CHI, K. N., SHORE, N. D., ARMSTRONG, A. J., FLAIG, T. W., FLECHON, A., MAINWARING, P., FLEMING, M., HAINSWORTH, J. D., HIRMAND, M., SELBY, B., SEELY, L. & DE BONO, J. S. 2012. Increased survival with enzalutamide in prostate cancer after chemotherapy. *N Engl J Med,* 367**,** 1187-97.

SCOTT, E. W., SIMON, M. C., ANASTASI, J. & SINGH, H. 1994. Requirement of transcription factor PU.1 in the development of multiple hematopoietic lineages. *Science,* 265**,** 1573-7.

SEIDEL, J. J. & GRAVES, B. J. 2002. An ERK2 docking site in the Pointed domain distinguishes a subset of ETS transcription factors. *Genes Dev,* 16**,** 127-37.

SEIDENFELD, J., SAMSON, D. J., HASSELBLAD, V., ARONSON, N., ALBERTSEN, P. C., BENNETT, C. L. & WILT, T. J. 2000. Single-therapy androgen suppression in men with advanced prostate cancer: a systematic review and meta-analysis. *Ann Intern Med,* 132**,** 566-77.

SEMENTCHENKO, V. I., SCHWEINFEST, C. W., PAPAS, T. S. & WATSON, D. K. 1998. ETS2 function is required to maintain the transformed state of human prostate cancer cells. *Oncogene,* 17**,** 2883-8.

SERUGA, B. & TANNOCK, I. F. 2011. Chemotherapy-based treatment for castration-resistant prostate cancer. *J Clin Oncol,* 29**,** 3686-94.

SETH, A. & WATSON, D. K. 2005. ETS transcription factors and their emerging roles in human cancer. *Eur J Cancer,* 41**,** 2462-78.

SHAHI, P., SEETHAMMAGARI, M. R., VALDEZ, J. M., XIN, L. & SPENCER, D. M. 2011. Wnt and Notch pathways have interrelated opposing roles on prostate progenitor cell proliferation and differentiation. *Stem Cells,* 29**,** 678-88.

SHAIKHIBRAHIM, Z., LINDSTROT, A., LANGER, B., BUETTNER, R. & WERNERT, N. 2011a. Comprehensive gene expression microarray analysis of Ets-1 blockade in PC3 prostate cancer cells and correlations with prostate cancer tissues: Insights into genes involved in the metastatic cascade. *Int J Mol Med,* 27**,** 811-9.

SHAIKHIBRAHIM, Z., LINDSTROT, A., LANGER, B., BUETTNER, R. & WERNERT, N. 2011b. Differential expression of ETS family members in prostate cancer tissues and androgen-sensitive and insensitive prostate cancer cell lines. *Int J Mol Med,* 28**,** 89-93.

SHAIKHIBRAHIM, Z. & WERNERT, N. 2012. ETS transcription factors and prostate cancer: the role of the family prototype ETS-1 (review). *Int J Oncol,* 40**,** 1748-54.

SHAO, L., TEKEDERELI, I., WANG, J., YUCA, E., TSANG, S., SOOD, A., LOPEZ-BERESTEIN, G., OZPOLAT, B. & ITTMANN, M. 2012. Highly specific targeting of the TMPRSS2/ERG fusion gene using liposomal nanovectors. *Clin Cancer Res,* 18**,** 6648-57.

SHARROCKS, A. D. 2001. The ETS-domain transcription factor family. *Nat Rev Mol Cell Biol,* 2**,** 827-37.

SHATNAWI, A., NORRIS, J. D., CHAVEROUX, C., JASPER, J. S., SHERK, A. B., MCDONNELL, D. P. & GIGUÈRE, V. 2014. ELF3 is a repressor of androgen receptor action in prostate cancer cells. *Oncogene,* 33**,** 862-871.

SHAW, A. & BUSHMAN, W. 2007. Hedgehog signaling in the prostate. *J Urol,* 177**,** 832-8.

SHEN, M. M. & ABATE-SHEN, C. 2010. Molecular genetics of prostate cancer: new prospects for old challenges. *Genes Dev,* 24**,** 1967-2000.

SHEN, R., DORAI, T., SZABOLES, M., KATZ, A. E., OLSSON, C. A. & BUTTYAN, R. 1997. Transdifferentiation of cultured human prostate cancer cells to a neuroendocrine cell phenotype in a hormone-depleted medium. *Urol Oncol,* 3**,** 67-75.

SHIMOGAWA, H., KWON, Y., MAO, Q., KAWAZOE, Y., CHOI, Y., ASADA, S., KIGOSHI, H. & UESUGI, M. 2004. A wrench-shaped synthetic molecule that modulates a transcription factor-coactivator interaction. *J Am Chem Soc,* 126**,** 3461-71.

SHIN, S. Y., RATH, O., ZEBISCH, A., CHOO, S. M., KOLCH, W. & CHO, K. H. 2010. Functional roles of multiple feedback loops in extracellular signal-regulated kinase and Wnt signaling pathways that regulate epithelial-mesenchymal transition. *Cancer Res,* 70**,** 6715-24.

SHORE, N. D. 2013. Experience with degarelix in the treatment of prostate cancer. *Ther Adv Urol,* 5**,** 11-24.

SHULTZ, L. D., SCHWEITZER, P. A., CHRISTIANSON, S. W., GOTT, B., SCHWEITZER, I. B., TENNENT, B., MCKENNA, S., MOBRAATEN, L., RAJAN, T. V., GREINER, D. L. & ET AL. 1995. Multiple defects in innate and adaptive immunologic function in NOD/LtSz-scid mice. *J Immunol,* 154**,** 180-91.

SIGNORETTI, S., PIRES, M. M., LINDAUER, M., HORNER, J. W., GRISANZIO, C., DHAR, S., MAJUMDER, P., MCKEON, F., KANTOFF, P. W., SELLERS, W. R. & LODA, M. 2005. p63 regulates commitment to the prostate cell lineage. *Proc Natl Acad Sci U S A,* 102**,** 11355-60.

SIGNORETTI, S., WALTREGNY, D., DILKS, J., ISAAC, B., LIN, D., GARRAWAY, L., YANG, A., MONTIRONI, R., MCKEON, F. & LODA, M. 2000. p63 is a prostate basal cell marker and is required for prostate development. *Am J Pathol,* 157**,** 1769-75.

SIMONS, B. W., HURLEY, P. J., HUANG, Z., ROSS, A. E., MILLER, R., MARCHIONNI, L., BERMAN, D. M. & SCHAEFFER, E. M. 2012. Wnt signaling though beta-catenin is required for prostate lineage specification. *Dev Biol,* 371**,** 246-55.

SIMPSON, R. J. 1997. Benign prostatic hyperplasia. *Br J Gen Pract,* 47**,** 235-40.

SINGAREDDY, R., SEMAAN, L., CONLEY-LACOMB, M. K., ST JOHN, J., POWELL, K., IYER, M., SMITH, D., HEILBRUN, L. K., SHI, D., SAKR, W., CHER, M. L. & CHINNI, S. R. 2013. Transcriptional regulation of CXCR4 in prostate cancer: significance of TMPRSS2-ERG fusions. *Mol Cancer Res,* 11**,** 1349-61.

SINGH, S. K., CLARKE, I. D., TERASAKI, M., BONN, V. E., HAWKINS, C., SQUIRE, J. & DIRKS, P. B. 2003. Identification of a cancer stem cell in human brain tumors. *Cancer Res,* 63**,** 5821-8.

SINH, N. D., ENDO, K., MIYAZAWA, K. & SAITOH, M. 2017. Ets1 and ESE1 reciprocally regulate expression of ZEB1/ZEB2, dependent on ERK1/2 activity, in breast cancer cells. *Cancer Sci,* 108**,** 952-960.

SMITH, A. M., FINDLAY, V. J., BANDURRAGA, S. G., KISTNER-GRIFFIN, E., SPRUILL, L. S., LIU, A., GOLSHAYAN, A. R. & TURNER, D. P. 2012. ETS1 transcriptional activity is increased in advanced prostate cancer and promotes the castrate-resistant phenotype. *Carcinogenesis,* 33**,** 572-80.

SMITH, B. A., SOKOLOV, A., UZUNANGELOV, V., BAERTSCH, R., NEWTON, Y., GRAIM, K., MATHIS, C., CHENG, D., STUART, J. M. & WITTE, O. N. 2015. A basal stem cell signature identifies aggressive prostate cancer phenotypes. *Proc Natl Acad Sci U S A*.

SMITH, M. R., BIGGAR, S. & HUSSAIN, M. 1995. Prostate-specific antigen messenger RNA is expressed in non-prostate cells: implications for detection of micrometastases. *Cancer Res,* 55**,** 2640-4.

SNEDDON, J. B. & WERB, Z. 2007. Location, location, location: the cancer stem cell niche. *Cell Stem Cell,* 1**,** 607-11.

SOBEL, R. E. & SADAR, M. D. 2005. CELL LINES USED IN PROSTATE CANCER RESEARCH: A COMPENDIUM OF OLD AND NEW LINES—PART 1. *The Journal of Urology,* 173**,** 342-359.

SOOD, A. K., SAXENA, R., GROTH, J., DESOUKI, M. M., CHEEWAKRIANGKRAI, C., RODABAUGH, K. J., KASYAPA, C. S. & GERADTS, J. 2007. Expression characteristics of prostate-derived Ets factor support a role in breast and prostate cancer progression. *Hum Pathol,* 38**,** 1628-38.

SPIOTTO, M. T. & CHUNG, T. D. 2000. STAT3 mediates IL-6-induced neuroendocrine differentiation in prostate cancer cells. *Prostate,* 42**,** 186-95.

SRAMKOSKI, R. M., PRETLOW, T. G., 2ND, GIACONIA, J. M., PRETLOW, T. P., SCHWARTZ, S., SY, M. S., MARENGO, S. R., RHIM, J. S., ZHANG, D. & JACOBBERGER, J. W. 1999. A new human prostate carcinoma cell line, 22Rv1. *In Vitro Cell Dev Biol Anim,* 35**,** 403-9.

STANFORD, J. L. & OSTRANDER, E. A. 2001. Familial prostate cancer. *Epidemiol Rev,* 23**,** 19-23.

STEFFAN, J. J. & KOUL, H. K. 2011. Prostate derived ETS factor (PDEF): a putative tumor metastasis suppressor. *Cancer Lett,* 310**,** 109-17.

STEGH, A. H. 2012. Targeting the p53 signaling pathway in cancer therapy - the promises, challenges and perils. *Expert Opin Ther Targets,* 16**,** 67-83.

STEPHENSON, R. A., DINNEY, C. P., GOHJI, K., ORDONEZ, N. G., KILLION, J. J. & FIDLER, I. J. 1992. Metastatic model for human prostate cancer using orthotopic implantation in nude mice. *J Natl Cancer Inst,* 84**,** 951-7.

STIELER, K., SCHUMACHER, U., HORST, A. K. & FISCHER, N. 2012. XMRV induces cell migration, cytokine expression and tumor angiogenesis: are 22Rv1 cells a suitable prostate cancer model? *PLoS One,* 7**,** e42321.

SUN, C., DOBI, A., MOHAMED, A., LI, H., THANGAPAZHAM, R. L., FURUSATO, B., SHAHEDUZZAMAN, S., TAN, S. H., VAIDYANATHAN, G., WHITMAN, E., HAWKSWORTH, D. J., CHEN, Y., NAU, M., PATEL, V., VAHEY, M., GUTKIND, J. S., SREENATH, T., PETROVICS, G., SESTERHENN, I. A., MCLEOD, D. G. & SRIVASTAVA, S. 2008. TMPRSS2-ERG fusion, a common genomic alteration in prostate cancer activates C-MYC and abrogates prostate epithelial differentiation. *Oncogene,* 27**,** 5348-53.

SUN, Y. X., WANG, J., SHELBURNE, C. E., LOPATIN, D. E., CHINNAIYAN, A. M., RUBIN, M. A., PIENTA, K. J. & TAICHMAN, R. S. 2003. Expression of CXCR4 and CXCL12 (SDF-1) in human prostate cancers (PCa) in vivo. *J Cell Biochem,* 89**,** 462-73.

SVENSSON, M. A., LAFARGUE, C. J., MACDONALD, T. Y., PFLUEGER, D., KITABAYASHI, N., SANTA-CRUZ, A. M., GARSHA, K. E., SATHYANARAYANA, U. G., RILEY, J. P., YUN, C. S., NAGY, D., KOSMEDER, J. W., PESTANO, G. A., TEWARI, A. K., DEMICHELIS, F. & RUBIN, M. A. 2011. Testing mutual exclusivity of ETS rearranged prostate cancer. *Lab Invest,* 91**,** 404-12.

TAI, S., SUN, Y., SQUIRES, J. M., ZHANG, H., OH, W. K., LIANG, C. Z. & HUANG, J. 2011. PC3 is a cell line characteristic of prostatic small cell carcinoma. *Prostate,* 71**,** 1668-79.

TAKAI, N., MIYAZAKI, T., FUJISAWA, K., NASU, K. & MIYAKAWA, I. 2000. Expression of c-Ets1 is associated with malignant potential in endometrial carcinoma. *Cancer,* 89**,** 2059-67.

TAKEBE, N., HARRIS, P. J., WARREN, R. Q. & IVY, S. P. 2011. Targeting cancer stem cells by inhibiting Wnt, Notch, and Hedgehog pathways. *Nat Rev Clin Oncol,* 8**,** 97-106.

TAPLIN, M. E., BUBLEY, G. J., KO, Y. J., SMALL, E. J., UPTON, M., RAJESHKUMAR, B. & BALK, S. P. 1999. Selection for androgen receptor mutations in prostate cancers treated with androgen antagonist. *Cancer Res,* 59**,** 2511-5.

TAUROZZI, A. J., BEEKHARRY, R., WANTOCH, M., LABARTHE, M. C., WALKER, H. F., SEED, R. I., SIMMS, M., RODRIGUES, G., BRADFORD, J., VAN DER HORST, G., VAN DER PLUIJM, G. & COLLINS, A. T. 2017. Spontaneous development of Epstein-Barr Virus associated human lymphomas in a prostate cancer xenograft program. *PLoS One,* 12**,** e0188228.

TAYLOR, B. S., SCHULTZ, N., HIERONYMUS, H., GOPALAN, A., XIAO, Y., CARVER, B. S., ARORA, V. K., KAUSHIK, P., CERAMI, E., REVA, B., ANTIPIN, Y., MITSIADES, N., LANDERS, T., DOLGALEV, I., MAJOR, J. E., WILSON, M., SOCCI, N. D., LASH, A. E., HEGUY, A., EASTHAM, J. A., SCHER, H. I., REUTER, V. E., SCARDINO, P. T., SANDER, C., SAWYERS, C. L. & GERALD, W. L. 2010. Integrative genomic profiling of human prostate cancer. *Cancer Cell,* 18**,** 11-22.

TAYLOR, R. A., TOIVANEN, R., FRYDENBERG, M., PEDERSEN, J., HAREWOOD, L., COLLINS, A. T., MAITLAND, N. J. & RISBRIDGER, G. P. 2012. Human epithelial basal cells are cells of origin of prostate cancer, independent of CD133 status. *Stem Cells,* 30**,** 1087-1096.

TERPE, H. J., STARK, H., PREHM, P. & GUNTHERT, U. 1994. CD44 variant isoforms are preferentially expressed in basal epithelial of non-malignant human fetal and adult tissues. *Histochemistry,* 101**,** 79-89.

TERRY, S. & BELTRAN, H. 2014. The many faces of neuroendocrine differentiation in prostate cancer progression. *Front Oncol,* 4**,** 60.

THALMANN, G. N., RHEE, H., SIKES, R. A., PATHAK, S., MULTANI, A., ZHAU, H. E., MARSHALL, F. F. & CHUNG, L. W. 2010. Human prostate fibroblasts induce growth and confer castration resistance and metastatic potential in LNCaP Cells. *Eur Urol,* 58**,** 162-71.

THIERY, J. P., ACLOQUE, H., HUANG, R. Y. & NIETO, M. A. 2009. Epithelial-mesenchymal transitions in development and disease. *Cell,* 139**,** 871-90.

THIRANT, C., BESSETTE, B., VARLET, P., PUGET, S., CADUSSEAU, J., TAVARES SDOS, R., STUDLER, J. M., SILVESTRE, D. C., SUSINI, A., VILLA, C., MIQUEL, C., BOGEAS, A., SURENA, A. L., DIAS-MORAIS, A., LEONARD, N., PFLUMIO, F., BIECHE, I., BOUSSIN, F. D., SAINTE-ROSE, C., GRILL, J., DAUMAS-DUPORT, C., CHNEIWEISS, H. & JUNIER, M. P. 2011. Clinical relevance of tumor cells with stem-like properties in pediatric brain tumors. *PLoS One,* 6**,** e16375.

THOMPSON, I. M., GOODMAN, P. J., TANGEN, C. M., LUCIA, M. S., MILLER, G. J., FORD, L. G., LIEBER, M. M., CESPEDES, R. D., ATKINS, J. N., LIPPMAN, S. M., CARLIN, S. M., RYAN, A., SZCZEPANEK, C. M., CROWLEY, J. J. & COLTMAN, C. A., JR. 2003. The influence of finasteride on the development of prostate cancer. *N Engl J Med,* 349**,** 215-24.

TIAN, X., LIU, Z., NIU, B., ZHANG, J., TAN, T. K., LEE, S. R., ZHAO, Y., HARRIS, D. C. & ZHENG, G. 2011. E-cadherin/beta-catenin complex and the epithelial barrier. *J Biomed Biotechnol,* 2011**,** 567305.

TOMLINS, S. A., LAXMAN, B., DHANASEKARAN, S. M., HELGESON, B. E., CAO, X., MORRIS, D. S., MENON, A., JING, X., CAO, Q., HAN, B., YU, J., WANG, L., MONTIE, J. E., RUBIN, M. A., PIENTA, K. J., ROULSTON, D., SHAH, R. B., VARAMBALLY, S., MEHRA, R. & CHINNAIYAN, A. M. 2007. Distinct classes of chromosomal rearrangements create oncogenic ETS gene fusions in prostate cancer. *Nature,* 448**,** 595-9.

TOMLINS, S. A., LAXMAN, B., VARAMBALLY, S., CAO, X., YU, J., HELGESON, B. E., CAO, Q., PRENSNER, J. R., RUBIN, M. A., SHAH, R. B., MEHRA, R. & CHINNAIYAN, A. M. 2008. Role of the TMPRSS2-ERG gene fusion in prostate cancer. *Neoplasia,* 10**,** 177-88.

TOMLINS, S. A., MEHRA, R., RHODES, D. R., SMITH, L. R., ROULSTON, D., HELGESON, B. E., CAO, X., WEI, J. T., RUBIN, M. A., SHAH, R. B. & CHINNAIYAN, A. M. 2006. TMPRSS2:ETV4 gene fusions define a third molecular subtype of prostate cancer. *Cancer Res,* 66**,** 3396-400.

TOMLINS, S. A., RHODES, D. R., PERNER, S., DHANASEKARAN, S. M., MEHRA, R., SUN, X. W., VARAMBALLY, S., CAO, X., TCHINDA, J., KUEFER, R., LEE, C., MONTIE, J. E., SHAH, R. B., PIENTA, K. J., RUBIN, M. A. & CHINNAIYAN, A. M. 2005. Recurrent fusion of TMPRSS2 and ETS transcription factor genes in prostate cancer. *Science,* 310**,** 644-8.

TRACHTENBERG, J., GITTLEMAN, M., STEIDLE, C., BARZELL, W., FRIEDEL, W., PESSIS, D., FOTHERINGHAM, N., CAMPION, M. & GARNICK, M. B. 2002. A phase 3, multicenter, open label, randomized study of abarelix versus leuprolide plus daily antiandrogen in men with prostate cancer. *J Urol,* 167**,** 1670-4.

TREROTOLA, M., RATHORE, S., GOEL, H. L., LI, J., ALBERTI, S., PIANTELLI, M., ADAMS, D., JIANG, Z. & LANGUINO, L. R. 2010. CD133, Trop-2 and alpha2beta1 integrin surface receptors as markers of putative human prostate cancer stem cells. *Am J Transl Res,* 2**,** 135-44.

TSAO, H. W., TAI, T. S., TSENG, W., CHANG, H. H., GRENNINGLOH, R., MIAW, S. C. & HO, I. C. 2013. Ets-1 facilitates nuclear entry of NFAT proteins and their recruitment to the IL-2 promoter. *Proc Natl Acad Sci U S A,* 110**,** 15776-81.

TU, J. J., ROHAN, S., KAO, J., KITABAYASHI, N., MATHEW, S. & CHEN, Y. T. 2007. Gene fusions between TMPRSS2 and ETS family genes in prostate cancer: frequency and transcript variant analysis by RT-PCR and FISH on paraffin-embedded tissues. *Mod Pathol,* 20**,** 921-8.

TUGORES, A., LE, J., SOROKINA, I., SNIJDERS, A. J., DUYAO, M., REDDY, P. S., CARLEE, L., RONSHAUGEN, M., MUSHEGIAN, A., WATANASKUL, T., CHU, S., BUCKLER, A., EMTAGE, S. & MCCORMICK, M. K. 2001. The epithelium-specific ETS protein EHF/ESE-3 is a context-dependent transcriptional repressor downstream of MAPK signaling cascades. *J Biol Chem,* 276**,** 20397-406.

TURNER, D. P., FINDLAY, V. J., MOUSSA, O., SEMENCHENKO, V. I., WATSON, P. M., LARUE, A. C., DESOUKI, M. M., FRAIG, M. & WATSON, D. K. 2011. Mechanisms and functional consequences of PDEF protein expression loss during prostate cancer progression. *Prostate,* 71**,** 1723-35.

TUXHORN, J. A., AYALA, G. E., SMITH, M. J., SMITH, V. C., DANG, T. D. & ROWLEY, D. R. 2002. Reactive stroma in human prostate cancer: induction of myofibroblast phenotype and extracellular matrix remodeling. *Clin Cancer Res,* 8**,** 2912-23.

TYMMS, M. J., NG, A. Y., THOMAS, R. S., SCHUTTE, B. C., ZHOU, J., EYRE, H. J., SUTHERLAND, G. R., SETH, A., ROSENBERG, M., PAPAS, T., DEBOUCK, C. & KOLA, I. 1997. A novel epithelial-expressed ETS gene, ELF3: human and murine cDNA sequences, murine genomic organization, human mapping to 1q32.2 and expression in tissues and cancer. *Oncogene,* 15**,** 2449-62.

TYRRELL, C. J., KAISARY, A. V., IVERSEN, P., ANDERSON, J. B., BAERT, L., TAMMELA, T., CHAMBERLAIN, M., WEBSTER, A. & BLACKLEDGE, G. 1998. A randomised comparison of 'Casodex' (bicalutamide) 150 mg monotherapy versus castration in the treatment of metastatic and locally advanced prostate cancer. *Eur Urol,* 33**,** 447-56.

VALASTYAN, S. & WEINBERG, R. A. 2011. Tumor metastasis: molecular insights and evolving paradigms. *Cell,* 147**,** 275-92.

VAN DER PLUIJM, G. 2011. Epithelial plasticity, cancer stem cells and bone metastasis formation. *Bone,* 48**,** 37-43.

VAN LEENDERS, G. J., AALDERS, T. W., HULSBERGEN-VAN DE KAA, C. A., RUITER, D. J. & SCHALKEN, J. A. 2001. Expression of basal cell keratins in human prostate cancer metastases and cell lines. *J Pathol,* 195**,** 563-70.

VANNUCCI, L., LAI, M., CHIUPPESI, F., CECCHERINI-NELLI, L. & PISTELLO, M. 2013. Viral vectors: a look back and ahead on gene transfer technology. *New Microbiol,* 36**,** 1-22.

VEERAVAGU, A., BABABEYGY, S. R., KALANI, M. Y., HOU, L. C. & TSE, V. 2008. The cancer stem cell-vascular niche complex in brain tumor formation. *Stem Cells Dev,* 17**,** 859-67.

VISVADER, J. E. & LINDEMAN, G. J. 2008. Cancer stem cells in solid tumours: accumulating evidence and unresolved questions. *Nat Rev Cancer,* 8**,** 755-68.

VOCKE, C. D., POZZATTI, R. O., BOSTWICK, D. G., FLORENCE, C. D., JENNINGS, S. B., STRUP, S. E., DURAY, P. H., LIOTTA, L. A., EMMERT-BUCK, M. R. & LINEHAN, W. M. 1996. Analysis of 99 microdissected prostate carcinomas reveals a high frequency of allelic loss on chromosome 8p12-21. *Cancer Res,* 56**,** 2411-6.

WANG, H., YU, Z., HUO, S., CHEN, Z., OU, Z., MAI, J., DING, S. & ZHANG, J. 2018. Overexpression of ELF3 facilitates cell growth and metastasis through PI3K/Akt and ERK signaling pathways in non-small cell lung cancer. *Int J Biochem Cell Biol,* 94**,** 98-106.

WANG, J., CAI, Y., REN, C. & ITTMANN, M. 2006. Expression of variant TMPRSS2/ERG fusion messenger RNAs is associated with aggressive prostate cancer. *Cancer Res,* 66**,** 8347-51.

WANG, J. L., CHEN, Z. F., CHEN, H. M., WANG, M. Y., KONG, X., WANG, Y. C., SUN, T. T., HONG, J., ZOU, W., XU, J. & FANG, J. Y. 2014. Elf3 drives beta-catenin

transactivation and associates with poor prognosis in colorectal cancer. *Cell Death Dis,* 5**,** e1263.

WANG, X., KRUITHOF-DE JULIO, M., ECONOMIDES, K. D., WALKER, D., YU, H., HALILI, M. V., HU, Y. P., PRICE, S. M., ABATE-SHEN, C. & SHEN, M. M. 2009. A luminal epithelial stem cell that is a cell of origin for prostate cancer. *Nature,* 461**,** 495-500.

WATSON, P. A., CHEN, Y. F., BALBAS, M. D., WONGVIPAT, J., SOCCI, N. D., VIALE, A., KIM, K. & SAWYERS, C. L. 2010. Constitutively active androgen receptor splice variants expressed in castration-resistant prostate cancer require full-length androgen receptor. *Proc Natl Acad Sci U S A,* 107**,** 16759-65.

WEICHERT, W., SCHMIDT, M., GEKELER, V., DENKERT, C., STEPHAN, C., JUNG, K., LOENING, S., DIETEL, M. & KRISTIANSEN, G. 2004. Polo-like kinase 1 is overexpressed in prostate cancer and linked to higher tumor grades. *Prostate,* 60**,** 240-5.

WISE, A. M., STAMEY, T. A., MCNEAL, J. E. & CLAYTON, J. L. 2002. Morphologic and clinical significance of multifocal prostate cancers in radical prostatectomy specimens. *Urology,* 60**,** 264-9.

WRIGHT, M. E., TSAI, M. J. & AEBERSOLD, R. 2003. Androgen receptor represses the neuroendocrine transdifferentiation process in prostate cancer cells. *Mol Endocrinol,* 17**,** 1726-37.

WU, J., DUAN, R., CAO, H., FIELD, D., NEWNHAM, C. M., KOEHLER, D. R., ZAMEL, N., PRITCHARD, M. A., HERTZOG, P., POST, M., TANSWELL, A. K. & HU, J. 2008. Regulation of epithelium-specific Ets-like factors ESE-1 and ESE-3 in airway epithelial cells: potential roles in airway inflammation. *Cell Res,* 18**,** 649-63.

XIA, J., TROCK, B. J., COOPERBERG, M. R., GULATI, R., ZELIADT, S. B., GORE, J. L., LIN, D. W., CARROLL, P. R., CARTER, H. B. & ETZIONI, R. 2012. Prostate cancer mortality following active surveillance versus immediate radical prostatectomy. *Clin Cancer Res,* 18**,** 5471-8.

XIE, Y. S., ZHANG, Y. H., LIU, S. P., LIU, S. Q., PENG, C. W., WU, L., LUO, H. S. & LI, Y. 2010. Synergistic gastric cancer inhibition by chemogenetherapy with recombinant human adenovirus p53 and epirubicin: an in vitro and in vivo study. *Oncol Rep,* 24**,** 1613-20.

XU, D., DWYER, J., LI, H., DUAN, W. & LIU, J. P. 2008. Ets2 maintains hTERT gene expression and breast cancer cell proliferation by interacting with c-Myc. *J Biol Chem,* 283**,** 23567-80.

YAN, J. & TANG, D. 2014. Prostate cancer stem-like cells proliferate slowly and resist etoposide-induced cytotoxicity via enhancing DNA damage response. *Exp Cell Res,* 328**,** 132-42.

YANG, C., CIRIELLI, C., CAPOGROSSI, M. C. & PASSANITI, A. 1995. Adenovirus-mediated wild-type p53 expression induces apoptosis and suppresses tumorigenesis of prostatic tumor cells. *Cancer Res,* 55**,** 4210-3.

YANG, X. & LEE, S. H. 2016. Identification of ESE1 as a beta-Catenin Binding Protein. *Anticancer Res,* 36**,** 2697-703.

YEUNG, T. L., LEUNG, C. S., WONG, K. K., GUTIERREZ-HARTMANN, A., KWONG, J., GERSHENSON, D. M. & MOK, S. C. 2017. ELF3 is a negative regulator of epithelial-mesenchymal transition in ovarian cancer cells. *Oncotarget,* 8**,** 16951-16963.

YU, J., YU, J., MANI, R. S., CAO, Q., BRENNER, C. J., CAO, X., WANG, X., WU, L., LI, J., HU, M., GONG, Y., CHENG, H., LAXMAN, B., VELLAICHAMY, A., SHANKAR, S., LI, Y., DHANASEKARAN, S. M., MOREY, R., BARRETTE, T., LONIGRO, R. J., TOMLINS, S. A., VARAMBALLY, S., QIN, Z. S. & CHINNAIYAN, A. M. 2010. An integrated network of androgen receptor, polycomb, and TMPRSS2-ERG gene fusions in prostate cancer progression. *Cancer Cell,* 17**,** 443-54.

YUAN, T. C., VEERAMANI, S. & LIN, M. F. 2007. Neuroendocrine-like prostate cancer cells: neuroendocrine transdifferentiation of prostate adenocarcinoma cells. *Endocr Relat Cancer,* 14**,** 531-47.

ZELEFSKY, M. J., FUKS, Z., HUNT, M., LEE, H. J., LOMBARDI, D., LING, C. C., REUTER, V. E., VENKATRAMAN, E. S. & LEIBEL, S. A. 2001. High dose radiation delivered by intensity modulated conformal radiotherapy improves the outcome of localized prostate cancer. *J Urol,* 166**,** 876-81.

ZELENT, A., GREAVES, M. & ENVER, T. 2004. Role of the TEL-AML1 fusion gene in the molecular pathogenesis of childhood acute lymphoblastic leukaemia. *Oncogene,* 23**,** 4275-83.

ZHANG, M., TAYLOR, C. E., PIAO, L., DATTA, J., BRUNO, P. A., BHAVE, S., SU, T., LANG, J. C., XIE, X., TEKNOS, T. N., MAPP, A. K. & PAN, Q. 2013. Genetic and chemical targeting of epithelial-restricted with serine box reduces EGF receptor and potentiates the efficacy of afatinib. *Mol Cancer Ther,* 12**,** 1515-25.

ZHENG, L., XU, M., XU, J., WU, K., FANG, Q., LIANG, Y., ZHOU, S., CEN, D., JI, L., HAN, W. & CAI, X. 2018. ELF3 promotes epithelial-mesenchymal transition by protecting ZEB1 from miR-141-3p-mediated silencing in hepatocellular carcinoma. *Cell Death Dis,* 9**,** 387.